Investigation of an unusual $GABA_A$ receptor - Studies on the promiscuous ε subunit

Tina Schwabe

A thesis submitted in partial fulfilment of the requirements of Nottingham Trent University for the degree of Doctor of Philosophy.

December 2010

Copyright statement

Abstract

γ-aminobutyric acid (GABA) type A ($GABA_A$) receptors are pentameric, chloride-selective ion channels. Nineteen different $GABA_A$ receptor subunits are known to exist in man and various subunit combinations are able to form receptor subtypes with different, subunit-specific pharmacological properties. $GABA_A$ receptors are targeted by many clinically-important drugs, for example, benzodiazepines. Unwanted side effects, such as tolerance and dependence, often occur due to non-selective receptor targeting. There is, therefore, a need for subtype-selective drugs. Comparatively little is known about the role of the ε subunit or ε-subunit-containing receptors *in vivo*. Recently, it has been recognised that a $GABA_A$ receptor subtype, that contains the $\alpha 3$ and ε subunits, is present in neurons within the forebrain that synthesise acetylcholine, and this may regulate neurotransmitter release. In Alzheimer's disease, cholinergic neurotransmission is reduced; therefore, this subtype might be a target for the development of anti-Alzheimer's disease drugs that would function by increasing acetylcholine release in forebrain regions where cholinergic neurons are dying. The pharmacological properties of a $GABA_A$ receptor that comprises the $\alpha 3$, $\beta 2$ and ε subunits were examined in *Xenopus laevis* oocytes using the two-electrode voltage-clamp technique. The results obtained confirm that the ε subunit confers unusual properties on the $GABA_A$ receptor. $\alpha 3\beta 2\varepsilon$ receptors were spontaneously active and displayed high agonist sensitivity. Next, a screening assay was established in human embryonic kidney 293 cells, which were transiently transfected with complementary DNAs for $GABA_A$ receptor subunits and a yellow fluorescence protein variant (YFP-H148Q/I152L). The latter is quenched by anion influx into cells upon receptor activation. Using this assay, receptor activity and GABA-concentration relationships could be demonstrated. It was, therefore, used to screen for compounds that modulate the activity of ε-subunit-containing receptors. Several interesting compounds were identified, and they were further examined using the two-electrode voltage-clamp technique. These compounds are potential candidates for drug development, and may help to identify the physiological role(s) of $GABA_A$ receptors that contain the ε polypeptide *in vivo*.

I would like to dedicate my thesis to my grandma Ursula Pöller.

Acknowledgements

I would like to thank my supervisor Professor Mark Darlison for giving me the opportunity to do my PhD in his laboratory, for the help and guidance I received from him and for introducing me to the exciting field of ion channel research. I would also like to thank my other supervisors Professor John Wallis and Dr Chris Garner for their support.

I am grateful to my co-supervisor Dr Ian Mellor for all his help throughout my PhD and, especially, for giving me the opportunity to work in his laboratory at the University of Nottingham on a regular basis. It has been a great experience and I very much enjoyed working with you. I would also like to thank Ian for proof-reading most parts of my thesis.

Next, I would like to thank all friends and colleagues at Nottingham Trent University, University of Nottingham and Edinburgh Napier University for the help they have given me during the various stages of my PhD. I very much appreciated the warm welcome, friendliness and support I received in Ians laboratory as well as in Edinburgh after I first arrived. I am thankful to Amy Poole who has been a great help for me, especially during the last two years. It was nice to getting to know you better.

Most importantly, I would like to thank my family, especially my parents and grandparents for their constant support and encouragement. I very much missed seeing you more often. Finally, I would like to thank my fiancï£¡e Shiva Marthandan who has been there for me throughout these past few years, helping, encouraging and comforting me. Thanks for having faith in me and my work; this has greatly helped me to get to the end and finish my thesis.

Finally, I am thankful to Prof. Erwin Sigel (Institute of Biochemistry and Molecular Medicine, University of Bern, Switzerland) for supplying the $GABA_A$ receptor α3-, β2- and γ2L-subunit cDNAs, to Dr Maurice Garret (Laboratoire de Neurophysiologie, Bordeaux, France) for providing the ε-subunit cDNA, to Dr Thomas Kuner (Institute of Anatomy and Cell Biology, Heidelberg University, Germany) for the pRK5-Clomeleon plasmid and to Prof. Alan Verkman (Department of Medicine, University of California, San Francisco, USA) for supplying the pEYFP H148Q/I152L mutant vector. I am also grateful to Prof. Anne Stephenson (The School of Pharmacy, University of London, UK) for providing HEK293 cells.

Table of Contents

List of Figures

List of Tables

Abbreviations

5-HT_3Rs	Serotonin 5-hydroxytryptamine$_3$ receptors
A	Absorbance
ACh	Acetylcholine
AD	Alzheimer's disease
AE1	Anion exchanger 1
BF	Baseline fluorescence
BLAST	Basic local alignment search tool
bp	Base pairs
cDNA	Complementary DNA
CFP	Cyan fluorescence protein
CFTR	Cystic fibrosis transmembrane conductance regulator protein
CNS	Central nervous system
cRNA	Complementary RNA
DEPC	Diethylpyrocarbonate
DMCM	methyl-6,7-dimethoxy-4-ethyl-beta-carboline-3-carboxylate
DMEM	Dulbecco's modified Eagle's medium
DMSO	Dimethyl sulfoxide
DPBS	Dulbecco's phosphate buffered saline
E.coli	*Escherichia coli*
ε_T	Truncated ε subunit
EC_{50}	Effective concentration for 50 % receptor activity
EDTA	Ethylenediaminetetraacetic acid
FBS	Fetal bovine serum
FLIPR	Fluorometric Imaging Plate Reader
FRET	Förster (or Fluorescence) Resonance Energy Transfer
GABA	γ-Aminobutyric acid
$GABA_A$	GABA type A
$GABA_B$	GABA type B
GAD	Glutamate decarboxylase
GFP	Green fluorescence protein
GlyRs	Glycine receptors
HEK	Human embryonic kidney
HTS	High throughput screening
IC_{50}	Effective concentration for 50 % receptor inhibition
K_{App}	Apparent dissociation constant
K_d	Dissociation constant
kb	Kilo bases
LB	Lysogeny broth
LC	Locus coeruleus

LGICs	Ligand-gated ion channels
MQAE	N-(ethoxycarbonylmethyl)-6-methoxyquinolinium bromide
MRK-016	3-tert-butyl-7-(5-methylisoxazol-3-yl)-2-(1-methyl-1H-1,2,4-triazol-5-ylmethoxy)-pyrazolo[1,5-d]-[1,2,4]triazine
mRNA	Messenger RNA
nAChRs	Nicotinic ACh receptors
NKCC	Na^+-K^+-Cl^- co-transporters
OD	Optical density
PCR	Polymerase chain reaction
PKC	Protein kinase C
rpm	Revolutions per minute
rTEV	Recombinant Tobacco Etch Virus
SD	Standard deviation
SEM	Standard error of the mean
SK	Sandell-Kolthoff
T_m	Melting temperature
TAE	Tris-acetate
TM	Transmembrane domain
UV	Ultraviolet
v/v	Volume per volume
w/v	Weight per volume
YFP	Yellow fluorescence protein
YFP-H148Q/I152L	YFP with mutation at positions 148 (histidine to glutamine) and 152 (isoleucine to leucine)

Chapter 1

General Introduction

1.1 Alzheimer's disease

Alzheimer's disease (AD) is a progressive neurodegenerative disorder and the most frequent form of dementia in elderly people. More than 25 million people worldwide are suffering from dementia, a number that is expected to double every 20 years as the general age of the human population increases (Ferri et al., 2005; Citron, 2010). Clinical features of AD include loss of memory, cognitive dysfunction as well as behavioural disturbances, such as mood disorders, agitation and psychosis, leading to death on average nine years after AD was first diagnosed. AD is the sixth leading cause of death in the USA. The illness not only has a dramatic effect on the patient, but there is also a considerable burden on close relatives and caregivers, and ultimately national economies due to the frequent requirement for institutionalisation. Total costs caused by AD worldwide are thought to be more than 200 billion dollars per annum (Citron, 2010).

The pathological hallmarks of AD are the presence of extracellular plaques containing β-amyloid peptides, which derive from the amyloid precursor protein, and neurofibrillary tangles, which contain abnormally phosphorylated forms of the cytoskeleton-associated protein tau, as well as the degeneration of synapses and neurons (Kar et al., 2004; Citron, 2010). It is also well established that there is a loss of cholinergic neurotransmission in the hippocampus and neocortex of the brain. This is the result of reduced choline uptake, acetylcholine

(ACh) release and choline acetyltransferase activity and, ultimately, the loss of basal forebrain cholinergic neurons. ACh is essential for cell-to-cell communication in the forebrain, and neuronal pathways regulated by this transmitter are important for cognition. The findings outlined above have led to the 'cholinergic hypothesis' of AD, in which the loss of basal forebrain cholinergic neurons and the interruption of cholinergic neurotransmission in the cerebral cortex and other areas is proposed to cause the observed cognitive impairments (Kar et al., 2004; Yuede et al., 2007). Currently, there is no cure for this debilitating illness. However, therapeutic approaches have been developed, for example ACh-esterase inhibitors, which increase ACh levels in the brain resulting in improved cognitive functions. There are currently four approved ACh-esterase inhibitors to treat mild to moderate AD: tacrine (Cognex®), donepezil (Aricept®), rivastigmine (Exelon®) and galantamine (Reminyl®; Yuede et al., 2007). The latter also potentiates the activity of neuronal nicotinic ACh receptors (nAChRs), which is believed to further improve neurotransmission (Seltzer, 2010). However, these drugs merely delay the progression of disease symptoms for one to two years. Moreover, the ACh-esterase inhibitor tacrine has been shown to trigger hepatotoxic effects and its use has been diminished (Watkins et al., 1994). Hence, to treat AD more efficiently, new drug targets and more effective treatments are urgently needed.

1.2 GABA and $GABA_A$ receptors

γ-Aminobutyric acid (GABA) is a four-carbon nonprotein amino acid. It is synthesised from L-glutamic acid catalysed by glutamate decarboxylase (GAD); GAD requires the cofactor pyridoxal phosphate (Martin & Rimvall, 1993). It exists in two isoforms, GAD_{65} (65 kDa isoform) and GAD_{67} (67 kDa isoform). The two forms are regulated separately and localised in different subcellular compartments. GAD_{67} is present throughout the cytoplasm of neurons, generating GABA for metabolic purposes rather than neurotransmission, for example protection after neuronal injury or regulation of redox potential in response to oxidative stress (Kaufman et al., 1991; Waagepetersen et al., 1999; Lamigeon et al., 2001; Buddhala et al., 2009). GAD_{65} is present in nerve terminal endings generating GABA for neurotransmission purposes. GABA is removed from the synaptic cleft by high-affinity transporters and bro-

ken down by GABA transaminase into succinic semialdehyde and glutamic acid (D'Hulst & Kooy, 2007).

GABA is the main inhibitory neurotransmitter in the mammalian central nervous system (CNS) and found in 30 % of neuronal synapses. Its effects are mediated via ionotropic GABA type A ($GABA_A$) receptors or via metabotropic GABA type B ($GABA_B$) receptors. The latter are coupled to G proteins, which mediate signal transduction via secondary messengers, whereas the former are directly gating Cl^- ions (Bormann, 2000). $GABA_A$ receptors are widespread throughout the mammalian CNS where they control the majority of physiological actions of GABA, including learning and memory processes, cognition, feeding and drinking behaviour and the modulation of anxiety (Bormann, 2000; Sieghart & Sperk, 2002; D'Hulst et al., 2009). Mutations or functional deficits of $GABA_A$ receptors have been implicated with a variety of neuropsychiatric diseases, such as anxiety, schizophrenia, fragile X syndrome and several genetic forms of epilepsy (D'Hulst & Kooy, 2007; Moult, 2009; Macdonald et al., 2010). The receptors importance is further reflected by the fact that it is targeted by a plethora of pharmacologically and clinically important drugs, including benzodiazepines and anaesthetics.

1.2.1 Molecular structure of $GABA_A$ receptors

$GABA_A$ receptors belong to the superfamily of Cys-loop ligand-gated ion channels (LGICs) that also includes nAChRs, serotonin 5-hydroxytryptamine$_3$ receptors (5-HT_3Rs), glycine receptors (GlyRs) and zinc-activated ion channels (Schofield et al., 1987; Olsen & Sieghart, 2008). Cys-loop LGICs mediate fast synaptic neurotransmission by conducting cations (nAChRs, 5-HT_3Rs and zinc-activated ion channels) or anions ($GABA_A$ receptors and GlyRs), mediating excitatory or inhibitory neurotransmission, respectively (Pless & Lynch, 2008). $GABA_A$ receptors consist of five subunits, each of which comprises a large extracellular amino terminal domain of about 220 amino acids, four hydrophobic, α-helical transmembrane domains (TM1-4) each of about 20 amino acids in length, a large intracellular loop between TM3 and TM4 and a short extracellular carboxyl-terminal domain (Figure 1.1 A). The extracellular amino terminal domain includes a 13 amino acid sequence flanked by

two cystein residues that form a disulphide bond. This characteristic structural feature, common to all Cys-loop LGICs, determined the superfamily's name (Simon et al., 2004). The receptor subunits are arranged in a circle to form a central ion-conducting channel, with the second TM of each subunit forming the channel pore (Figure 1.1 B; Hevers & Lüddens, 1998). Residues within the amino terminal domain of two adjacent subunits form the ligand binding sites. Binding of two GABA molecules to a $GABA_A$ receptor triggers a conformational change in the receptor, resulting in the opening of the intrinsic channel pore, the influx of extracellular ions (primarily Cl^- ions) via diffusion and subsequent hyperpolarisation of the post-synaptic membrane, which leads to an increase in the inhibitory tone (Darlison et al., 2005).

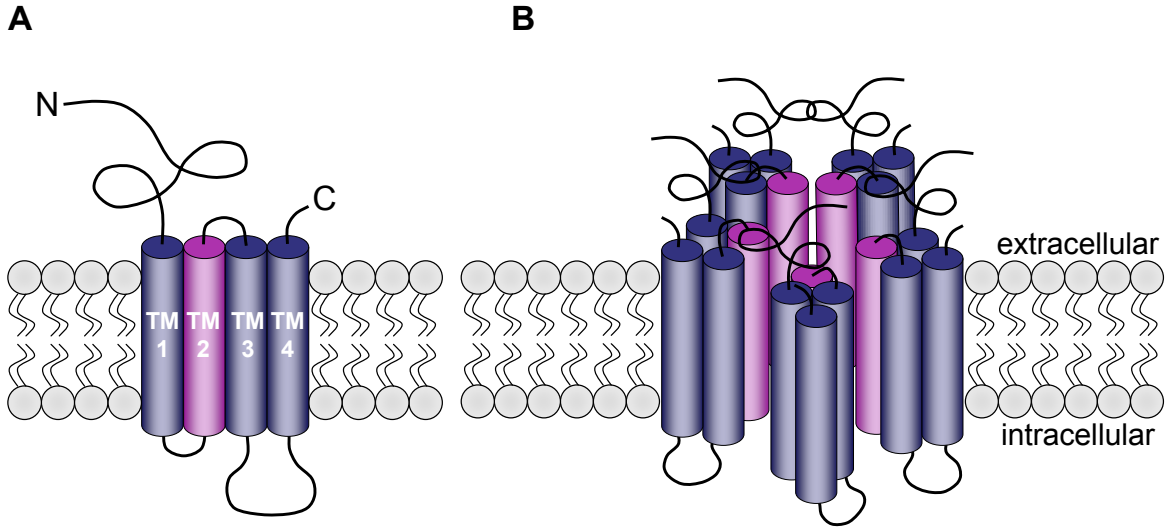

Figure 1.1: $GABA_A$ receptor structure. (A) Schematic representation of a receptor subunit and (B) the pentameric receptor structure.

1.2.2 $GABA_A$ receptor subunit diversity

Nineteen different $GABA_A$ receptor subunits are known to exist in man; analysis of the human genome database revealed that there are no further $GABA_A$ receptor subunit genes (Simon et al., 2004). The subunit genes are subdivided into classes according to their amino acid sequence homology. Sequence similarities between members of the same family are around 70 % and between different families around 20 to 40 % (Darlison et al., 2005). There are six alpha (α1-α6), three beta (β1-β3), three gamma (γ1-γ3), one delta (δ), one epsilon

(ε), one theta (θ) and one pi (π) subunit as well as three rho (ρ1-ρ3) subunits. The latter were formerly classified as GABA type C receptors due to their distinct pharmacological characteristics and the fact that they are highly expressed in the vertebrate retina and do not co-localise with other $GABA_A$ receptor subtypes (Bormann, 2000; Olsen & Sieghart, 2008). A number of receptor subunits exhibit splice variants, among others the α6, γ2 and ε subunits, generating further structural diversity of $GABA_A$ receptors (see also Section 3.1.2, Chapter 3; Whiting et al., 1990, 1997; Korpi et al., 1994; Simon et al., 2004). Furthermore, two other subunits, β4 and γ4, have been identified in lower vertebrates which lack the ε and θ subunits (Bateson et al., 1991; Harvey et al., 1993). Based on sequence similarities between the ε and γ4 subunits (49 % identity) as well as between the θ and β4 subunits (56 % identity) and gene mapping studies, it has been concluded that the ε and θ subunits are orthologues of the γ4 and β4 subunits, respectively (Simon et al., 2004; Darlison et al., 2005).

Each receptor subunit is encoded by a distinct gene; most of which are clustered on different chromosomes in the human genome (see Table 1.1; Simon et al., 2004; Darlison et al., 2005). The subunit genes are expressed independently from other genes of the same cluster and associate together in different combinations to form a variety of receptor subtypes. This explains the large number of different $GABA_A$ receptor subtypes present in the vertebrate brain (see below). However, co-regulation of clustered genes may play a role in some receptor subtypes, for example in $\alpha1\beta2\gamma2$ receptors. All three subunits are clustered on chromosome 5; the β2 and α1 genes are separated by the α6 subunit gene (β2-α6-α1-γ2). It was shown in α6 'knockout' mice that α1 and β2 subunits are most likely regulated together by a common regulatory element, since expression of both subunits was reduced in mice lacking the α6 subunit (Uusi-Oukari et al., 2000). Furthermore, α1 and β2 subunits are widely expressed and exhibit a nearly identical expression pattern in the mammalian brain. Expression of the γ2 subunit was not affected in α6 'knockout' mice compared to wild-type mice. Nevertheless, these results suggest that subunit gene-clustering may partly contribute to $\alpha1\beta2\gamma2$ receptor assembling and may also play a role in subunit assembling of certain other receptor subtypes.

Table 1.1: $GABA_A$ receptor subunit clusters in the human genome

$GABA_A$ receptor subunits	Chromosome
$\alpha 2$, $\alpha 4$, $\beta 1$, $\gamma 1$	4p12-p13
$\alpha 1$, $\alpha 6$, $\beta 2$, $\gamma 2$	5q31-q35
$\alpha 5$, $\beta 3$, $\gamma 3$	15q11-q12
$\alpha 3$, θ, ε	Xq28
$\rho 1$, $\rho 2$	6q14-q21

The π subunit gene is located on chromosome 5 (5q34-q35), but apart from the $\beta 2$-$\alpha 6$-$\alpha 1$-$\gamma 2$ subunit gene cluster. The δ subunit is present separately from all other $GABA_A$ receptor genes on chromosome 1 (1p36.3; Simon et al., 2004; Darlison et al., 2005).

1.2.3 $GABA_A$ receptor stoichiometry and distribution in the brain

Hypothetically, if all existing $GABA_A$ receptor subunits could co-assemble at random, the number of potential receptor subtypes would be huge. However, cell type-specific regulation mechanisms control subcellular localisation, trafficking and subunit assembly (Fritschy & Brünig, 2003; Lüscher & Keller, 2004), resulting in the existence of only a fraction of those potential $GABA_A$ receptors *in vivo*. Sieghart (2000) estimated that there could be more than 500 different receptor subtypes expressed in the brain. Although, the presence of α and β subunits is sufficient to form functional GABA-gated channels, most of the native receptors are composed of three different types of subunits, usually two α subunits, two β subunits and one γ subunit with a common stoichiometry of α-β-α-β-γ (Baumann et al., 2002; Sieghart & Sperk, 2002). The γ subunit is in certain receptor subtypes replaced by a δ or ε subunit.

The distribution of the different $GABA_A$ receptor subtypes is brain area and cell type specific; distinct neurons can express more than one receptor subtype. Subunit co-localisation in different brain areas is important for receptor subunit composition. *In situ* hybridisation and immunohistochemistry experiments revealed that $\alpha 1$, $\beta 1$, $\beta 2$, $\beta 3$ and $\gamma 2$ subunits are widely expressed throughout the brain, albeit with different distribution patterns (Sieghart & Sperk, 2002; Olsen & Sieghart, 2009). Expression of $\alpha 2$, $\alpha 3$, $\alpha 4$, $\alpha 5$, $\alpha 6$, $\gamma 1$ and δ subunits is less abundant and restricted to specific brain areas. The $\alpha 2$ subunit, for example, is predominately expressed in the forebrain, whereas the $\alpha 6$ subunit is located only in granule cells of the cerebellum and the cochlear nucleus (Pirker et al., 2000). Furthermore, the majority of serotonergic neurons located in the raphne nuclei contain $\alpha 3$ subunits, but lack

$\alpha 1$ subunits (Gao et al., 1993). In contrast, GABAergic neurons in this area express both α subunits and, hence, contain different receptor types.

The most common receptor subtype is the $\alpha 1\beta 2\gamma 2$ receptor, which is present in most areas of the brain and makes up for 60 % of all $GABA_A$ receptors (Möhler, 2006, 2007). Other common receptor subtypes are $\alpha 2\beta 3\gamma 2$ and $\alpha 3\beta\gamma 2$ receptors, which count for 15 to 20 % and 10 to 15 % of all receptors, respectively. Despite extensive research in the area, only ten different native receptor subtypes have been identified indubitably by taking into account specific criteria for receptor identification, including localisation, subunit composition, stoichiometry and receptor pharmacology (see Olsen & Sieghart, 2008, 2009). Further receptor subtypes have been proposed to exist with high probability or tentatively (see Table 1.2).

Table 1.2: Native $GABA_A$ receptors in the brain

Identified	Existing with high probability	Tentative
$\alpha 1\beta 2\gamma 2$	$\alpha 1\beta 3\gamma 2$	$\rho 1$
$\alpha 2\beta\gamma 2$	$\alpha 1\beta\delta$	$\rho 2$
$\alpha 3\beta\gamma 2$	$\alpha 5\beta 3\gamma 2$	$\rho 3$
$\alpha 4\beta\gamma 2$	$\alpha\beta 1\gamma/\alpha\beta 1\delta$	$\alpha\beta\gamma 1$
$\alpha 4\beta 2\delta$	$\alpha\beta$	$\alpha\beta\gamma 3$
$\alpha 4\beta 3\delta$	$\alpha 1\alpha 6\beta\gamma/\alpha 1\alpha 6\beta\delta$	$\alpha\beta\theta$
$\alpha 5\beta\gamma 2$		$\alpha\beta\varepsilon$
$\alpha 6\beta\gamma 2$		$\alpha\beta\pi$
$\alpha 6\beta\delta$		$\alpha_x\alpha_y\beta\gamma 2$
ρ		

By investigating different aspects of $GABA_A$ receptors, including localisation, subunit composition and receptor pharmacology, ten native receptor subtypes have been unequivocally identified, further receptor subtypes exist with high probability and others tentatively (adapted from Olsen & Sieghart, 2009).

Although most receptors contain only one type of α or β subunits several studies have suggested that there may be receptor subtypes co-expressing two different α or β subunits in the brain (Sieghart & Sperk, 2002; Benke et al., 2004; Olsen & Sieghart, 2009). Immunoprecipitation and -purification experiments and expression of $\alpha 1$, $\alpha 6$, $\beta 2$ and $\gamma 2$ subunits in *Xenopus laevis* oocytes suggested that $\alpha 1$ and $\alpha 6$ subunits can co-exist in $\alpha 1\alpha 6\beta 2\gamma 2$ receptor subtypes (Jechlinger et al., 1998; Sigel & Baur, 2000). Similarly, Fisher & Macdonald (1997) showed that two different β subunits can co-exist in recombinant $GABA_A$ receptors

expressed in L929 fibroblasts conferring different properties to the receptor compared to receptors containing only one of the two β subunits.

Different receptor subtypes exhibit distinct functional, physiological and pharmacological characteristics. The specific subunit composition as well as the subunits position in the pentameric receptor structure determine the receptors affinity for GABA, its pharmacological profile as well as the receptors assembling patterns and targeting to different subcellular domains (Ebert et al., 1994; Connolly et al., 1996; Whiting et al., 1999).

1.2.4 Pharmacology of $GABA_A$ receptors

As mentioned above, $GABA_A$ receptors have two GABA binding sites. They are located at the interface between the α and β subunits and amino acid residues on both subunits form the agonist binding pocket (Figure 1.2; Sigel & Buhr, 1997). Additionally, $GABA_A$ receptors possess multiple other binding sites for a variety of pharmacologically and clinically important drugs, such as benzodiazepines, general anaesthetics, neurosteroids, barbiturates and convulsants (Figure 1.2 A; Bateson, 2004).

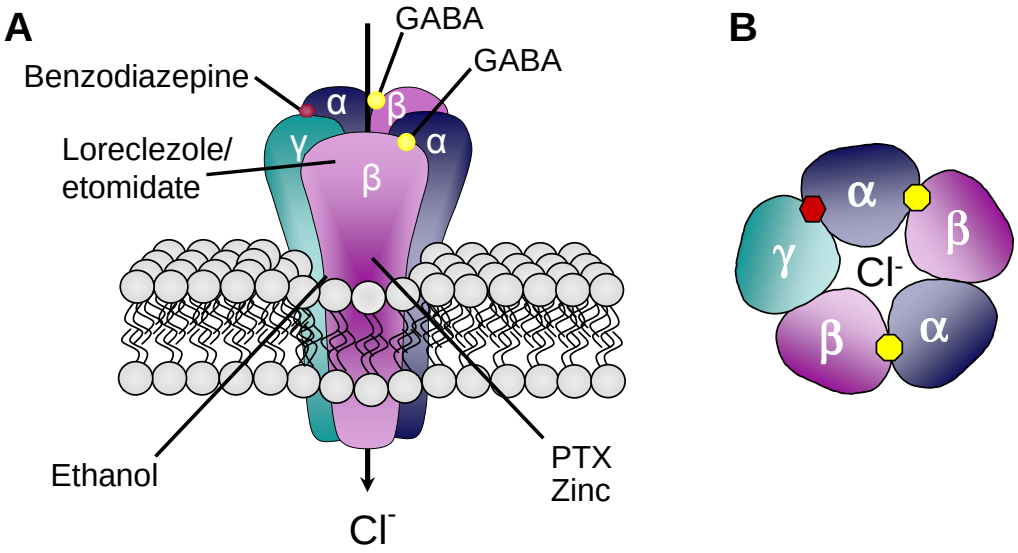

Figure 1.2: (A) Schematic illustration of the $GABA_A$ receptor and some of the several drug binding sites. (B) Cross section of the pentameric receptor structure. Yellow circles represent the agonist GABA, which binds to the receptor between the α and β subunits. The binding site for benzodiazepines (red circles) is located at the interface of α and γ subunits.

The benzodiazepine binding site has received notable interest due to the clinical importance of benzodiazepines. Full agonists, such as diazepam, antagonists, such as methyl-6,7-dimethoxy-4-ethyl-beta-carboline-3-carboxylate (DMCM), or inverse agonists, such as flumazenil, but no endogenous ligands have been identified to bind to the site (van Niel et al., 2005). Full benzodiazepine agonists have been used since the 1960s in a wide range of clinical applications, such as treatment of anxiety disorders and insomnia and as anti-epileptic and muscle relaxing agents (Bateson, 2004; Rudolph & Möhler, 2006). Inverse agonists have been used as research tools only, due to their proconvulsant effects (van Niel et al., 2005). The allosteric binding site is located at the interface between the α and γ subunits (Pritchett et al., 1989b; Stephenson et al., 1990) and benzodiazepine ligand pharmacology is determined by both the α and γ subunits of a receptor subtype (Pritchett et al., 1989a; Hadingham et al., 1993; Wafford et al., 1993). Amino acid residues of the benzodiazepine binding pocket are homologues to those in the GABA binding site (Olsen et al., 2004). It has been shown that the $\gamma 2$ subunit confers high sensitivity to classical benzodiazepines, such as diazepam and triazolam, whereas receptors containing $\gamma 1$ or $\gamma 3$ subunits show decreased affinity (Knoflach et al., 1991; Wafford et al., 1993). The $\alpha 1$, $\alpha 2$, $\alpha 3$ and $\alpha 5$ subunits also confer sensitivity to classical benzodiazepines (Pritchett et al., 1989a; Smith & Olsen, 1995; Sigel & Buhr, 1997), whereas receptors containing the $\alpha 4$ and $\alpha 6$ subunits are insensitive to most clinically used benzodiazepines (Wisden et al., 1991; Möhler et al., 2002). Receptor subtypes containing the δ and ε subunits are also benzodiazepine insensitive (Saxena & Macdonald, 1994; Whiting et al., 1997).

Work with genetically engineered mice and studies using subunit specific ligands revealed that the various effects of benzodiazepines (sedative/hypnotic, anxiolytic, anticonvulsant, muscle relaxing and amnesic) are mediated by different $GABA_A$ receptor subtypes (McKernan & Whiting, 1996; Rudolph et al., 1999; Rudolph & Möhler, 2006). In these mice, point-mutations were introduced in $\alpha 1$, $\alpha 2$, $\alpha 3$ or $\alpha 5$ subunits, which caused insensitivity of the specific subunit to diazepam (Rudolph & Möhler, 2004). Deficits in the behaviour of the mutant mice were then examined and revealed the actions mediated by the mutated subunit (Figure 1.3). By this means, it was demonstrated that receptors containing the $\alpha 1$ subu-

nit mediate the sedative, amnesic as well as partly the anticonvulsant effects of diazepam (Rudolph et al., 1999). In contrast, the anxiolytic and myorelaxing effects of diazepam are mediated by receptors containing the $\alpha 2$ subunit (Löw et al., 2000; Rudolph et al., 2001). It was further revealed that $\alpha 3$ subunits mediate myorelaxation as well as an anxyolytic effect at high receptor occupation. Several studies investigating $\alpha 5$ subunit functions revealed a role in learning and memory, for example, mice lacking the $\alpha 5$ subunit performed better in a spatial learning exercise than wild type mice (Rudolph & Möhler, 2006).

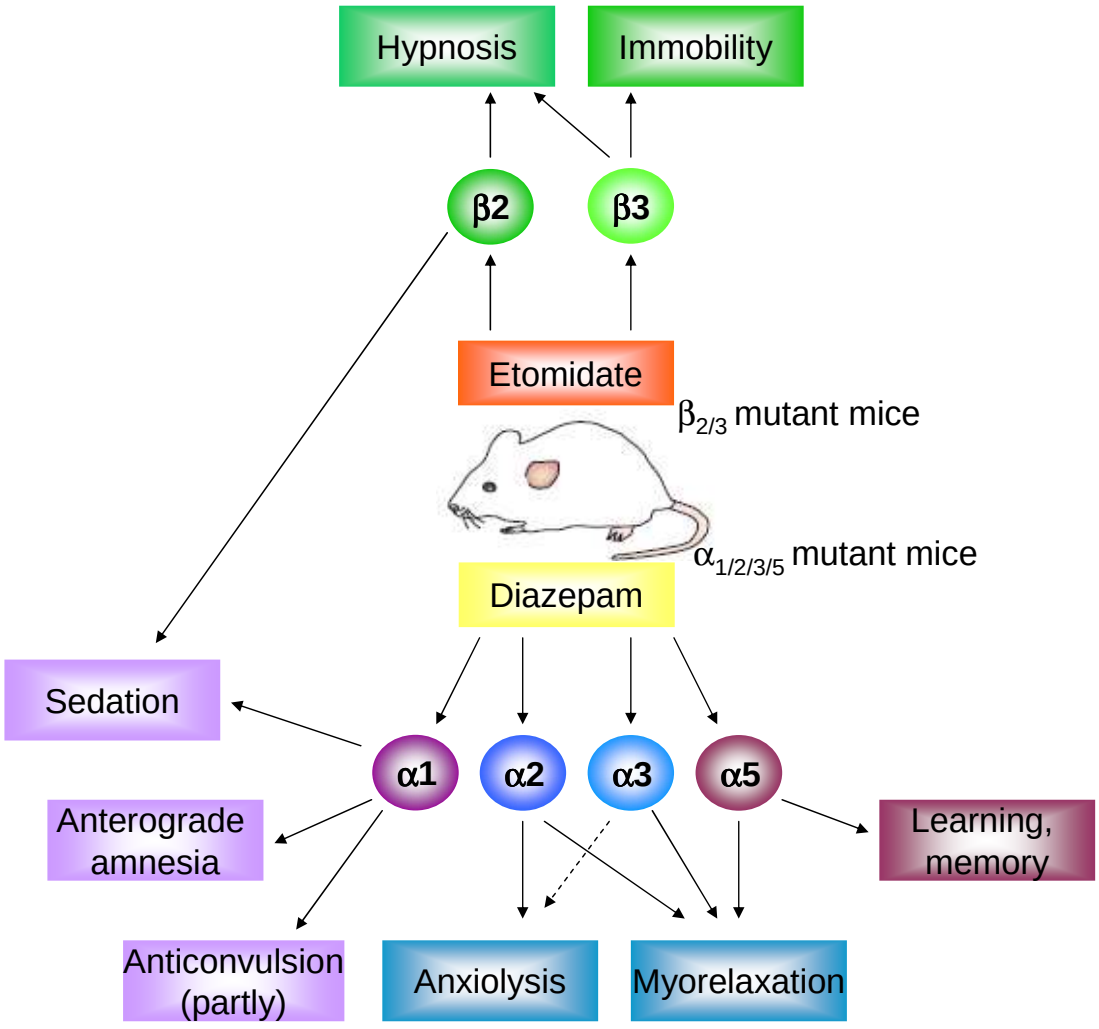

Figure 1.3: Genetic engineering studies in mice revealed distinct actions of diazepam and etomidate on different $GABA_A$ receptor subtypes.

Point-mutations in specific α or β subunits rendered them insensitive to diazepam or etomidate, respectively. Behavioural deficits in these genetically engineered mice gave information about the actions mediated by these specific receptor subtypes. For example, $\alpha 1$-containing receptors are mediating the sedative action of benzodiazepines (adapted from Agid et al., 2007).

Subunit specific ligands have been shown to also demonstrate $GABA_A$ receptor subunit functions and could confirm results obtained from genetically engineered mice (Chambers et al., 2004; Sternfeld et al., 2004; Atack et al., 2006; Rudolph & Möhler, 2006). For example, compound MRK-016 is an inverse agonist on the benzodiazepine binding site and acts primarily on α5-subunit-containing receptors mediating enhanced cognition (Chambers et al., 2004; Atack et al., 2009). Another example is the hypnotic, non-benzodiazepine zolpidem. It binds preferentially to receptors containing the α1 subunit and with less or no affinity to receptors containing α2, α3 or α5 subunits (Pritchett & Seeburg, 1990). Crestani et al. (2000) have demonstrated that the anticonvulsant and sedative effects mediated by zolpidem are solely conferred by the α1 subunit. The described compounds are subunit selective, however, they cannot discriminate between different receptor subtypes. Therefore, native $GABA_A$ receptor subtypes cannot be identified using these compounds.

The application of classical benzodiazepines is often accompanied by adverse side effects, such as dependence, withdrawal or tolerance limiting their clinical suitability (Buffett-Jerrott & Stewart, 2002; Möhler et al., 2002; Bateson, 2004; Agid et al., 2007). It was suggested that this was due to the lack of selectivity for a given receptor subtype. Ligands acting on smaller subpopulations of $GABA_A$ receptors, such as zolpidem, are thought to produce specific actions and show fewer side effects compared with the classical benzodiazepine drugs. Currently there are a number of subtype specific ligands under investigation, which may substitute the use of classical benzodiazepines in the future to contain the occurrence of side effects (see Möhler et al., 2002; Rudolph & Möhler, 2006; Whiting, 2006). These are, for example, zaleplone, a compound with high affinity for α1 subunits, but decreased sensitivity to α2, α3, or α5 subunits or dihydroquinoline that has shown to exhibit agonist efficacy at α2 subunits, but lacks affinity for α1-containing receptors (Johnstone et al., 2004; Rudolph & Möhler, 2006). L-655,708 is a memory enhancing drug preferentially binding to the α5 subunit (Navarro et al., 2002; Rudolph & Möhler, 2006; Whiting, 2006).

$GABA_A$ receptors are also targeted by volatile and intravenous anaesthetics, which exhibit three different modes of action on the receptors: (1) allosteric receptor activation at low concentrations, (2) at higher concentrations they directly activate receptors in the absence of

GABA and (3) at very high concentrations they block the chloride channel (Thompson et al., 1996). A number of studies have demonstrated the importance of β subunit isoforms for the action of certain anaesthetics, such as etomidate (Harris et al., 1995; Sanna et al., 1995, 1997). Etomidate produces modulatory actions on recombinant receptors containing any of the β subunits, but has been shown to be less potent on β1-containing receptors compared to β2- and β3-containing receptors (Hill-Venning et al., 1997; Sanna et al., 1997). The direct action of etomidate, in contrast, is dependent on the presence of β2 and/or β3 subunits, since receptors containing the β1 subunit did not show GABA-mimetic actions (Belelli et al., 1996; Hill-Venning et al., 1997; Pistis et al., 1997; Sanna et al., 1997). These findings have led to the suggestion that the modulatory and GABA-mimetic actions of etomidate are mediated via distinct binding sites on the $GABA_A$ receptor.

Similar studies as described above using genetically engineered mice have shown that the different actions of anaesthetics are also mediated by different $GABA_A$ receptor subtypes. Point mutations of residue N265 in β2 (N265S) and β3 (N265M) subunits were introduced in mice. The effects of etomidate in these mice were compared to the effects seen in wild type mice (Jurd et al., 2003; Reynolds et al., 2003). Missing or reduced behavioural pattern in mutant mice was suggested to be mediated by the mutated subunit. Via this means it was demonstrated that the β3 subunit mediates the immobilising as well as in part the hypnotic effect of etomidate. The β2 subunit was found to also mediate the hypnotic action of etomidate (Figure 1.3).

Neurosteroids are the only endogenously synthesised $GABA_A$ receptor modulators. They interact with many different receptor subtypes and lack specificity, although several reports suggested a more potent action on extrasynaptic δ-containing receptors (Belelli et al., 2002; Wohlfarth et al., 2002; Mitchell et al., 2008). It was proposed that neurosteroids mediate their action via two different binding pockets (Belelli & Lambert, 2005; D'Hulst et al., 2009; Olsen & Sieghart, 2009), since they enhance GABA-mediated effects at low concentrations whereas at higher concentrations they directly activate $GABA_A$ receptors. The binding site for the former action has recently been shown to consist of highly conserved amino acid residues in the TM domains of α subunits, whereas the site for direct receptor activation is

located in the interface between α and β subunits (Hosie et al., 2007, 2009).

As described before, there are various further drug binding sites located at the $GABA_A$ receptor (for a detailed review see Korpi et al., 2002) and the examples described illustrate the complexity of allosteric ligand binding on $GABA_A$ receptor subtypes. They also indicate the great potential of $GABA_A$ receptors for future drug development, especially in terms of subtype selective compounds. Currently, most drugs in use are not subtype selective, but act on multiple subunits/receptor subtypes. Consequences are frequent appearance of adverse side effects. Hence, new subtype-selective compounds are needed.

1.2.5 Minor $GABA_A$ receptors

As mentioned above, most $GABA_A$ receptors comprise of α, β and γ subunits. However, in certain areas of the brain receptors containing minor subunits are expressed and may play important roles. ε, θ and π subunits were the last identified $GABA_A$ receptor subunits. They were discovered by searching DNA databases (Davies et al., 1997; Hedblom & Kirkness, 1997; Whiting et al., 1997; Bonnert et al., 1999). All three have been assigned into their own subunit classes, due to the relative low sequence similarities with members of other subunit classes. ε and θ subunits are closest to γ and β subunits (Section 1.2.1), whereas the π subunit shows closest homology to β (37 % identity), δ (35 % identity) and ρ (33 % identity) subunits (Hedblom & Kirkness, 1997).

Little is known about properties and functions of these subunits and their roles *in vivo* are still not known. It seems as if there has been a lack of interest in investigating these subunits, since only a relatively small number of studies have been performed, compared to other $GABA_A$ receptor subtypes. This may be partly, due to the fact that receptor subtypes containing ε, θ or π subunits are insensitive to benzodiazepine-type drugs and no subunit-specific pharmacologies could yet be established. Furthermore, their expression patterns are restricted to few brain areas or, in case of the π subunit, are mainly expressed in peripheral tissues and barely in the brain (Hedblom & Kirkness, 1997). However, these subunits may have important functions in some areas of the brain.

1.2.5.1 The $GABA_A$ receptor ε subunit

The ε subunit was first described in 1997 by Davies et al., Garret et al. and Whiting et al.. It was detected in several peripheral tissues, such as heart, liver, testis and placenta, as well as in the mammalian brain, where its expression pattern is restricted to specific areas (Whiting et al., 1997; Erlitzki et al., 2000; Davies et al., 2002). *In situ* hybridisation and Northern blot analyses in primates and rodents have revealed distinct ε subunit expression in several areas of the forebrain, such as basal ganglia, thalamus, hypothalamus and amygdala as well as in the locus coeruleus (LC; Whiting et al., 1997; Moragues et al., 2000; Sinkkonen et al., 2000; Sieghart & Sperk, 2002). ε subunit gene expression has also been demonstrated in all forebrain and a few hindbrain cholinergic cell groups; many of these also contain the $\alpha 3$ subunit (Moragues et al., 2002). Furthermore, the expression pattern of the ε subunit widely overlaps with that of the θ subunit in the brain, for example in hypothalamus, amygdala and LC (Bonnert et al., 1999; Sieghart & Sperk, 2002). The θ subunit also exhibits a restricted expression pattern in the brain. It is noteworthy that both subunit genes as well as the one encoding the $\alpha 3$ subunit are clustered together on chromosome Xq28 in the human genome (see Section 1.2.2; Wilke et al., 1997). Therefore, it is likely that the three subunits alone or containing a further subunit form functional receptor channels in some areas of the brain, for example in the LC or other areas in the forebrain, where all three subunits are co-expressed (Moragues et al., 2000; Sieghart & Sperk, 2002).

Kasparov et al. (2001) proposed that neurons of the caudal nucleus of the solitary tract express ε-containing receptors. The authors investigated rat brain slices electrophysiologically as well as performed immunocytochemistry analyses, and concluded that the observed benzodiazepine insensitivity of these neurons could be due to expression of ε-subunit-containing receptors. Another area where ε-subunit-containing receptors are expressed is the LC. $GABA_A$ receptors expressed in the LC have interesting properties. It was assumed that they comprise of $\alpha 3$, θ, ε and probably $\beta 1/3$ subunits, but do not contain γ subunits (Chen et al., 1999; Belujon et al., 2009). Indeed, *in situ* hybridisation experiments in brains from 21-day old rats did not detect γ subunit expression in LC neurons. However, conflicting data were obtained when investigating benzodiazepine sensitivity in these neurons. Chen

et al. (1999) reported diazepam did not effect the GABA-induced firing rate of LC neurons using LC slice preparations. Belujon et al. (2009) performed *in vivo* extracellular and *in vitro* patch-clamp recordings in adult rats and slice preparations from juvenile rats, respectively, to investigate the effects of flunitrazepam and diazepam on LC neurons. The former had no effect, but surprisingly, diazepam at micromolar concentrations was able to potentiate GABA-induced currents *in vitro*. Functions of ε-subunit-containing receptors in these brain regions are not known yet.

The ε subunit exhibits a great level of sequence divergence across species. Furthermore, several ε subunit splice variants have been found (see also Section 3.1.2, Chapter 3; Whiting et al., 1997). Northern blot analysis revealed an incomplete ε subunit splice variant of 5.5 kilobases (kb) in several peripheral tissues, such as placenta and pancreas, and a correctly spliced messenger RNA (mRNA) of 3.5 kb in several brain areas, and, to a lesser extent, in the heart. Davies et al. (2002) showed that only the 3.5 kb version of the ε subunit mRNA results in a full length protein. Exclusively in rodents, a splice variant containing a large Pro/Glx domain that consists of 483 amino acid residues (mostly proline/glutamic acid and proline/glutamine tandem repeats) has also been recognised as well as a splice variant lacking this insertion (Moragues et al., 2000; Sinkkonen et al., 2000). Even without this large insertion at the amino-terminus, the amino acid sequence homology between the human and rodent ε subunits is only 68 %, whereas it is between 88 % and 99 % for other orthologous $GABA_A$ receptor subunits from different species.

In recombinant expression systems, the ε subunit forms functional receptor channels when co-expressed with α and β subunits (Davies et al., 1997; Whiting et al., 1997). It may, therefore, substitute for the γ or δ subunit in native receptors. However, two recent studies have examined alternative stoichiometry in ε-subunit-containing receptors (Jones & Henderson, 2007; Bollan et al., 2008). Most studies expressing recombinant ε-containing $GABA_A$ receptors used subunit ratios of 1:1:1 for α, β and ε subunits. Jones & Henderson (2007) investigated the influence of a range of transfection ratios of ε versus α and β subunits and discovered that spontaneous current density, receptor deactivation time and a shift in rectification from outward to inward changed with increased ε subunit expression. It was suggested

that, unlike in recombinant $\alpha\beta\gamma$ receptors, which exhibit a fixed stoichiometry of two α, two β and one γ subunit (Baumann et al., 2002), receptor stoichiometry may vary, depending on the amount of ε subunit expression. It was proposed that higher ε subunit abundance may create receptors containing two ε subunits, where one subunit substitutes for the γ subunit and the second for a β subunit (Figure 1.4 C).

A different attempt to solve ε-containing receptor stoichiometry was approached by Bollan et al. (2008), who used concatenated subunits. These subunit constructs, consisting of two or three different subunits, enable investigation of receptor stoichiometry and characteristics of receptors with different subunit isoforms in specific locations (Minier & Sigel, 2004). Bollan et al. (2008) proposed, upon functional expression of different concatenated subunits in *Xenopus laevis* oocytes, that the ε subunit can assemble at different positions in receptor pentamers. However, most likely it is located at position four in $\alpha1\beta2\varepsilon$ receptors (α1-β2-α1-ε-β2), substituting for the β2 subunit, or at position one in $\alpha1\beta2\gamma2\varepsilon$ receptors (ε-β2-α1-β2-γ2), substituting for the α1 subunit (Figure 1.4 A, B).

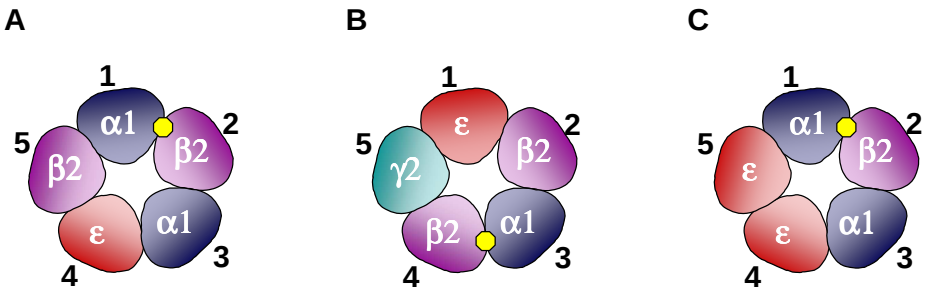

Figure 1.4: Schematic representation of possible subunit arrangement in ε-containing $GABA_A$ receptors. Subunit positions in (A) $\alpha1\beta2\varepsilon$ receptors, (B) $\alpha1\beta2\gamma2\varepsilon$ receptors (both suggested by Bollan et al., 2008) and (C) $\alpha1\beta2\varepsilon$ receptors (proposed by Jones & Henderson, 2007). Yellow circles represent the agonist GABA.

As mentioned above, subunit position in the receptor pentamer contributes to different receptor properties, for example agonist binding. The proposed ε subunit positions in $\alpha\beta\varepsilon$ or $\alpha\beta\gamma\varepsilon$ receptors as well as in receptors containing two ε subunits would all result in receptors with no benzodiazepine binding site and only one GABA binding site (Figure 1.4). The latter could explain the low Hill coefficient seen in ε-containing receptors exposed to

GABA (Whiting et al., 1997; Neelands et al., 1999; Jones et al., 2006). However, the subunit combination and stoichiometry of ε-containing $GABA_A$ receptors *in vivo* is still unknown.

The ε subunit has often been described as γ-like, due to its highest sequence similarity with γ subunits and the fact that it forms functional channels with α and β subunits in recombinant expression systems (Whiting et al., 1997; Bollan et al., 2008). Jones & Henderson (2007) demonstrated that the ε subunit exhibits β-subunit-like characteristics too, in particular β3-subunit-like. A series of experiments showed that the ε subunit is able to access the cell surface on its own as well as in conjunction with the α1 subunit, but not together with the β2 or γ2 subunit. This is also the case for β subunits. Moreover, the ε subunit possesses similar assembly domains as the β3 subunit (Jones & Henderson, 2007). This could enable the ε subunit to also assemble at a different position in the receptor complex and to replace a β subunit. However, unlike the β3 subunit, the ε subunit expressed alone or together with the α1 subunit was unable to form functional, GABA-sensitive channels at the cell surface (Jones & Henderson, 2007; Bollan et al., 2008).

ε-containing $GABA_A$ receptors possess unique pharmacological properties, for instance insensitivity to benzodiazepines (mentioned above; Davies et al., 1997; Whiting et al., 1997). This is not surprising, because benzodiazepine binding requires amino acid residues from α and γ subunits (Section 1.2.4). Several studies have been conducted to acquire the pharmacological profile of ε-containing $GABA_A$ receptors (Davies et al., 1997; Whiting et al., 1997; Thompson et al., 1998; Neelands et al., 1999; Maksay et al., 2003; Ranna et al., 2006). Results obtained examining the effect of general anaesthetic agents, such as propofol, pentobarbital or etomidate on ε-containing receptors were conflicting. Investigations in native neurons expressing ε subunits have shown reduced sensitivity to anaesthetics (Irnaten et al., 2002; Sergeeva et al., 2005). Davies et al. (1997, 2001) also reported that ε-subunit-containing receptors are insensitive to pentobarbital and propofol in heterologous expression systems. In contrast, several other studies showed that general anaesthetics potentiate the effect of submaximal GABA concentrations (Whiting et al., 1997; Thompson et al., 1998; Neelands et al., 1999). Since the level of enhancement was similar in $\alpha\beta\varepsilon$ and $\alpha\beta\gamma$ receptors, but lower compared to $\alpha\beta$ receptors, it was suggested that the inclusion of a third subunit

into the receptor complex lowers the potency of anaesthetic agents, such as pentobarbital. Thompson et al. (2002) investigated the discrepancies in sensitivity to general anaesthetics between the different *in vitro* studies described above. It was concluded that they were caused by the use of different expression vectors, which resulted in an overexpression of the ε subunit versus α and β subunits in the studies by Davies et al. (1997, 2001). Thompson et al. (2002) presumed that receptor stoichiometry varied in the different studies, which was corroborated by a study mentioned earlier by Jones & Henderson (2007). Nevertheless, all studies demonstrated direct receptor activation after applying high concentrations of the anaesthetic agents.

Recombinant ε-containing receptors are highly sensitive to GABA, but they also exhibit agonist-independent channel activity (Neelands et al., 1999; Davies et al., 2001; Maksay et al., 2003; Wagner et al., 2005). Spontaneous currents have also been seen in homomeric $\beta1$ receptors or heteromeric receptors containing the $\beta1$ and $\alpha2$ or $\gamma2$ subunits, but not in receptors containing all three subunits (Miko et al., 2004). Thus, $\alpha\beta\varepsilon$ receptors are the first receptors comprising of three different subunits that exhibit constitutive receptor activity *in vitro*. Davies et al. (2001) reported that receptors containing α, β, ε and γ subunits also exhibited spontaneous receptor activity. A possible reason for this may be that the open state of ε-containing receptors is energetically more favourable than the closed receptor form (Neelands et al., 1999; Maksay et al., 2003). Whether or not ε-containing receptors *in vivo* exhibit spontaneous activity remains unclear. *In vitro* studies by Belujon et al. (2009), Irnaten et al. (2002) and Sergeeva et al. (2005) in LC neurons, native parasympathetic cardiac neurons and hypothalamic neurons, respectively, could not detect significant spontaneous receptor activity, whereas Jones et al. (2006) described the occurrence of constitutive receptor activity in cultured ganodotrophin-releasing hormone neurons, which was comparable to that described in human embryonic kidney (HEK) 293 cells expressing $\alpha2\beta3\varepsilon$ receptors.

From numerous studies investigating the pharmacological profile of ε-subunit-containing receptors, it can be summarised that the receptors exhibit different pharmacological characteristics compared to receptors expressing α and β subunits only or $\alpha\beta\gamma$ receptors (Davies et al., 1997; Whiting et al., 1997; Thompson et al., 1998; Neelands et al., 1999; Maksay et al.,

2003; Ranna et al., 2006). However, to this date no ε-subunit-specific pharmacology could be identified. Moreover, it is not known whether ε-subunit-containing receptors are located at the synapse or extrasynaptic and subunit composition in ε-containing receptors *in vivo* as well as the function of the ε subunit remain still elusive.

1.3 Investigating ion channel properties

Ion channels are involved in a wide range of different diseases, for example epilepsy. Over recent years, pharmaceutical industries developed an enhanced interest in ion channel drug targets, due to an increased availability of chemical compounds and the advancement in the field of genomic research, providing a large amount of previously unknown drug targets. Among the 100 top selling drugs worldwide are, at present, 15 % ion channel modulators generating more than six billion dollars yearly (Gill et al., 2003). As mentioned above, $GABA_A$ receptors exhibit a wide range of structural diversity and possess a number of different modulatory binding sites that are targeted by a plethora of different drugs. In order to lessen the appearence of adverse side effects commonly implicated with current drugs on the market, new subtype-selective drugs are needed. Many methods are available to study ion channel/$GABA_A$ receptor properties, including expression studies, assays to gain structural or pharmacological insights, gene targeting, for instance knockout mice, as well as electrophysiological studies to directly assess ionic current flow (for a review see Smith & Simpson, 2003).

Although it is technically challenging to screen chloride channels for modulatory compounds, over recent years, a number of assay formats have been developed to screen for compounds that target ion channels/$GABA_A$ receptors. Important assay characteristics are sensitivity, specificity, throughput and information content, among others (Xu et al., 2001). Many of these thwart each other, as pictured in Figure 1.5. For instance, highly informative assays, such as electrophysiological methods, usually have a low throughput, whereas high throughput techniques, for example fluorescence-based techniques, lack informational content. Thus, it is important to select the right assay type for a specific project.

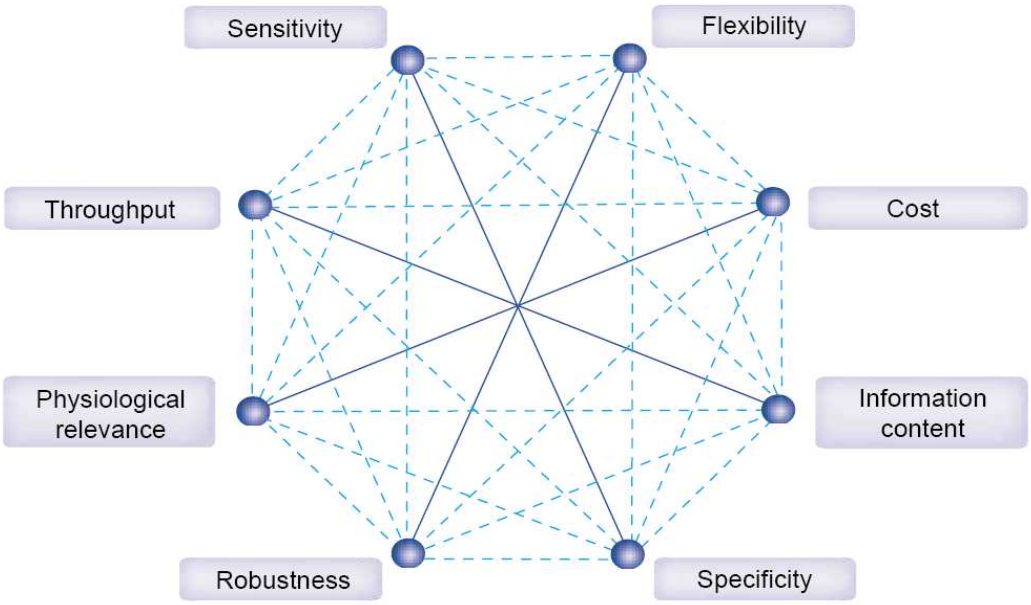

Figure 1.5: Interrelations between different attributes of ion channel assays. Solid lines mark antagonising features; dashed lines display other relationships between them (from Xu et al., 2001).

There are biochemical as well as cell-based assays to examine ion channel properties or screen for compounds. However, the latter are often the preferred method since they provide a physiologically relevant environment (An & Tolliday, 2009). Several possibilities exist to express functional channels for ion channel screening, such as primary cell culture or engineered cell lines. Relevant and frequently applied biological systems for $GABA_A$ receptor expression are, for example, mammalian cells or *Xenopus laevis* oocytes (Sections 1.3.1 and 1.3.2). As mentioned before, the choice of a suitable assay approach is a further important factor when investigating ion channels. Electrophysiological methods, like the two-electrode voltage-clamp and the patch-clamp technique (Section 1.3.3), measure ionic conductance accross the cell membrane and provide high quality and informational content when assessing ion channel function and drug-channel interactions (Xu et al., 2001). However, only a limited number of cells can be examined per experiment, because the method is technically challenging and labour intensive yielding only 10-20 data points per day. It is, therefore, used in basic research as well as for secondary or safety screenings applying a smaller number of compounds (Gonzalez & Maher, 2002). However, since the method provides high quality data, systems for automated electrophysiological recordings have been developed to improve

throughput. Nevertheless, further miniaturisation and, thus, improving throughput remains difficult, due to the complexity of the assay setup (Xu et al., 2001). Miniaturisation plays an important role in high throughput screening (HTS), since a smaller assay scale requires less reagents, hence, reducing the overall costs. Automated recording methods are implicated with high costs that limit their use in HTS.

Several alternative assay technologies with high throughput have been developed to identify ion channel modulators from large chemical compound libraries. In most cases, ion flux assays or fluorescence-based methods, such as chloride-sensitive indicator dyes, membrane potential fluorescence probes or the use of halide-sensing mutant green fluorescent proteins (GFP), are applied in preliminary, large-scale screening assays (Xu et al., 2001). Both can be set up in microtiter plate format with the possibility of measuring multiple samples at the same time (see Sections 1.3.4 and 1.3.5 and Sections 4.1.2 and 4.1.3, Chapter 4).

Many factors influence the choice of the assay system to investigate ion channel function and to screen for compounds that modulate them, which include the level of sensitivity required, assay resolution, safety issues, costs, the ability to handle low volumes and the availability of a suitable measuring device.

1.3.1 Mammalian expression systems

Heterologous expression systems, such as mammalian cell lines or *Xenopus laevis* oocytes (Section 1.3.2) are commonly used to investigate structure-function relationships of recombinant proteins (Sigel & Minier, 2005). Studying a protein in a foreign host cell rather than in its genuine environment is advantageous because of the relative 'pure' environment and the possibility of choosing the cell type for expression according to the type of experiment planned as well as practical and cost reasons.

Mammalian cell lines are a popular expression system for recombinant proteins. Plasmid vectors carrying genetic information of the gene of interest can be introduced stably or transiently into the cells which in turn translate, modify and express the desired protein (Witchel

et al., 2002). Producing stably transfected cell lines requires great initial effort and time. However, once produced they are easier and more convenient to use than transiently transfected cells. Advantages of a stable cell line are the homogeneous cell population as well as the fact that errors in protein assembly are reduced. However, if several different proteins are being investigated, it would be necessary to prepare stable cell lines for each protein of interest. In this case, it is often more practical to transiently transfect the different proteins into the cell line of choice. Mammalian expression systems benefit from the fact that numerous cells can be transfected at the same time. Also advantageous is that mammalian cell lines may resemble the physiological system in humans more than alternative expression systems and experiments can be carried out at physiological temperature (37°C; Witchel et al., 2002; Hogg et al., 2008). However, experiments using transiently transfected cells often suffer from a change in receptor expression over time as well as relatively low transfection efficiencies. For certain applications, such as electrophysiological measurements, this problem can be overcome by using a detection system for successfully transfected cells. For instance, a plasmid that expresses GFP can be simultaneously transfected with the protein of interest, highlighting transfected cells.

The HEK293 cell line is a frequently used expression system for recombinant proteins, such as ligand-gated ion channels (Thomas & Smart, 2005). HEK293 cells exhibit similarities with early differentiating neurons by expressing many mRNAs which are present in neurons, such as neurofilament proteins. The cells also contain several signalling pathways found in native neurons. Therefore, the expression of foreign neuronal proteins in HEK293 cells resembles expression in their native cell environment (Thomas & Smart, 2005). Furthermore, HEK293 cells are relatively easy and cheap to maintain, they are robust, have a quick cell division rate (between 24 to 36 hours) and a good size for electrophysiological measurements. Several different transfection techniques have been applied successfully, resulting in sufficient protein expression for many different applications, ranging from electrophysiological recordings to biochemical assays. HEK293 cells express a number of endogenous receptors (for details see Thomas & Smart, 2005), and experiments should be carefully monitored for interference of these proteins using adequate controls. Nevertheless, the expression levels

of recombinant proteins are usually high enough that endogenous proteins are outnumbered and the risk of interference is minimal.

1.3.2 *Xenopus laevis* oocytes

The oocytes of the South African clawed frog *Xenopus laevis* have been commonly used as a heterologous expression system for over 30 years (Sigel & Minier, 2005), for example for comparing the functions of wild-type and mutated ion channels or to investigate drug actions on expressed proteins. Oocytes undergo six developmental stages (I-VI), which take place asynchronous, i.e. the ovary contains oocytes of all stages (Dumont, 1972). Most electrophysiological studies are performed using oocytes from stages V and VI. Characteristic for *Xenopus* oocytes is the 'two-toned colour scheme': the animal pole containing the nucleus is dark brown whereas the vegetal pole exhibits a yellowish colouration (Figure 1.6).

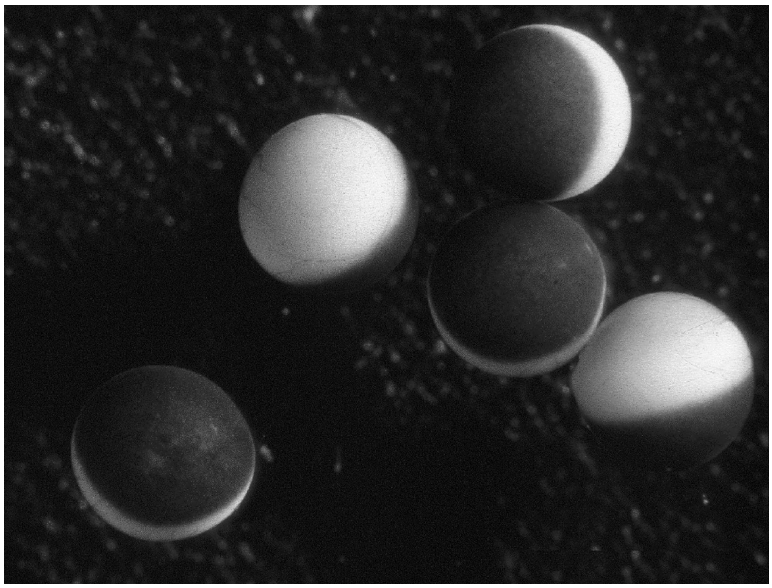

Figure 1.6: *Xenopus laevis* oocytes (from Sigel & Minier, 2005).

Oocytes are able to express foreign genetic material precisely and at high levels (Sigel, 1990; Sigel & Minier, 2005). Complementary DNA (cDNA) can be microinjected into the nucleus of an oocyte or, alternatively, RNA can be introduced into the cytoplasm (Figure 1.7). Afterwards, the nucleic acid is efficiently transcribed (in the case of cDNA injection) and transla-

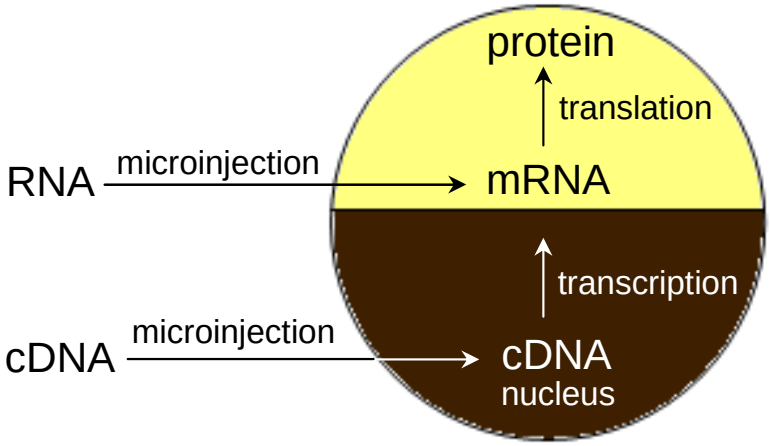

Figure 1.7: Schematic representation of the functional expression of genetic information in *Xenopus* oocytes (after Sigel, 1990).

ted by the oocyte. The resulting protein is then assembled, post-translationally modified and finally targeted to the surface membrane or an appropriate subcellular compartment.

Proteins are usually expressed within 24 hours after RNA or cDNA microinjection and oocytes can then be used for up to 14 days (Wagner et al., 2000; Sigel & Minier, 2005). RNA injection usually results in protein expression in > 98 % of the injected cells, whereas microinjection of cDNA is often successful in only a small percentage of the injected oocytes (Sigel & Minier, 2005). There are several advantages of using oocytes over mammalian cells. Oocytes are available at low cost and easy to handle in the laboratory due to their large size (1-1.2 mm in diameter) and robustness (Wagner et al., 2000; Sigel & Minier, 2005). Furthermore, the number of endogenously expressed (surface) proteins is relatively low (Dascal, 1987). The quantity of electrophysiological data which can be obtained from a single oocyte is relatively high; the robust setup permits recording for more than an hour (Witchel et al., 2002). However, there are a number of limitations to the use of oocytes: (1) each oocyte needs to be injected separately, (2) oocytes are less suitable for studying very fast cellular events, due to their large size and associated slow fluid exchange rate and slow changes in membrane potential, (3) the intracellular ionic composition cannot be influenced, (4) compounds can be absorbed by the egg yolk, which may result in lower sensitivity, (5) oocytes show seasonal differences in expression and quality and (6) frogs are poikilothermic ani-

mals. For that reason, experiments need to be carried out at room temperature rather than at physiological temperature of 37°C (Wagner et al., 2000; Xu et al., 2001; Sigel & Minier, 2005; Hogg et al., 2008). This may hamper certain applications, for instance kinetic studies. Moreover, findings should be evaluated carefully, since there may be variations between the expression in oocytes and the native tissue, as a result of different signalling pathways.

1.3.3 Electrophysiological techniques

Electrophysiological techniques measure differences in current carried by ions accross a cell membrane of a whole cell or a membrane patch (Xu et al., 2001). The two-electrode voltage-clamp technique is often used to study ion channel properties in large cells, such as *Xenopus laevis* oocytes. The technique measures whole-cell currents by impaling two glass microelectrodes into an oocyte; one electrode acts as a current-delivering electrode (i), which clamps the membrane potential to a desired voltage, and the other measures the membrane potential (V; see Figure 1.8). The measured membrane potential is compared with the command voltage (delivered by the current delivering electrode) and the difference is set to zero by the amplifier. Thus, it is possible to measure ionic current flow across the membrane (deviation from the baseline current) mediated by either ion channels or transporters (see also Section 1.3.2; Baumgartner et al., 1999; Wagner et al., 2000).

The patch-clamp method is the 'gold standard' for measuring ion channel functions, providing high quality and physiologically relevant data. It is a highly flexible technique with different configurations, such as whole-cell recording, inside-out and outside-out patches (Hamill et al., 1981). The first configuration allows the recording of ionic currents from ion channels expressed in the whole cell membrane (Figure 1.9), whereas the latter two are single channel configurations. They enable the study of individual ion channels in isolation in a small membrane patch to obtain, for example, data on channel gating and kinetics. The main difference to the two-electrode voltage-clamp technique is that a single micropipette is pressed against the membrane of a cell forming an electrical "giga-seal" (high resistance seal in the gigaohm range) between the membrane and the micropipette. Giga-seals enable most of the ionic currents to go into the pipette, reducing the 'leak current'; they are me-

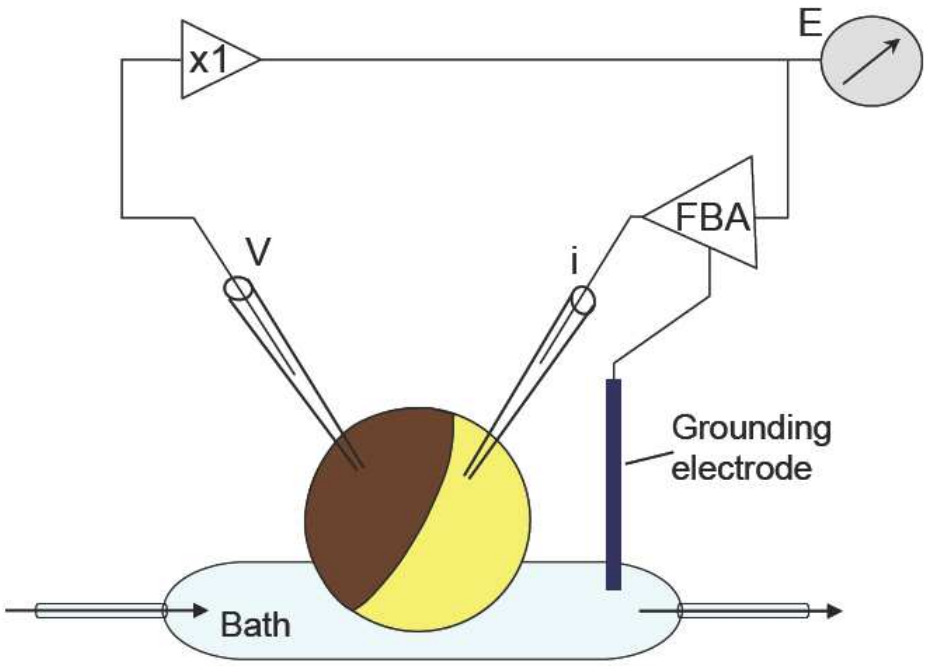

Figure 1.8: Schematic representation of the two-electrode voltage-clamp technique.
The membrane potential is measured by an electrode (V) that is linked to a voltage follower (triangle) and it is then compared with the command voltage (E; given by a generator) via the feedback amplifier (FBA). The amplified difference between the signals is delivered as a current through the current-delivering electrode (i), which clamps the membrane potential to a desired voltage and further over the cell membrane to the grounding electrode in the bath. Changes in the ion flux across the membrane can then be monitored as variation from the baseline current (adapted from Wagner et al., 2000).

chanically stable and offer a low background noise (Hamill et al., 1981). The advantages of this technique are that the intracellular environment can be controlled, due to the mixing of pipette solution and cytosol (whole-cell recording), it can be performed at physiological temperatures and fast cellular events can be studied, due to a rapid solution exchange rate and a high temporal resolution.

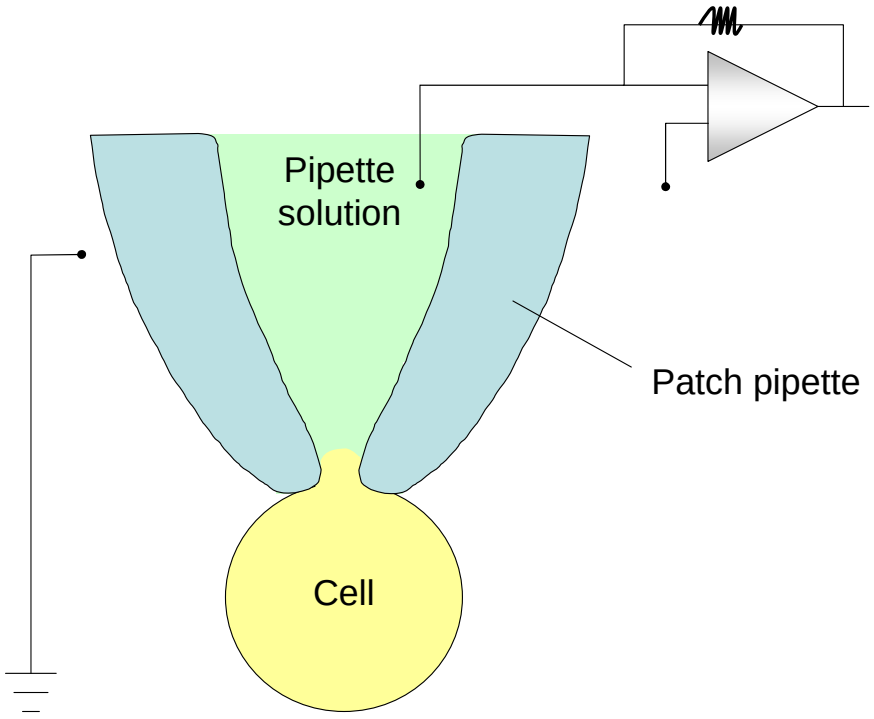

Figure 1.9: Schematic representation of the patch-clamp whole-cell configuration.
This method enables the recording of ionic currents from ion channels expressed in the whole membrane of the cell. To acquire the whole-cell configuration, a glass microelectrode is lowered onto the cell surface (cell-attached mode), slight suction is then applied to obtain a high-resistance seal between cell membrane and glass pipette. Subsequently, the membrane is ruptured and the amplifier can control and measure voltage accross the entire cell membrane (adapted from Wood et al., 2004).

1.3.4 Flux assays

Commonly used ion flux assays apply radioactive tracer ions, such as $^{36}Cl^-$ or $^{125}I^-$ which can be used to measure ion influx or efflux through ion channels, thereby measuring ion channel activity directly (Smith & Simpson, 2003; Terstappen, 2005; Verkman & Galietta, 2009). The throughput of these assays is considerably higher than with electrophysiological recordings, since assays are usually performed in 96- or 384-well plates, however, it is lower compared to fluorescence-based methods. Radioactive flux assays are easy to perform, reliable

and robust and exhibit high sensitivity. Nevertheless, slow temporal resolution, reduced reproducibility, difficulties of further assay miniaturisation and low informational content as well as high costs and safety issues are major drawbacks (Gill et al., 2003). Tang & Wildey (2004) recently presented a non-radioactive flux assay using iodide as an indicator of chloride channel activity (Section 4.1.2, Chapter 4). The advantages of this assay setup are lower costs and increased safety. However, sample mixtures and buffers of the assay are relatively unstable and fast reading is required, which may limit its use in HTS. Furthermore, flux assays suffer from long incubation times needed to load the cells with tracer molecules and require high levels of ion channel expression to lower the signal-to-noise ratio (Xu et al., 2001).

1.3.5 Fluorescence-based assays

Fluorescence-based methods are ideally suited for assay miniaturisation, because they are volume-independent. There are several different fluorescence-based methods to screen for ion channel modulators, for instance chloride indicator dyes or membrane potential-sensing dyes (Gill et al., 2003; Molokanova & Savchenko, 2008; Verkman & Galietta, 2009). Assays applying membrane permeable, quinoline-derived chloride indicator dyes, such as MQAE, are easy to set up and exhibit relatively high chloride sensitivity (Marandi et al., 2002). However, they suffer from high background noise, leakage from the cells and the low half-life of the fluorescence dye (Gill et al., 2003; Verkman & Galietta, 2009). Another method is to measure changes in intracellular pH, using proton-sensitive dyes and a fluorometric imaging plate reader (FLIPR; Gill et al., 2003; Verkman & Galietta, 2009). Voltage-sensing Förster (or Fluorescence) Resonance Energy Transfer (FRET)-based, ratiometric dyes are also commonly used for ion channel screening. FRET is the transfer of energy from an excited fluorophore (donor) to another fluorescent molecule (acceptor), which is dependent on the distance between them (Piston & Kremers, 2007). These dyes are lipophilic molecules and can be easily introduced into the cell membrane. Changes in membrane potential can then be measured with fast resolution using a voltage/ion probe reader; it is also possible to quantify membrane potential changes. A wide range of different dyes is available to measure

changes in membrane potential. They differ in chloride sensitivity, response kinetics and sensing mechanisms (Verkman & Galietta, 2009). The main drawback of these dyes is that the membrane potential can be influenced by many different factors, such as cytoplasmic composition or activity of other ion channels or transporters in the membrane rather than only the channel of interest. The latter leads to a high rate of false positive readings which is further increased by test compounds exhibiting autofluorescence. Furthermore, such systems are more suitable for stably transfected cell lines, since the dye molecules are present in every cell's membrane. False negative results can also be obtained due to the high background noise masking weaker signals.

There are also assay technologies using halide-sensing mutant GFPs, such as Clomeleon. Clomeleon is a ratiometric, FRET-based and genetically-encoded chloride-ion indicator protein. It was developed by Kuner & Augustine (2000) and consists of a chloride-sensitive yellow fluorescence protein (YFP) linked to a chloride-insensitive cyan fluorescence protein (CFP) and can be targeted to specific cellular compartments (see Section 4.1.1, Chapter 4). Compared to chloride-sensitive indicator dyes, such as MQAE, Clomeleon exhibits slower kinetics and its chloride sensitivity is relatively low. YFP mutants with higher chloride sensitivity have, therefore, been developed, such as YFP-H148Q/I152L (Section 4.1.3, Chapter 4; Galietta et al., 2001a; Verkman & Galietta, 2009). Although fluorescence membrane potential-sensing dyes and YFP mutant proteins both have similar signal-to-noise ratios and dynamic ranges, there are several advantages of YFP-based assays: they are faster, less expensive, YFP is genetically encoded and cannot leak out of the cells and the assay does not require ion channel expression in a stable cell line, but can also be used in transiently transfected cells, which is advantageous when investigating several of the various $GABA_A$ receptor subtypes (Kruger et al., 2005).

1.4 Aims and objectives of the study

As mentioned in Section 1.2.5.1, expression of the $GABA_A$ receptor ε subunit is relatively restricted in the mammalian brain; it is mainly expressed in the forebrain as well as in all

major neuronal groups, including cholinergic cells (Moragues et al., 2000, 2002). 84-95 % of cholinergic neurons also express the $\alpha 3$ subunit (Gao et al., 1995). Due to the co-expression of $\alpha 3$ and ε subunits in cholinergic neurons, it was hypothesised that the subunits form functional channels in these neurons, which may regulate ACh release (McGehee & Role, 1996; Cervetto & Taccola, 2008). The $\alpha 3$- and ε-subunit-containing receptor subtype is, therefore, a potential target for the development of anti-AD drugs that would function by increasing ACh release in forebrain regions where cholinergic neurons are dying.

The initial aim of this project was to functionally express and pharmacologically characterise the $GABA_A$ receptor subtype that contains the $\alpha 3$ and ε subunits applying an electrophysiological approach. It was shown in several studies, that the β subunit has no significant effect on the benzodiazepine modulation of the $GABA_A$ receptor (Pritchett et al., 1989b; Hadingham et al., 1993). Therefore, the $\alpha 3$ and ε subunits were co-expressed with the rat $\beta 2$ subunit, a subunit combination that has not been pharmacologically characterised before. However, it is likely that receptor subtypes of this combination exist in the brain, since the $\beta 2$ subunit is the most widely expressed β subunit in the brain. At first, it was planned to establish the patch-clamp method at Nottingham Trent University using HEK293 cells transiently transfected with rat cDNAs encoding the respective $GABA_A$ receptor subunits. This would have also provided information about correct assembly of the subunits in HEK293 cells, important for the subsequent cell-based screening assay setup (see below). However, problems with the setup of the electrophysiological rig at Nottingham Trent University caused a slight change in the project and electrophysiological recordings were performed in *Xenopus laevis* oocytes microinjected with complementary RNA (cRNA) in the laboratory of Dr Ian Mellor at the University of Nottingham instead.

After the pharmacological characterisation of the $\alpha 3\beta 2\varepsilon$ receptor, the aim was to establish a cell-based screening system using HEK293 cells and search for compounds that modulate the activity of this $GABA_A$ receptor subtype. It is generally accepted that modulation of the agonist binding site of ligand-gated ion channels is not a productive avenue for drug discovery. Therefore, as part of the project, search was narrowed down to compounds that bind elsewhere on this multi-subunit receptor complex. Whiting (1999) suggested the existence

of a new modulatory site on ε-containing receptors, since steroids, barbiturates and anaesthetics have no significant influence on these receptors. Since $GABA_A$ receptor subunits exhibit strong sequence similarity to one another (Section 1.2.2), it was hoped to identify a site between the $\alpha 3$ and ε subunits that is analogous to the benzodiazepine binding site that is found at the interface between α and γ subunits. For this purpose, a search for lead compounds from a chemical compound library that, in the presence of GABA, modulate receptor activity was conducted. Such compounds could not only serve as potential future drugs on ε-containing receptor subtypes, but may also help providing important information to uncover the role of the ε subunit in future studies.

Chapter 2

Materials and Methods

2.1 General molecular biology techniques

2.1.1 Preparation of competent *Escherichia coli (E. coli)* cells

100 µl already competent *E. coli* XL1 blue cells were added to 5 ml lysogeny broth (LB) medium (10 g/l peptone from casein, 5 g/l yeast extract, 10 g/l sodium chloride, Miller), supplemented with tetracycline (25 µg/ml) and incubated overnight in an orbital shaking incubator (S150, Stuart) at 37°C and 200 rpm. On the next day, 2 ml of the overnight culture was added to 100 ml LB medium supplemented with tetracycline (25 µg/ml) and incubated further at 37°C and 200 rpm for several hours, measuring the optical density (OD) of the culture at regular intervals at a wavelength of 660 nm until an OD660 of 0.4 to 0.5 was reached. The inoculated LB medium was then split and transferred to two 50 ml tubes (Sartstedt) and centrifuged 3,000 rpm for 15 minutes (Beckman Coulter) at room temperature (18-25°C). Supernatants were discarded subsequently and the bacterial cell pellets resuspended in 20 ml cold, sterile-filtered TFB1 buffer (30 mM KAc, 50 mM $MnCl_2$, 100 mM KCl, 10 mM $CaCl_2$ and 15 % (v/v) glycerol; pH 5.8) each by briefly vortexing the tubes. Next, the bacteria were incubated on ice for 30 minutes, followed by centrifugation at 1,750 rpm for 20 minutes at 4°C. Supernatants were discarded and bacterial cell pellets carefully resuspended in 2 ml ice-cold TFB2 buffer (10 mM MOPS buffer, 76 mM $CaCl_2$, 10 mM KCl and 15 % (v/v) glycerol). Finally, the competent *E. coli* Xl1 blue cells were aliquotted into microfuge tubes

and stored at -80°C until usage.

2.1.2 Transformation of plasmid DNA into competent *E. coli* cells

1 to 5 µg plasmid DNA was added to 50 µl competent *E. coli* Xl1 blue cells and incubated on ice for 30 minutes. The cells were then heat-shocked by incubating them at 42°C for 50 seconds and subsequently cooled on ice for another two minutes. 100 µl SOC medium (20 g/l 2 % (w/v) Bacto tryptone, 0.5 % (w/v) Bacto yeast extract, 10 mM NaCl, 10 mM KCl, 20 mM $MgCl_2$, 20 mM glucose) was added followed by incubation at 37°C, 200 rpm for 45 minutes. Transformed bacteria were cultured on LB agar plates (10 g/l peptone from casein, 5 g/l yeast extract, 10 g/l NaCl, 12 g/l agar-agar, Miller) containing 0.1 % (w/v) ampicillin overnight at 37°C.

2.1.3 Plasmid preparation

2.1.3.1 Minipreparation

Plasmid DNA transformed into *E. coli* cells was isolated by selecting single colonies from a LB agar plate using a sterile pipette tip. 2 ml LB medium supplemented with 0.1 % (w/v) ampicillin were inoculated with a single bacterial colony and incubated overnight at 37°C, 200 rpm. On the following day, the plasmid DNA was purified from the overnight cultures using a GenElute™ Plasmid Miniprep Kit (Sigma) or QIAprep Spin Miniprep Kit (Qiagen) following the manufacturer's protocols. Isolated plasmid DNA was finally eluted in 50 µl 0.1 % (v/v) diethylpyrocarbonate (DEPC)-treated water and stored at -20°C.

2.1.3.2 Maxipreparation

In order to generate multiple copies of plasmid DNA, single bacterial colonies containing the desired plasmid were transferred into 5 ml LB medium supplemented with 0.1 % (w/v) ampicillin and incubated for 8 hours at 37°C, 200 rpm. Next, 2 to 3 ml of the bacterial culture was transferred to 100 ml LB medium (containing 0.1 % (w/v) ampicillin) and incubated overnight at 37°C, 200 rpm. On the following day the plasmid DNA was isolated using a

Plasmid Maxi Kit (Qiagen) following the manufacturer's instructions. The purified DNA was resuspended in 200 µl 0.1 % (v/v) DEPC-treated water and stored at -20°C for further use.

2.1.4 Restriction endonuclease digestion

Purified plasmid DNAs and polymerase chain reaction (PCR) products were digested using one or two (depending on further applications) restriction enzymes (Promega). First, enough 0.1 % (v/v) DEPC-treated water was added into 0.5 ml microcentrifuge tubes to make up a final volume of 10 or 20 µl. Reactions were then further assembled by adding the respective 10 x buffer, 0.2 to 1.5 µg DNA and respective restriction endonuclease, using a tenfold excess of enzyme over DNA (see Section 2.2.3 for details). After incubating the mixtures for 1 to 2 hours at 37°C, the digested as well as corresponding undigested plasmid DNAs were analysed by gel electrophoresis on a 1 % (w/v) agarose gel, containing ethidium bromide (10 mg/ml), in 1 × tris-acetate (TAE)-buffer (40 mM Trizma Base, 1.14 % (v/v) Glacial acetic acid, 1 mM disodium EDTA (pH 8)) and visualised by UV trans illumination (InGenius or G:Box, Syngene).

2.1.5 Measuring nucleic acid concentrations

Nucleic acids were diluted and concentrations were measured using a UV spectrophotometer (DU530 or DU800, Beckman). Based on the absorbance (A) at 260 nm the concentrations were calculated as shown below:

$$\text{concentration [ng/µl]} = A_{260} \times \text{dilution factor} \times \text{conversion factor} \tag{2.1}$$

The conversion factors for nucleic acids are as follows (Maniatis et al., 1982):

Double-stranded DNA	:	50 ng/µl
Single-stranded DNA & RNA	:	40 ng/µl
Single-stranded oligonucleotides	:	20 ng/µl

2.1.6 Ethanol precipitation

Nucleic acids were precipitated using 2.5 × volume 100 % (v/v) ethanol and 1/10 volume 3 M NaAc (pH 5.2), incubated at -20°C for at least 30 minutes and subsequently centrifuged at 13,000 rpm, 4°C for 30 minutes. Supernatants were discarded and pellets were washed with 75 % (v/v) ethanol and centrifuged again at 13,000 rpm, 4°C for five minutes. Nucleic acid pellets were briefly air-dried before resuspension in DEPC-treated water.

2.1.7 Sequencing

15-20 µl DNA at a concentration of 60-100 ng/µl were added into a 1.5 ml microfuge tube. Tubes containing DNA samples were sent to Eurofins MWG Operon (London) for sequencing. Sequencing results were aligned and compared with corresponding $GABA_A$ receptor subunit or other respective sequences in the nucleotide sequence database using a basic local alignment search tool (BLAST; URL: http://www.ncbi.nlm.nih.gov/BLAST/) and a sequence alignment tool (ClustalW; URL: http://www.justbio.com/aligner/index.php), respectively, to confirm their identity.

2.1.8 Side-directed mutagenesis - Generating a truncated ε subunit

2.1.8.1 Primer design

A truncated ε (ε_T) subunit version, lacking 26 amino acids ranging from within TM2 until TM3 compared to the full length ε subunit version (Figure 3.1, Chapter 3), was constructed using overlap PCR and cDNA encoding the rat ε subunit (in pcDNA3 vector). Two sets of sequence specific primers were designed according to the ε subunit cDNA sequence (Table 2.1).

Table 2.1: Oligonucleotide design to generate a $GABA_A$ receptor ε_T subunit

Oligonucleotide	Sequence	T_m
rGABRE-T_F1	5'-GCC AGT GTG CTG GAA TTC TG-3'	56.6°C
rGABRE-T_R1	5'-AGA AGT CCA AAG CTA CAG AGG CCC T-3'	61.6°C
rGABRE-T_F2	5'-AGG GCC TCT GTA GCT TTG GAC TTC T-3'	61.6°C
rGABRE-T_R2	5'-CTA GAT GCA TGC TCG AGC GG-3'	58.1°C

Forward and reverse primers (rGABRE-T_F1 and rGABRE-T_R2), flanking the entire ε subunit sequence, overlapped with the multiple cloning site of the ε-subunit-containing vector and contained an *Eco*RI or *Xho*I endonuclease restriction site (underlined), respectively. The introduction of restriction sites facilitated the insertion of the ε_T subunit cDNA into the pcDNA3.1+ vector after generating the correct sequence. The oligonucleotides positioned within the ε subunit sequence, rGABRE-T_R1 and rGABRE-T_F2, were flanking both sites of the mutation which was located in the middle of the primers. All four oligonucleotides had closely matched melting temperatures (T_m) for optimal amplification which were calculated using the following website: URL:http://eu.idtdna.com/analyzer/applications/oligoanalyzer/default.aspx. Figure 2.1 illustrates the different amplification steps used in order to generate the respective deletion.

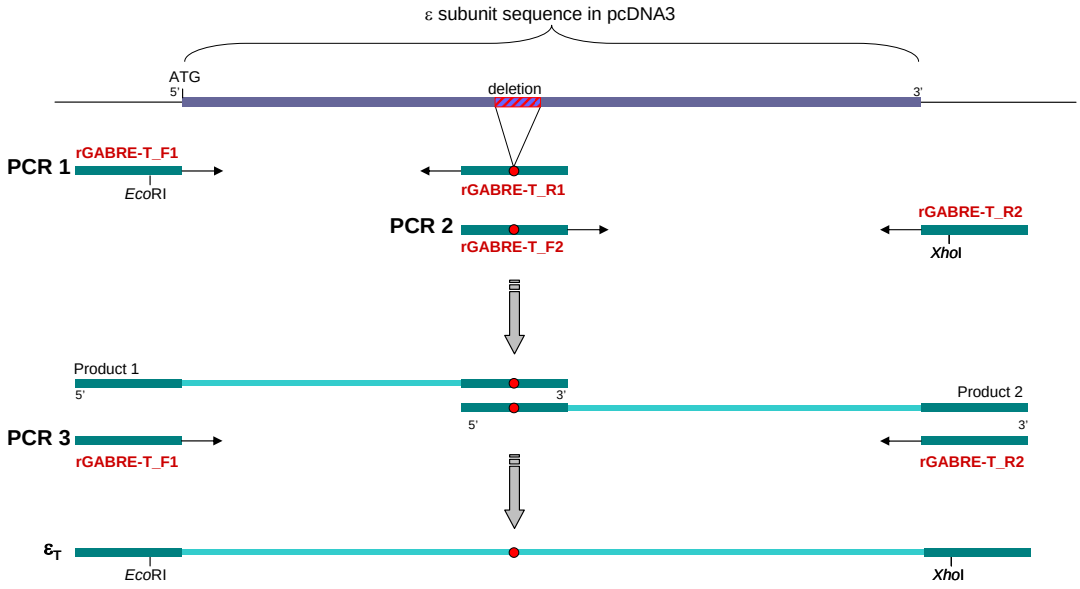

Figure 2.1: Side-directed mutagenesis using overlap PCR to create the ε_T subunit.
The forward primer rGABRE-T_F1 is located before the start codon of the ε subunit sequence and contains an EcoRI restriction site. The reverse primer rGABRE-T_R1 is spanning the sequence immediate before and after the 26 amino acid mutation, excluding the sequence which was deleted. The second primer pair consists of the reverse complement of rGABRE-T_R1 (rGABRE-T_F2) and rGABRE-T_R2. The latter is located after the stop codon of the ε subunit sequence extending into the multiple cloning site of the vector and including a XhoI restriction site. PCR products 1 and 2 were used as templates in PCR 3, using oligonucleotides rGABRE-T_F1 and rGABRE-T_R2. rGABRE-T_R1 and rGABRE-T_F2 which are comprised in PCR products 1 and 2 anneal together resulting in the amplification of the whole length ε_T subunit sequence.

2.1.8.2 Polymerase chain reaction

All PCRs were performed using *Pfu* DNA polymerase (Promega) or Phusion™ high fidelity DNA polymerase (Finnzymes). Both enzymes exhibit proofreading activity to minimise errors due to incorporation of wrong bases by the enzyme. PCR 1 and 2 (see Figure 2.1) were assembled in sterile 0.5 ml PCR tubes as follows:

Pfu DNA polymerase 10 × buffer (200 mM Tris-HCl (pH 8.8 at 25°C), 100 mM KCl, 100 mM $(NH_4)_2SO_4$, 20 mM $MgSO_4$, 1.0% Triton® X-100 and 1 mg/ml nuclease-free BSA, Promega)	5 µl
dNTP mix (10 mM each, Sigma)	1 µl
Forward primer (200 ng/µl)	1 µl
Reverse primer (200 ng/µl)	1 µl
DNA template (1 pg/µl (PCR 1) or 5 pg/µl (PCR 2))	1 µl
pfu DNA polymerase (2-3 U/µl, Promega)	1 µl
DEPC-treated water to a final volume of	50 µl

Negative controls contained water instead of the DNA template. PCRs were performed in a thermal cycler (TC-512 or TC-3000, Techne) at the following conditions:

Initial Denaturation	94°C	5 min
32 cycles		
Denaturation	94°C	1 min
Annealing	59°C	1 min
Extension	72°C	4.5 min
Final extension	72°C	10 min

PCR products were visualised on a 1% agarose gel (Section 2.1.4) and amplicons of the right size, ~960 bp (PCR 1) and ~2100 bp (PCR 2), were excised from the gel with a clean scalpel and purified using a GFX™ PCR DNA and Gel Band Purification Kit (GE Healthcare) according to the manufacturer's instructions. Purified PCR products were ethanol precipita-

ted (Section 2.1.6). The two PCR products then served as template DNA for a further PCR (PCR 3) using the forward primer of the first (rGABRE-T_F1) and the reverse primer of the second primer pair (rGABRE-T_R2) and Phusion™ high fidelity DNA polymerase (Finnzymes). The PCR was assembled as follows:

5 × Phusion® HF buffer (containing 7.5 mM $MgCl_2$)	10 µl
10 mM dNTPs (200 µM each, Sigma)	1 µl
Forward primer (200 ng/µl)	1 µl
Reverse primer (200 ng/µl)	1 µl
purified PCR product 1 (1 in 10 dilution)	1 µl
purified PCR product 2 (undiluted)	0.5 µl
DMSO (100 %)	1 µl
Phusion® DNA Polymerase (2 U/µl)	0.5 µl
DEPC-treated water to a final volume of	50 µl

Negative controls contained water instead of purified PCR products. The PCR was carried out in a Techne TC-3000 thermal cycler at the following conditions:

Initial Denaturation	98°C	30 sec
35 cycles		
Denaturation	98°C	10 sec
Annealing	64°C	30 sec
Extension	72°C	1.5 min
Final extension	72°C	10 min

The resulting product was visualised on a 1% agarose gel. The amplicon of the right size (~3000 bp) was excised from the gel, purified and ethanol precipitated (see above).

2.1.8.3 Ligation of the ε_T subunit cDNA into the pcDNA3+ vector

The purified ε_T subunit cDNA (PCR product 3) was digested in a 0.5 ml microfuge tube as follows:

Purified PCR product 3	14.5 µl
pcDNA3.1+ vector (20 ng/µl)	1.5 µl
10 × buffer H (0.9 M Tris-HCl, 100 mM $MgCl_2$, 0.5 M NaCl, pH 7.5, Promega)	2 µl
*Eco*RI (12 U/µl, Promega)	1 µl
*Xho*I (10 U/µl, Promega)	1 µl
DEPC-treated water to a final volume of	20 µl

The sample was incubated for 2 hours at 37°C before it was again ethanol precipitated to purify the DNA (Section 2.1.6). Afterwards, the digested PCR product was ligated into the linearised pcDNA3.1+ vector in a final volume of 10 µl, by adding 1 µl T4 DNA ligase (1-3 U/µl, Promega) and 1 µl 10 × reaction buffer (300 mM Tris-HCl (pH 7.8 at 25°C), 100 mM $MgCl_2$, 100 mM DTT and 10 mM ATP, Promega) and incubating it at 4°C overnight. On the following day, the ligated product (10 µl) was transformed into 50 µl competent *E. coli* cells (Section 2.1.2). Bacterial colonies, containing plasmid DNA, were cultured overnight and subsequently purified using GenElute™ Plasmid Miniprep Kit (Section 2.1.3). 0.5 µl of purified plasmid DNA was digested using *Eco*RI and *Xho*I in a final volume of 20 µl as described above and subsequently visualised on a 1% agarose gel in order to display the insertion of the ε_T subunit DNA into the vector. Samples, which contained an insert, were sent for DNA sequencing (Section 2.1.7) to confirm their correct identity and orientation in the pcDNA3.1+ vector.

2.2 $GABA_A$ receptor subunits & fluorescence proteins

2.2.1 Recovery of vectors harbouring $GABA_A$ receptor subunits

Rat $GABA_A$ receptor $\alpha 3$, $\beta 2$, $\gamma 2L$ and ε subunit cDNAs were kindly provided by Prof. Erwin Sigel (Institute of Biochemistry and Molecular Medicine, University of Bern, Switzerland) and Dr Maurice Garret (Laboratoire de Neurophysiologie, Bordeaux, France). The $\alpha 3$ subunit cDNA was subcloned into the pcDNA3.1+ vector (Invitrogen), the $\beta 2$ and $\gamma 2L$ subunit cDNAs were in the pCMV vector and the ε subunit cDNA was present in the pcDNA3 vector (Invitrogen; see Appendix A for vector maps). Plasmids that harboured the $\alpha 3$, $\beta 2$ and $\gamma 2L$ cDNAs were recovered from filter paper by cutting out the area on the paper, where the DNA was placed, with sterile scissors and transferring the paper to sterile 1.5 ml microfuge tubes. Next, 50 µl 10 mM Tris-HCl (pH 7.6) was added to the tubes; they were vortexed, incubated at room temperature (18-25°C) for 5 minutes and briefly centrifuged for 30 seconds. The supernatants containing the plasmid DNAs were transferred into fresh tubes and stored at -20°C for further use. The ε-subunit-containing vector was obtained as aqueous stock solution (0.2 mg/ml) and stored at -20°C. The human $GABA_A$ receptor $\alpha 1$ subunit was present in the pBS vector (Stratagene) and stored in ethanol at -20°C.

2.2.2 Recovery of pRK5-Clomeleon and pEYFP H148Q/I152L vectors

The pRK5-Clomeleon plasmid was generously provided by Dr Thomas Kuner (Institute of Anatomy and Cell Biology, Heidelberg University, Germany) and recovered from filter paper as described above (Section 2.2.1), but instead of Tris-HCl, 50 µl 0.1 % (v/v) DEPC-treated water was added to the filter paper in the microfuge tube. This was vortexed, incubated at room temperature (18-25°C) for 5 minutes and briefly centrifuged for 30 seconds. The supernatant, containing the plasmid DNA, was transferred to a fresh tube and stored at -20°C until further use.

A pcDNA3.1+ vector containing the coding sequence for the pEYFP H148Q/I152L mutant protein was kindly supplied by Prof. Alan Verkman (Department of Medicine, University of California, San Francisco, USA). The vector was obtained as aqueous stock solutions

(0.2 mg/ml) and stored at -20°C.

2.2.3 Examination of received vectors

Before the cDNAs described above (Sections 2.2.1 & 2.2.2) could be used in experiments, their sequence identity was analysed. On this account, the plasmid vectors were transformed into competent *E. coli* Xl1 blue cells and subsequently purified and, in case of the $GABA_A$ receptor subunits, digested using restriction endonucleases (Promega) listed in Table 2.2 (Sections 2.1.2 to 2.1.4). After digesting the plasmid cDNAs, they were visualised on a 1% agarose gel (Section 2.1.4) to verify the presence of $GABA_A$ receptor subunit cDNA in the vector. Finally, $GABA_A$ receptor subunit as well as pEYFP H148Q/I152L cDNAs and the pRK5-Clomeleon plasmid were sent for sequencing (Section 2.1.7).

Table 2.2: Restriction enzymes used to digest different $GABA_A$ receptor cDNAs

	Enzymes	10 × buffer (buffer composition)
$\alpha 3$	*Hind*III, *Xba*I	Buffer B (60 mM Tris-HCl, 60 mM $MgCl_2$, 0.5 M NaCl, 10 mM DTT, pH 7.5)
$\beta 2$	*Eco*RI, *Xba*I	Buffer H (0.9 M Tris-HCl, 100 mM $MgCl_2$, 0.5 M NaCl, pH 7.5)
$\gamma 2$L	*Eco*RI, *Xba*I	Buffer H
ε	*Eco*RI, *Xba*I	Buffer H
$\alpha 1$	*Hind*III, *Eco*RI	Buffer E (60 mM Tris-HCl, 60 mM $MgCl_2$, 1 M NaCl, 10 mM DTT, pH 7.5)

2.2.4 Subcloning

The sequencing results revealed that the $\alpha 3$ subunit cDNA was present in the wrong orientation in the pcDNA3.1+ vector and had to be reversed. The $\alpha 1$ subunit cDNA was present in the pBS vector and needed to be re-cloned into a mammalian expression vector (pcDNA3.1+) in order to express the subunit in mammalian cells in later experiments. Furthermore, for the purpose of cRNA synthesis using T7 RNA polymerase (Section 2.3.1), the $\beta 2$ and $\gamma 2$L subunit cDNAs were sub-cloned into the pcDNA3.1+ vector. Plasmids containing the $GABA_A$ receptor subunit cDNAs were digested using restriction endonucleases as described before (Sections 2.1.4 and 2.2.3).

In case of the $\alpha 3$ subunit, the plasmid was digested using *Eco*RI restriction endonuclease

only (this is where the subunit cDNA was cloned originally into the multiple cloning site of the vector). Next, the digested vector was ethanol precipitated (Section 2.1.6) and the DNA pellet was resuspended in 8 µl 0.1 % (v/v) DEPC-treated water. Afterwards, vector and subunit cDNA were religated using 1 µl T4 DNA ligase (1-3 U/µl; Promega) with 1 µl 10 × reaction buffer (300 mM Tris-HCl (pH 7.8 at 25°C), 100 mM $MgCl_2$, 100 mM DTT and 10 mM ATP) at 4°C overnight.

The pBS vector containing the α1 subunit was digested using *Hind*III and *Eco*RI restriction endonucleases. The β2 and γ2L subunit cDNAs were digested using *Eco*RI and *Xba*I restriction endonucleases. 30 ng pcDNA3.1+ vector was digested for each subunit cDNA using the respective restriction enzymes in a separate microfuge tube (Sections 2.1.4 and 2.2.3). Digested plasmids containing the subunit cDNAs were run on a 2 % (w/v) agarose gel and visualised by UV trans illumination (Section 2.1.4). Bands corresponding to α1, β2 and γ2L subunit cDNAs were excised from the gels with a clean scalpel and purified using a GFX™ PCR DNA and Gel Band Purification Kit (GE Healthcare; Section 2.1.8.2). Purified subunit cDNAs as well as digested pcDNA3.1+ vector DNA were ethanol precipitated and subsequently ligated using T4 DNA ligase (see above).

Ligation products were transformed into competent *E. coli* XL1 blue cells, amplified and then isolated from the bacterial cultures. Subsequently, purified plasmid DNA was digested and visualised on a 2 % (w/v) agarose gel. Plasmid DNAs containing an insert of the correct size were sent for sequencing to confirm their identity and correct orientation in the vectors (Sections 2.1.2 to 2.1.7).

2.3 Electrophysiological recordings in *Xenopus* oocytes

2.3.1 Making cRNA from cDNA

cRNA was made from cDNA using a T7 mMessage mMachine® Kit (Ambion) according to the manufacturer's protocol. $GABA_A$ receptor subunit cDNAs were present in the pcDNA3.1+ (α3, α1, β2, γ2L and ε_T) or the pcDNA3 vector (ε); these vectors contain a

promoter sequence for T7 RNA polymerase. At first, the plasmid DNA was linearised by cutting it after the end of the $GABA_A$ receptor subunit sequence. For this, 5 µg plasmid DNA, containing the different $GABA_A$ receptor subunit cDNAs, respectively, was digested using *Xba*I restriction endonuclease (8-12 U/µl, Promega) and 10 × buffer D (10 mM Tris-HCl (pH 7.4), 300 mM NaCl, 0.1 mM EDTA, 1 mM DTT, 0.5 mg/ml BSA, 50 % glycerol) in a total volume of 40 µl (Section 2.1.4). 2 µl of each linearised product was visualised on a 1.5 % (w/v) agarose gel to confirm the completion of the digest, which was then terminated by adding 1/20 volume 0.5 M EDTA (pH 8), 1/10 volume 3 M NaAc (pH 5.2) and 2 × volume 100 % (v/v) ethanol and incubated at -20°C for 30 minutes. Next, plasmid DNAs were centrifuged for 15 minutes at 13,000 rpm and 4°C. Supernatants were removed and DNA pellets resuspended in 0.1 % (v/v) DEPC-treated water to yield a final concentration of 0.5 µg/µl. Capped cRNA was transcribed *in vitro* using the T7 mMessage mMachine® Kit. The transcription reaction was set up at room temperature (18-25°C) in the following order and with a final volume of 20 µl:

Nuclease-free water	4 µl
2 × NTP/CAP (15 mM of each ATP, CTP, UTP, 3 mM GTP, 12 mM cap analog)	10 µl
10 × reaction buffer	2 µl
linearised cDNA template (0.5 µg/µl)	2 µl
T7 enzyme mix	2 µl

The mixture was incubated at 37°C for 70 minutes. Subsequently, 1 µl TURBO DNase (2 U/µl) was added to each sample, which was incubated at 37°C for a further 15 minutes. The resulting cRNA was recovered by performing a lithium chloride precipitation. 30 µl nuclease-free water and 30 µl lithium chloride precipitation solution (7.5 M lithium chloride, 50 mM EDTA) were added to the cRNA and precipitated at -20°C for 40 minutes. The microfuge tube was then centrifuged at 13,000 rpm, 4°C for 15 minutes and the supernatant was carefully removed. The cRNA pellet was washed with 70 % ethanol and once more centrifuged for 15 minutes before the ethanol was removed and the cRNA pellet was resuspended in an appropriate amount of nuclease-free water. Concentrations of the cRNAs were measured

using a UV spectrophotometer (DU530 or DU800, Beckman) as described in Section 2.1.5. 2 µl aliquots of cRNA samples at concentrations of 1 µg/µl or 2.5 µg/µl were stored at -80°C until needed. Remaining cRNA was stored in 2.5 × volume 100 % (v/v) ethanol at -80°C.

2.3.2 Selection of *Xenopus laevis* oocytes

All following experiments using *Xenopus laevis* oocytes were performed in the laboratory of Dr Ian Mellor (University of Nottingham). Oocytes that had been enzymatically separated and defolliculated with 2 mg/ml collagenase type 1A for 40-60 minutes were provided. Healthy, large, round stage V and VI oocytes (1 to 1.2 mm diameter and 1.2 to 1.3 mm in diameter, respectively) featuring a distinctive two-toned colour scheme (dark brown animal hemisphere and yellow vegetal hemisphere) were selected for $GABA_A$ receptor subunit cRNA expression (Figure 2.2).

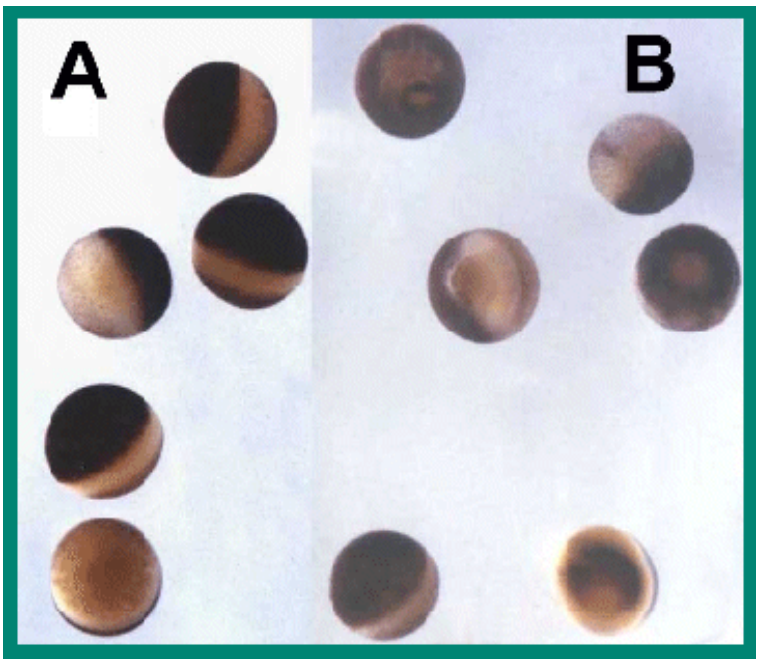

Figure 2.2: (A) Healthy and (B) impaired *Xenopus laevis* oocytes

The selection of healthy oocytes with a distinctive two-toned colour scheme and spherical or round shape is vital for an effective expression of foreign proteins (from http://www.rothamsted.ac.uk/ppi/staff/TonyMiller/plantele_xenopus.html)

2.3.3 Injection of cRNA into *Xenopus laevis* oocytes

Oocytes were injected on the same day or one day after removal from the animal. Injection pipettes were pulled from glass capillaries (No. 4878, World Precision Instruments, Inc.) in one stage using a vertical pipette puller (Model 700C, David Kopf Instruments). Pipette tips were shortened by gently tapping them against the lid of a sterile 35 mm Petri dish to a diameter of approximately 15 µm. Subsequently, the pipette was backfilled with sterile-filtered paraffin oil, using a hypodermic needle (25G) and 2 ml syringe, to seal the pipette from air. It was then mounted onto a 50 nl microinjector (A203XVB, World Precision Instruments, Inc.). The pipette was gradually filled with 4 µl cRNA mixture, containing one or more cRNAs and sterile, DEPC-treated water. Selected oocytes were lined up in a 35 mm Petri dish containing filter-sterilised modified Barth's solution (96 mM NaCl, 2 mM KCl, 1.8 mM $CaCl_2$, 1 mM $MgCl_2$, 5 mM HEPES, 2.5 mM pyruvic acid, 0.5 mM theophylline, 0.05 mg/ml gentamycin; pH 7.5) and several silicone strips to keep oocytes separated and in place. Oocytes were impaled with the injection pipette and 50 nl cRNA mixture was injected into each oocyte at the following ratios: 1:1 for $\alpha 3\beta 2$ receptors, 1:1:1 for $\alpha 1/\alpha 3\beta 2\varepsilon/\varepsilon_T$ receptors (12.5 ng of each subunit per oocyte) and 1:1:10 for $\alpha 3\beta 2\gamma 2$L receptors (6.25 ng of $\alpha 3$ and $\beta 2$ subunit cRNA and 62.5 ng of $\gamma 2$L subunit cRNA per oocyte). Oocytes were incubated in modified Barth's medium at 18°C for a minimum of 36 hours to allow $GABA_A$ receptor expression. Oocytes, when injected with cRNAs encoding for $\alpha 1$ or $\alpha 3$, $\beta 2$ and ε subunits, were incubated in the presence of 100 µM Picrotoxin to block current through spontaneously open channels. Oocytes were checked every day and dead oocytes were removed from the medium. Barth's medium was changed on the second day and on a regular basis afterwards.

2.3.4 Two-electrode voltage-clamp

Microelectrodes were pulled from thin wall borosilicate glass tubes (1.5 /1.12 OD/ID (mm); Model no. TW150F-4, World Precision Instruments, Inc.) using a programmable, horizontal pipette puller (P-97, Sutter Instruments) in two steps. Next, microelectrodes were bent in the middle to about 150 degree using a spirit burner and backfilled with 3 M KCl using a modified 1 ml syringe to about two thirds full. To remove air bubbles in the microelectrode tip, it

was gently flicked until bubbles disappeared. It was then inserted into a microelectrode holder mounted on a headstage (H2-RA, Axon Instruments) controlled by a micromanipulator (Leitz). Microelectrodes had a resistance of 0.5 to 3 MΩ when submerged in the frog Ringer solution (95 mM NaCl, 2 mM KCl, 2 mM $CaCl_2$, 5 mM HEPES; pH 7.5). An oocyte was placed into the oocyte bath chamber (RC-3Z, Warner Instruments) and constantly perfused with a frog Ringer solution at a flow rate of approximately 6-8 ml/min. Two microelectrodes were impaled into the oocyte; one electrode recorded the voltage, the other injected the current (Figure 1.8, Chapter 1). Oocytes were clamped at a chosen holding potential, normally -60 mV, using a GeneClamp 500 (Axon Instruments) or Axoclamp 2-A (Axon Instruments) amplifier. Data were recorded to the hard disk of a PC using Strathclyde Electrophysiology Software WinEDR2.9.2. (Dr J. Dempster, Department of Physiology and Pharmacology, University of Strathclyde, UK). All drugs were bath applied by switching from frog Ringer solution to drug solution using a ValveLink 8 or ValveBank 8 perfusion system (Automate Scientific). Oocytes were washed for at least four minutes between each drug application to avoid receptor desensitisation. $GABA_A$ receptor agonists were applied alone and antagonists and allosteric modulators were administered simultaneously with GABA at a concentration that produced 20 % of the maximum response (EC_{20}). GABA alone at EC_{20} concentrations served as control. GABA, muscimol and zinc sulphate were prepared as 10 mM stock solutions and picrotoxin was dissolved as a 100 µM stock solution in frog Ringer and diluted before use. Flunitrazepam and etomidate were dissolved in 100 % (v/v) DMSO before dilution into frog Ringer solution. The final solution did not exceed a DMSO level of 0.1 % (v/v), which had no effect either alone or on GABA-elicited currents (Figure B.1 in Appendix B). All experiments were performed at room temperature (18-25°C). A minimum of two batches of oocytes were used per experiment.

2.3.5 Data analysis

Two-electrode voltage-clamp data were analysed using Strathclyde Electrophysiology Software WinEDR V2.9.2 (Dr J. Dempster, Department of Physiology and Pharmacology, University of Strathclyde, UK) by measuring the amplitudes of peak-currents of recorded traces.

Concentration-response curves were fitted using GraphPad Prism 5.0 software (San Diego, USA). Data were normalised and shown as percentage of the maximal response or percentage of the control response, respectively, and fitted using a non-linear regression fit with variable slope to the following equation:

$$\text{response} = \begin{cases} 100/(1+10^{((\log EC_{50}-\mathrm{X})\times n)}) & \text{for agonists and positive modulating drugs} \\ 100/(1+10^{((\log IC_{50}-\mathrm{X})\times n)}) & \text{for antagonists} \end{cases} \tag{2.2}$$

Where X is the log of drug concentration, EC_{50}/IC_{50} is the drug concentration evoking a half-maximal response and n is the Hill coefficient. Data are given as means $\pm$ standard error of the mean (SEM). EC_{50}/IC_{50} values from different receptor subtypes were analysed statistically using unpaired Student's t-test and considered significant when $p < 0.05$.

2.4 Patch clamping mammalian cells

Glass coverslips (VWR) were cut into ~5.5 mm $\times$ 22 mm pieces using a diamond cutter. Coverslip pieces were then sterilised by baking them at 180°C for 3 hours. Transiently transfected HEK293 cells were reseeded at a low density onto sterile pieces of glass coverslip in 35 mm Petri dishes (Nunc) 24 hours after transfection with $GABA_A$ receptor cDNAs (see Sections 2.5.4 and 2.6.3). Recordings were performed using the whole-cell patch-clamp configuration 24 to 48 hours after plating (Figure 1.9, Chapter 1).

Whole-cell recordings were performed in the laboratory of Dr Ian Mellor (University of Nottingham). Glass borosilicate capillaries (Model no. 1B150-4, World Precision Instruments, Inc.) were pulled in two steps using a programmable, horizontal pipette puller (P-97, Sutter Instruments). Pipettes were filled approximately two thirds with pipette solution (140 mM CsCl, 1 mM $CaCl_2$, 1 mM $MgCl_2$, 11 mM EGTA and 5 mM HEPES; pH 7.2 adjusted with CsOH) and air bubbles in the tip were removed by gently tapping the pipette. It was then inserted into a pipette holder mounted on a CV 201AU headstage (Axon Instruments), which was controlled by a micromanipulator (PCS - 5000 Series, Burleigh). Pipettes had a resistance of ~5 to ~8 MΩ when lowered into the bath. A RC-27 bath chamber (Warner Ins-

truments) was placed on the stage of a microscope (Olympus). Coverslips with cells were transferred into the chamber and continuously perfused with a mammalian Ringer solution (135 mM NaCl, 5.4 mM KCl, 1 mM $CaCl_2$, 1 mM $MgCl_2$, 5 mM HEPES and 10 mM Glucose; adjusted to pH 7.4 with NaOH). Membrane currents were recorded using an Axopatch 200A amplifier (Axon Instruments). Cells were clamped at a holding potential of -50 mV. Drugs were bath applied using a QMM micromanifold (ALA Scientific Instruments, Inc.) by switching from mammalian Ringer solution to drug solution. 2 second pulses of agonists or antagonists at specific concentrations were applied using a DAD-12 superfusion system (ALA Scientific Instruments, Inc.). Cells were washed for at least 30 seconds between each drug application. The amplifier, perfusion system and data recording to a PC were controlled and synchronized by Strathclyde Electrophysiology Software WinWCP V2.9.2 (Dr J. Dempster, Department of Physiology and Pharmacology, University of Strathclyde, UK). All experiments were carried out at room temperature (18-25°C).

2.5 Cell culture

2.5.1 Culturing HEK293 cells

HEK293 cells were kindly provided by Prof. Anne Stephenson (The School of Pharmacy, University of London, UK). Cells were grown in sterile-filtered Dulbecco's modified Eagle's medium (DMEM), containing 4.5 g/l glucose and 4 mM L-glutamine, supplemented with 10 % (v/v) fetal bovine serum (FBS) and intermittently with 10 ml/l Penicillin-Streptomycin (10,000 U/ml penicillin and 10 mg/ml streptomycin). Cells were maintained at 37°C in a humidified atmosphere with 95 % (v/v) air and 5 % (v/v) carbon dioxide. Cells were routinely grown in 75 cm^2 or 25 cm^2 tissue culture flasks (Sarstedt/Iwaki) and sub-cultured twice a week (when 80-90 % confluent). For this, the growth medium was pipetted out and cells were washed once with Dulbecco's phosphate buffered saline (DPBS; 130 mg/l $CaCl_2 \cdot 2\ H_2O$, 200 mg/l KCl, 200 mg/l KH_2PO_4, 100 mg/l $MgCl_2 \cdot 6\ H_2O$, 8 g/l NaCl, 2.16 g/l $Na_2HPO_4 \cdot 7\ H_2O$) to remove traces of serum. Next, cells were incubated with trypsin/EDTA (900 mg/l NaCl, 500 mg/l Trypsin, 200 mg/l Versene (EDTA)·2 Na·2 H_2O) at 37°C

until they detached from the plastic flask and fresh growth media was added to quench the action of the trypsin/EDTA. Cells were centrifuged at 300 rcf, 22°C for 5 minutes (Models 5415R, Eppendorf or Universal 320R, Hettich); the supernatant was discarded and the cell pellet resuspended in 1 ml fresh medium by pipetting the cells gently up and down several times. Afterwards, a suitable quantity of cells was transferred into a tissue culture flask containing fresh growth medium and incubated as stated above. Cells were cultured for about 20 passages before a new stock was regenerated. All reagents were purchased from Lonza.

2.5.2 Long term storage of HEK293 cells in liquid nitrogen

For cryopreservation, HEK293 cells of a low passage number were grown and harvested as described above (Section 2.5.1). Cell pellets were carefully resuspended with a pipette until cells were free of clusters. Next, cells were counted using a hemocytometer with Neubauer improved grid pattern (C-Chip (DHC-N01), Incyto) by transferring 20 µl resuspended cells to a microfuge tube containing an appropriate volume of growth medium, depending on the size of the tissue culture vessel where cells grew in. Cells were further diluted 1:1 (final concentration of 4 to 6 $\times$ 10^6 cells per ml) using a Trypan blue solution (0.4 % in 0.81 % NaCl and 0.06 % K_2HPO_4, Sigma), which stained non-viable cells blue. 10 µl of the mixture were loaded into the counting chamber and viable cells were counted in 5 large squares. The number of viable cells per ml was calculated as follows:

$$\frac{\text{no. of cells counted}}{5} \times \text{dilution factor} \times 10^4 = \text{cells/ml} \tag{2.3}$$

Afterwards, cells were pelleted again and resuspended in sufficient freezing medium (DMEM supplemented with 10 % (v/v) FBS and 5 % (v/v) DMSO) to get a final concentration of 2 $\times$ 10^6 cells per ml. 1 ml of cell suspension was pipetted into each cryovial and frozen at -80°C for 24 hours before vials were transferred into liquid nitrogen for long term storage.

2.5.3 Thawing cells stored in liquid nitrogen

Cryovials of HEK293 cells from frozen stock were thawed quickly by incubating the vials at 37°C and transferring the cells to 20 ml prewarmed growth medium. Next, the cell suspension was centrifuged at 300 rcf, 22°C for 5 minutes and cell pellets were resuspended in 1 ml fresh growth medium before transferring them to a tissue culture flask containing fresh growth medium and incubating them at 37°C, 95 % (v/v) air and 5 % (v/v) carbon dioxide until 80 to 90 % confluent (Section 2.5.1).

2.5.4 Transient transfection of HEK293 cells

Cells were seeded into different tissue culture vessels (depending on the number of cells needed) in DMEM containing 10 % FBS, but no antibiotics, and grown for 24 hours as described in Section 2.5.1 and Table 2.3.

Table 2.3: Transient transfection using TransPass^{TM} D2 in different culture vessels

Culture vessel	No. of cells seeded	Volume of medium	total amount plasmid DNA in DMEM	TransPass^{TM} D2
24-well plate	1.5×10^5	250 µl	0.7 µg in 50 µl	1.75 µl
6-well plate	7.2×10^5	1 ml	3 µg in 250 µl	8.75 µl
T25 flask	1.85×10^6	3.2 ml	9 µg in 600 µl	22 µl
T75 flask	5.55×10^6	9.6 ml	27 µg in 1800 µl	66 µl

After 24 hours, cells were 70-80 % confluent and transfected using TransPass^{TM} D2 transfection reagent (New England Biolabs) according to the manufacturer's protocol. Briefly, plasmid DNA was pipetted into DMEM as in Table 2.3, when transfecting several different DNAs the quantity was divided equally or at certain ratios. Next, 22 µl TransPass^{TM} D2 was added, mixed carefully and incubated for 20 to 30 minutes at room temperature (18-25°C) to facilitate formation of tranfection complexes. Subsequently, the mixture was added to the cells and incubated for 4 to 6 hours as described before (Section 2.5.1). Medium containing excess transfection complexes was then replaced by fresh growth medium in order to prevent toxic effects to the cells. Transient transfection was optimised using pRK5-Clomeleon as a reporter protein (Section 2.5.4.1).

2.5.4.1 Evaluation of transient transfection efficiency

Transient transfection efficiency was optimised by transfecting HEK293 cells with pRK5-Clomeleon, which served as fluorescence marker of transfected cells. Cells were seeded into and transfected in 24-well plates as described in Section 2.5.4, but varying the number of cells as well as the plasmid DNA to TransPass^{TM} D2 transfection reagent ratio. Approximately 24 hours after the transfection, cells were removed from the wells by using trypsin/ EDTA (as described in 2.5.1). Transfection efficiency was examined by placing cells in solution onto a glass microscope slide and visualising them using an Olympus BX51 fluorescence microscope. A minimum of 1000 cells were counted per experiment using Cell^{F} software (Olympus) in order to determine the ratio of transfected (fluorescent) cells versus untransfected cells. The conditions resulting in highest transfection efficiency after performing each experiment in duplicates were used for all further transient transfection experiments (Section 2.5.4, Table 2.3).

2.5.5 Reseeding cells into appropriate tissue culture plasticware

Typically, cells had to be reseeded into cell culture plastic ware suited for respective experiments 24 hours after transient transfection. For this, cells were washed once using DPBS and subsequently detached from the surface by adding trypsin/EDTA and incubating them at 37°C until dissociated from the plastic. Sufficient growth medium was added to the cells to quench the trypsin/EDTA. Cells were then centrifuged at 300 rcf for 5 minutes at room temperature (18-25°C). Cell pellets were resuspended and counted (Section 2.5.2); the required number of cells was plated into microtiter plates or coverslips placed in 35 mm Petri dishes and incubated further until usage in respective experiments (see below).

2.6 Assay development to screen compound libraries

2.6.1 A cell-based assay using the chloride-ion indicator Clomeleon

2.6.1.1 Excitation and emission spectra of Clomeleon

Sequencing the pRK5-Clomeleon plasmid revealed a discrepancy of one amino acid with the sequence data provided by Dr Thomas Kuner. Therefore, the excitation and emission spectra of Clomeleon were investigated using a spectrofluorometer (QuantaMaster, Photon Technology International,Inc.). HEK293 cells were seeded into 24-well plates and transfected 24 hours later with $GABA_A$ receptor subunit cDNA (α3 and β2 and γ2L) and pRK5-Clomeleon at a ratio of 1:1:1:1 (Section 2.5.4). On the next day, cells were reseeded onto sterile coverslips (10 $\times$ 24 mm, Chance Propper Ltd.) placed in 35 mm dishes (Nunc) at a cell density of 7 to 10 $\times$ 10^5 in 500 µl medium. Cells were incubated as described above (Scetion 2.5.1) until the following day.

Excitation and emission screens were performed using a spectrofluorometer (QuantaMaster, Photon Technology International,Inc.). Cells on a coverslip were immersed into a fluorimeter cuvette (Sigma) containing mammalian Ringer solution (Section 2.4), which was subsequently fitted into the spectrofluorometer. The emission scan was performed at wavelengths of 450 nm to 650 nm, with an excitation of 440 nm; the excitation scan was carried out from 350 nm to 485 nm with the emission being set to 527 nm. Both were performed with cells transfected with Clomeleon alone or Clomeleon and $\alpha3\beta2\gamma2$L $GABA_A$ receptors. Additionally, untransfected HEK293 cells, a cuvette with mammalian Ringer solution and a cuvette alone were scanned as controls. Experiments were performed at 37°C.

2.6.1.2 Evaluating a screening assay using Clomeleon

HEK293 cells were seeded into 25 cm^2 tissue culture flasks and 24 hours later transfected with $GABA_A$ receptor subunit cDNAs (α3 and β2 or α3, β2 and γ2L) and pRK5-Clomeleon at ratios of 1:1:1 or 1:1:1:1, respectively (Section 2.5.4). On the following day, cells were plated into Poly-D-Lysine coated, black 96-well plates with clear, flat bottom (BD Biosciences)

at cell densities of 1.5 $\times$ 10^5 and 2 $\times$ 10^5 cells per well in 200 µl medium. Poly-D-Lysine coating enhanced cell growth and attachment to the wells and black polystyrene plates were used to lower background noise and well-to-well crosstalk. Cells were incubated for another day before performing the assay using a FLUOstar Optima microplate reader (BMG Labtech) fitted with one reagent injector, a 430 $\pm$ 10 nm excitation and 480 $\pm$ 10 nm and 520-P emission filters.

On the day of the assay, the growth medium was removed from each well and replaced with 90 µl prewarmed mammalian Ringer solution (Section 2.4) per well. Cells were then incubated for a further one hour (as described in 2.5.1) before placing the plate into the FLUOstar Optima plate reader, which was set to excite and read Clomeleon emission from the bottom of the plate. Baseline fluorescence was measured for 20 seconds (0.2 second intervals) for both Clomeleon emission wavelengths (480 nm and 520 nm), together as well as separately. Next, 10 µl GABA (1 mM) in mammalian Ringer solution was injected into each well (100 µM final GABA concentration). To intermix the added solution, the plate was shaken for 1 second before the fluorescence signal was continued to be read for a further 30 seconds at 0.2 second intervals. Experiments were performed at 37°C and repeated twice. Data were analysed by normalising averaged baseline fluorescence signal to 100 % and fluorescence signals recorded after GABA solution injection were shown as percentage of baseline fluorescence. Data are given as means $\pm$ SEM.

2.6.2 Setting up an iodide-flux assay

The assay was set up as described in Tang & Wildey (2004) and Tang & Wildey (2006). HEK293 cells were seeded into 25 cm^2 tissue culture flasks and transfected 24 hours later with $GABA_A$ receptor subunit cDNAs (α3, β2 and γ2L, ratio 1:1:1; Section 2.5.4). On the following day, cells were plated into Poly-D-Lysine coated 96-well microplates with flat bottom (BD Biosciences) at cell densities of 25 $\times$ 10^3 cells per well in 100 µl growth medium. At a later date, cells were tested at lower densities of 12.5 $\times$ 10^3 and 17.5 $\times$ 10^3 cells per well. Cells were incubated for another day before proceeding with the iodide-flux assay. Untransfected HEK293 cells served as negative controls.

DMEM was removed from the wells and cells were loaded with 100 or 200 µl filter-sterilised, prewarmed iodine-loading buffer (150 mM NaI, 2 mM $CaCl_2$, 0.8 mM NaH_2PO_4, 1 mM $MgCl_2$, 5 mM KI, 2 % FBS; adjusted to pH 7.4 with NaOH). Subsequently, cells were incubated for a further 4 hours at 37°C, 95 % (v/v) air, 5 % (v/v) carbon dioxide to allow cell loading. Cells were then washed 3 to 4 times with 200 µl DPBS to remove excess iodide, before adding 100 µl DPBS containing increasing concentrations of GABA and incubated for a further 5 minutes at room temperature (18-25°C). Next, the DPBS containing GABA and the 'effluxed' iodide was transferred to a fresh plate. Cells on the first plate were lysed by adding 100 µl lysis buffer (1 % (v/v) triton X-100). Colorimetric detection was accomplished on both plates (lysed cells as well as DPBS) by adding to each 100 µl detection buffer II (2 mM $Ce(NH_4)_4(SO_4)_4 \cdot 2H_2O$, 5.2 % (v/v) fuming H_2SO_4 in distilled H_2O) followed by 100 µl detection buffer I (1.25 % (v/v) NH_4OH solution, 100 mM As_2O_3, 3.2 % (v/v) fuming H_2SO_4, 467.38 mM NH_4Cl). Subsequently, the plate was incubated at room temperature for 15 minutes. Next, it was inserted into a microplate reader (ASYS, Expert 96), shaken for 2 seconds to evenly disperse the liquid and the OD405 was read.

The results obtained were rather random, therefore, several assay modifications and optimisations were tested. Since the OD405 readings were relatively low, not only less cells were seeded, but also it was examined whether the results could be improved by diluting the lysed cells and DPBS (1:2 and 1:5) before performing the colorimetric assay. In order to test functionality of $GABA_A$ receptors, cells were incubated in DPBS with 50 µM bicuculline and 1 or 100 µM GABA or in DPBS containing 50 µM picrotoxin and 1 or 100 µM GABA as well as 1 or 100 µM GABA and DPBS alone. Untransfected cells served as controls. Different agonist incubation times of 10 seconds up to 5 minutes (DPBS containing 10 µM GABA) were also investigated to optimise efflux. In every assay for every test variable 8 replicates were prepared per plate. Different setups were repeated at least 2 times.

A standard curve was generated by adding 100 µl per well in a 96-well plate of ascending concentrations of NaI (3 nM to 300 µM) as well as distilled water as negative control. Afterwards, 100 µl detection buffer II and 100 µl detection buffer I were added into each well, contents were mixed and incubated at room temperature for 10 to 70 minutes before reading

the OD405 on the microplate reader. 8 standard replicates per NaI concentration were prepared and the experiment was repeated 3 times on different days. Data points were averaged. The assay detection limit was defined as minimal NaI concentration that fulfils the following argument (Tang & Wildey, 2004):

$$OD405_{\text{sample}} - OD405_{\text{control}} > 3SD_{\text{control}} \tag{2.4}$$

Where $OD405_{\text{sample}}$ is the OD405 of the sample containing NaI, $OD405_{\text{control}}$ is the OD405 of the control sample that contains no NaI and SD_{control} is the standard deviation (SD) of the control.

OD405 readings of the iodide-flux assay were averaged and the SD was calculated. Values were analysed statistically using unpaired Student's t-test and considered significant when $p < 0.05$. In some cases, channel conductivity (% activity) was calculated as follows (Tang & Wildey, 2004):

$$(OD405_{\text{sample}} - OD405_{\text{low}})/(OD405_{\text{high}} - OD405_{\text{low}}) \times 100 \tag{2.5}$$

Where $OD405_{\text{sample}}$ was the reading of the wells incubated with different GABA concentrations, $OD405_{\text{high}}$ was the reading of the cells treated with the highest concentration of GABA and $OD405_{\text{low}}$ was measured from cells incubated with distilled water instead.

2.6.3 Setup and optimisation of a mutant YFP-based assay

HEK293 cells were seeded into 25 cm^2 or 75 cm^2 tissue culture flasks. On the next day, when 70 - 80 % confluent, cells were transfected with $GABA_A$ receptor subunit cDNAs and the pEYFP H148Q/I152L vector (as described in 2.5.4). $GABA_A$ receptor subunit cDNAs to pEYFP H148Q/I152L vector ratios were as listed below:

$\alpha1$	:	$\beta2$		:		pEYFP H148Q/I152L	$\rightarrow$	1:1:2
$\alpha3$	:	$\beta2$		:		pEYFP H148Q/I152L	$\rightarrow$	1:1:2
$\alpha1$	:	$\beta2$	:	ε	:	pEYFP H148Q/I152L	$\rightarrow$	1:1:1:2
$\alpha3$	:	$\beta2$	:	ε	:	pEYFP H148Q/I152L	$\rightarrow$	1:1:1:2
$\alpha3$	:	$\beta2$	:	$\gamma2$L	:	pEYFP H148Q/I152L	$\rightarrow$	1:1:1:2

Untransfected cells served as control cells. On the following day, cells were plated into Poly-D-Lysine coated, black-sided 96-well plates with clear, flat bottom (BD Biosciences) and incubated for a minimum of a further 24 hours. For assay optimisation, different numbers of cells were seeded per well (in 200 µl growth medium). Approximately 1.5 $\times$ 10^5 cells per well (in 200 µl medium) were decided to give the best results and used in all further experiments.

On the day of the assay, one hour prior to the start of an experiment, growth medium was removed from the wells and replaced by 50 µl prewarmed NaCl bathing solution per well (140 mM NaCl, 5 mM KCl, 2 mM $CaCl_2$, 1 mM $MgCl_2$, 10 mM HEPES, 10 mM Glucose; pH 7.3 using NaOH). Following incubation, the plate was placed into a FLUOstar Optima microplate reader (BMG Labtech) fitted with two reagent injectors, a 500 $\pm$ 10 nm excitation and a 520-P emission filter. Assays were performed at 37°C. The mutant YFP-H148Q/I152L was excited and its emission was measured from the bottom of the plate; each well was scanned orbitally at a radius of 3 mm. Baseline fluorescence was recorded for 5 seconds (one second intervals) before injection of 150 µl NaI test solution only (140 mM NaI, 5 mM KCl, 2 mM $CaCl_2$, 1 mM $MgCl_2$, 10 mM HEPES, 10 mM Glucose; pH 7.3 using NaOH) or NaI test solution supplemented with GABA or picrotoxin at specific concentrations (injection speed 100 µl/sec). After solution was injected, the fluorescence signal was recorded at 0.5 second intervals for a further 30 seconds. Experiments were repeated 3 times, each with at least 3 wells on the same plate and at least one of the replicates was performed on a separate plate.

As it became clear that the assay was functional, GABA concentration-response relation curves were determined for $\alpha1\beta2$, $\alpha1\beta2\varepsilon$ and $\alpha3\beta2\gamma2$ receptors by injecting ascending

GABA concentrations (in NaI test solution) ranging from 30 nM to 3 mM. By adding NaI test solution containing flunitrazepam (1 µM final concentration) and an EC_{30} concentration of GABA to cells expressing $\alpha 3\beta 2\gamma 2$ receptors it was demonstrated that the assay was suitable to detect positive modulation of the receptors. Flunitrazepam stock solution was prepared by dissolving it in 100 % (v/v) DMSO. Before the assay, flunitrazepam was diluted into NaI test solution. The final solution did not exceed a DMSO level of 0.5 % (v/v), which had no effect on GABA-elicited currents (Figure B.2 in Appendix B).

2.6.3.1 Data analysis

Data were analysed by subtracting the averaged fluorescence measured from non-transfected control cells (baseline fluorescence and after addition of NaI test solution) resulting in the net fluorescence signal. This was then normalised by setting the averaged baseline fluorescence to 100 % and fluorescence changes (after adding solutions) were calculated as percentage of the baseline fluorescence. The percentage of fluorescence quench was calculated as follows (Gilbert et al., 2009a):

$$\% \text{ fluorescence quench} = (1 - (F_{\text{final}}/F_{\text{BF}})) \times 100 \tag{2.6}$$

F_{BF} is the averaged baseline fluorescence signal and F_{final} is the averaged final fluorescence signal. Values were presented as means ± SEM. To assess the assays quality without test compounds the Z'factor was calculated as described below (Zhang et al., 1999):

$$Z' = 1 - \frac{(3\sigma_{\text{c+}} + 3\sigma_{\text{c-}})}{|\mu_{\text{c+}} - \mu_{\text{c-}}|} \tag{2.7}$$

σ_{c+} or σ_{c-} represent the SD of positive and negative controls, μ_{c+} or μ_{c-} states the means of positive and negative controls. Positive controls were readings from cells treated with a high GABA concentration (100 µM), for negative controls NaI test solution only was applied to the cells. Concentration-response curves were fitted using GraphPad Prism 5.0 software (San Diego, USA). Data were shown as percentage of baseline fluorescence and fitted using

a non-linear regression fit with variable slope according to the following equation:

$$\text{response} = \{\text{bottom} + (\text{top} + \text{bottom})/(1 + 10^{((\log EC_{50} - \text{X}) \times n)}) \tag{2.8}$$

Where X is the log of drug concentration, EC_{50} is the drug concentration evoking a half-maximal response, n is the Hill coefficient and the response starts at bottom and goes to top. Data are given as means ± SEM.

2.7 Compound screening using mutant YFP-H148Q/I152L

2.7.1 Chemical compound library

800 compounds covering a broad range of structural motifs and biological space were acquired from the Maybridge HitFinder™ collection of screening compounds (Maybridge Ltd.). Compound quality was guaranteed to have a minimum of 90 % purity. Compounds were arrayed individually in ten separate 96-well plates (80 compounds per plate) as dry films of 1 µmol per compound and stored at -80°C until usage.

Compounds were resuspended in 100 µl DMSO per well. Plates were placed on an orbital shaker (Stuart) and left until compounds were dissolved. Subsequently, 20 µl aliquot plates were prepared. All plates were sealed using parafilm and stored at -20°C until needed. Concentrations of these compound stock solutions ranged from ~10.1 to ~11.9 mM.

2.7.2 Screening assay

HEK293 cells were seeded in 75 cm^2 flasks, transfected with α1, β2, ε or α3, β2, γ2L $GABA_A$ receptor subunit cDNAs and YFP-H148Q/I152L cDNA and reseeded into Poly-D-Lysine coated 96-well plates (Sections 2.5.4, 2.6.3). On the next day, the assay was performed as described in Section 2.6.3. Application of 100 µM GABA, 1 mM picrotoxin with an EC_{30} GABA concentration as well as EC_{30} GABA with or without 0.5 % DMSO (all were applied in NaI test solution) served as controls.

1 µl of compound stock solution was transferred manually, using a multichannel pipette, to each well of the microtiter plate containing 50 µl NaCl bath solution. Next, the plate was returned to the plate reader and shaken for 10 seconds to intermix the added compound. 150 µl of low concentration GABA (EC_{30}) in NaI test solution was injected into the first well and the fluorescence signal was read for 30 seconds (0.5 second intervals), before GABA in NaI test solution was added to the next well to measure the fluorescence signal for 30 seconds until all compounds were screened for their possible modulating or antagonist activity. Time elapsed between the addition of a chemical compound to the wells until the injection of NaI test solution and subsequent fluorescence measurement was between approximately 5 and 60 minutes. In later assays this time was reduced to shorter periods.

The initial screening was performed with relatively high compound concentrations (final concentrations were between 50.3 and 59.29 µM). Due to the high number of 'hit' compounds, which enhanced or inhibited submaximal GABA-evoked receptor activity, the screenings were repeated several times using gradually decreased compound concentrations (compound solutions were further diluted using DMSO). During these preliminary screens, each compound was tested in singlets until the number of 'hit' compounds was whittled down sufficiently. The remaining 'hit' compounds were then tested in at least three wells on the same plate, repeated at least three times. Compounds applied with NaI test solution only were examined for possible agonist activity of 'hit' compounds and cells transfected with YFP-H148Q/I152L cDNA only served as control cells to rule out compound activity via receptors expressed endogenously in the cells. Data were analysed as in Section 2.6.3 described.

2.7.2.1 Data analysis

The effect of test compounds was compared to the EC_{30} GABA-control response and analysed statistically using Student's t-test. Results were considered significant when $p < 0.05$.

2.7.3 Further testing of 'hit' compounds

A selection of 'hit' compounds which exhibited receptor modulation or inhibition during the preliminary screening assay was further tested in *Xenopus laevis* oocytes expressing $\alpha 1 \beta 2 \varepsilon$

or $\alpha 3\beta 2\gamma 2$ receptors using the two-electrode voltage-clamp technique (Section 2.3). Test compounds were dissolved in DMSO as 100 mM stock solutions before dilution into frog Ringer solution. The final solution did not exceed a DMSO level of 0.1 % (v/v), which had no effect either alone or on GABA-elicited currents (Figure B.1, Appendix B).

Chapter 3

Pharmacological characterisation of the $\alpha 3\beta 2\varepsilon$ $GABA_A$ receptor subtype

3.1 Introduction

3.1.1 The $GABA_A$ receptor ε subunit

The $GABA_A$ receptor ε subunit belongs to a minor receptor population with unknown function (Olsen & Sieghart, 2009). Its expression in the brain is restricted to specific areas, mainly areas in the forebrain, such as the hypothalamus, as well as nuclei containing major modulatory systems of the brain, including cholinergic cell groups (Moragues et al., 2000; Sieghart & Sperk, 2002). The latter also express the $\alpha 3$ subunit. The ε subunit is clustered together with the $\alpha 3$ and θ subunits on chromosome Xq28 of the human genome (Wilke et al., 1997) and it has been shown that these subunits are co-expressed in several areas of the brain (Moragues et al., 2000; Sieghart & Sperk, 2002). It is therefore likely that they form functional receptor channels in some brain areas. Heterologous expression studies have shown that the ε subunit can replace the γ subunit to form functional $GABA_A$ receptors, when co-expressed with α and β subunits (Davies et al., 1997; Whiting et al., 1997). These receptors respond to a wide range of allosteric modulators, but exhibit unusual characteristics compared to other known native $GABA_A$ receptors, such as increased desensitisation rate, high agonist sensitivity and spontaneous channel opening (see Section 1.2.5.1, Chapter 1; Whiting et al., 1997;

Neelands et al., 1999).

The subunit compositions of ε-containing receptors *in vivo* and their precise functions are largely unknown. Previously, the pharmacological profile of ε-subunit-containing receptors has been investigated in heterologous expression systems in several different subunit combinations. Nonetheless, despite co-expression of $\alpha3$ and ε subunits in a number of brain areas, only one study examined pharmacological properties of recombinant receptors containing these subunits in conjunction with the $\beta1$ subunit (Ranna et al., 2006). However, the $\beta2$ subunit is more abundant and the most widely expressed β subunit in the brain. In several areas of the brain, $\alpha3$ and ε subunits are co-expressed with $\beta2$ subunits, for example in hypothalamus and amygdala (Zhang et al., 1991; Moragues et al., 2000; Pirker et al., 2000; Sieghart & Sperk, 2002) and it is likely that these subunits may form functional receptors in some of those areas. In order to learn more about the role of the ε subunit it is, therefore, important to know the pharmacological profile of $\alpha3\beta2\varepsilon$ receptors.

In this study, pharmacological properties of the $\alpha3\beta2\varepsilon$ receptor subtype were investigated and compared with $\alpha3\beta2$ and $\alpha3\beta2\gamma2$ receptors. The initial plan was to express cDNA encoding the different subunits in HEK293 cells, which were also used later in the cell-based screening assay (see Chapters 4 and 5). In this way, not only the pharmacological profile of this novel subunit combination could be examined, but the correct subunit assembly in HEK293 cells could be investigated too (which would be advantageous for setting up the screening assay). However, problems with the electrophysiological rig at Nottingham Trent University caused a slight change in the project and electrophysiological recordings were instead performed in *Xenopus laevis* oocytes microinjected with cRNA in the laboratory of Dr Ian Mellor at the University of Nottingham.

3.1.2 ε subunit splice variants

As mentioned in Chapter 1 (Section 1.2.2), subunit splicing adds even more complexity and diversity to the $GABA_A$ receptor family. It has been shown, that several of the $GABA_A$ receptor subunits exist in different splice variants, including $\alpha2$, $\alpha4$, $\alpha5$, $\alpha6$, $\beta2$, $\beta3$, $\gamma2$, $\gamma3$

and ε subunits (Simon et al., 2004). Often, there are two different splice forms, a long and a short version of the protein, for example the $\beta 2$ and $\gamma 2$ subunits exist in both forms. In the case of the $\gamma 2$ subunit, the long form exhibits an eighth amino acid insertion into the large intracellular loop between TM3 and TM4, introducing a site for phosphorylation by protein kinase C (PKC; Whiting et al., 1990).

The ε subunit gene consists of nine exons (Sinkkonen et al., 2000; Simon et al., 2004) and several mRNA splice variants have been demonstrated in brain as well as in several other peripheral tissues. Four splice forms were described by Wilke et al. (1997): (1) the full length, functional transcript, which is expressed in brain, but also found in heart and spinal cord, (2) a version where the first three exons are spliced out and (3) a variant like 2, but with an additional deletion in the centre of exon four; both variants are expressed in peripheral tissues, but not found in the brain, and (4) a deletion of exon one only. Moreover, Sinkkonen et al. (2000) described a 483 amino acid long insertion encoding a Pro/Glx motif, which was identified exclusively in rodents. However, Moragues et al. (2000) identified a rodent ε version lacking this long insertion, and, therefore, resembling the human sequence to a greater extent. It was demonstrated that both versions are expressed in the brain as well as mRNA of a further, truncated version (described below, Figure 3.2; Kasparov et al., 2001). Davies et al. (2002) investigated the functionality of the long rodent splice variant by expressing it in HEK293 cells. Functional properties as well as the transcripts expression pattern were examined, but failed to show its incorporation into functional channels. However, since there was no premature stop codon and the sequence is in frame, it was concluded that there may be a different function of this long transcript. The splice properties of the ε subunit are relatively unusual compared to other subunits, since splicing can be introduced at several different positions. Many of the truncated subunit transcripts are found in several different tissues, where they may exhibit unknown functions, and, also, several splice variants exist in the brain.

In this project, the truncated ε subunit version (ε_T) found in brain (Kasparov et al., 2001) was generated and functionally examined. This variant possesses a 26 amino acid deletion, starting in the centre of TM2 until the end of the extracellular loop between TM2 and TM3

(Figures 3.1 and 3.2). In order to find further clues about the role of this unusual subunit, it was investigated whether the truncated version forms functional channels *in vitro* when co-expressed with the $\alpha 3$ and $\beta 2$ subunits.

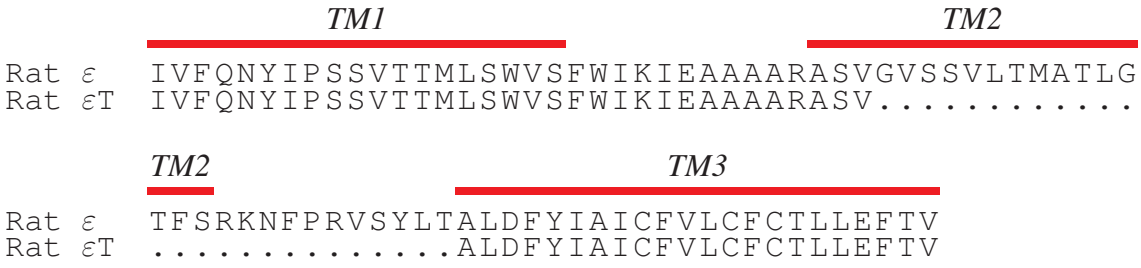

Figure 3.1: Alignment of the partial rat $GABA_A$ receptor ε subunit amino acid sequence (single-letter code) in the region of TM1 to TM3.

The truncated version (εT; accession number AF255385) shows a 26 amino acid deletion from the middle of TM2 to the start of TM3, compared to the full length version (accession number AF255612).

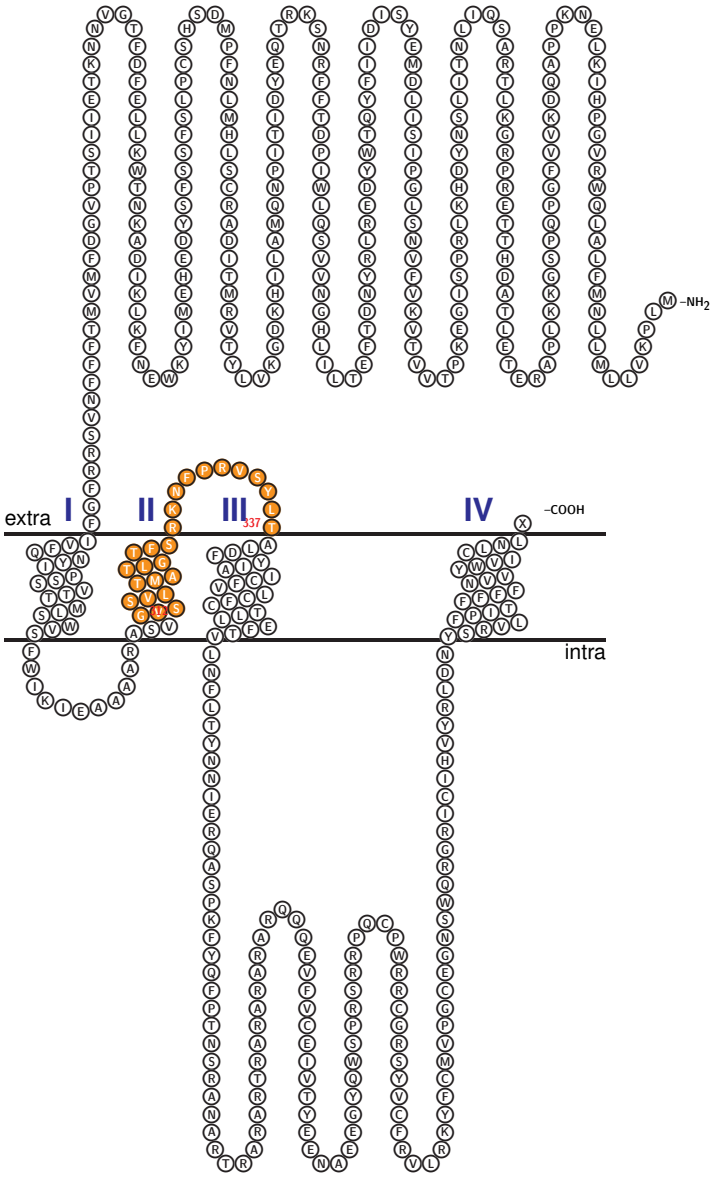

Figure 3.2: Structure of the ε subunit; amino acid sequence is displayed in single-letter code. Orange circles represent the 26 amino acid deletion in the truncated subunit version.

3.2 Results

3.2.1 Agonist sensitivity

$\alpha3\beta2$, $\alpha3\beta2\varepsilon$ and $\alpha3\beta2\gamma2$ $GABA_A$ receptor subtypes were expressed in *Xenopus laevis* oocytes and examined using the two-electrode voltage-clamp technique. To characterise the pharmacological and biophysical properties of the receptors, they were first examined for their sensitivity to the agonists GABA and muscimol. In all cases both agonists elicited concentration-dependent inward currents (see Figure 3.3 for GABA-evoked traces), whereas no currents were detected upon the application of 1 mM GABA in oocytes expressing $\alpha3$, $\beta2$, $\gamma2$ and ε subunits alone (n = 10 for $\alpha3$, $\beta2$ and ε subunits and n = 16 for $\gamma2$ subunits). It is noteworthy that maximal currents elicited by GABA were relatively small in $\alpha3\beta2\varepsilon$ receptors compared to $\alpha3\beta2$ and $\alpha3\beta2\gamma2$ receptors (Figure 3.3).

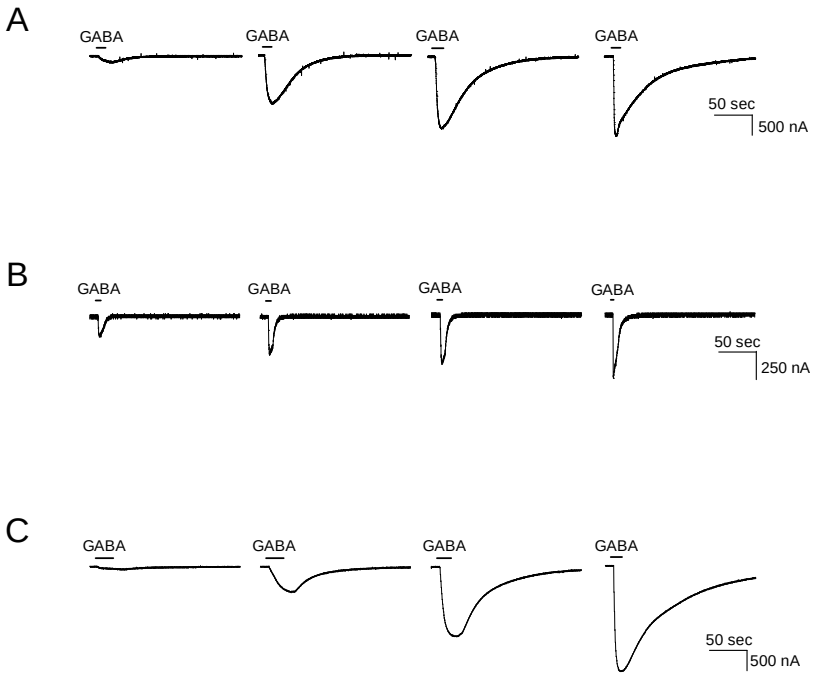

Figure 3.3: Sample current traces evoked by ascending GABA concentrations in oocytes expressing $\alpha3\beta2$ (A), $\alpha3\beta2\varepsilon$ (B) and $\alpha3\beta2\gamma2$ subunit receptors (C).
Sample currents were elicited by GABA concentrations of 1 µM, 10 µM, 100 µM and 1 mM. The holding potential was -60 mV.

Concentration-response curves of GABA as well as muscimol for the different receptor subtypes are depicted in Figures 3.4 and 3.5 and EC_{50} and Hill slope data obtained are summa-

rised in Table 3.1. EC_{50} values differed significantly between the receptor subtypes. $\alpha3\beta2\varepsilon$ receptors were the most sensitive receptors to both agonists, whereas the $\alpha3\beta2\gamma2$ receptor subtype was the least sensitive. In addition to the high agonist sensitivity, the $\alpha3\beta2\varepsilon$ receptor subtype also exhibited a moderate Hill slope for both agonists, whereas Hill slopes for the other two receptor types were more steep (Table 3.1).

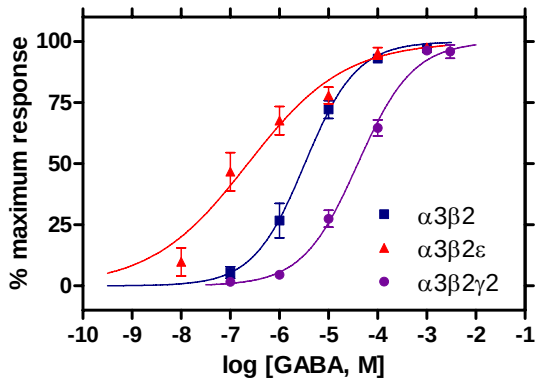

Figure 3.4: GABA concentration-response curves for $GABA_A$ receptors expressed in *Xenopus laevis* oocytes.

GABA concentration-response curves of $\alpha3\beta2$ (n = 11), $\alpha3\beta2\varepsilon$ (n = 12) and $\alpha3\beta2\gamma2$ receptor subtypes (n = 10). The data correspond to means ± SEM; n states the number of oocytes examined. EC_{50} values and Hill coefficients are presented in Table 3.1. Curves were fitted using a non-linear regression fit with variable slopes as described in Section 2.3.5.

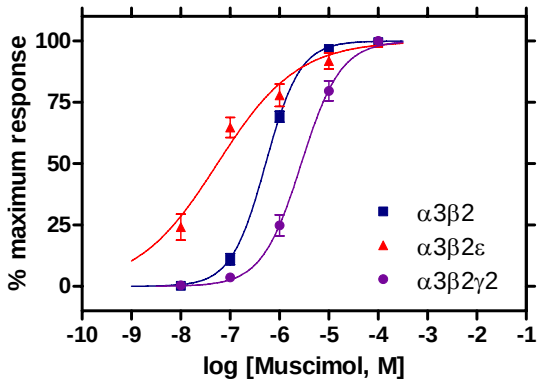

Figure 3.5: Muscimol activation of $GABA_A$ receptors expressed in *Xenopus laevis* oocytes.

Muscimol concentration-response curves of $\alpha3\beta2$ (n = 6), $\alpha3\beta2\varepsilon$ (n = 6) and $\alpha3\beta2\gamma2$ receptor subtypes (n = 7). Data correspond to means ± SEM; n represents the number of oocytes tested. EC_{50} values and Hill coefficients are presented in Table 3.1. Curves were fitted using a non-linear regression fit with variable slopes as described in Section 2.3.5.

Table 3.1: Effects of GABA and muscimol on different $GABA_A$ receptor subtypes

	GABA		Muscimol	
	EC_{50} (μM)	Hill slope	EC_{50} (μM)	Hill slope
$\alpha3\beta2$	3.30 ± 1.17 (n = 11)	0.82 ± 0.18	0.53 ± 1.65 (n = 6)	1.24 ± 0.14
$\alpha3\beta2\varepsilon$	0.23 ± 0.89 (n = 12)	0.44 ± 0.13	0.06 ± 1.02 (n = 6)	0.54 ± 0.06
$\alpha3\beta2\gamma2$	39.57 ± 1.35 (n = 10)	0.77 ± 0.10	2.77 ± 1.37 (n = 7)	1.08 ± 0.18

Data represent mean values (± SEM). EC_{50} and Hill slope values were obtained by non-linear regression fit with variable slopes as described in Section 2.3.5. n represents the number of oocytes used per experiment. GABA EC_{50} values were significantly different in oocytes expressing $\alpha3\beta2\varepsilon$ ($p < 0.001$) and $\alpha3\beta2\gamma2$ receptors ($p < 0.0001$), when compared with values obtained for $\alpha3\beta2$ receptors (unpaired t-tests). Likewise, muscimol EC_{50} values differed significantly in oocytes expressing $\alpha3\beta2\varepsilon$ ($p < 0.0001$) and $\alpha3\beta2\gamma2$ receptors ($p < 0.01$; compared to $\alpha3\beta2$ receptors).

3.2.2 Current-voltage relationships

Current-voltage relations for the $\alpha3\beta2$, $\alpha3\beta2\varepsilon$ and $\alpha3\beta2\gamma2$ $GABA_A$ receptor subtypes were determined by administrating submaximal GABA concentrations (EC_{20}) at different holding potentials (ranging from -90 to -10 mV; Figure 3.6). The reversal potential for $\alpha3\beta2$ receptors was -26.95 $\pm$ 1.96 mV (n = 5), for $\alpha3\beta2\gamma2$ receptors it was -20.57 $\pm$ 0.77 mV (n = 4) and for $\alpha3\beta2\varepsilon$ receptors -24.53 $\pm$ 6.99 mV (n = 6). These values are consistent with the chloride equilibrium potential in oocytes (approximately -25 mV) and, therefore, provide confirmation for chloride-ion flux across the membrane upon agonist binding (Dascal, 1987).

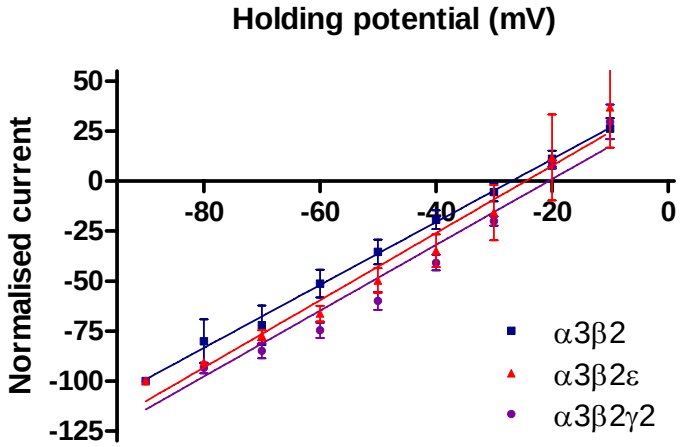

Figure 3.6: Current-voltage relationships of GABA-induced currents in *Xenopus* oocytes expressing $\alpha3\beta2$, $\alpha3\beta2\varepsilon$ and $\alpha3\beta2\gamma2$ receptors.

Reversal potentials for $\alpha3\beta2$, $\alpha3\beta2\varepsilon$ and $\alpha3\beta2\gamma2$ receptors were -26.95 $\pm$ 1.96 mV (n = 5), -24.53 $\pm$ 6.99 mV (n = 6) and -20.57 $\pm$ 0.77 mV (n = 4), respectively. Data represent x-axis intercepts $\pm$ SEM; n represents the number of oocytes examined. Data were fitted by linear regression analysis.

3.2.3 Effect of zinc

It is known that zinc ions inhibit $GABA_A$ receptor function and are most potent on α- and β-subunit-containing receptors and least potent on receptors containing α, β and γ subunits (Draguhn et al., 1990). Receptors containing the ε or δ subunits have been shown to exhibit medium sensitivity to zinc inhibition (Whiting et al., 1997; Krishek et al., 1998). Thus, zinc can be used as a marker for subunit co-assembly (i.e. relative insensitivity to zinc in-

dicates the existence of the γ subunit in the receptor complex). To verify correct subunit co-assembling, increasing concentrations of zinc with submaximal GABA concentrations (EC_{20}) were applied to *Xenopus* oocytes expressing $\alpha3\beta2$, $\alpha3\beta2\varepsilon$ or $\alpha3\beta2\gamma2$ receptor subtypes. GABA-induced currents in the receptor subtypes examined were inhibited with distinct potency by zinc (Figure 3.7). $GABA_A$ receptors containing the $\alpha3\beta2$ subunits were most sensitive to zinc inhibition with an IC_{50} value of 0.51 $\pm$ 1.18 µM (n = 7). Oocytes expressing $\alpha3\beta2\varepsilon$ receptors were about 90 times less sensitive to the action of zinc and exhibited an IC_{50} of 46.67 $\pm$ 1.08 µM (n = 8; $p < 0.01$, unpaired t-test). Receptors containing the $\alpha3\beta2\gamma2$ subunits were least sensitive to zinc. Their IC_{50} was 587.49 $\pm$ 1.17 µM (n = 7; $p < 0.01$, compared with $\alpha3\beta2$, unpaired t-test).

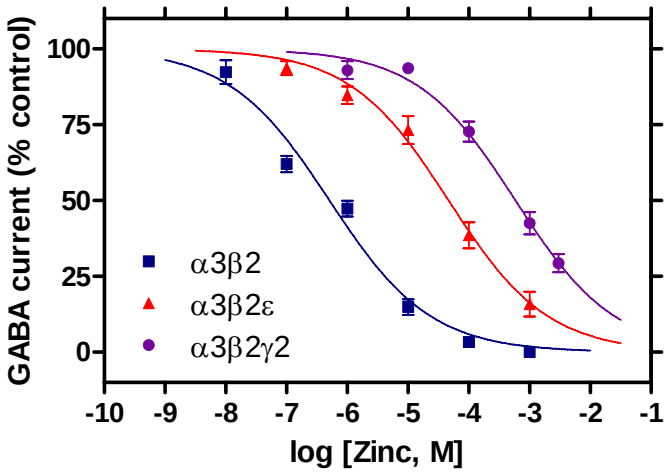

Figure 3.7: Zinc concentration-response curves for $GABA_A$ receptors expressed in *Xenopus laevis* oocytes.

Concentration-response curves for the inhibition of GABA (EC_{20} concentration) by zinc in oocytes expressing $\alpha3\beta2$ (n = 7), $\alpha3\beta2\varepsilon$ (n = 8) and $\alpha3\beta2\gamma2$ receptor subtypes (n = 7). Currents were normalised to the maximal response induced by GABA. IC_{50} values are specified in the text (Section 3.2.3). Data correspond to means $\pm$ SEM; n represents the number of oocytes examined. Curves were fitted using a non-linear regression fit with variable slopes as described in Section 2.3.5.

3.2.4 Application of the benzodiazepine flunitrazepam

In order to gain further confirmation for the correct subunit co-assembling, modulation by the benzodiazepine flunitrazepam was tested in oocytes expressing $\alpha3\beta2\gamma2$ and $\alpha3\beta2\varepsilon$ receptor subtypes, respectively. It is known that the benzodiazepine binding site consists of residues

from both α and γ subunits (Pritchett et al., 1989b) and ε-subunit-containing receptors are insensitive to benzodiazepines (Whiting et al., 1997). Currents evoked by GABA (EC_{20}) were enhanced with 1 µM flunitrazepam by 68.5 $\pm$ 10.01 % (compared to GABA alone) in oocytes expressing $\alpha 3\beta 2\gamma 2$ receptors (n = 4). This positive receptor modulation further verified presence and assembly of the γ subunit into the receptor complex. In contrast, $\alpha 3\beta 2\varepsilon$ receptors showed no response to 1 µM flunitrazepam administration (97.26 $\pm$ 2.33 % of GABA control response, n = 6, $p < 0.0001$; see Figure 3.8).

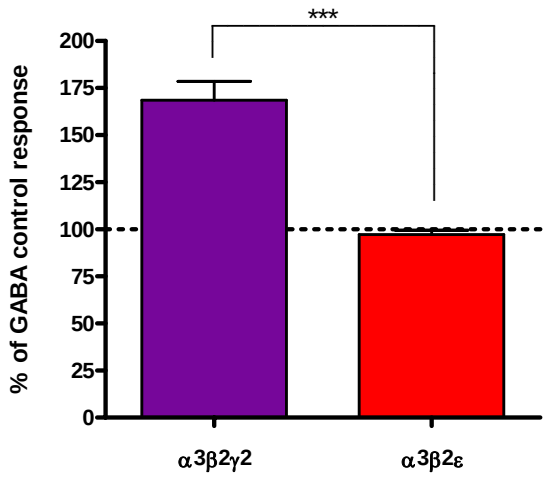

Figure 3.8: Effect of flunitrazepam on $GABA_A$ receptors expressed in *Xenopus laevis* oocytes.

*Oocytes expressing $\alpha 3\beta 2\gamma 2$ receptors were positively modulated by 1 µM flunitrazepam (168.5 $\pm$ 10.01 % of GABA control response, n = 4); data were determined by application of GABA (EC_{20}) alone (control) or co-administered with 1 µM flunitrazepam. In contrast, flunitrazepam did not affect GABA-control currents in oocytes expressing the $\alpha 3\beta 2\varepsilon$ receptor subtype (97.26 $\pm$ 2.33 % of control response, n = 6). Currents were normalised to the maximal response induced by GABA at EC_{20} concentrations. Columns represent mean values ($\pm$ SEM). *** indicates a significant difference between the two receptor subtypes ($p < 0.0001$).*

3.2.5 Constitutive activity of the $\alpha 3\beta 2\varepsilon$ $GABA_A$ receptor subtype

Previous studies have shown that ε-subunit-containing receptors exhibit spontaneous activity in the absence of GABA (Neelands et al., 1999; Davies et al., 2001; Maksay et al., 2003; Wagner et al., 2005). It was also noticed that those receptors required an unusually large holding current to clamp the cells at a specific voltage. The latter was also evident in

this study and it was tested whether $\alpha3\beta2\varepsilon$ receptors also exhibit constititive receptor activity. Administration of 100 µM picrotoxin to oocytes expressing $\alpha3\beta2\varepsilon$ receptors caused clear "outward" currents of 21.49 $\pm$ 1.98 % (of total response capacity (maximal GABA response + response to picrotoxin = 100 %), n = 8; Figure 3.9 B), indicating agonist-independent receptor activity. In contrast, picrotoxin had only a marginal effect on oocytes expressing $\alpha3$ and $\beta2$ subunits (n = 5; Figure 3.9 A). Furthermore, it was evident throughout all experiments that oocytes expressing $\alpha3\beta2\varepsilon$ receptors exhibited large baseline (leak) currents when clamped at -60 mV.

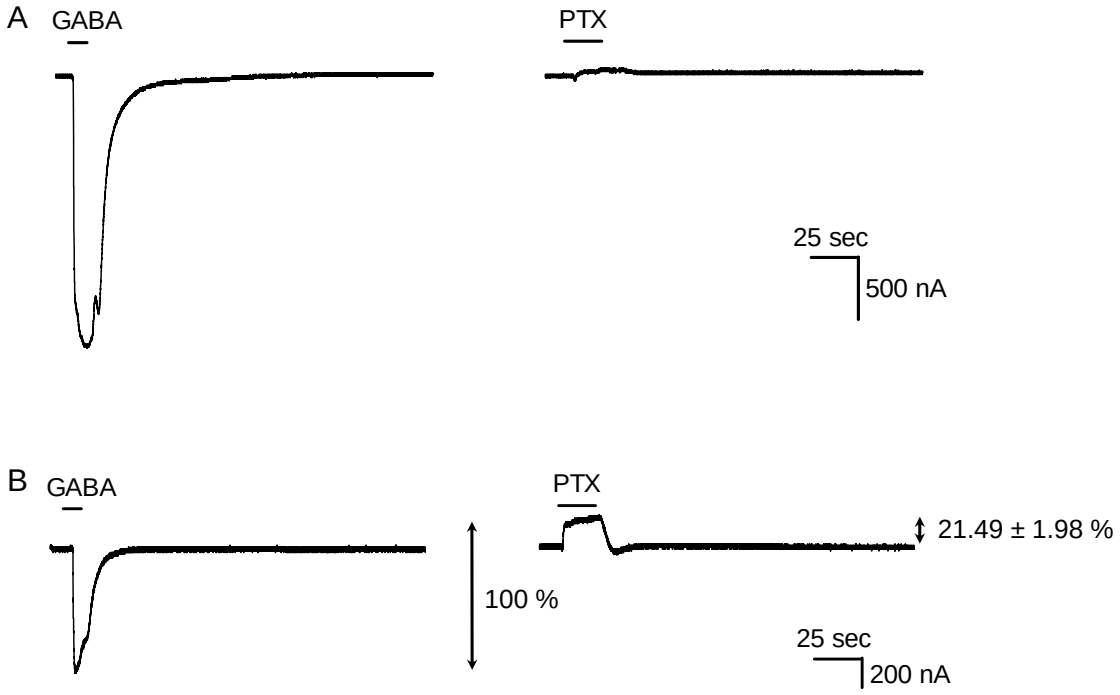

Figure 3.9: Representative current traces evoked by 1 µM GABA and 100 µM picrotoxin in oocytes expressing $\alpha3\beta2$ subunits (A) and by 1 mM GABA and 100 µM picrotoxin in oocytes expressing $\alpha3\beta2\varepsilon$ receptor subtypes (B).

3.2.6 Effect of etomidate on $\alpha3\beta2\varepsilon$ $GABA_A$ receptors

Anaesthetics, such as etomidate, exhibit potentiation and at high concentrations direct activation of $GABA_A$ receptors (Thompson et al., 1996; Pistis et al., 1997). The receptor modulation has been shown to be dependent on the type of β subunit expressed in the receptor

subtype (Hill-Venning et al., 1997). Here, the influence of the presence of the ε subunit in the $\alpha3\beta2$ receptor complex was investigated in view of modulation and direct activation by etomidate. Data were compared with those obtained for the $\alpha3\beta2$ receptor subtype. Etomidate enhanced GABA-elicited currents (EC_{20}) in oocytes expressing the latter by up to 402.1 $\pm$ 77.27 % (n = 8; Figure 3.10 A and C). In contrast, the level of etomidate efficacy was greater in oocytes expressing the $\alpha3\beta2\varepsilon$ receptors (up to 917.3 $\pm$ 83.45 %; n = 7; Figure 3.10 B and C). However, $\alpha3\beta2\varepsilon$ receptors were significantly less sensitive to etomidate (EC_{50} 13.34 $\pm$ 1.18 µM; $p < 0.0001$) compared to $\alpha3\beta2$ receptors (EC_{50} 1.71 $\pm$ 0.31 µM). Both receptor subtypes were also activated in the absence of GABA by 100 µM etomidate alone. Oocytes expressing the $\alpha3\beta2\varepsilon$ receptor showed a greater level of activation (651.5 $\pm$ 57.35 % of GABA control response (EC_{20}), n = 6) compared to $\alpha3\beta2$ receptors (146.7 $\pm$ 1.24 % of GABA control response, n = 3; Figure 3.10 D).

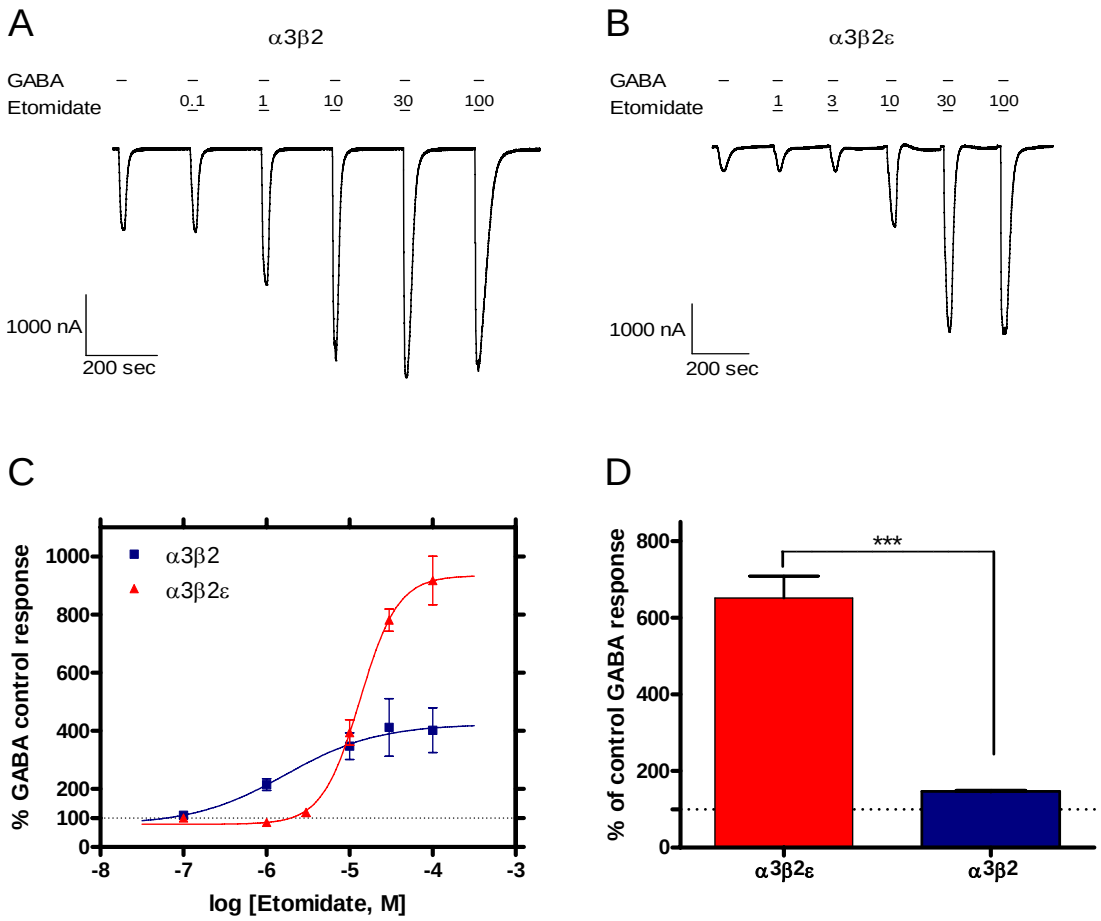

Figure 3.10: Effect of etomidate on oocytes expressing $\alpha3\beta2$ and $\alpha3\beta2\varepsilon$ receptor subtypes, respectively.

*(A) and (B) Current traces evoked by application of GABA (EC_{20}) alone or with successive concentrations of etomidate (in µM) in oocytes expressing the $\alpha3\beta2$ (A) and $\alpha3\beta2\varepsilon$ receptor subtypes (B). Horizontal bars represent drug application. (C) Etomidate concentration-response relationships were determined by administering increasing concentrations of etomidate with GABA (EC_{20}). Application of GABA at EC_{20} concentrations alone served as control (set to 100 %). Datapoints are means ± SEM (n = 8 for $\alpha3\beta2$ and n = 7 for $\alpha3\beta2\varepsilon$). Curves were fitted using a non-linear regression fit with variable slopes as described in Section 2.3.5. Currents were normalised to the maximal response induced by GABA at EC_{20} concentrations. EC_{50} values are specified in the text (Section 3.2.6); n represents the number of oocytes examined. (D) Columns represent mean direct activation of the receptors by 100 µM etomidate (± SEM; $\alpha3\beta2$ receptor activation: 146.7 ± 1.24 % of GABA control response, n = 3; $\alpha3\beta2\varepsilon$ receptor activation: 651.5 ± 57.35 % of GABA control response, n = 6). Currents were normalised to the maximal response induced by GABA at EC_{20} concentrations. *** indicates a significant difference between the two receptor subtypes ($p < 0.001$).*

3.2.7 Expression of a truncated ε splice variant

Recently, Kasparov et al. (2001) described a truncated ε subunit version (ε_T) expressed in the rat brain that exhibits a 26 amino acid deletion starting in the middle of TM2 of the subunit. The ε_T subunit was generated using site-directed mutagenesis and co-expressed with $\alpha3$ and $\beta2$ subunits in *Xenopus laevis* oocytes, in order to investigate, whether the ε_T subunit could form functional channels with $\alpha3$ and $\beta2$ subunits *in vitro*. Initially, GABA concentration-response relations were investigated (see Figure 3.11 A). EC_{50} values for $\alpha3\beta2\varepsilon_T$ receptors were 6.48 $\pm$ 0.98 µM (Hill slope: 0.7 $\pm$ 0.24, n = 6). These results were very similar to results obtained for the $\alpha3\beta2$ receptor (EC_{50}: 3.30 $\pm$ 1.17 µM, p = 0.07; see Section 3.2.1). Furthermore, the concentration-response curves to zinc inhibition for these two receptor types were also greatly similar (IC_{50} 0.78 $\pm$ 0.84 µM, n= 7, p = 0.33, compared to results obtained for $\alpha3\beta2$ receptors; Figure 3.11 B). These findings suggest that the ε_T subunit examined here was probably not incorporated into functional channels in *Xenopus laevis* oocytes and channels expressed consisted solely of $\alpha3\beta2$ receptors.

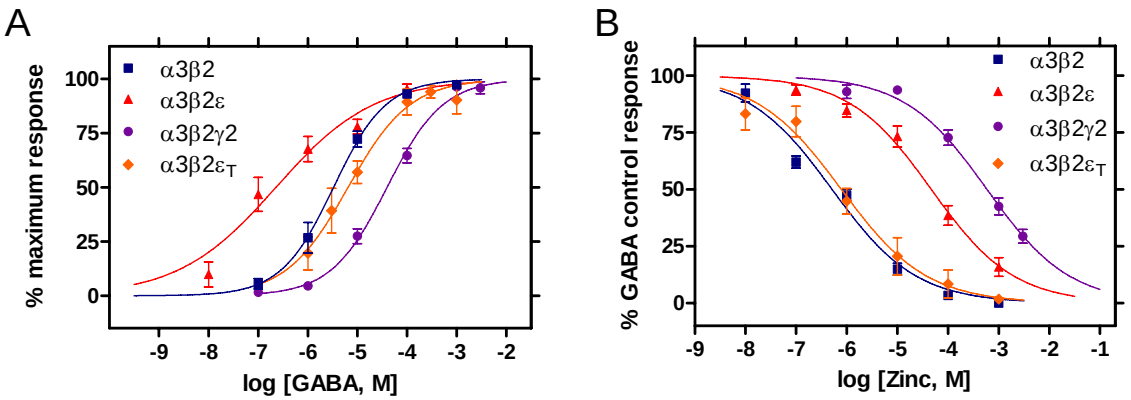

Figure 3.11: Concentration-response curves for GABA activation and zinc inhibition in oocytes expressing $\alpha3\beta2\varepsilon_T$ receptor subtypes.

(A) GABA concentration-response curves of $\alpha3\beta2$ (n = 11), $\alpha3\beta2\varepsilon$ (n = 12), $\alpha3\beta2\gamma2$ (n = 10) and $\alpha3\beta2\varepsilon_T$ receptor subtypes (n = 6). EC_{50} values are specified in the text (Sections 3.2.1 and 3.2.7). (B) Concentration-response curves for the inhibition of an EC_{20} concentration of GABA by zinc in oocytes expressing $\alpha3\beta2$ (n = 7), $\alpha3\beta2\varepsilon$ (n = 8), $\alpha3\beta2\gamma2$ (n = 7) and $\alpha3\beta2\varepsilon_T$ receptor subtypes (n = 7). Currents were normalised to the maximal response induced by GABA at EC_{20} concentrations; IC_{50} values are specified in the text (Sections 3.2.3 and 3.2.7). Data correspond to means $\pm$ SEM; n represents the number of oocytes examined. Curves were fitted using a non-linear regression fit with variable slopes as described in Section 2.3.5.

3.3 Discussion

3.3.1 Pharmacological characteristics of the ε subunit

The $GABA_A$ receptor ε subunit represents a minor subunit population with restricted expression pattern in the brain. There have been only a few studies investigating the functions and characteristics of recombinant and native receptors, and the exact role, receptor subtype structure, and assembling characteristics remain widely unknown. In this study, co-expression of the ε subunit with the $\alpha3$ subunit (both genes are clustered on the Xq28 chromosome; Wilke et al., 1997) and the $\beta2$ subunit, which is the most widespread β subunit in the brain (Olsen & Sieghart, 2008), were examined. It is likely that $\alpha3$ and $\beta2$ subunits form functional receptors with the ε subunit in some areas of the brain. The data obtained emphasise that the inclusion of the ε subunit into the $\alpha3\beta2$ $GABA_A$ receptor complex confers distinct pharmacological properties to the receptor which also differ significantly from properties of $\alpha3\beta2\gamma2$ receptors.

The inclusion of the ε subunit conferred high GABA sensitivity to the $\alpha3\beta2$ receptor subtype and results obtained were consistent with results seen in previous studies by Neelands et al. (1999) and Whiting et al. (1997), although in these latter studies the $\alpha1$ instead of the $\alpha3$ subunit was expressed with the ε and $\beta3$ or $\beta1$ subunits, respectively. In contrast, Ranna et al. (2006) expressed $\alpha3\beta1\varepsilon$ receptor subtypes and reported a reduced sensitivity to GABA compared to $\alpha1$- and ε-subunit-containing receptors (Whiting et al., 1997; Neelands et al., 1999). A study by Ebert et al. (1994) demonstrated reduced GABA sensitivity in $\alpha3\beta1\gamma2$ receptors, compared to $\alpha3\beta2\gamma2$ receptors and it was shown that both α and β subunits are able to contribute to the affinity to GABA (Ebert et al., 1994; Ducic et al., 1995). This could explain the differences observed in this study compared to the work by Ranna et al. (2006). Muscimol is a structural GABA analogue found in the mushroom *Amanita muscaria* (Snodgrass, 1978) and its potency is known to be higher when compared to GABA (Harris et al., 1997). Consistent with this, in this study, all receptor subtypes expressed showed higher sensitivity to muscimol compared to GABA. Again, ε-containing receptors were the most potent subtype to the agonist.

The Hill coefficients of GABA and muscimol agonist curves measured in oocytes expressing $\alpha3\beta2\varepsilon$ receptors were lower when compared to Hill slopes of $\alpha3\beta2$ and $\alpha3\beta2\gamma2$ receptors. This was also reported previously by Maksay et al. (2003) and Whiting et al. (1997). The reason for this is not known. In contrast to $\alpha\beta$ or $\alpha\beta\gamma$ receptors, which usually need binding of two agonist molecules to sufficiently open the receptor channel, ε-subunit-containing receptors may have only one agonist binding site, as described above (Section 1.2.5.1, Chapter 1; Jones & Henderson, 2007; Bollan et al., 2008). The low Hill coefficient seen in ε-containing receptors would support the hypothesis of one agonist binding site in ε-containing receptors, because the Hill slope reflects the minimal number of interacting binding sites in positively cooperating reactions (Abeliovich, 2005). However, an additional explanation could be that the lower Hill slopes are partly due to the increased desensitisation rate seen in ε-subunit-containing receptors, since desensitisation also influences the Hill coefficient (Celentano & Wong, 1994; Dominguez-Perrot et al., 1996; Whiting et al., 1997).

Zinc inhibition has been suggested to be a good marker for correct $GABA_A$ receptor assembly, as $GABA_A$ receptors containing α and β subunits are highly sensitive to zinc inhibition, whereas receptors which include the γ subunit are less affected by the action of zinc (Draguhn et al., 1990). Receptors containing the δ or ε subunit have been shown to exhibit medium sensitivity to zinc inhibition. The results obtained here were in consent with this information. IC_{50} values for all three receptor subtypes were similar to the results obtained by Neelands et al. (1999) and Whiting et al. (1997) and indicated correct subunit co-assembling of the three receptor subtypes by showing significant differences in sensitivity to zinc inhibition.

It is well known that the presence of the γ subunit within the $GABA_A$ receptor complex is needed for benzodiazepine binding to the receptor and recombinant receptors, substituting the γ with the ε subunit, have been shown to be insensitive to benzodiazepine modulation (Davies et al., 1997; Whiting et al., 1997). Here, the benzodiazepine flunitrazepam was applied to further test the correct assembly of $\alpha3\beta2\varepsilon$ and $\alpha3\beta2\gamma2$ receptors. As expected, GABA-induced currents in $\alpha3\beta2\gamma2$ receptors were potentiated by 1 µM flunitrazepam, whereas the current measured in oocytes expressing the $\alpha3\beta2\varepsilon$ receptor remained unchanged to

the GABA-evoked control response. Although there is a lack of a benzodiazepine binding site in ε-containing receptors, there may be a similar modulatory site for a yet unknown compound at the interface of ε and α subunits.

Sensitivity of $GABA_A$ receptors to the intravenous anaesthetic etomidate is known to be dependent on the β subunit expressed in the receptor subtype, with $\beta2$ and $\beta3$ subunits being highly sensitive to etomidate potentiation compared to the $\beta1$ subunit, which is least sensitive (Belelli et al., 1997; Hill-Venning et al., 1997). Etomidate potentiates $GABA_A$ receptors at lower concentrations as well as directly activates receptors at high concentrations. It was shown that the ε subunit confers distinct pharmacological properties in response to etomidate when incorporated into the $\alpha3\beta2$ $GABA_A$ receptor. Currents evoked by submaximal GABA concentrations (EC_{20}) were enhanced to a greater level in $\alpha3\beta2\varepsilon$ receptors compared to $\alpha3\beta2$ receptors. However, inclusion of the ε subunit into the $\alpha3\beta2$ receptor complex resulted in an approximately eightfold higher EC_{50} value compared to the $\alpha3\beta2$ receptor. Previous studies had also shown that including a third subunit, γ or ε, into the $\alpha\beta$ receptor complex reduces the potency of certain anaesthetic agents (Thompson et al., 1998). Etomidate at high concentrations triggered a GABA-mimetic effect in both receptor subtypes. The potentiation of the GABA-control response, however, was greater in $\alpha3\beta2\varepsilon$ receptors compared to $\alpha3\beta2$ receptors. Previous studies by Thompson et al. (1998) demonstrated a greater level of potentiation in $\alpha1\beta2$ compared to $\alpha1\beta2\varepsilon$ receptors. The reason for this difference is not clear, since the β subunit is the major determinant of sensitivity to the modulating effects of etomidate (Hill-Venning et al., 1997). Nevertheless, Hill-Venning et al. (1997) showed that $\alpha3$-subunit-containing receptors can contribute to differences in maximal potentiation by etomidate compared to other α subunits, and Ranna et al. (2006) and Thompson et al. (1998) demonstrated that the inclusion of the ε subunit into $\alpha\beta1$ receptors can have some influencing effects on GABA-mimetic properties. It was shown that direct receptor activation by etomidate is normally minimal or absent in receptors containing the $\beta1$ subunit. However, inclusion of the ε into the receptor complex resulted in small direct effects.

As also seen in previous recombinant expression studies, receptors containing the ε subunit exhibited spontaneous receptor activity (Whiting et al., 1997; Neelands et al., 1999; Maksay

et al., 2003). The level of spontaneous activity in $\alpha3\beta2\varepsilon$ receptors was similar to the results obtained by Mortensen et al. (2003) expressing $\alpha1\beta3\varepsilon$ receptors in *Xenopus* oocytes. Furthermore, a large holding current was required to sustain a potential of -60 mV in *Xenopus laevis* oocytes, which was not seen in the other receptor combinations investigated, indicative for constitutive receptor activity (Neelands et al., 1999; Maksay et al., 2003). This was confirmed when applying picrotoxin, a channel blocking agent, to oocytes expressing the receptor, resulting in "outward" currents, which demonstrated the blockade of spontaneously open channels (Maksay et al., 2003). Several amino acids located in the channel-lining TM2 are involved in chloride conduction, sensitivity to channel blockers and channel gating of $GABA_A$ receptors and the related nAChRs (Filatov & White, 1995; Labarca et al., 1995; Scheller & Forman, 2002). Different mutations of amino acids in the TM2 have identified several residues that increase unliganded openings of the receptors and play a role in channel gating, for example the 9' leucine residue. Another residue critical for channel gating is the 15' serine residue. Mutations of the latter amino acid residue have been shown to influence channel gating and spontaneous receptor activity in $\beta1$, $\alpha1$ and $\alpha2$ $GABA_A$ receptor subunits (Findlay et al., 2001; Scheller & Forman, 2002; Miko et al., 2004). The ε subunit is the only $GABA_A$ receptor subunit with a glycine residue at this position. Point mutations of the 15' serine in $\beta1$ subunits to glycine or tryptophan increased spontaneous currents blocked by picrotoxin (Findlay et al., 2001; Miko et al., 2004). Therefore, it is likely that the presence of the glycine residue at this position entails constitutive receptor activity in ε-containing receptors (Wagner et al., 2005). As mentioned before, whether or not native ε-containing receptors exhibit constitutive activity is still not clear, and functional implications of such a receptor type *in vivo* would depend on many factors, such as the location of the receptor.

It is important to verify the correct receptor assembly, because it is known that $\alpha3\beta2\gamma2$ receptors can sometimes assemble as a mixture of $\alpha3\beta2$ and $\alpha3\beta2\gamma2$ receptors (Boileau et al., 2002, 2003). However, Jones & Henderson (2007) showed by applying zinc with high GABA concentrations that the majority of receptors formed by α, β and ε subunits consisted of all three subunits at a transfection ratio of 1:1:1 and $\alpha\beta$ receptors are mostly absent. To verify correct subunit co-assembling, it was shown that $\alpha3\beta2\gamma2$ receptors were

relatively insensitive to zinc and GABA-control responses were enhanced by application of flunitrazepam. $\alpha 3\beta 2\varepsilon$ receptors were also assembled correctly, which was demonstrated by medium zinc sensitivity, an outward current after the application of the channel blocker picrotoxin, a high leak current when voltage clamped at -60 mV and relatively small GABA-evoked currents compared to currents obtained from other receptor subtypes.

3.3.2 Investigation of a truncated ε subunit variant

Several previous studies reported a number of different splice variants seen in the human and rodent ε subunit (Whiting et al., 1997; Sinkkonen et al., 2000; Kasparov et al., 2001). In rodent brain, an appropriate spliced mRNA, a large version, including a Pro/Glx motif, and a truncated version have been described. The latter exhibits a 26 amino acid deletion in the second putative TM domain. Since such a deletion would have a major impact on receptor structure and function, and the role of the ε subunit is still not understood, it was investigated whether the truncated version would form functional receptors with the $\alpha 3$ and $\beta 2$ subunit in *Xenopus laevis* oocytes. GABA concentration-response relationships were very similar to the ones seen in $\alpha 3\beta 2$ receptors. The same applied to the inhibition of the receptor by zinc. These results suggested that the truncated subunit is not incorporated into the receptor, which does not seem to come as a surprise, due to the fact that amino acids of the TM2 and the entire extracellular loop between TM2 and TM3 are missing. Those amino acids have been shown to be important for channel pore formation (TM2) and channel gating upon agonist binding (extracellular loop between TM2 and TM3). Therefore, a deletion would have a major impact on receptor structure and function (Smith & Olsen, 1995; Kash et al., 2004). Furthermore, a recently published study by Pape et al. (2009) showed Western blot analysis of ε subunit expression in the spinal cord and hypothalamus of twelve days old rats. The results revealed a 70 kDa band (appropriate spliced ε subunit) and a large ε subunit version of 120 kDa (the large version described by Moragues et al. (2000)), but no band which would correspond to the truncated version. These findings indicate that the truncated version is not translated into proteins in these brain regions, which would support our results. Although a number of ε splice variants have been investigated, none of the splice forms have

been shown to be incorporated into functional receptors *in vitro* or *in vivo* up until now.

3.3.3 Summary

In summary, the rat $GABA_A$ receptor ε subunit as well as a truncated ε splice version together with the $\alpha3$ and $\beta2$ subunits were co-expressed in *Xenopus laevis* oocytes and pharmacological properties of $\alpha3\beta2\varepsilon$ receptors were examined. This subunit combination has not been investigated previously, but it is likely that $\alpha3\beta2\varepsilon$ receptors exist in certain areas of the brain *in vivo*. Data obtained revealed that the $\alpha3\beta2\varepsilon$ receptor exhibits unusual pharmacological characteristics, previously described in other ε-subunit-containing receptor subtypes. Furthermore, it was shown that receptors were enhanced to a greater level by the anaesthetic etomidate compared to $\alpha3\beta2$ receptors. However, as stated previously, inclusion of a third subunit into the $\alpha\beta$ receptor complex also lowered etomidate potency in $\alpha3\beta2\varepsilon$ receptors. So far, no subunit-selective pharmacology could be recognised. Nevertheless, the ε subunit may represent an important pharmaceutical target for future drug development and further research is needed to uncover the promiscuous role of this subunit. It was also shown that the truncated ε splice variant was not included into functional $\alpha3\beta2$ receptor channels in *Xenopus laevis* oocytes.

Chapter 4

Development of an assay to screen compound libraries

4.1 Introduction

The structural diversity of $GABA_A$ receptors and the plethora of drug binding sites make them attractive targets for drug discovery, especially since it was demonstrated that the various subunits regulate different drug effects (Section 1.2.4, Chapter 1; Möhler, 2006). Although several studies have been conducted in order to identify the pharmacological profile of ε-subunit-containing receptors, no subunit-specific pharmacology could be identified (Davies et al., 1997; Whiting et al., 1997; Thompson et al., 1998; Neelands et al., 1999; Maksay et al., 2003; Ranna et al., 2006). However, these receptors possibly have specific modulatory binding sites which may be important for future drug development. The next aim of this project was to set up a cell-based system to screen the ε-containing receptor against compounds from a commercially available library and, with luck, to identify compounds that modulate this specific $GABA_A$ receptor subtype.

As described in Section 1.3, Chapter 1, screening ion channels for modulating compounds is a challenging research area, however, several assay technologies are available. Electrophysiological recordings are the gold standard method to measure ion channel function (Smith & Simpson, 2003; Verkman & Galietta, 2009). However, they are very labour intensive

and, hence, time consuming. Therefore, in the majority of studies the primary screening for compounds is performed via high throughput assays to detect lead compounds. Many screening methods require specialised measurement devices, such as voltage/ion probe readers, FLIPRs or scintillation counters and only few can be set up easily and at low costs using commercially available measuring devices. In this project, a suitable method was sought to screen ε-subunit-containing $GABA_A$ receptors for novel modulatory compounds. Such compounds are thought to be important to uncover the role of the $GABA_A$ receptor ε subunit and they may even act as future drugs on these receptor subtypes. The assay technologies applied in this study were first set up using $\alpha3\beta2$ or $\alpha3\beta2\gamma2$ receptors before testing constitutively open ε subunit receptors, which may add some additional challenges to the setup.

4.1.1 Clomeleon

GFP was originally isolated from jellyfish (*Aequorea victoria*) and has been used extensively in the field of molecular biology as a fluorescence probe (Tsien, 1998; Wachter et al., 1998). YFP, a derivative of GFP, exhibits enhanced brightness and a longer wavelength compared to other GFP variants. It is the only fluorescent protein that can be quenched by small anions and, thus, it can be used as a chloride-ion indicator (Wachter & Remington, 1999; Jayaraman et al., 2000). Kuner & Augustine (2000) have constructed a FRET-based, ratiometric, genetically-encoded chloride-ion indicator protein termed Clomeleon. It was generated by linking a CFP, which is insensitive to chloride, to a YFP using a flexible recombinant Tobacco Etch Virus (rTEV) protease peptide linker. In the absence or at low concentrations of chloride in the cell, upon excitation of the CFP, Clomeleon emits energy to the YFP, which can be measured at ~530 nm (Figure 4.1 A). At rising concentrations of chloride (e.g. upon $GABA_A$ receptor activation), chloride binds to the YFP. This changes its absorption coefficient and leads to a reduction of the FRET efficacy and increased CFP emission that can be measured at 485 nm (Figure 4.1 B, C). The ratio of fluorescence emission of the YFP to that of the CFP is chloride concentration dependent.

Clomeleon has been shown to be a good indicator of intracellular chloride concentrations in living cells, for example neurons, as well as in transgenic mice, where it was used to

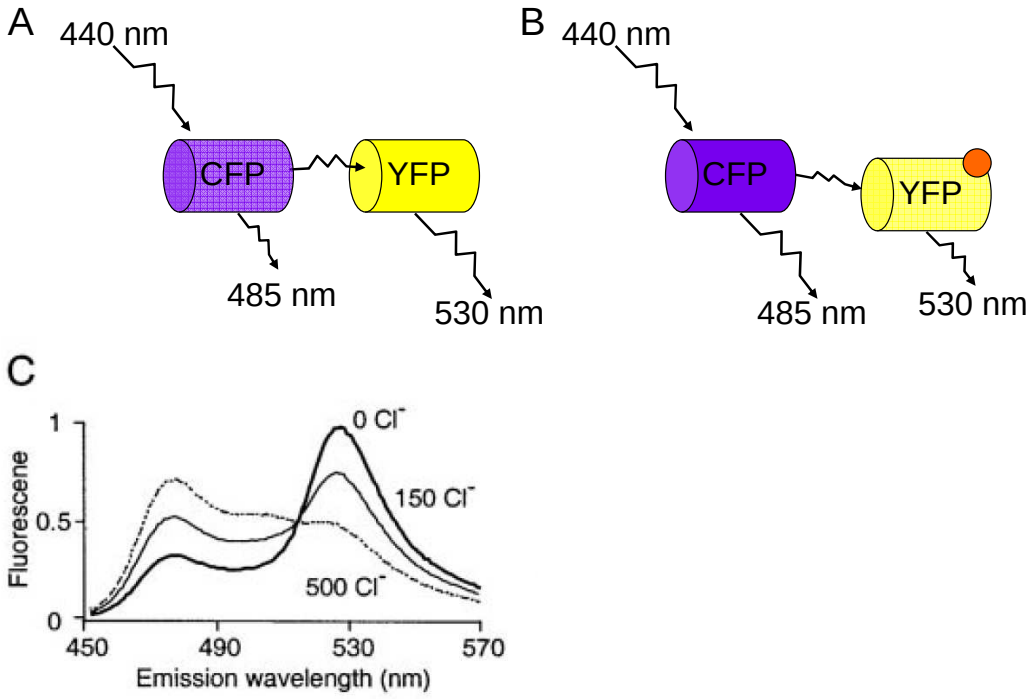

Figure 4.1: Clomeleon is a FRET-based chloride-indicator protein consisting of two distinct fluorescence proteins.

(A) At no or low concentrations of chloride, the excited CFP (donor) transfers most of its energy to the linked YFP (acceptor). (B) If chloride (depicted as orange circle) binds to the YFP, FRET efficiency is reduced leading to increased CFP emission. (C) Emission spectrum of Clomeleon in the presence of different concentrations of chloride ions (in mM; from Kuner & Augustine, 2000).

monitor chloride distribution and concentration changes (Kuner & Augustine, 2000; Haverkamp et al., 2005; Duebel et al., 2006; Berglund et al., 2008). It was also applied to measure chloride shifts after $GABA_A$ receptor activation in cultured hippocampal neurons (Kuner & Augustine, 2000). However, it has not been used in compound screening assays before. Clomeleon has several advantages over other chloride indicators: it has a good signal-to-noise ratio, cannot be influenced by other physiologically important anions, it can be easily loaded into cells via transfection methods, its fluorescence is very stable and it can be targeted to specific locations/cells (Kuner & Augustine, 2000; Bregestovski et al., 2009). Its relative large size (~59 kDa) prevents diffusion from the cell and it is possible to determine absolute chloride concentration changes. However, there are several disadvantages, including its sensitivity to pH changes, the slow response kinetics and low chloride affinity as well as the different bleaching of the CFP and YFP. This could lead to an overestimation of the chloride concentration and, thus, careful setup and optimisation are important for a successful application.

In this study, it was examined whether Clomeleon can be used in a cell-based screening assay by expressing it together with $GABA_A$ receptors in HEK293 cells. The cells were seeded into 96-well microtitre plates and it was tested whether $GABA_A$ receptor activation would result in a fluorescence shift from 530 to 485 nm by comparing the baseline fluorescence before adding the receptor agonist with the fluorescence signal afterwards. If GABA application could elicit a change of the fluorescence signal, the compound screening assay could be optimised.

4.1.2 Iodide-flux method

Chloride ion channels are not only permeable to chloride, but also to other small anions, namely NO_3^-, Br^-, I^-, HCO_3^-, SCN^- and small organic acids (Tang & Wildey, 2004; Verkman & Galietta, 2009). However, chloride is the most abundant anion in biological systems, hence, the name chloride channels. Anions can pass through the channels in either direction (influx or efflux) according to the electrochemical driving force. Movement of ions can be directly quantified using ion flux assays, which can be used to characterise ion channel functions.

Flux assays often employ radiolabelled tracers, such as $^{36}Cl^-$ or $^{125}I^-$. Ion channels are activated in the presence of a known concentration of tracer ions and ion flux through the opened channels takes place. Subsequently, the medium is moved to a new plate, cells are lysed and radioactive tracer concentration in both cell lysate and medium, are measured. Receptor activity, inhibition or modulation can be detected by determining the ratio of intracellular to extracellular radioactivity. The signal strength is dependent on tracer ion concentration and the number of cells (Gill et al., 2003). Screening assays using radiolabelled tracer molecules are robust, easy to perform and provide data with high sensitivity. However, there are some major concerns with this method. The application of radioactive tracers raises safety issues and also implies relatively high costs of the material and the special requirements for its disposal.

In this project a non-radioactive, colorimetric iodide-flux assay was tested, where iodide acts as the indicator of chloride channel activity (Tang & Wildey, 2004, 2006). The assay was derived from the Sandell-Kolthoff (SK) reaction (Sandell & Kolthoff, 1937; Tang & Wildey, 2004):

$$Ce^{4+}(yellow) + As^{3+} \xrightarrow{I^-} Ce^{3+}(colourless) + As^{4+} \tag{4.1}$$

The principle of the reaction is that the iodide catalyses the conversion of yellow-coloured cerium ions (Ce^{4+}) to colourless Ce^{3+} by arsenic III acids. The remaining Ce^{4+} in the sample can be detected by reading the absorbance at a wavelength of 405 nm. The OD405 readings enable to draw conclusions to the intra- and extracellular iodide concentrations and, thus, ion flux upon receptor activation (Figure 4.2).

The colorimetric ion flux technology has the advantages of lower costs and improved safety. Furthermore, the method does not require a confluent cell monolayer and already small concentrations of iodide can be detected due to the low intracellular concentration (Tang & Wildey, 2004). Since test compounds are removed from the cells after incubation, there is also the benefit that they cannot interfere with the assay readout of the lysed cells, a problem that commonly leads to false positive results in other screening formats, such as fluorescence-based methods. However, flux assays have certain disadvantages, including

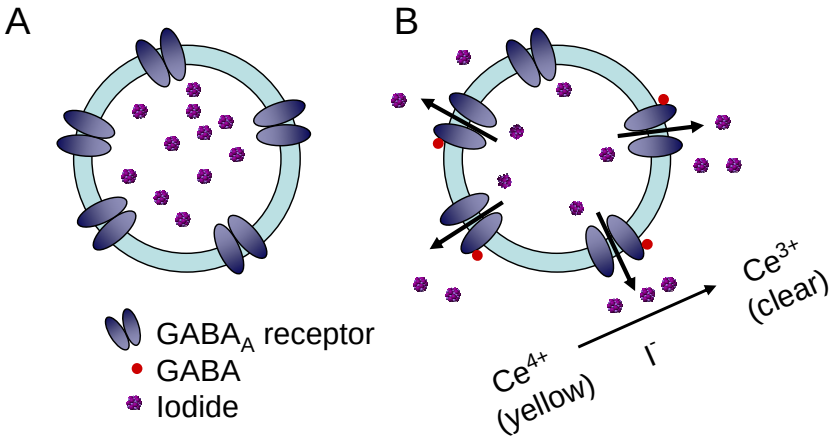

Figure 4.2: Assay principle of the colorimetric iodide-flux assay.
(A) Iodide-loaded cells in iodide-free solution. (B) Channels open upon agonist binding and iodide exerts into extracellular solution due to electrochemical gradient (adapted from Lynch, 2005)

low temporal resolution, the long cell-loading incubation times, low informational content, reduced reproducibility and a high signal-to-noise ratio that is influenced by the channel expression levels (Xu et al., 2001; Gill et al., 2003). A further drawback of the assay is the relative short stability of the sample-buffer mixture making a fast reading and optimal timing necessary. The high signal-to-noise ratio is presumably the reason why the assays Z'-factor obtained by Tang & Wildey (2004) was relatively low (0.42), which indicates a small signal detection window (Zhang et al., 1999). The Z'-factor provides a mean to assess the quality and optimisation of an assay in regard to the assay's signal dynamic range as well as data variation (Zhang et al., 1999). Z'-factors between 1 and 0.5 represent an assay with excellent quality, whereas smaller values indicate a smaller signal separation between the positive and negative controls. Values near zero or negative Z'-factors indicate that the assay was either not optimised or that a robust setup is not achievable in this format.

In this project, the iodide-flux assay was performed and optimised by expressing $\alpha 3\beta 2\gamma 2$ $GABA_A$ receptors in HEK293 cells, which were seeded into 96-well plates. Cells were loaded prior to the assay with iodide. Receptors were activated and iodide efflux from the cells was determined by performing the SK assay with both, cell lysates and supernatants. By assessing the OD405 readings, the iodide concentration in the samples, which gives information on the receptor activity, could be determined (Tang & Wildey, 2004; Lynch, 2005).

4.1.3 YFP-based assays

As displayed below, the attempted assays described before were not suitable for screening of $GABA_A$ receptors transiently expressed in HEK293 cells. Therefore, a further method was examined applying a YFP-based assay format. This assay was similar to the first assay examined, applying the chloride-indicator protein Clomeleon (Section 4.1.1), as it was based on the halide sensitivity of YFPs. However, the assay used a single fluorophore with increased sensitivity to halides that could be used to detect anionic influx into a cell using a fluorescence plate reader (Kruger et al., 2005).

Due to the fact that YFP has a low sensitivity to chloride, YFP variants were constructed, among others the YFP-H148Q (Wachter & Remington, 1999). This mutant version showed an improved sensitivity to chloride (K_d 100 mM; K_d represents the anion concentration at a half-maximal YFP quench) as well as iodide (K_d 21 mM; Jayaraman et al., 2000). Iodide does not occur naturally in cells and can be toxic at high concentrations. In order to prevent such effects, solutions applied to cells should contain low iodide concentrations. Hence, sensitivities for chloride and iodide of YFP-H148Q were still too low and YFPs with enhanced properties were sought. Galietta et al. (2001a) generated random mutations of certain amino acid residues at the halide binding site. This approach identified several mutant YFP variants that showed improved halide sensitivity. The mutant version YFP-H148Q/I152L exhibited a very high iodide affinity (K_d 3 mM) as well as improved chloride sensitivity (K_d 88 mM). Performing assays with iodide rather than chloride has the advantage that anion co-transporters or exchangers, for example NKCC (Na^+-K^+-Cl^- co-transporter) or AE1 (anion exchanger 1), transport iodide less efficiently than chloride (Galietta et al., 2001b).

In this project, the YFP mutant version YFP-H148Q/I152L was used as a chloride-indicator protein in a cell-based screening assay as described by Kruger et al. (2005). It was shown that YFP-H148Q/I152L is suitable for screening assays by permitting detection of fluorescence signal changes upon $GABA_A$ receptor activation. This is because, in a medium that contains a high concentrations of iodide, activation of the $GABA_A$ receptor will result in a reduction of intracellular fluorescence as iodide enters the cell, which can be measured using

a fluorescence plate reader (Figure 4.3).

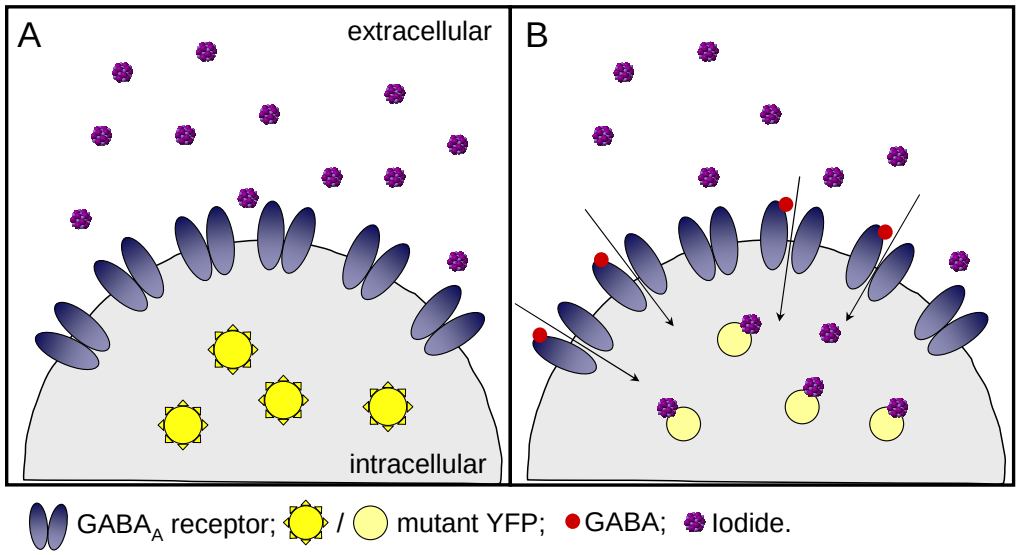

Figure 4.3: Schematic diagram showing the principle of the YFP-H148Q/I152L screening assay.

(A) Cells co-expressing the mutant YFP-H148Q/I152L and GABA$_A$ receptors were present in an iodide-containing solution. (B) GABA application triggers the channels to open and iodide enters the cells upon the electrochemical gradient. Subsequently, the YFP-H148Q/I152L inside the cells is quenched, reducing the fluorescence signal emitted.

This assay format has a range of advantages over other existing methods: (1) it does not require time-consuming cell loading or washing steps, (2) the YFP mutant version exhibits excellent optical properties and photostability, (3) it can be excited in the visible range of light, (4) it is genetically encoded and can be targeted to the required cell type, (5) its kinetics are faster compared to voltage-sensitive dyes, (6) due to its high molecular weight of 27 kDa, it is retained in cells and (7) stable expression of the protein(s) of interest is not required (Galietta et al., 2001b; Bregestovski et al., 2009; Gilbert et al., 2009a). A disadvantage of the YFP-H148Q/I152L is its relatively slow kinetics (Bregestovski et al., 2009). Nevertheless, different YFP mutant variants have successfully been used in screening assays of cystic fibrosis transmembrane conductance regulator protein (CFTR) chloride transport agonists (Galietta et al., 2001a). Furthermore, it was shown that the mutant YFP is suitable for HTS of GlyR and GABA$_A$ receptors (Kruger et al., 2005; Gilbert et al., 2009b).

4.2 Results

4.2.1 Evaluating a screening assay using Clomeleon

The chloride-sensitive protein Clomeleon was first scanned for its excitation and emission spectrum using a spectrofluorometer. This was to test protein functionality, because the DNA sequence acquired from sequencing differed in one amino acid from the sequence received from Dr Thomas Kuner. HEK293 cells were transfected with Clomeleon alone or Clomeleon and $\alpha 3\beta 2$ subunit receptors; untransfected cells served as negative control. Cells were excited at a wavelength of 440 nm and emission was scanned over a range of 460 to 650 nm. The obtained spectrum showed a large peak at a wavelength of 527 nm and a smaller peak at 475 nm (Figure 4.4). Control scans with untransfected cells, mammalian Ringer solution and the cuvette alone resulted in one or two minor peaks in case of the first two controls, which were of different wavelengths compared to the two large peaks obtained for Clomeleon (Figure 4.4). An excitation spectrum obtained for wavelengths from 350 to 450 nm, when measuring emission at 527 nm, showed no clear peak, but a gradual increase of the signal (Figure 4.5). Furthermore, it was tested whether a shift in the fluorescence signal could be measured by manually adding GABA (100 µM final concentration) to the cuvette, but no change of the Clomeleon emission could be detected. It was suggested that receptor activity may be too fast paced to see a change using the equipment.

Excitation and emission scans of Clomeleon were similar to those described by Kuner & Augustine (2000) and the protein was, therefore, further tested in a microtitre screening assay setup using a fluorescence plate reader. Clomeleon was expressed in HEK293 cells together with $GABA_A$ receptor $\alpha 3$ and $\beta 2$ subunits. On the day of the assay, baseline fluorescence was measured for 20 seconds, before adding 10 µl mammalian Ringer solution with GABA (100 µM final concentration) to each well and further reading the fluorescence signal for another 30 seconds at either 527 or 480 nm. Readings obtained from the assay setup did not show the expected fluorescence shift from 527 nm to 480 nm. Instead, there was little or no change at both wavelengths. Figure 4.6 A represents the normalised gross fluorescence signals obtained at 527 as well as 480 nm over 30 seconds after addition of the agonist GABA.

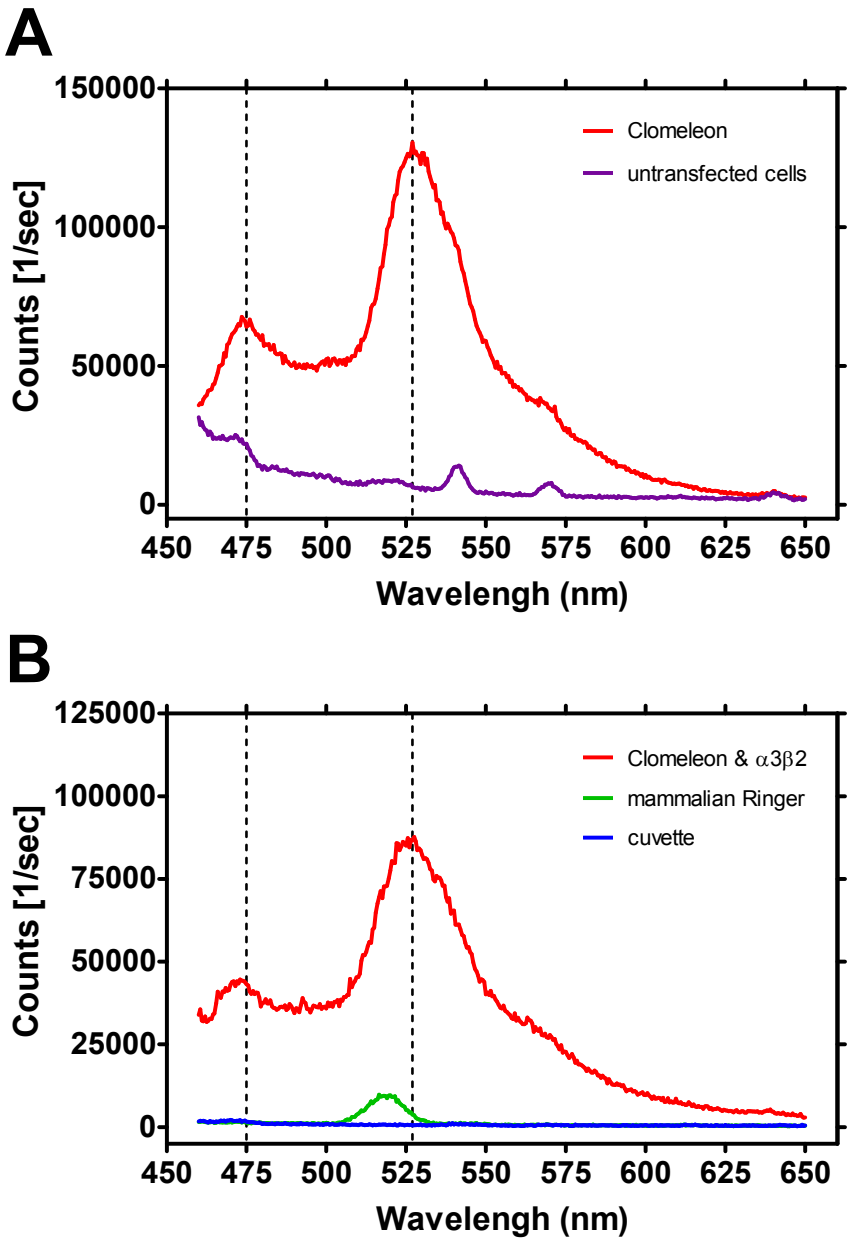

Figure 4.4: Emission scan of the chloride-indicator Clomeleon expressed in HEK293 cells.
Fluorescence signal of cells expressing Clomeleon versus untransfected cells (A) and spectrum of cells expressing Clomeleon and $\alpha 3\beta 2$ $GABA_A$ receptors as well as of mammalian Ringer solution alone and a cuvette only (B). Dashed lines highlight the two peaks of the fluorescence signal emitted by Clomeleon.

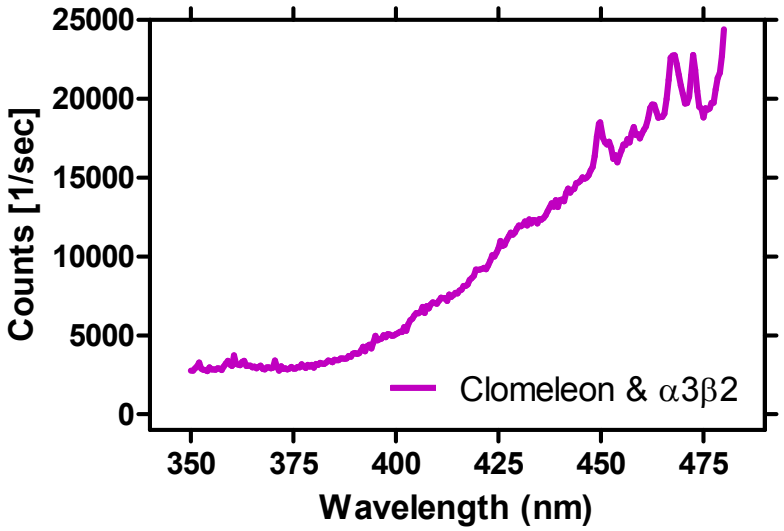

Figure 4.5: Excitation spectrum of HEK293 cells expressing Clomeleon and $\alpha 3\beta 2$ $GABA_A$ receptors.

Figure 4.6 B displays the normalised net fluorescence signals after subtracting the signal of untransfected control cells. Data depicted show a small, non-significant decrease of fluorescence signal compared to baseline fluorescence after agonist injection at both wavelengths. This was most likely an artefact of the assay setup, since the signal at both emission wavelengths decreased and no increase could be seen for CFP emission. Altering cell densities could not improve the measurement's outcome.

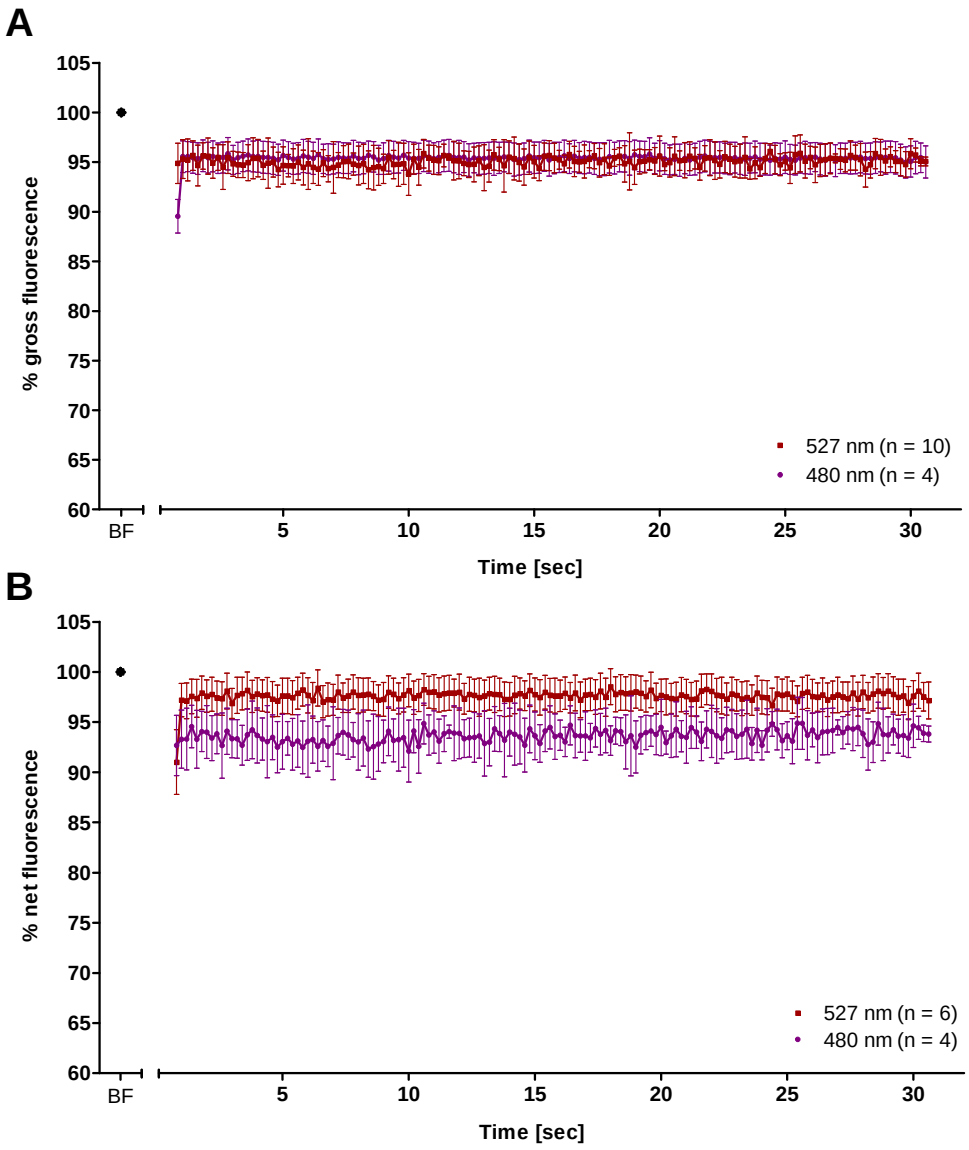

Figure 4.6: Fluorescence signal of Clomeleon in HEK293 cells also expressing $\alpha 3\beta 2$ $GABA_A$ receptors after addition of GABA.

(A) Gross fluorescence signal. (B) Net fluorescence signal. Fluorescence was measured at emission wavelengths of 527 nm or 480 nm for 30 seconds after injecting GABA (100 µM final concentration). Data correspond to means ± SEM; n states the number of wells measured. Fluorescence was normalised by setting the averaged baseline fluorescence (BF) to 100 % and fluorescence changes (after adding GABA) were calculated as percentage of the baseline fluorescence.

4.2.2 Iodide-flux assay

Due to the fact that the Clomeleon-based assay setup did not provide the required outcome, a colorimetric iodide-flux screening assay, based on the modified SK method, was tested next. Tang & Wildey (2004) demonstrated that a modified SK reaction could indicate $GABA_A$ receptor activity in WSS-1 cells by measuring iodide concentration changes after incubation of iodide-loaded cells with the agonist GABA. In order to determine the assays linear range and sensitivity, standard curves were established by measuring the OD405 of increasing concentrations of NaI subjected to the SK reaction (Figure 4.7). The linear range of the assay was estimated from the standard curves in Figure 4.7 B; it was between 300 nM and 3 µM after 15 minutes incubation time and between 100 nM and 1 µM after 30 minutes incubation time, demonstrating a shift towards the left, depending on the assay incubation time. Further, it was evident that the OD405 readings of the SK reaction decrease with incubation time (Figure 4.7 B). The assays lowest detection limit after 15 minutes incubation time was estimated from the standard curve data as described in Section 2.6.2. The $OD405_{control}$ was 2.972 with a SD of 0.030. The determined lowest detection limit was 407 nM (OD405 at 407 nM was 2.88, ΔOD405 was 0.092 and $3SD_{Control}$ was 0.09; Figure 4.7 A).

After obtaining a standard curve, HEK293 cells were transfected with $\alpha 3\beta 2\gamma 2$ $GABA_A$ receptors and seeded into 96-well microtitre plates. At first it was tested whether it was possible to measure a GABA concentration-dependent effect performing the assay as described by Tang & Wildey (2004, 2006). Figure 4.8 and Table 4.1 illustrate the results obtained from cell lysates subjected to the SK assay. Those did not show a clear GABA concentration-dependent pattern, but rather random values. The same applied to the % activity of the receptors which was calculated as described in Section 2.6.2 (Tang & Wildey, 2004). Furthermore, OD405 values of untransfected control cells were expected to be low, due to a high iodide concentration in the cells, however, the values obtained were relatively high and similar to the data from cells expressing $\alpha 3\beta 2\gamma 2$ receptors. It is worth mentioning that results shown were not reproducible, but varied widely, despite repeating the assay several times.

The OD405 of the cell supernatant, the DPBS solution containing different agonist concen-

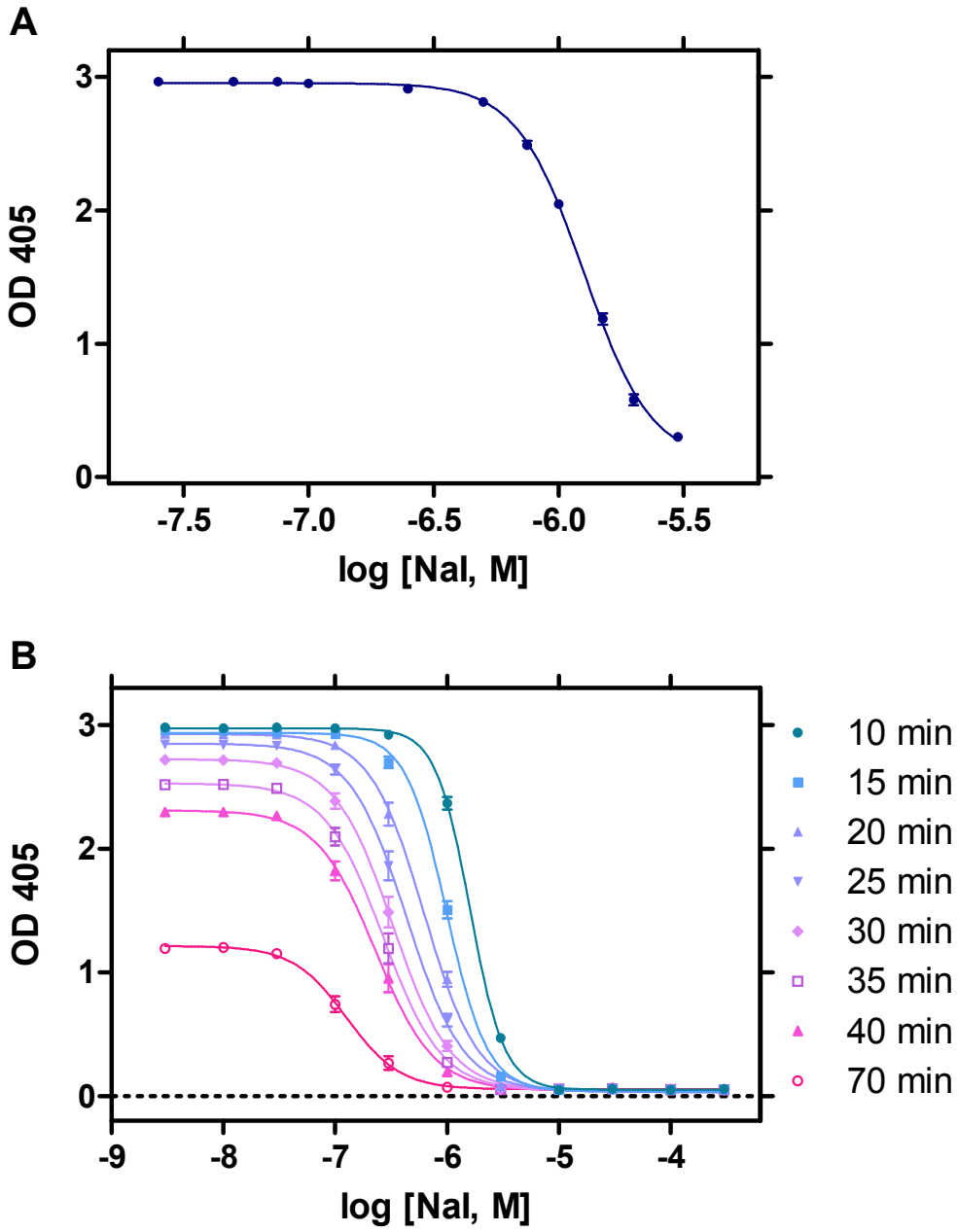

Figure 4.7: NaI flux assay standard curve. (A) NaI concentrations of 3 µM to 25 nM were applied to the modified SK method. OD405 was read after 15 minutes incubation time. (B) The modified SK assay was performed on samples containing different NaI concentrations (300 µM to 3 nM). OD405 was determined after different incubation times ranging from 10 to 70 minutes. Data were averaged from eight data points ± SEM.

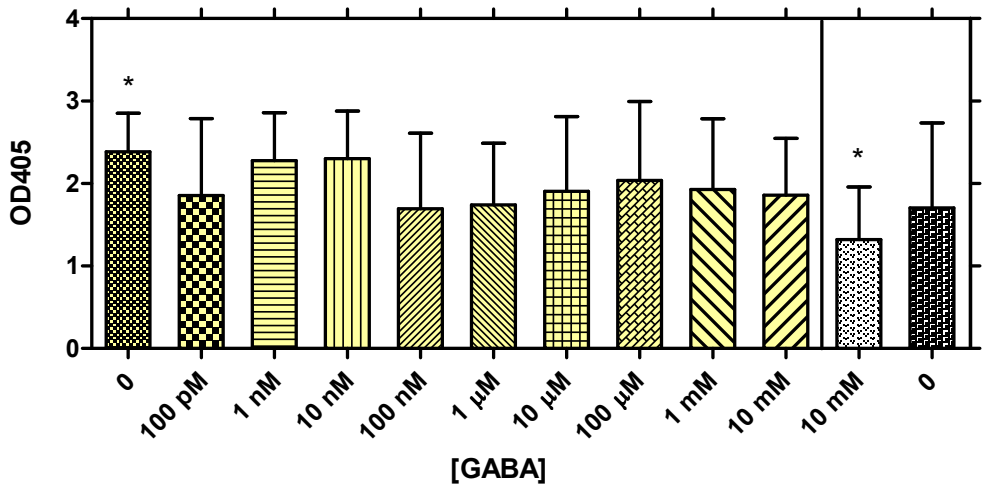

Figure 4.8: A modified SK assay was used to measure chloride conductivity in HEK293 cells expressing $\alpha 3\beta 2\gamma 2$ $GABA_A$ receptors (yellow columns) and untransfected HEK293 cells (white columns).

*Before the assay, cells were loaded with iodide-loading buffer and incubated with increasing concentrations of GABA as described in the text. OD405 was measured after 15 minutes incubation of SK reaction. Values were means ± SD from 16 data points from two different microtitre plates. * indicates $p < 0.05$ compared to highest GABA concentration of 10 mM.*

Table 4.1: OD405 readings and analysis of results obtained from modified SK assay in HEK293 cells expressing $\alpha 3\beta 2\gamma 2$ $GABA_A$ receptors.

	$\alpha 3\beta 2\gamma 2$ receptors											untransfected cells
GABA	0 µM	100 pM	1 nM	10 nM	100 nM	1 µM	10 µM	100 µM	1 mM	10 mM	10 mM	0 µM
OD405 mean	2.387	1.854	2.279	2.303	1.696	1.740	1.904	2.037	1.927	1.857	1.321	1.706
SD	0.464	0.936	0.579	0.575	0.917	0.747	0.907	0.957	0.859	0.691	0.636	1.029
% activity	0.00	100.66	20.28	15.73	130.41	122.06	91.12	65.94	86.84	100.00		

Cells were loaded with iodide-loading buffer and incubated with increasing concentrations of GABA as described in the text. The SK assay was conducted for 15 minutes before determining OD405 readings. Mean values were calculated from 16 data points from two different microtitre plates, % activity as described in Section 2.6.2.

trations added to the iodide-loaded cells, was also investigated. After the incubation time, the supernatant was transferred to a separate plate and further subjected to the SK assay. Depending on $GABA_A$ receptor activity, the supernatant should contain distinct concentrations of iodide. Compared to the results obtained from lysed cells, the OD405 readings of the supernatant were very low throughout, indicating a high extracellular concentration of iodide (Figure 4.9 A). Because the assay has a relatively small detection range (see above) and iodide concentration of supernatant seemed to be very high in all samples, it was examined whether diluting the supernatants would improve the results. It was therefore transferred to a new plate after incubation and diluted 1:2 or 1:5. Although the OD405 readings were higher with increased dilution, the results did again show no concentration-dependent pattern but seemed arbitrary (Figure 4.9 B, C). Furthermore, supernatants from untransfected control cells had a relatively low OD, indicating iodide efflux from the cells into the supernatant via other means than the examined $GABA_A$ receptors.

GABA incubation time for iodide-loaded cells was examined by performing a time-response course in order to establish the optimal time to improve the assay outcome. After washing the cells, they were incubated with 10 µM GABA in DPBS or DPBS only for 10, 20, 30 or 45 seconds or 1, 2, 3 or 5 minutes. The results obtained from the cell lysate, after performing the SK assay, are shown in Figure 4.10. OD405 readings for cells treated with GABA or DPBS were similar and overall relatively high. Figure 4.11 represents OD405 values from the supernatants (undiluted or diluted) after performing the SK assay. Samples from the undiluted plate have low OD405 values throughout, indicating a high iodide concentration. Therefore, samples were diluted in the following tests to be able to distinguish between different iodide concentrations. Although there were significant differences between GABA and DPBS treated cells in some cases, results obtained varied on each plate tested (see also Figures B.3 and B.4, Appendix B). Due to the discrepancies obtained throughout, it was difficult to decide on an optimal GABA incubation time. Therefore, the incubation time of five minutes applied by Tang & Wildey (2004) was further applied.

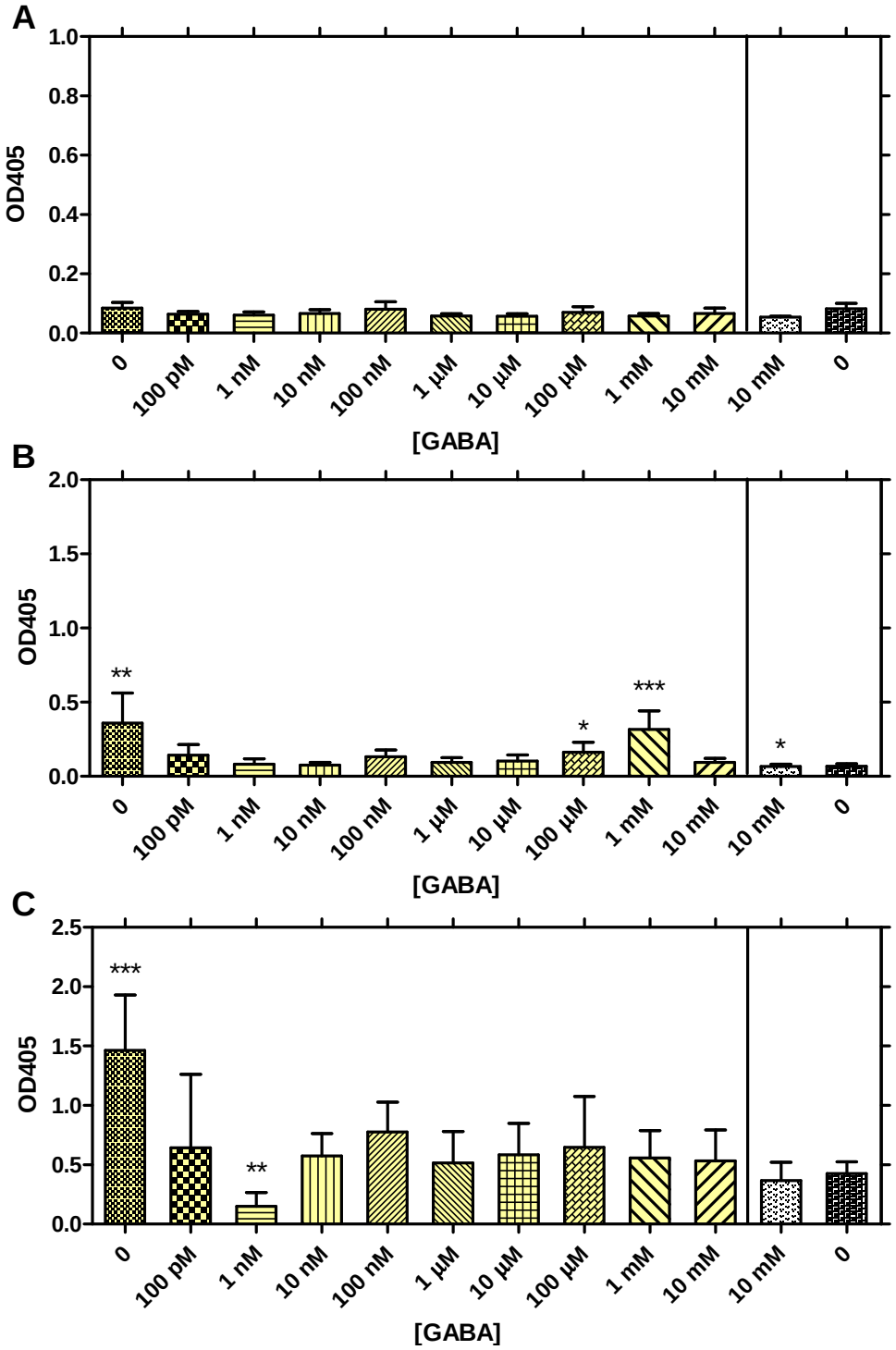

Figure 4.9: SK assay determining iodide efflux from HEK293 cells expressing $\alpha 3\beta 2\gamma 2$ $GABA_A$ receptors (yellow columns) and untransfected HEK293 cells (white columns).

*Before the assay, cells were loaded with iodide-loading buffer and incubated with increasing concentrations of GABA as described. The solution containing GABA was transferred to a separate plate. The SK assay was performed on undiluted (A), 1:2 (B) and 1:5 (C) diluted supernatant. After 15 minutes incubation the OD405 was measured. All values were means ± SD from eight data points on one microtitre plate. * indicates $p < 0.05$, ** = $p < 0.01$, *** = $p < 0.001$ compared to highest GABA concentration of 10 mM.*

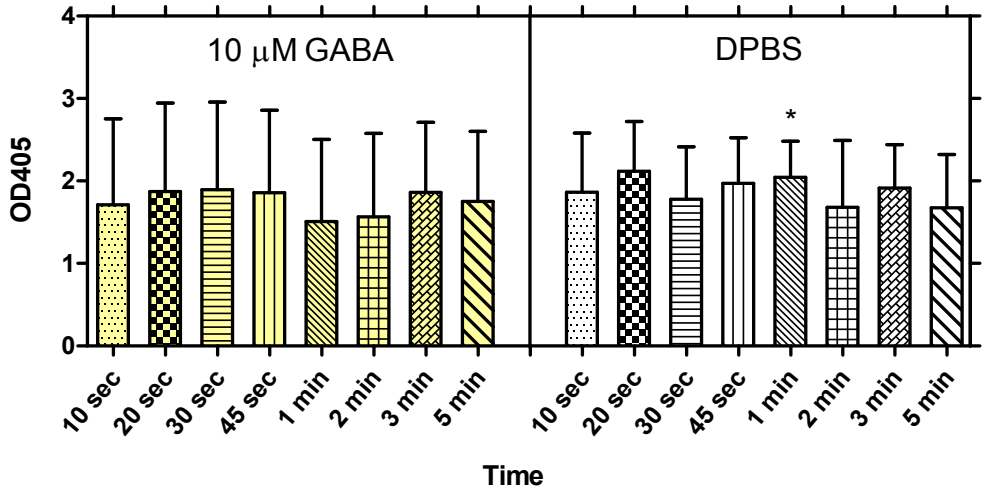

Figure 4.10: OD405 values from iodide-flux assay in HEK293 cells expressing $\alpha 3\beta 2\gamma 2$ $GABA_A$ receptors. Before performing the SK assay, 10 μM GABA (yellow columns) or DPBS (white columns) were incubated for ten seconds to five minutes, respectively.

*Readings represent data from SK assay from undiluted cell lysate. Values are means ± SD from six data points each on three microtitre plates. * indicates $p < 0.05$ comparing GABA-treated cells with their respective DPBS controls.*

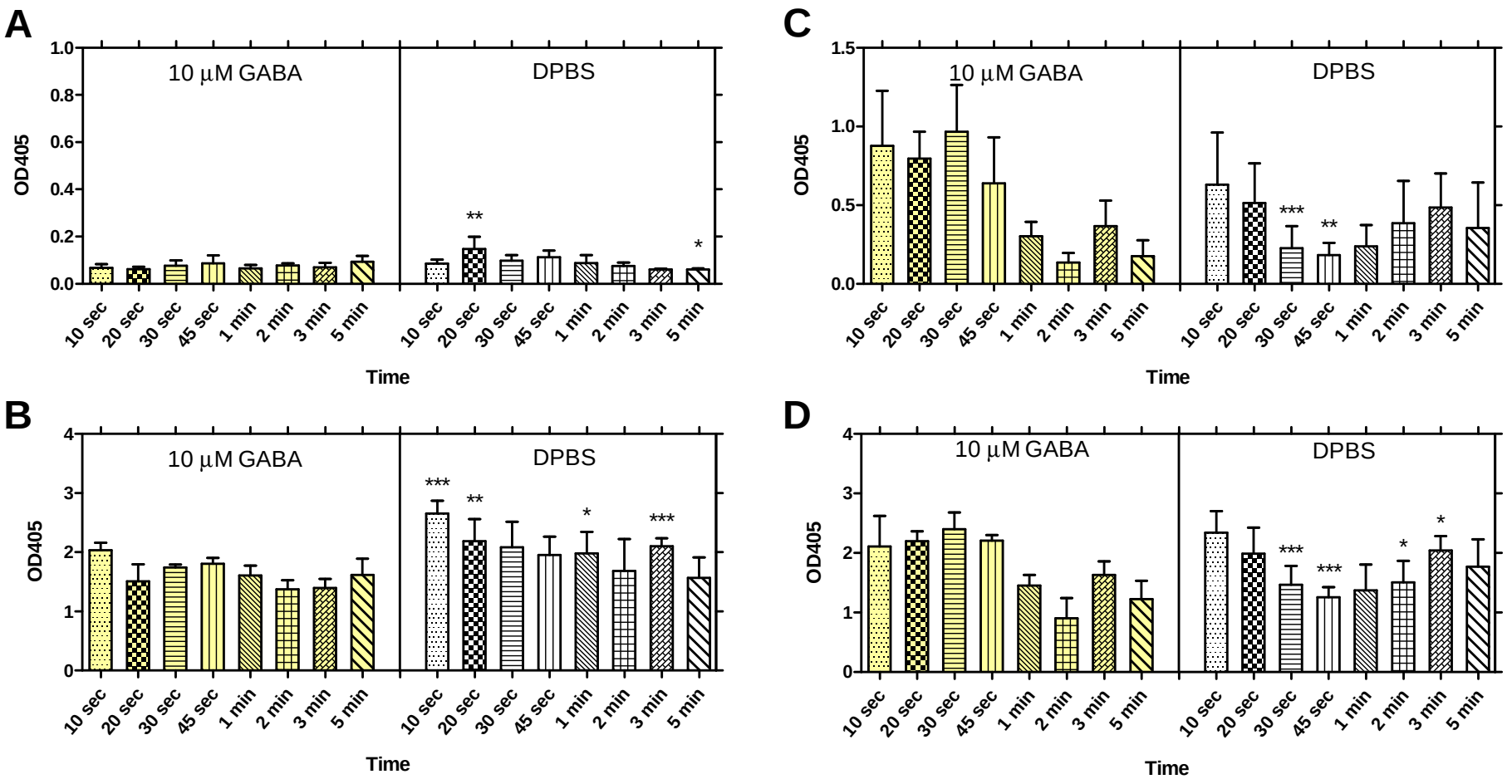

Figure 4.11: Iodide-flux assay. HEK293 cells expressing $\alpha 3\beta 2\gamma 2$ $GABA_A$ receptors were exposed to GABA for different incubation times.

*Before performing the SK assay, 10 µM GABA in DPBS (yellow columns) or DPBS only (white columns) were incubated for ten seconds to five minutes. DPBS was transferred to new plates and the SK assay was performed on undiluted supernatant (A), on supernatant diluted 2:3 (B), 1:2 (C) or 1:5 (D). OD405 values are means ± SD from six data points. * indicates p < 0.05, ** = p < 0.01, *** = p < 0.001 comparing GABA-treated cells with their respective DPBS-incubated controls.*

In a further attempt, the influence of the cell density was examined. The effect of different concentrations of GABA at a cell density of 25×10^3 cells per well was compared with its effect on decreased densities of 17.5×10^3 and 12.5×10^3 cells per well. The SK assay was performed on lysed cells as well as the undiluted supernatant. The latter showed very low OD405 readings throughout, indicating a high concentration of iodide (Figure 4.12 B). In contrast, the readings for the lysed cells differed between different cell densities and GABA concentrations. In general, the readings had a tendency towards higher values for higher GABA concentrations, indicating a low iodide concentration inside the cells (Figure 4.12 A), which would be the desirable assay outcome, but the results obtained were not consistent.

Due to the fact that the data obtained so far did not show well-defined results, it was investigated whether the observed iodide efflux from HEK293 cells was GABA receptor-mediated by applying bicuculline and picrotoxin to the cells. Bicuculline is a competitive antagonist of $GABA_A$ receptors. Treating the receptors expressed with bicuculline would inhibit the iodide flux compared to GABA alone in case of a GABA-mediated response. Exposing cells to the non-competitive channel blocker picrotoxin would indicate $GABA_A$ receptor blockade. The results showed comparatively high readings for all samples of cell lysate, indicating low iodide concentration inside the cells (Figure 4.13 A). There were some significant differences between the various treatments. However, the values were random, for example OD405 readings of cells exposed to 1 µM GABA were significantly higher than those of cells treated with 100 µM, although there should have been lower iodide concentrations in the latter cells. Readings obtained from the cell supernatant solutions showed low OD405 values for all wells, except for those containing DPBS with GABA and picrotoxin (Figure 4.13 B). The latter exhibited similar OD405 readings to the data obtained for cell lysates, indicating a low iodide concentration in the cell supernatants, thus blocking iodide efflux from those cells. Untransfected control cells were treated with GABA alone or GABA and picrotoxin and showed similar OD405 values as transfected cells. Interestingly, in picrotoxin treated control cells iodide efflux was also blocked (Figure 4.13 B).

Although optimisation of the iodide-flux assay setup was tested extensively, results varied and no robust assay setup could be achieved. Since iodide efflux was high in transfected and

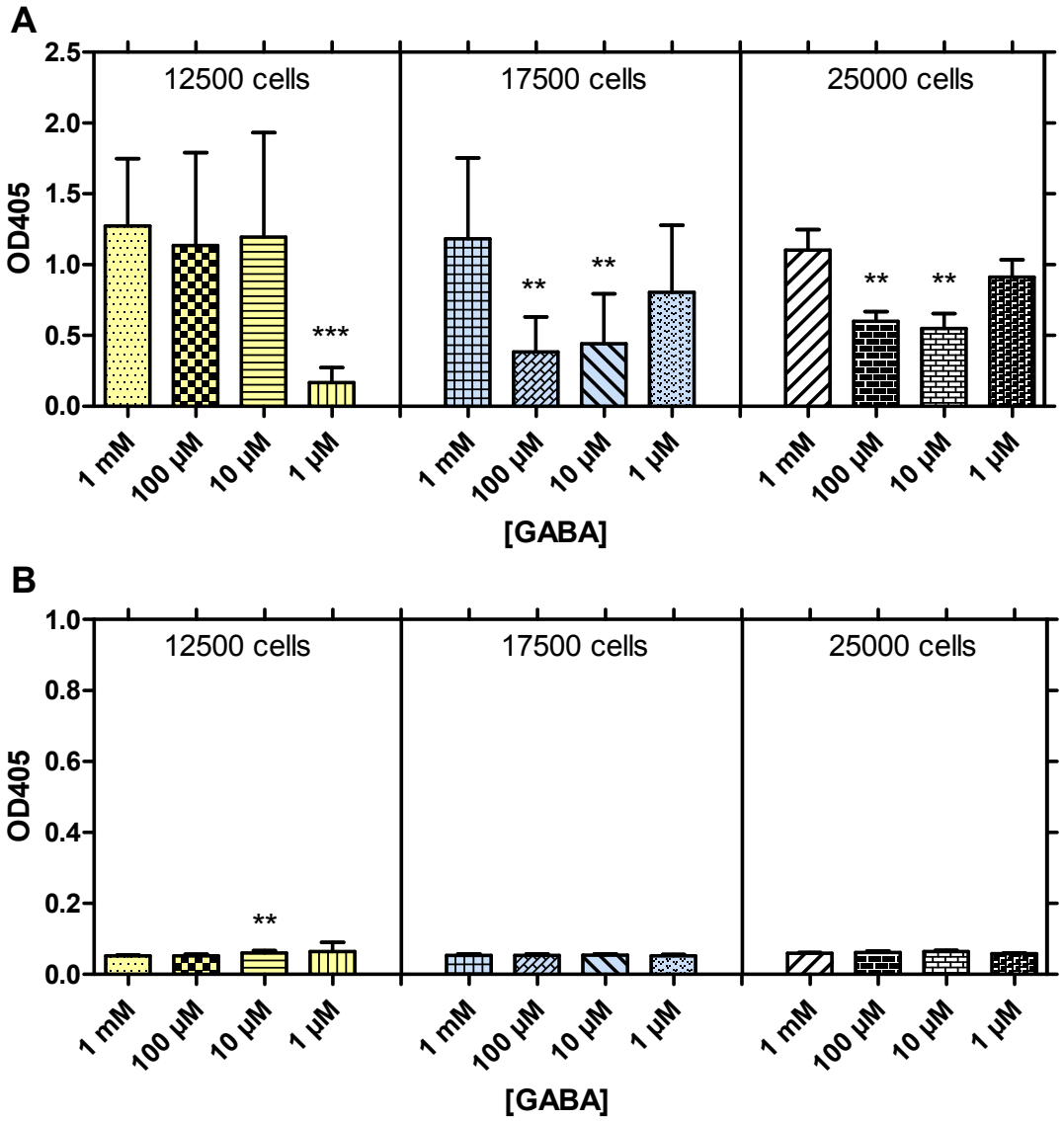

Figure 4.12: SK assay measuring iodide flux in HEK293 cells expressing $\alpha 3\beta 2\gamma 2$ $GABA_A$ receptors. Different cell densities were seeded: 12.5×10^3 cells per well (yellow columns), 17.5×10^3 cells per well (blue columns) and 25×10^3 cells per well (white columns).

*Before the assay, cells were loaded with iodide-loading buffer and incubated with increasing concentrations of GABA as described. The SK assay was performed on undiluted cell lysate (A) and supernatant (B). After 15 minutes incubation, the OD405 was measured. All values were means ± SD from eight data points on one microtitre plate. * indicates p < 0.05 and ** = p < 0.01 compared to highest GABA concentration of 1 mM.*

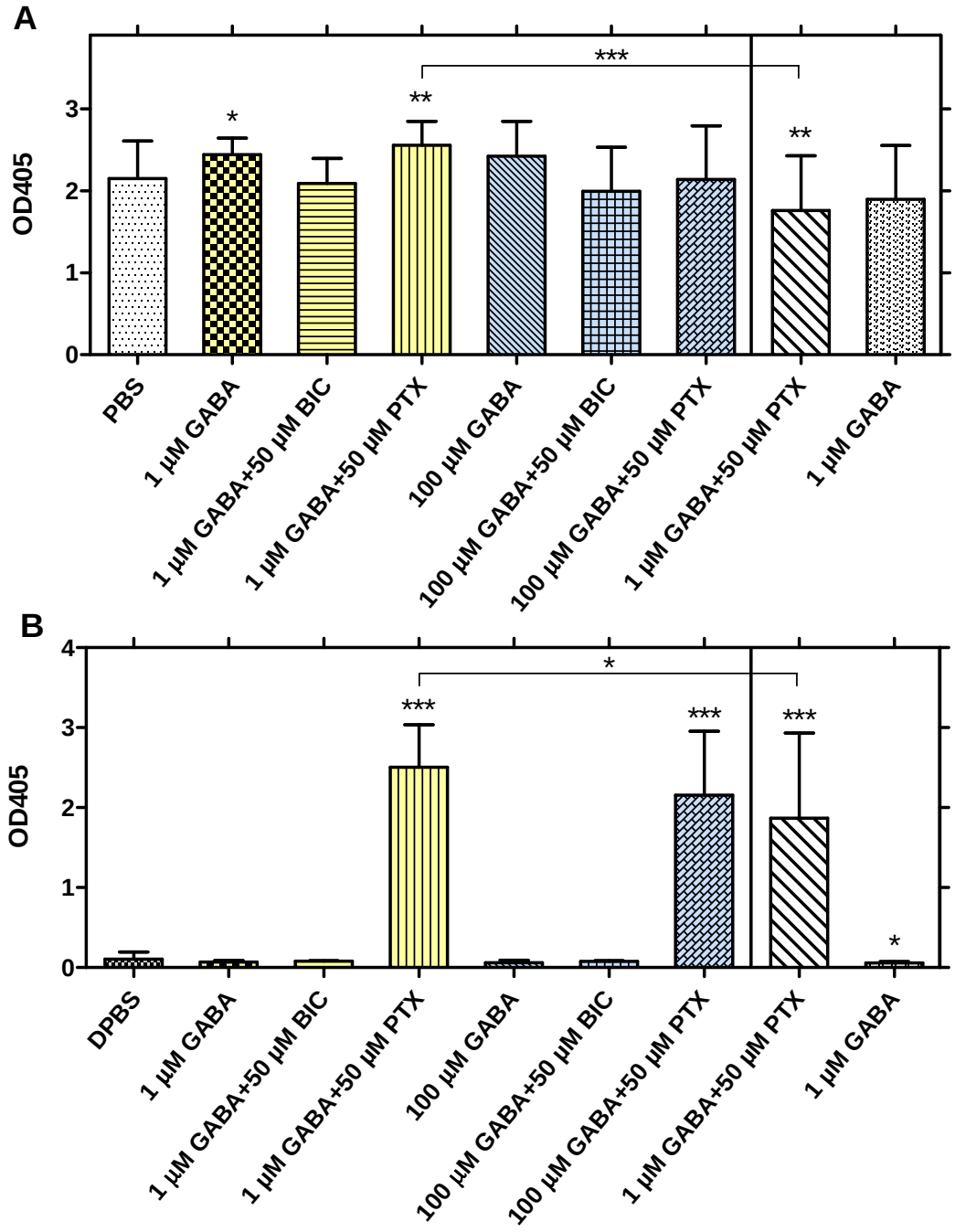

Figure 4.13: OD405 readings of SK assay after applying GABA, bicuculline and picrotoxin to HEK293 cells expressing $\alpha 3\beta 2\gamma 2$ $GABA_A$ receptors.

*Cells were loaded with iodide-loading buffer and subsequently incubated with 50 µM bicuculline or 50 µM picrotoxin and 1 µM GABA (yellow columns) or 100 µM GABA (blue columns). Untransfected control cells were also exposed to picrotoxin and 1 µM GABA (white columns). The SK assay was performed on undiluted cell lysate (A) and cell supernatant (B). After 15 minutes incubation time, OD405 was measured. All values were means ± SD from eight data points each on two microtitre plates. * indicates p < 0.05, ** = p < 0.01 and *** = p < 0.001 compared to DPBS treatment only (grey column). OD405 readings from experiments using PTX were also compared.*

untransfected cells and the last assay attempt using the channel blocker picrotoxin indicated the possibility that the observed iodide efflux may be in part due to spontaneous channel activity, HEK293 cells expressing $\alpha3\beta2\gamma2$ $GABA_A$ receptors were investigated using the patch-clamp method. Administration of 100 µM picrotoxin to the cells showed small outward currents in cells expressing the receptors with an agonist-independent receptor activity of 9.04 $\pm$ 1.75 % of total response capacity (maximal GABA response + response to picrotoxin = 100 %, n = 8; Figure 4.14). [1]

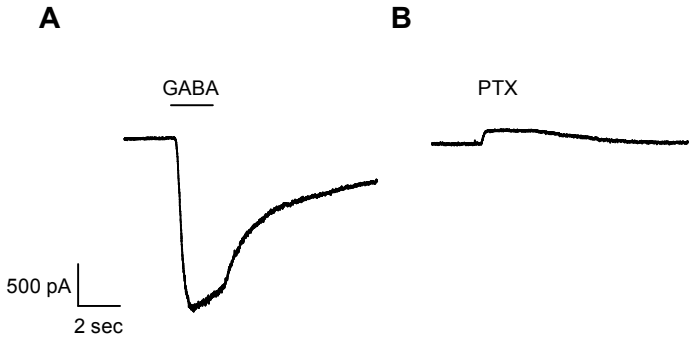

Figure 4.14: Representative current traces evoked by 100 µM GABA (A) and 100 µM picrotoxin (B) in HEK293 cells expressing $\alpha3\beta2\gamma2$ $GABA_A$ receptors.

4.2.3 Optimisation of a YFP-based screening assay

A third possible assay option, a YFP mutation with increased chloride and iodide sensitivity, was tested using a fluorescence plate reader. HEK293 cells transiently transfected with the mutated YFP-H148Q/I152L as well as $\alpha3\beta2\gamma2$ $GABA_A$ receptors were seeded into 96-well plates. On the following day, cells were incubated in NaCl bath solution an hour before the assay. Afterwards, the microtitre plates were put into a fluorescence plate reader and NaI test solution only or together with 100 µM GABA were injected into the wells and changes in the fluorescence signal were measured. The latter resulted in a clear fluorescence decrease, which could be prevented by injecting 100 µM GABA together with 1 mM picrotoxin (Figure 4.15 A). These results indicated that $\alpha3\beta2\gamma2$ $GABA_A$ receptor activity, elicited by a high agonist concentration could be detected with this assay. It was, therefore, further

[1] During this set of experiments GABA concentration-response relations were also examined for the $\alpha3\beta2\gamma2$ receptors (see Figure B.6, Appendix B).

tested in HEK293 cells transfected with YFP-H148Q/I152L and $\alpha3\beta2$ or $\alpha3\beta2\varepsilon$ $GABA_A$ receptors. Cells expressing the former receptors also exhibited a fluorescence quench, which was not seen when picrotoxin was applied. However, the fluorescence quench was only 12.41 $\pm$ 3.55 % (n = 9) compared to 54.62 $\pm$ 4.14 % (n = 15) obtained from cells expressing $\alpha3\beta2\gamma2$ receptors (Figure 4.15 B). When examining cells expressing $\alpha3\beta2\varepsilon$ receptors, the fluorescence signal did not show distinct changes after adding the agonist or channel blocker (n = 9; Figure 4.15 C). From the results obtained, it was suggested that the assay could probably be used for certain $GABA_A$ receptor combinations, such as the $\alpha3\beta2\gamma2$ subtype. However, the assay seemed unsuitable for the receptor subtype containing the ε subunit, since no receptor activity could be detected.

Since the various subunit combinations resulted in different assay outcomes, i.e. different percentage of fluorescence quench, it was tested whether another α subunit, namely the human $\alpha1$ subunit, would improve the fluorescence readings when combined with $\beta2$ and ε subunits. HEK293 cells expressing $\alpha1\beta2$ and $\alpha1\beta2\varepsilon$, respectively, were examined as described above and produced some interesting results. Cells expressing the $\alpha1\beta2$ receptor showed a 39.4 $\pm$ 3.32 % quench (n = 9) which was significantly different compared to the results obtained with the $\alpha3\beta2$ receptor ($p > 0.0001$, unpaired t-test; Figure 4.16 A). Similarly, a fluorescence quench of 24.65 $\pm$ 2.13 % (n = 9) was measured in cells expressing $\alpha1\beta2\varepsilon$ receptors after adding 100 µM GABA to the wells (Figure 4.16 B). This could be prevented by adding a high concentration of picrotoxin.

In order to assess the quality of the assay, the Z'-factor for each receptor subtype was calculated as described in Section 2.6.3.1 (Equation 2.7, Chapter 2). Although the fluorescence quench for $\alpha3\beta2\gamma2$ receptors was the highest obtained, the Z'-factor was 0.48. Further Z'-factors were -0.16 for $\alpha3\beta2$, 0.58 for $\alpha1\beta2$ and -0,01 for $\alpha1\beta2\varepsilon$.

Next, GABA concentration-response relations were examined in cells expressing $\alpha3\beta2\gamma2$, $\alpha1\beta2$ and $\alpha1\beta2\varepsilon$ receptors, respectively. Figure 4.17 displays that different subunit combinations resulted in different GABA concentration-response curves, when investigating GABA concentrations ranging from 30 nM to 3 mM. $\alpha3\beta2\gamma2$ receptors were most sensitive to

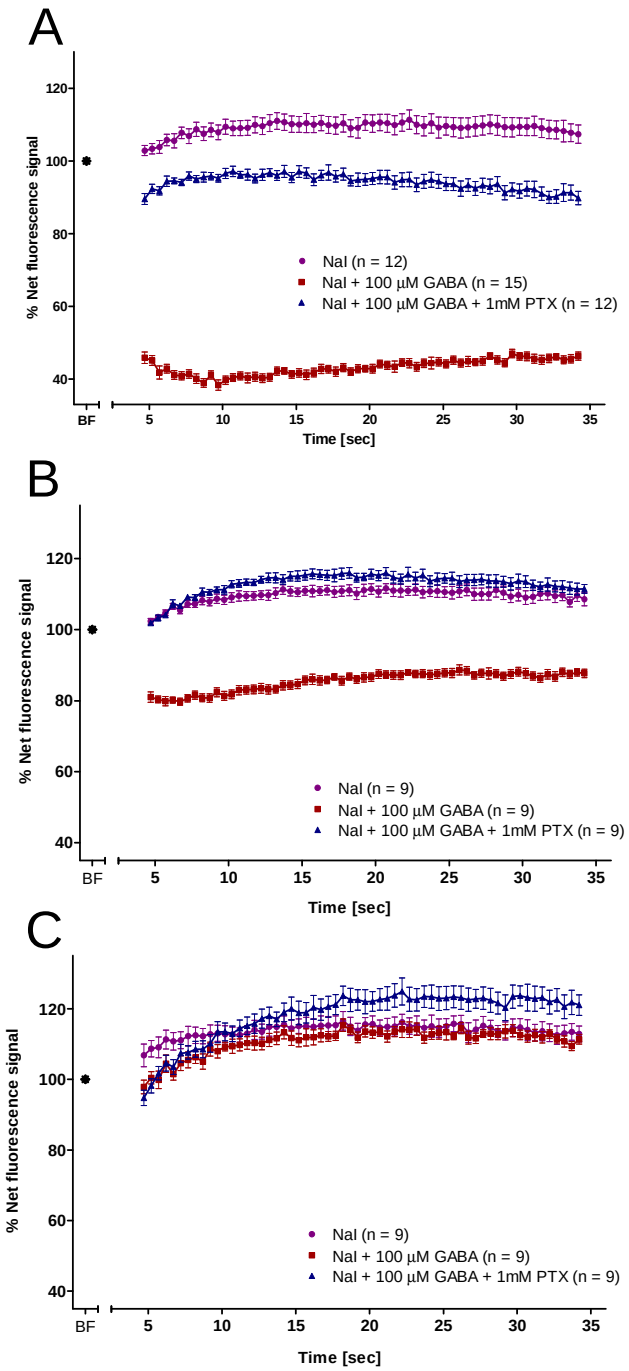

Figure 4.15: Net fluorescence signal of mutant YFP-H148Q/I152L in HEK293 cells expressing α3-subunit-containing $GABA_A$ receptors.

Fluorescence was measured for 30 seconds after addition of NaI test solution only or together with 100 µM GABA or with 100 µM GABA and 1 mM picrotoxin in cells expressing $\alpha3\beta2\gamma2$ (A), $\alpha3\beta2$ (B), $\alpha3\beta2\varepsilon$ (C) $GABA_A$ receptors. Data correspond to means $\pm$ SEM; n states the number of wells measured. Net fluorescence was normalised by setting the averaged baseline fluorescence to 100 % and fluorescence changes (after adding solutions) were calculated as percentage of baseline fluorescence.

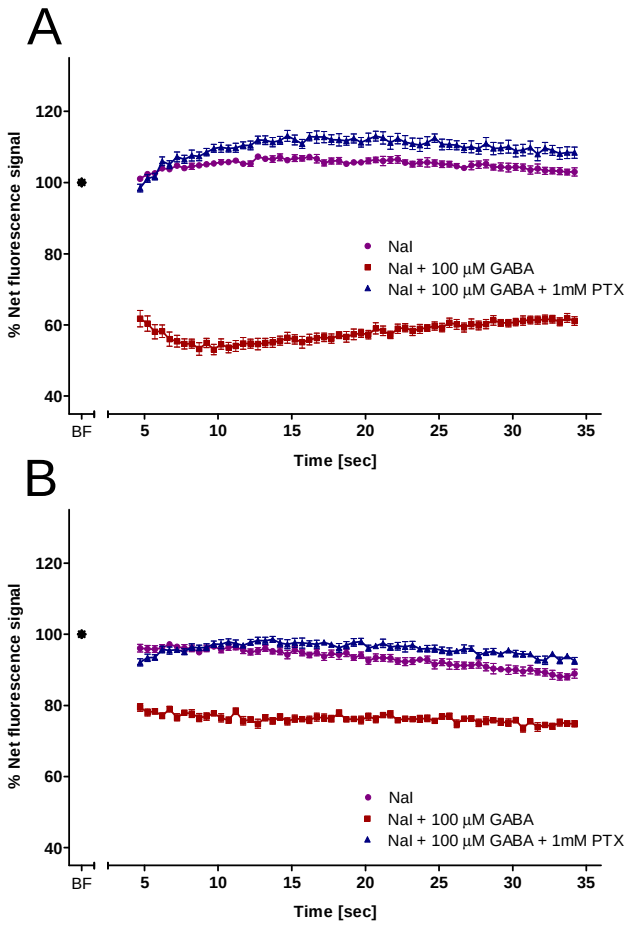

Figure 4.16: Net fluorescence signal of mutant YFP-H148Q/I152L in HEK293 cells expressing α1-subunit-containing $GABA_A$ receptors.

Fluorescence was measured for 30 seconds after addition of NaI test solution only (n = 9) or together with 100 µM GABA (n = 9) or with 100 µM GABA and 1 mM picrotoxin (n = 9) in cells expressing $\alpha1\beta2$ (A) and $\alpha1\beta2\varepsilon$ (B) $GABA_A$ receptors. Data correspond to means ± SEM; n states the number of wells measured. Net fluorescence was normalised by setting the averaged baseline fluorescence to 100 % and fluorescence changes (after adding solutions) were calculated as percentage of the baseline fluorescence.

GABA (EC_{50} 3.37 ± 0.42 µM, n = 14). $\alpha1\beta2$ receptors had an EC_{50} of 8.47 ± 0.48 µM (n = 10) and $\alpha1\beta2\varepsilon$ receptors where least sensitive with an EC_{50} of 17.1 ± 5.4 µM (n = 9). The Hill slope for $\alpha1\beta2\varepsilon$ receptors was lower (1.17 ± 2.70) compared to those obtained for $\alpha3\beta2\gamma2$ (2.26 ± 0.36) and $\alpha1\beta2$ (2.57 ± 0.14) receptors. However, the difference was not significant.

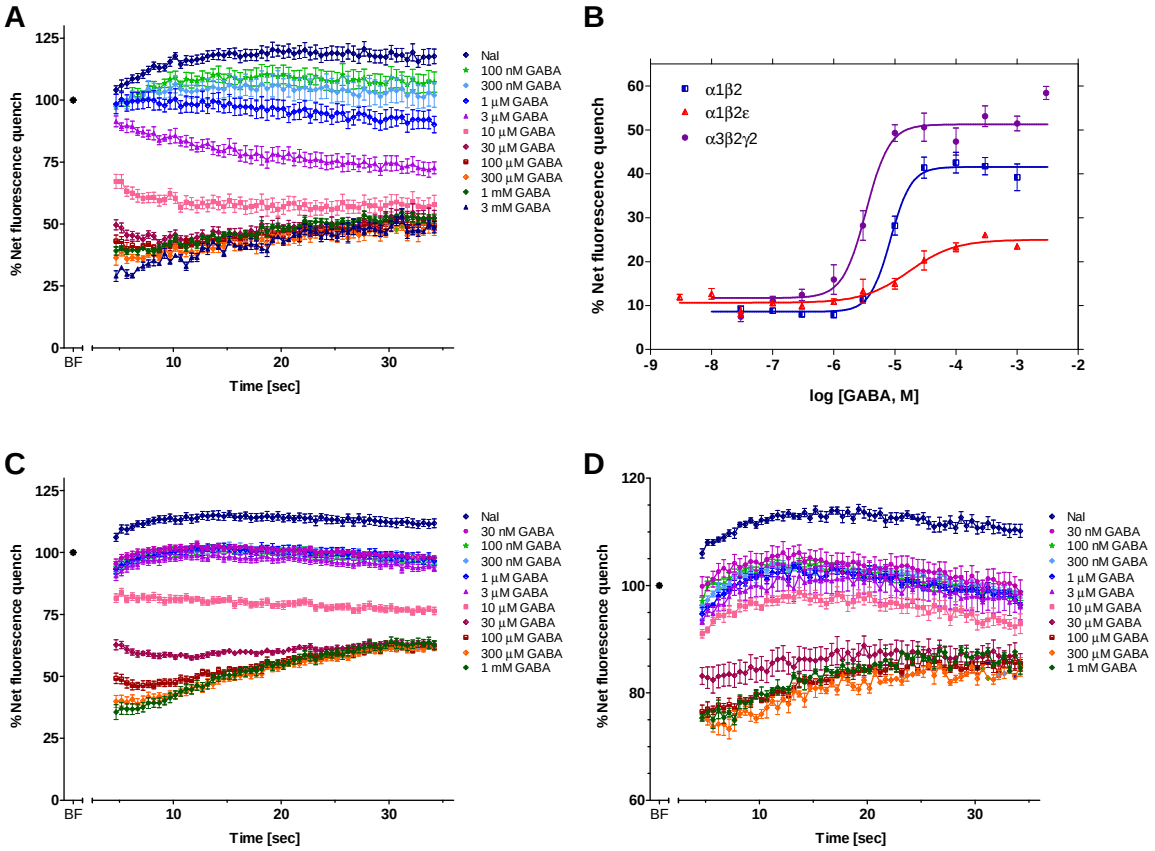

Figure 4.17: GABA concentration-response relations examined for $GABA_A$ receptors expressed in HEK293 cells using the YFP-based screening assay.

Time-course showing GABA-induced net fluorescence quench using increasing concentrations of GABA in cells expressing (A) $\alpha3\beta2\gamma2$, (C) $\alpha1\beta2$ and (D) $\alpha1\beta2\varepsilon$ receptor subtypes. (B) GABA concentration-response curves of $\alpha1\beta2$ (n = 10), $\alpha1\beta2\varepsilon$ (n = 9) and $\alpha3\beta2\gamma2$ receptor subtypes (n = 14). Data correspond to means ± SEM; n states the number of wells measured. EC_{50} values and Hill coefficients are stated in the text. Curves were fitted using a non-linear regression fit with variable slopes as described in Section 2.6.3.

1 µM of the benzodiazepine flunitrazepam (together with the EC_{30} concentration of GABA) was applied to cells expressing YFP-H148Q/I152L and $\alpha3\beta2\gamma2$ $GABA_A$ receptors. Results were compared to the action of an EC_{30} concentration of GABA alone (Figure 4.18). In cells exposed to 2.45 µM GABA alone, the fluorescence drop was 30.3 ± 5.88 % compa-

red to the baseline fluorescence, whereas it was 39 ± 5.76 % in cells exposed to 2.45 µM GABA with 1 µM flunitrazepam, demonstrating the positive modulation of the receptor by the benzodiazepine.

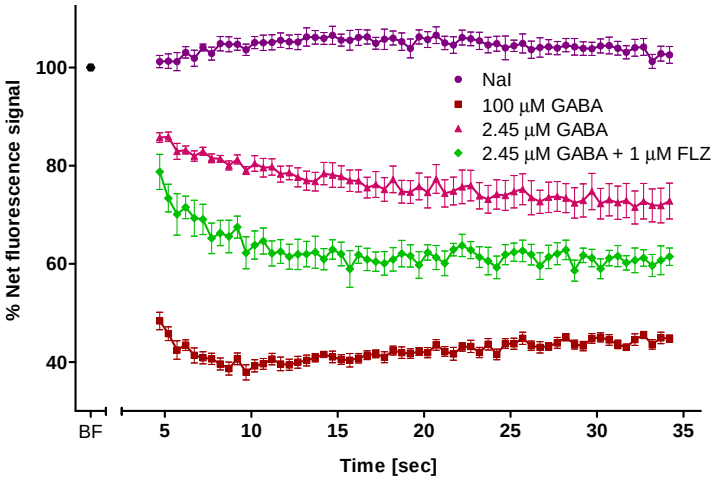

Figure 4.18: Fluorescence signal change after addition of 1 µM flunitrazepam to HEK293 cells expressing $\alpha 3\beta 2\gamma 2$ $GABA_A$ receptors.

Fluorescence was measured for 30 seconds after addition of NaI test solution only (n = 8) or together with 100 µM GABA (n = 12), 2.45 µM GABA (n = 12) or 2.45 µM GABA and 1 µM flunitrazepam (n = 9) in cells expressing $\alpha 3\beta 2\gamma 2$ receptors. Concentrations are final concentrations per well. Data correspond to means ± SEM; n states the number of wells measured. Net fluorescence was normalised by setting the averaged baseline fluorescence to 100 % and fluorescence changes (after adding solutions) were calculated as percentage of the baseline fluorescence.

4.3 Discussion

4.3.1 Clomeleon-based screening assay

The results presented in this chapter highlight that chloride-ion channel screening is challenging. Several methods had to be tested to find a suitable assay technique. The different assays were first tested and optimised with cells expressing $\alpha 3\beta 2$ or $\alpha 3\beta 2\gamma 2$ receptors, since those subtypes did not exhibit constitutive receptor activity. The latter meant a further challenge for the assay setup when using ε-containing receptors.

The initial plan was to set up a cell-based system to screen for compounds that modulate the $GABA_A$ receptor using the chloride-ion indicator protein Clomeleon (Kuner & Augustine, 2000). It had been shown that Clomeleon is suitable for chloride concentration measure-

ments in neurons of the hippocampus as well as transgenic mice (Kuner & Augustine, 2000; Duebel et al., 2006). However, Clomeleon had not been used in a cell-based screening assay to scan $GABA_A$ receptors for modulating compounds as attempted in this project. The excitation and emission spectra obtained from HEK293 cells expressing Clomeleon were in consent with the data published by Kuner & Augustine (2000). Therefore, Clomeleon was next expressed with $\alpha 3\beta 2$ $GABA_A$ receptors and the cells were seeded into 96-well microtitre plates. Using a fluorescence plate reader, the fluorescence signal was monitored before and after adding a high concentration of the agonist GABA to the cells. However, data obtained did not result in the expected fluorescence shift, with no or occasionally small, non-significant signal changes compared to baseline fluorescence. This slight fluorescence reductions could be measured in few wells at both emission wavelengths of Clomeleon. It was suggested that these changes were not Clomeleon-specific, but rather an artefact of the assay setup. This is because fluorescence was only read at a small-sized area of the wells. In some cases, cells probably got detached from the plate when injecting the agonist-solution which lead to reduction of cells in the area of the signal detection, decreasing the fluorescence signal. It was supposed that chloride-sensitivity of Clomeleon was too low to detect receptor mediated changes in the cells even at high agonist concentrations and, thus, no chloride-specific signal changes could be detected. In fact, the physiological range of chloride concentrations in different cell types lies between 3 to 60 mM (Rohrbough & Spitzer, 1996; Kuner & Augustine, 2000; Berglund et al., 2008; Markova et al., 2008; Bregestovski et al., 2009), but sensitivity of Clomeleon to chloride is much lower (K_{App} > 160 mM). Hence, it was concluded that Clomeleon is not suitable for the intended assay type due to its low chloride-sensitivity.

Since the initially planned screening assay setup did not produce the desired outcome and proved unsuitable for screening compounds, an alternative screening technique had to be found. There were two possible methods, which seemed suitable due to their relatively easy setup and no need for specialised measuring devices: a colorimetric-flux assay and a YFP-based screening assay.

4.3.2 Colorimetric iodide-flux assay

The next assay tested was the colorimetric iodide-flux assay described by Tang & Wildey (2004, 2006) which was based on a modified SK method. For this, HEK293 cells expressing the $\alpha 3\beta 2\gamma 2$ receptor were loaded with iodide. Subsequent application of GABA to the cells caused the ion channel receptors to open, triggering iodide efflux through the ion channel receptors into the supernatant solution. By determining the intra- and extracellular iodide concentrations, it would be possible to evaluate $GABA_A$ receptor activity. No or low concentrations of GABA result in low receptor activity, hence, the amount of iodide in the cells should be high, resulting in low OD405 values, whereas applying high concentrations of GABA results in high receptor activity. This causes most of the iodide to flow out of the cells due to the electrochemical gradient, causing a low intracellular iodide concentration and, hence, high OD405 values (see Equation 4.1). When determining extracellular iodide concentrations, OD405 values should be low at high receptor activity and high at low or no receptor function.

Standard curves obtained after increasing incubation times displayed a clear reduction of the OD405 readings over time, confirming the relatively short stability of the mixture of iodide-containing samples and detection buffers reported by Tang & Wildey (2004). The minimal detection limit estimated from the standard curve was higher than the one described by Tang & Wildey (2004). This may arise from the fact that the OD values obtained here were lower and probably due to well-to-well variations, since the 3 $\times$ SD is comprised to evaluate the detection limit. The assays linear range was determined from the NaI standard curves exhibiting a range of about 300 nM to 3 µM after 15 minutes assay incubation time or after 30 minutes between 100 nM and 1 µM. The lower value determined after 30 minutes was similar to the value presented by Tang & Wildey (2004), who reported a linear range of 130 nM to 13 µM after 30 minutes incubation time. However, the upper linear range limit gained was 10-fold lower than the one described by Tang & Wildey (2004), who showed a 100-fold molar linear range of the method. Thus, the SK assay detection range obtained here was relatively small compared to the data represented by Tang & Wildey (2004). The reasons for these variations are not clear, since detection buffers used were prepared as described (Tang

& Wildey, 2004, 2006). There may have been slight variations in NaI solutions or detection buffers due to fluctuation in measuring, weighing or pipetting, however, it is unlikely that these deviations are responsible for the indicated differences, especially since standard curves were repeated a few times using different solutions and buffers.

Next, the assay was tested in HEK293 cells transiently transfected with $\alpha 3\beta 2\gamma 2$ $GABA_A$ receptors using 96-well microtitre plates. As mentioned above, high OD405 values indicate a low iodide concentration inside the cells, whereas low OD405 readings represent high intracellular iodide concentrations. However, readings obtained from cell lysates after applying ascending GABA concentrations to the cells were rather random and did not show specific ion flux or GABA concentration-related patterns. Furthermore, untransfected control cells exhibited similar OD405 readings as transfected cells, although they did not express the exogenous $GABA_A$ receptors. Cell supernatants were also subject to the modified SK reaction. The supernatant solution was iodide free before adding it to the cells and should contain different concentrations of iodide depending on the level of receptor activation and, hence, the iodide efflux level. OD405 readings obtained from undiluted supernatants were low, indicating high iodide concentrations in the wells and confirming that iodide effused from the cells. Due to the small detection window, supernatant solutions were diluted in order to detect differences in the iodide concentrations per well that could distinguish $GABA_A$ receptor activity in the differently treated wells. However, the data obtained were not GABA concentration-related but random in transfected as well as untransfected cells. The fact that readings from untransfected control cells were similar to the ones obtained from cells transiently expressing $GABA_A$ receptors indicated a very low signal-to-noise ratio. This could be due to an imperfect removal of extracellular iodide after loading the cells or due to a continuous leakage of iodide from the cells before receptor stimulation (Zheng et al., 2004). However, cells were washed three to four times after the loading step, which most likely excludes the former possibility. A non-specific iodide leakage through the cell membrane could happen via passive diffusion, chloride pumps or spontaneous active $GABA_A$ receptors and may be one possible explanation for the low signal-to-noise ratio (Smith et al., 2001).

After repeating the assay a few times with no clear concentration-dependent effects, dif-

ferent assay components were varied and tested in order to improve and optimise the assay and to increase the signal-to-noise ratio. The agonist incubation time is an important factor for ideal flux responses that are dependent on the balance between ion channel activation and desensitisation (Smith et al., 2001). Also, iodide-leakage that may play a part in the low signal-to-noise ratio detected, could probably be reduced with shorter agonist incubation time which should then result in more accurate readings. Different GABA incubation times between ten seconds to five minutes were examined to optimise iodide efflux from the cells. Data obtained were compared with control data from DPBS incubation at the different time points in order to subtract non-specific iodide efflux from efflux induced by GABA. Supernatant data from certain time points differed significantly between GABA- and DPBS-treated cells. However, the test results were inconsistent and not reproducible. Also, often GABA-treated and control cell OD405 values were similar or occasionally flux from control cells seemed to be significantly more than from $GABA_A$ receptor expressing cells, although the opposite was expected. Due to the discrepancies obtained throughout the data, no optimal incubation time could be determined and it was decided to use the incubation time suggested by Tang & Wildey (2004) while other test variables were tried to be optimised instead. The question remained, why could the signal-to-noise ratio not be improved by different agonist incubation times and why were the results so difficult to reproduce?

It was also tested whether changes in cell density would improve the assay outcome. In previous experiments, iodide concentrations in the supernatants were relatively high whereas it was low in cell lysates, which could indicate high receptor activity, which may have not been suitable for the small detection range of the assay. Thus, it was examined whether lower cell numbers would improve intra- and extracellular iodide concentrations for better OD405 readouts. At all cell densities tested OD405 values were very low for supernatant solutions and no differences could be seen between the different cell densities without further supernatant dilutions. However, results obtained from cell lysates with 25×10^3 or 17.5×10^3 cells per well showed significant differences in OD405 readouts between different GABA concentrations, but no concentration-related pattern could be detected. Cell lysates of wells containing 12.5×10^3 cells per well, however, exhibited a significant lower reading for 1 µM

GABA compared to the three higher concentrations tested. Although this could have been a concentration-related difference, it was assumed, considering the high error bars obtained, that this was part of the variation seen throughout the plates and, hence, overlooked and not further examined. By hindsight, it would have been perspicacious to further decrease the number of cells. However, since the results were again not well-defined and Tang & Wildey (2004) used 2.5 $\times$ 10^4 WSS-1 cells per well, it was decided to continue with cell densities used by Tang & Wildey (2004), because WSS-1 cells, which stably express $GABA_A$ receptors, were derived from HEK293 cells (Wong et al., 1992).

Due to the fact that all assay optimisation attempts failed to improve the assay by producing a well-defined signal window, the functionality of the expressed $GABA_A$ receptors was investigated by applying the competitive antagonist bicuculline and the channel blocker picrotoxin. Again, OD405 data obtained for cell lysates were relatively high; only few differences were seen between the distinctly treated transfected and untransfected cells. However, results obtained from the supernatants were interesting. In all but the picrotoxin-treated wells, OD405 values were very low indicating a high iodide efflux from the cells. However, picrotoxin-treated cells, transfected as well as untransfected, exhibited significantly higher OD405 values, indicating a low concentration of iodide and, thus, blockage of the iodide-efflux from the cells. Since picrotoxin is a chloride channel blocker, the results indicated that mainly chloride channels were responsible for the iodide leakage detected in previous experiments, rather than chloride pumps or spontaneously active channels. Although, patch-clamp experiments using $\alpha 3\beta 2\gamma 2$ receptor expressing HEK293 cells revealed small constitutive activity of the expressed $GABA_A$ receptors. It is not clear why iodide concentrations were very high in cell supernatants containing bicuculline, since bicuculline is a receptor antagonist.

The colorimetric iodide-flux assay setup exhibited difficulties that could not be successfully amended when trying to optimise certain assay parameters. An important feature of compound screening assays is the assays reliability as well as a good information content and a robust assay setup (Xu et al., 2001), which could not be achieved with this assay format using HEK293 cells. There were three major issues, the variability between replicates, the random readings between different treatments and the fact that transfected as well as untransfected

cells had similar results. It is likely that several factors contributed to the assays failure. One is that the assay's detection range was very small. Therefore, already small iodide carry-overs could completely invalidate an experiment. Great care was taken to avoid carry-overs, but since the many pipetting steps involved were carried out manually, this may have been one contributing factor for the assays random readings and poor reproducibility between experiments. Another cause could have been the variable receptor population among the cells and especially between the different experiments due to variations in transient transfection efficacy. It is proposed that transient transfection efficiencies vary between 10 to 50 %, depending on cell type, cDNA and transfection reagent (Witchel et al., 2002; Thomas & Smart, 2005; Gilbert et al., 2009b) and it is likely that many cells in the wells were untrasfected. This heterogeneous cell population also likely added to the low signal-to-noise ratio seen throughout (Lynch, 2005). In comparison, Tang & Wildey (2004) demonstrated the assays functionality and reproducibility in cells expressing $GABA_A$ receptors stably and even then the Z'-factor that determines the assay's quality lay below 0.5, indicating a relatively small signal window that is not ideal for the assay's application in HTS (Zhang et al., 1999; Tang & Wildey, 2004). Even when considering a relatively low transfection efficacy, one question remained: why was the iodide efflux in cells expressing the $GABA_A$ receptors and control cells similar? It was suggested that agonist-independent iodide fluctuations, due to passive diffusion, active chloride pumps and spontaneous receptor activity (at least in transfected cells) partly contributed. A study by Galietta et al. (2001b) showed that the assay temperature can significantly influence basal halide permeability. In most cell types, non-specific halide permeability is significantly reduced when performing an assay at 37°C compared to room temperature, where it was relatively high. This likely explains the high iodide-efflux measured from untransfected control cells. Nevertheless, results obtained from applying picrotoxin to the cells indicated that the observed iodide-efflux blockade probably occurred via chloride channels. HEK293 cells endogenously express $\beta 3$, $\gamma 3$ and ε $GABA_A$ receptors (Thomas & Smart, 2005). They also express GlyR β subunits. However, the latter do not form functional homomeric channels (Lynch, 2009). There have been reports that endogenously expressed $GABA_A$ receptors can trigger GABA-activated currents (Ueno et al., 1996;

Thomas & Smart, 2005), however, patch-clamp studies on untransfected cells performed in this project did not detect GABA-activated currents. It is also worth mentioning that pre-incubation of cells with iodide-containing buffers can affect cell viability (Galietta et al., 2001b), which may have also contributed to the assay's outcome. Although the reasons for the assay's failure are not entirely clear, it was clearly not reliable or robust in the current assay format using transiently transfected HEK293 cells. Therefore, a further alternative plate reader assay was examined.

4.3.3 YFP-based screening assay

The final screening assay setup tested was based on the iodide-sensitivity of the mutant YFP-H148Q/I152L that can be used to determine iodide influx into cells via membrane proteins, such as the $GABA_A$ receptor (Galietta et al., 2001a; Kruger et al., 2005; Gilbert et al., 2009b). By using this assay format with HEK293 cells expressing YFP-H148Q/I152L and $\alpha3\beta2\gamma2$ receptors, it could be demonstrated that it was possible to measure changes in the fluorescence signal due to iodide influx into the cells upon $GABA_A$ receptor activation. The fluorescence change obtained was around 50 % and, thus, similar in magnitude as seen in other studies using $GABA_A$ receptors (Kruger et al., 2005; Gilbert et al., 2009b). Gilbert et al. (2009b) detected a larger fluorescence quench with $\alpha1\beta1$ receptors compared to changes obtained when adding a γ subunit to the receptor complex, whereas here the largest fluorescence quench was obtained from $\gamma2$-containing receptors compared to $\alpha1\beta2$ receptors. Several studies have investigated kinetic properties of different receptor isoforms, concluding that $GABA_A$ receptor channel gating is dependent on receptor subunit composition (Verdoorn, 1994; Gingrich et al., 1995; Lavoie et al., 1997; Haas & Macdonald, 1999). It was shown that the $\gamma2$L subunit confers longer duration openings and longer bursts of opening to a receptor subtype, compared to $\alpha\beta$-containing receptors (Haas & Macdonald, 1999), which could explain the higher fluorescence quench obtained. It was proposed that the fluorescence variation seen for the different receptor subtypes could be due to the distinct kinetics and gating properties of the receptor subtypes investigated, that conducted different levels of iodide influx. A further factor may be differences in transfection efficiency as shown

by Gilbert et al. (2009b). It is unclear why $\alpha3\beta2\varepsilon$ receptors could not trigger sufficient iodide influx to reduce the level of fluorescence inside the cells whereas a reduction in fluorescence could be measured in cells expressing $\alpha1\beta2\varepsilon$ receptors. The spontaneous receptor activity is most likely one factor contributing to the lower fluorescence quench achieved in ε-containing receptors. Furthermore, Whiting et al. (1997) reported a rapid desensitisation rate in $\alpha1\beta1\varepsilon$ receptors expressed in HEK293 cells. This would explain a lower and less sufficient iodide influx compared to other receptor subtypes exhibiting slower deactivation and desensitisation rates.

Before testing different GABA concentrations and compounds using the assay setup, its quality was evaluated and results obtained for different $GABA_A$ receptor subtypes were compared among each other by determining the assays' Z'-factors. The Z'-factor incorporates the assay's signal dynamic range as well as data variation between replicates, without interference of test compounds (Zhang et al., 1999). Results obtained indicated that the setup of the assay is acceptable when using cells expressing both $\alpha1\beta2$ (Z' = 0.58) and $\alpha3\beta2\gamma2$ receptors (Z' = 0.48; Inglese et al., 2007a). However, in cells expressing $\alpha1\beta2\varepsilon$ receptors the signal window was relatively small that positive and negative signal variation bands overlapped slightly, which caused a negative Z'-factor. Although the assays outcome was improved and a fluorescence quench could be detected when substituting the $\alpha3$ subunit with the $\alpha1$ subunit, the assay's quality using cells expressing the ε subunit was not ideal. Hence, it was decided to screen the compound library on both $\alpha3\beta2\gamma2$ receptors as well as on $\alpha1\beta2\varepsilon$ receptors. Cells expressing the latter were used despite the small signal window, as it was proposed that positively modulating as well as inhibiting compounds could still be identified by using this method.

Next, GABA concentration-response relations were investigated. By this means it was possible to compare the results of the assay with data obtained from electrophysiological methods as well as to determine a suitable submaximal GABA concentration for the screening assay. The findings gained were very different to the ones obtained from electrophysiological recordings (see Section 3.2.1, Chapter 3). EC_{50} values from cells expressing $\alpha3\beta2\gamma2$ receptors were lower than those from cells expressing $\alpha1\beta2$ and $\alpha1\beta2\varepsilon$ receptors; the latter

exhibited the highest values. Using electrophysiological recordings in oocytes it was shown that the ε subunit confers high agonist sensitivity to the receptor (Section 3.2.1, Chapter 3), which was also shown in several other studies (Whiting et al., 1997; Neelands et al., 1999; Maksay et al., 2003; Ranna et al., 2006). Furthermore, in case of $\alpha3\beta2\gamma2$ receptors, the EC_{50} value of the plate reader assay was lower compared to the ones obtained from oocytes (39.37 µM) or HEK293 cells (14.65 µM; Figure B.6, Appendix B) using electrophysiological methods, whereas the EC_{50} value for $\alpha1\beta2\varepsilon$ receptors was higher than the one obtained in oocytes (3.55 µM; Figure B.5, Appendix B). Kruger et al. (2005) measured concentration-response relations in cells expressing the mutant YFP and $\alpha1$ GlyR using an imaging-based assay system as well as a fluorescence plate reader. It was reported that the EC_{50} values obtained with the latter method were five-times higher compared to the former technique. Due to the high deviation seen with the fluorescence plate reader assay, compared to the other systems tested, the reliability of the assay format was doubted (Kruger et al., 2005). However, it is not surprising that the results obtained here vary, considering the variation between the different measuring techniques. The YFP-based assay was performed in a plate reader that measured values from the whole cell population in the wells, the measuring time was extended and an indirect, secondary effect (the YFP quench) was detected. In comparison, electrophysiological recordings are performed on single cells for a short time and current flow across the membrane upon receptor activation can be measured directly (Wafford et al., 2009). Furthermore, mutant YFP variants exhibited relatively slow chloride association and disassociation kinetics (iodide binding kinetics were not shown; Galietta et al., 2001a) and Colquhoun (1998) stated that to gain precise concentration-response curves fast agonist application is vital due to the fast desensitisation rates of ion channels.

By comparing the fluorescence signals of rising concentrations of GABA it was decided to use EC_{30} GABA concentrations when screening the compounds. This is because fluorescence signals obtained for EC_{30} GABA concentrations could be clearly distinguished between positive (high GABA concentration) and negative controls (NaI test solution only or GABA (EC_{30}) with picrotoxin). This was in consent with work done by Wafford et al. (2009), who also used EC_{30} concentrations, although in a different screening assay type (FLIPR).

Benzodiazepines are known to positively modulate $GABA_A$ receptors and flunitrazepam potentiated submaximal GABA concentrations in $\alpha3\beta2\gamma2$ receptors (Section 3.2.4, Chapter 3). Using the YFP-based assay setup it could be demonstrated that the potentiating effect by flunitrazepam could also be detected with the fluorescence plate reader.

The different tests performed using the YFP-based screening assay demonstrated that the assay was suitable to detect GABA-induced receptor activity when using cells expressing $\alpha3\beta2\gamma2$ and, to a certain degree $\alpha1\beta2\varepsilon$ receptors. It was also shown that the fluorescence signal change was GABA concentration-dependent and that the benzodiazepine-induced potentiation of a submaximal GABA concentration could be detected in cells expressing $\alpha3\beta2\gamma2$ receptors. This confirmed the suitability of the assay for pharmacological investigations.

4.3.4 Summary

The results presented in this chapter clearly display the difficulties associated with setting up a chloride-ion channel screening assay. The data show that a specific assay setup, that works for a certain cell line and chloride channel or $GABA_A$ receptor subtype, not necessarily works equally well with other receptor (sub)types or cell lines, even after optimisation steps. For example, attempts were made to optimise many parameters when setting up the iodide-flux assay. However, at the end it could be concluded that the assay format described by Tang & Wildey (2004) was unsuitable when using transiently transfected HEK293 cells expressing $GABA_A$ receptors. Nevertheless, an acceptable assay to screen certain $GABA_A$ receptor subtypes was found. However, there were certain limitations and difficulties when investigating spontaneously open ε-containing receptors and special care should be taken when evaluating screening results, due to the small signal detection window of the assay.

Chapter 5

Screening a chemical compound library using the mutant YFP-H148Q/I152L

5.1 Introduction

Not much is known about the ε-subunit-containing $GABA_A$ receptor. Studies conducted previously could not determine a subunit-specific pharmacological profile and its functions *in vivo* are still not known. It was proposed that ε-containing receptors have a specific modulatory site, similar to the benzodiazepine binding site. For these reasons, the next aim of this study was to screen an ε-containing $GABA_A$ receptor subtype against a chemical compound library and, with luck, to find compounds that modulate receptor activity in the presence of GABA. ε-subunit-selective compounds will be of great use to elucidate the subunit's role *in vivo* by indicating ε-specific pharmacological effects or possibly a specific phenotype. Furthermore, amino acids important for the compound's binding site could be identified by using molecular approaches, which would further help to study the subunit's role. Moreover, a novel lead compound could be a possible future drug acting on the receptor, for example to treat AD (Section 1.4, Chapter 1).

Several cell-based screening assays are available, such as flux or YFP-based assays, and many aspects have to be considered when developing and setting up a suitable approach, for example assay format and detection instrumentation (Inglese et al., 2007b). In the previous

chapter (Chapter 4), a number of screening assay formats were tested for their suitability to screen compounds against certain $GABA_A$ receptor subtypes. A cell-based screening assay using the mutant YFP-H148Q/I152L gave robust data when using HEK293 cells expressing $\alpha3\beta2\gamma2$ receptors. Results obtained for ε-containing receptors exhibited a relatively small signal dynamic range, limiting the assay's suitability. However, it was proposed that effects of inhibiting and enhancing compounds could be distinguished from submaximal GABA-control responses. Due to the lack of other alternative assay formats, the YFP-based assay was applied to screen compounds and search for $\alpha3\beta2\gamma2$ and $\alpha1\beta2\varepsilon$ $GABA_A$ receptor subtype modulators. By this means, the effects and specificity of hit compounds of the two receptor subtypes could be compared, and ε-subunit-specific compounds could be identified more easily. A similar study by Wafford et al. (2009) sought compounds specific to the δ subunit and also compared effects of the hit compounds with their effect on $\alpha\beta\gamma$ receptors.

The compound library purchased (Maybridge HitFinder™Collection) comprised of drug-like molecules with a broad range of structural motifs and biological space. The collection is rich in diverse pharmacophores, and compounds follow Lipinski guidelines (Lipinski et al., 2001). The Maybridge HitFinder™Collection consists of 14,400 compounds in total, of which a small selection of 800 compounds has been tested here. Due to the fact that nothing is known about specific compound-binding sites on the ε subunit, it was important to screen compounds with great structural diversity, which is a key factor concerning chemical libraries, especially since the drug target site is unknown (Gillet, 2008). It is likely that similar compound structures would exhibit similar activities. Therefore, chances to find chemical leads are enhanced when using a broad range of structural motifs. Finally, serendipity is also an important factor to find an ε-subunit-selective compound among the 800 compounds investigated in this study.

The aim of this chapter was to identify subtype-selective compounds modulating $\alpha1\beta2\varepsilon$ and $\alpha3\beta2\gamma2$ $GABA_A$ receptor subtypes by performing preliminary screens using the mutant YFP-H148Q/I152L. Afterwards, it was aimed to confirm the identity of hit compounds and further examine the compounds in more detail using the two-electrode voltage-clamp technique.

5.2 Results

5.2.1 Preliminary screening

Test compounds were screened against both $\alpha3\beta2\gamma2$ and $\alpha1\beta2\varepsilon$ $GABA_A$ receptor subtypes. Note that compounds were designated 'TS-' and in addition numbered (1-41). The preliminary screen was carried out using relatively high concentrations of the compounds (final concentrations between 50.3 and 59.29 µM). 1 µl of a compound (in DMSO, see Sections 2.7.1 and 2.7.2, Chapter 2) was added to each well containing 50 µl NaCl bath solution, and an EC_{30} concentration of GABA in NaI test solution was subsequently injected into the wells. By this means, compounds were identified that exhibit positive or negative modulatory effects on the receptor subtypes by exhibiting a reduced or increased fluorescence quench compared to cells treated with EC_{30} GABA concentrations only or cells subjected to GABA (EC_{30}) and 0.5 % DMSO (compound vehicle only negative control). The results acquired indicated that the majority of test compounds had no effect on the receptors. In the case of $\alpha1\beta2\varepsilon$ receptors 73.74 % of all compounds were inactive; Figure 5.1 represents a selection of negative screening results. In comparison, 87.31 % of test compounds had no effect on $\alpha3\beta2\gamma2$ receptors (Figure 5.2).

Figures 5.3 and 5.4 display representative results of test compounds that showed an inhibitory (5.3 A, B and 5.4 A) or positive (5.3 C and 5.4 B, C) effect on receptor activation. In the case of $\alpha1\beta2\varepsilon$ receptors, there were 209 compounds at this concentration range of which 151 inhibited and 58 increased the YFP fluorescence quench. In comparison, 101 compounds seemed to evoke an explicit effect on cells expressing $\alpha3\beta2\gamma2$ receptors of which 10 were inhibiting and 91 were increasing the YFP quench.

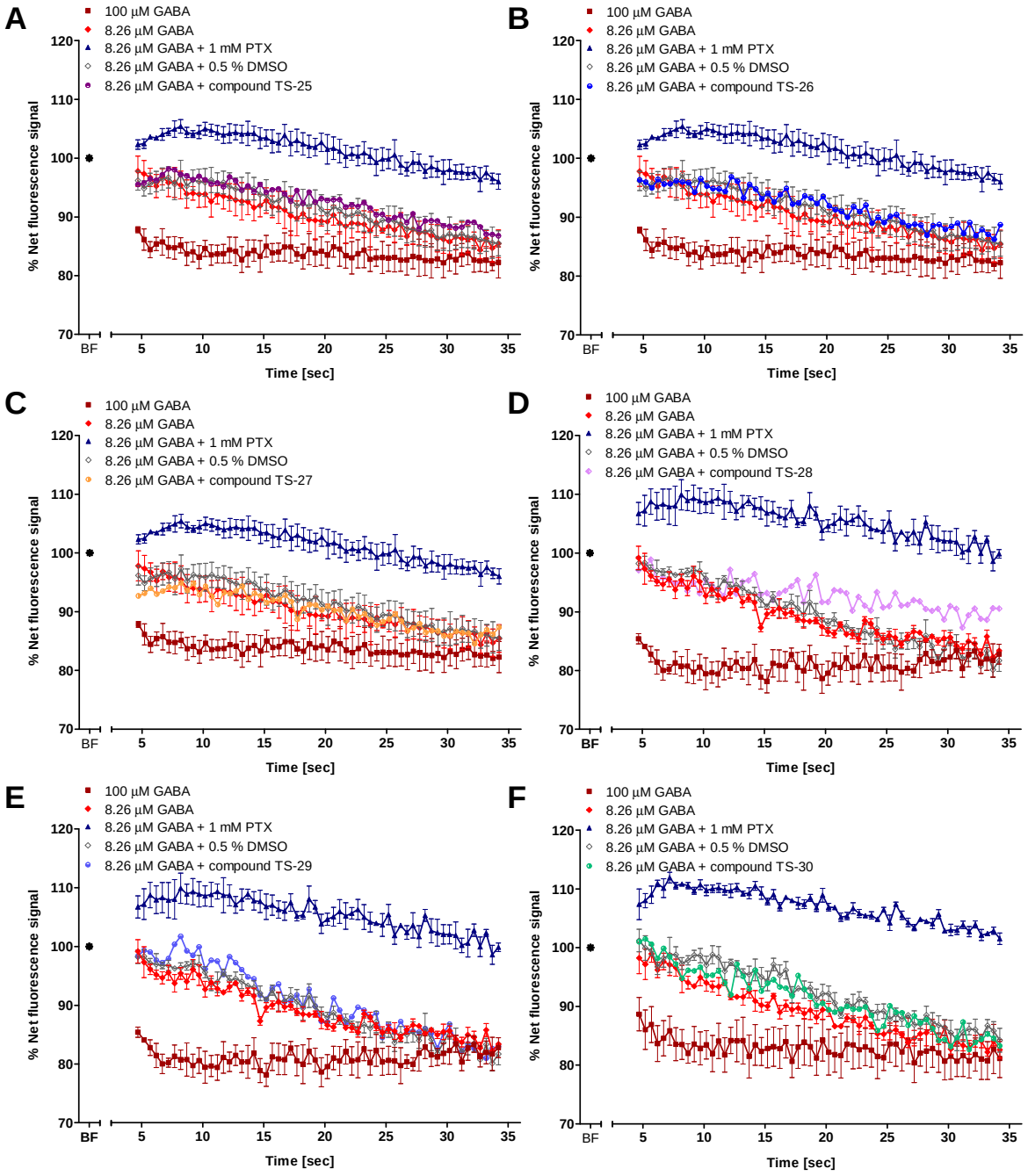

Figure 5.1: Sample negative results from the preliminary screening of HEK293 cells expressing mutant YFP-H148Q/I152L and $\alpha 1\beta 2\varepsilon$ $GABA_A$ receptors.

Fluorescence was measured for 30 seconds after addition of 100 µM GABA (n = 3), 8.26 µM GABA (EC_{30}) and 1 mM picrotoxin (n = 3), 8.26 µM GABA and 0.5 % DMSO (n = 3), 8.26 µM GABA alone (n = 3) or 8.26 µM GABA with test compound (n = 1): (A) compound TS-25 (54.37 µM), (B) compound TS-26 (53.81 µM), (C) compound TS-27 (53.92 µM), (D) compound TS-28 (56.72 µM), (E) compound TS-29 (52.52 µM), (F) compound TS-30 (58.47 µM). Compound concentrations are final concentrations per well after injection of GABA. Data correspond to means ± SEM; n states the number of wells tested. Net fluorescence was normalised by setting the averaged baseline fluorescence to 100 % and fluorescence changes (after adding solutions) were calculated as percentage of the baseline fluorescence.

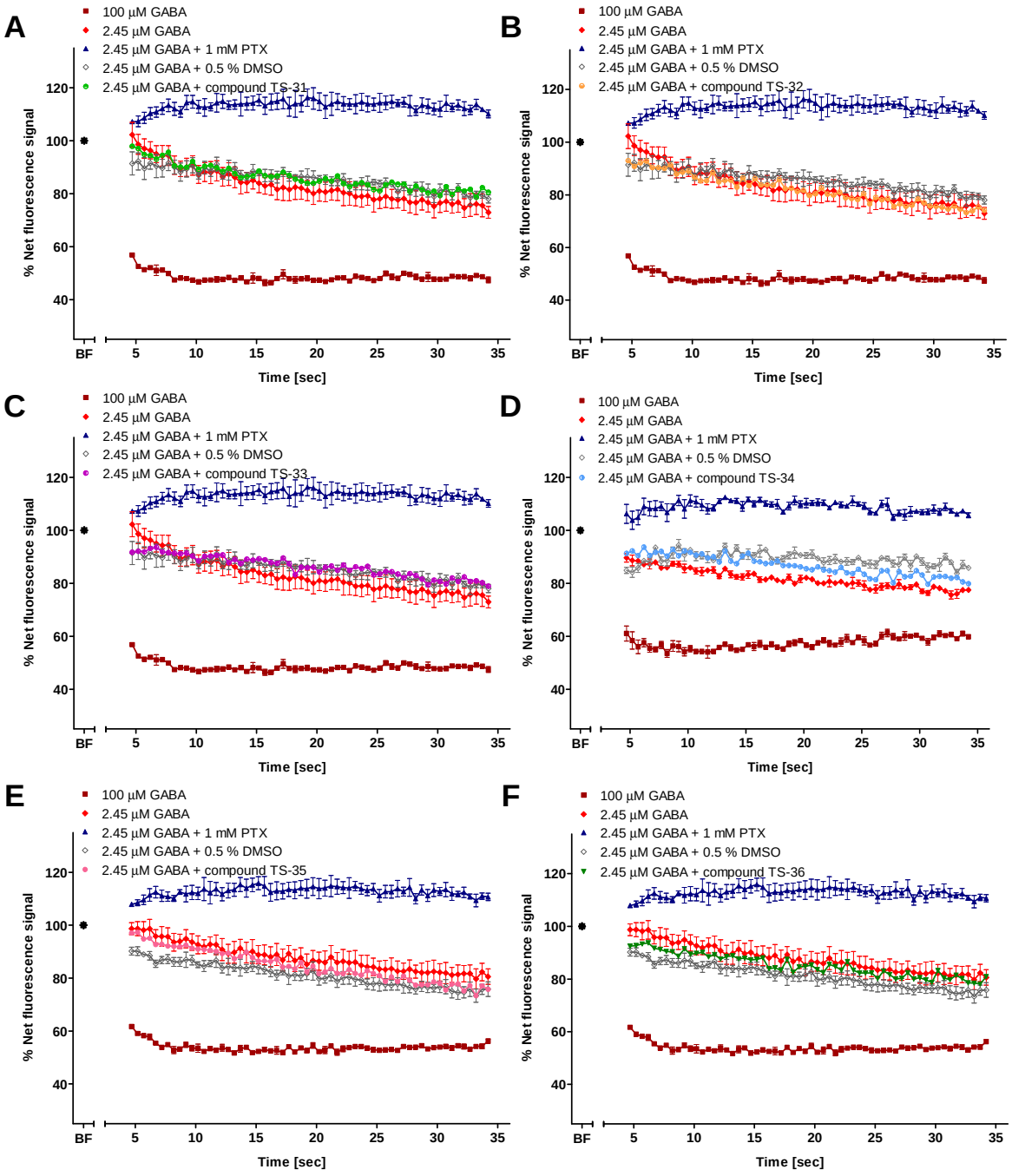

Figure 5.2: Sample negative results from the preliminary screening of HEK293 cells expressing mutant YFP-H148Q/I152L and $\alpha3\beta2\gamma2$ $GABA_A$ receptors.

Fluorescence was measured for 30 seconds after addition of 100 µM GABA (n = 3), 2.45 µM GABA (EC_{30}) and 1 mM picrotoxin (n = 3), 2.45 µM GABA and 0.5 % DMSO (n = 3), 2.45 µM GABA alone (n = 3) or 2.45 µM GABA with test compound (n = 1): (A) compound TS-31 (54.58 µM), (B) compound TS-32 (54.31 µM), (C) compound TS-33 (54.88 µM), (D) compound TS-34 (54.08 µM), (E) compound TS-35 (55.66 µM), (F) compound TS-36 (57.12 µM). Compound concentrations are final concentrations per well after injection of GABA. Data correspond to means ± SEM; n states the number of wells measured. Net fluorescence was normalised by setting the averaged baseline fluorescence to 100 % and fluorescence changes (after adding solutions) were calculated as percentage of the baseline fluorescence.

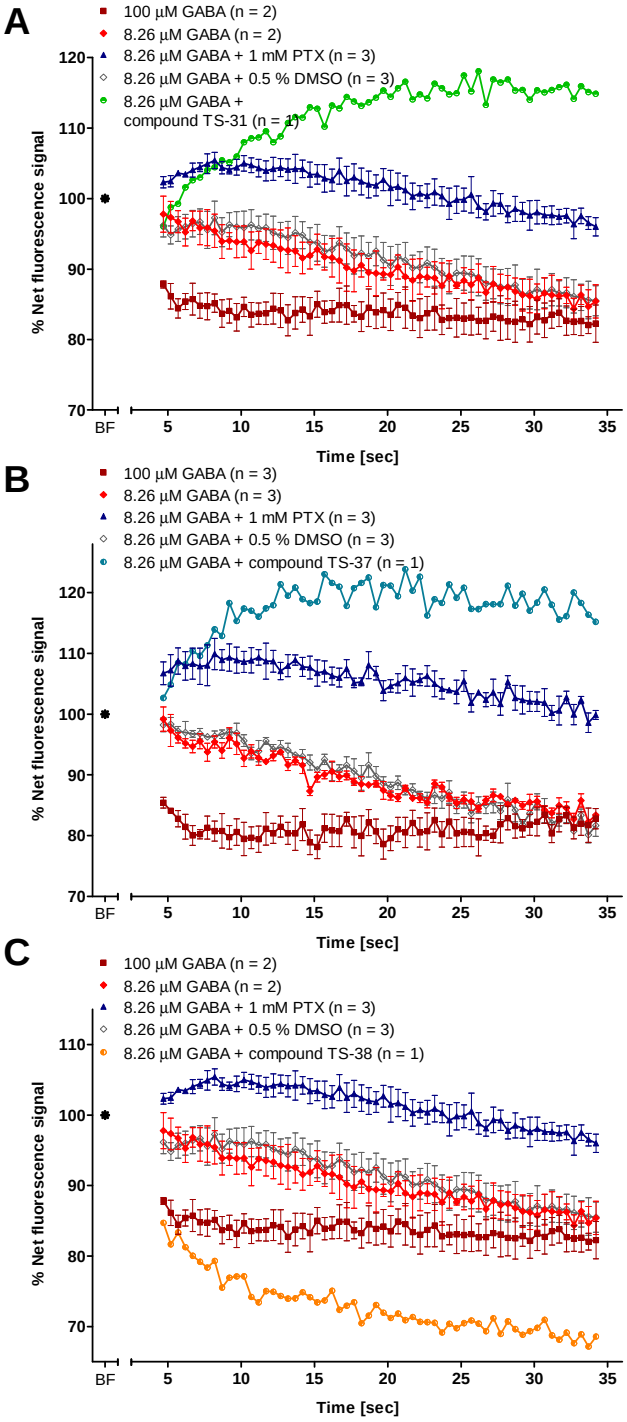

Figure 5.3: Representative positive screening results for HEK293 cells expressing mutant YFP-H148Q/I152L and $\alpha 1\beta 2\varepsilon$ $GABA_A$ receptors.

Fluorescence was measured for 30 seconds after addition of 100 µM GABA, 8.26 µM GABA and 1 mM picrotoxin, 8.26 µM GABA and 0.5 % DMSO, 8.26 µM GABA alone or 8.26 µM GABA with test compound: (A) compound TS-31 (54.58 µM), (B) compound TS-37 (55.04 µM), (C) compound TS-38 (55.24 µM). Concentrations are final concentrations per well after injection of solutions. Data correspond to means ± SEM; n states the number of wells tested. Net fluorescence was normalised by setting the averaged baseline fluorescence to 100 % and fluorescence changes (after adding solutions) were calculated as percentage of the baseline fluorescence.

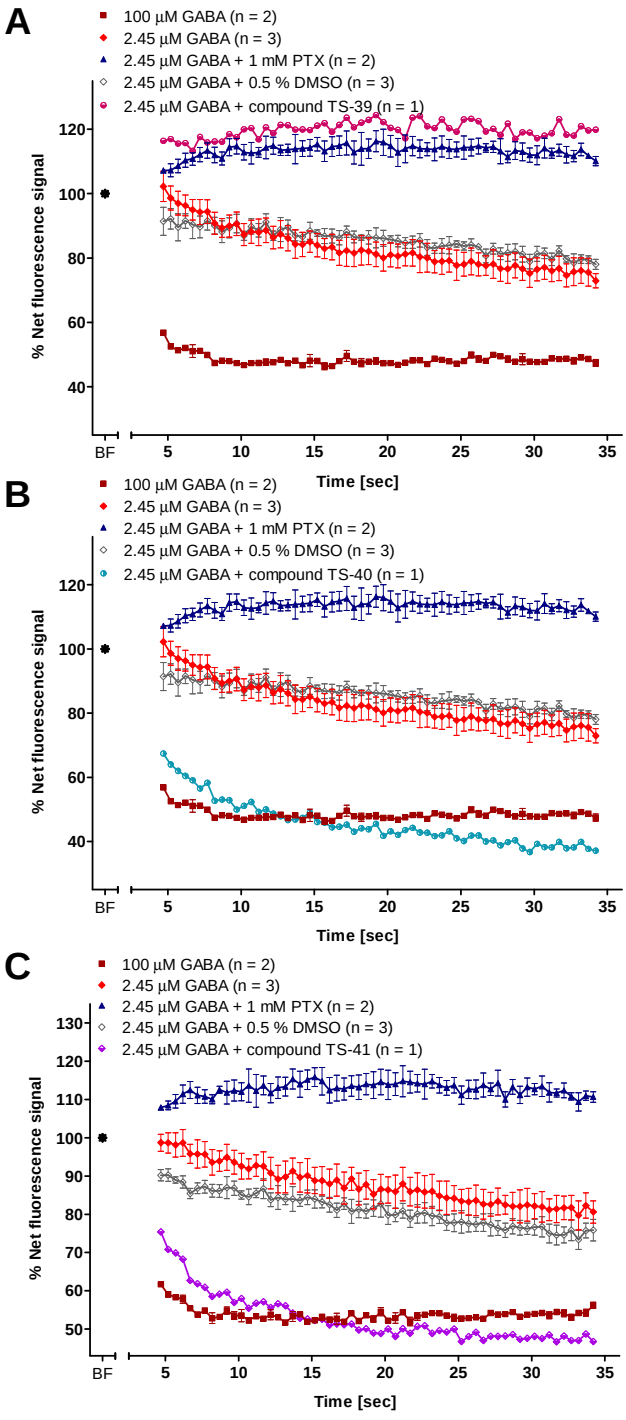

Figure 5.4: Representative positive screening results for HEK293 cells expressing mutant YFP-H148Q/I152L and $\alpha3\beta2\gamma2$ $GABA_A$ receptors.

Fluorescence was measured for 30 seconds after addition of 100 µM GABA, 2.45 µM GABA and 1 mM picrotoxin, 2.45 µM GABA and 0.5 % DMSO, 2.45 µM GABA alone or 2.45 µM GABA with test compound: (A) compound TS-39 (55.32 µM), (B) compound TS-40 (56.32 µM), (C) compound TS-41 (55.82 µM). Concentrations are final concentrations per well after injection of solutions. Data correspond to means ± SEM; n states the number of wells tested. Net fluorescence was normalised by setting the averaged baseline fluorescence to 100 % and fluorescence changes (after adding solutions) were calculated as percentage of the baseline fluorescence.

The number of compounds which had an effect on the two $GABA_A$ receptor subtypes was very high during the initial screen. Therefore further screens were performed by gradually decreasing the concentration of the test compounds in order to identify the most potent compounds. In a second screen all compounds which indicated positive receptor modulation or inhibition at the initial high concentrations were tested again with a tenfold diluted concentration (between 5.03 and 5.93 µM). Following this scan, the number of active compounds on $\alpha1\beta2\varepsilon$ receptors decreased to 95 (86 inhibiting and 9 enhancing the receptor activity). 32 compounds still showed an effect on cells expressing $\alpha3\beta2\gamma2$ receptors (10 inhibiting and 22 increasing the fluorescence quench). A third scan was conducted with the remaining active test compounds that were again tenfold diluted (final concentrations of compounds per well were between 503 and 593 nM). After that there were 47 active compounds on $\alpha1\beta2\varepsilon$ receptors (41 inhibiting and 6 enhancing the receptor activity) and seven on $\alpha3\beta2\gamma2$ receptors (one showed an inhibitory and 6 enhancing effects). Figures 5.5 and 5.6 represent results of compounds that exhibited an effect on $\alpha1\beta2\varepsilon$ and $\alpha3\beta2\gamma2$ $GABA_A$ receptors, respectively, at high concentrations, but both compounds failed to produce a similar effect at a lower screening concentration. However the number of compounds which triggered an effect in $\alpha1\beta2\varepsilon$ receptor-expressing cells during that last scan was still relatively high. Therefore a further dilution of the remaining test compounds was carried out (concentrations from 50.3 to 59.3 nM) and tested. 17 compounds showed an effect on cells expressing $\alpha1\beta2\varepsilon$ receptors whereas one compound enhanced receptor activity in cells expressing $\alpha3\beta2\gamma2$ receptors. The remaining 17 active compounds for $\alpha1\beta2\varepsilon$ receptors plus 2 further compounds that enhanced the fluorescence signal when using the next higher concentration were subject to further investigation. Also applied in subsequent assays were the 7 compounds exhibiting an effect on cells expressing $\alpha3\beta2\gamma2$ receptors.

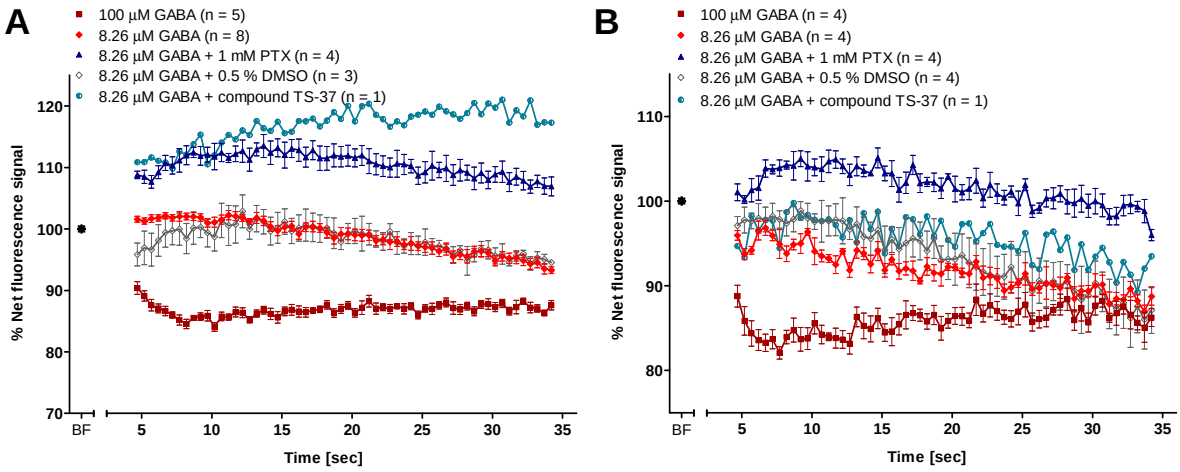

Figure 5.5: Results obtained for decreasing concentrations of a test compound in HEK293 cells expressing $\alpha 1\beta 2\varepsilon$ $GABA_A$ receptors.

Fluorescence was measured for 30 seconds after addition of 100 µM GABA, 8.26 µM GABA alone (EC_{30}), 8.26 µM GABA and 1 mM picrotoxin, 8.26 µM GABA and 0.5 % DMSO or 8.26 µM GABA with test compound TS-37. (A) 5.5 µM; (B) 550.4 nM. Concentrations are final concentrations per well after injection of GABA. Data correspond to means ± SEM; n states the number of wells tested. Net fluorescence was normalised by setting the averaged baseline fluorescence to 100 % and fluorescence changes (after adding solutions) were calculated as percentage of the baseline fluorescence.

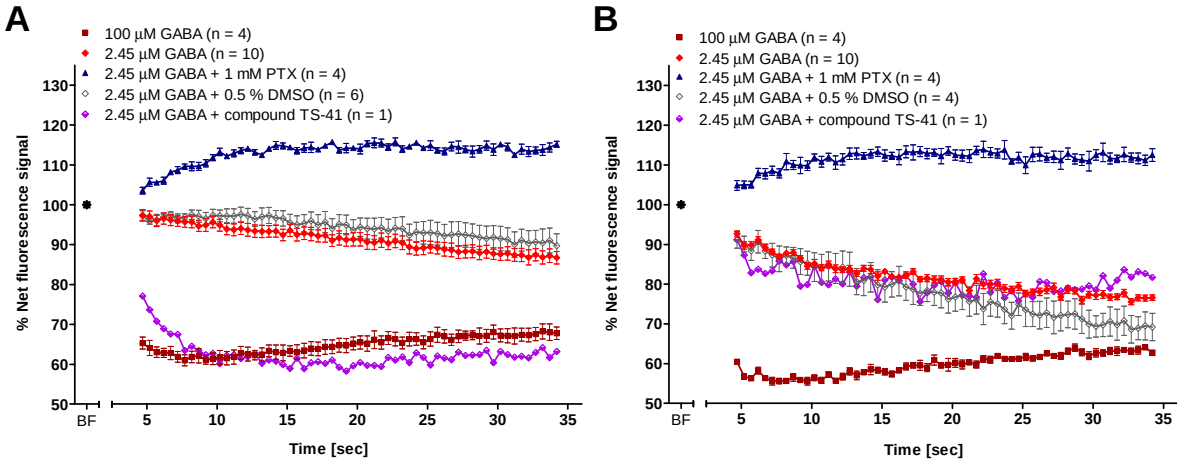

Figure 5.6: Results obtained for decreasing concentrations of a test compound in HEK293 cells expressing $\alpha 3\beta 2\gamma 2$ $GABA_A$ receptors.

Fluorescence was measured for 30 seconds after addition of 100 µM GABA, 2.45 µM GABA alone (EC_{30}), 2.45 µM GABA and 1 mM picrotoxin, 2.45 µM GABA and 0.5 % DMSO or 2.45 µM GABA with test compound TS-41. (A) 5.58 µM concentration of test compound, (B) 558.2 nM. Concentrations are final concentrations per well after injection of solutions. Data correspond to means ± SEM; n states the number of wells tested. Net fluorescence was normalised by setting the averaged baseline fluorescence to 100 % and fluorescence changes (after adding solutions) were calculated as percentage of the baseline fluorescence.

5.2.2 Investigation of 'hit' compounds on $\alpha 1\beta 2\varepsilon$ receptors

So far, test compounds were examined as singlets using only few controls (vehicle-only controls and controls testing receptor functions). In order to rule out false positive results, the remaining chemical compounds were examined in more detail using additional controls. Each compound was tested in triplicates and on at least three different plates. Compounds were applied at the lowest effective concentrations, determined before, to HEK293 cells expressing YFP-H148Q/I152L and the respective $GABA_A$ receptor subtype. NaI test solution containing GABA at an EC_{30} concentration was added subsequently. Compounds were also tested in the absence of GABA, injecting NaI test solution only. This would indicate possible GABA-independent effects of a test compound. Finally, compounds were applied at high concentrations to HEK293 cells expressing mutant YFP-H148Q/I152L only. If fluorescence changes would be seen in these cells, it would indicate that a test compound acts on endogenously expressed proteins of the cells rather than the specific $GABA_A$ receptor subtype. The latter two controls were more effective for compounds enhancing receptor activity. Neither an agonist-independent effect nor an effect on endogenously expressed ion channels could be seen from compounds that inhibit the receptors activity. However controls were performed on all compounds in order to identify any possible irregularities.

Figures 5.7 to 5.25 display the results obtained for test compounds that showed an effect on $\alpha 1\beta 2\varepsilon$ $GABA_A$ receptor activation during the initial screening assays in HEK293 cells, described above. At a concentration of 54.58 nM, test compound TS-1 had shown an inhibiting effect on the cells expressing the receptor subtype (Figure 5.7 A). However, after repeating the screening assay using the compound in triplicates, the effect was less distinctive (but significant) than before (Figure 5.7 B). Controls with test compounds only, in the absence of GABA, or using cells expressing YFP-H148Q/I152L only, showed no YFP quench, which was expected (see above; Figure 5.7 C, D).

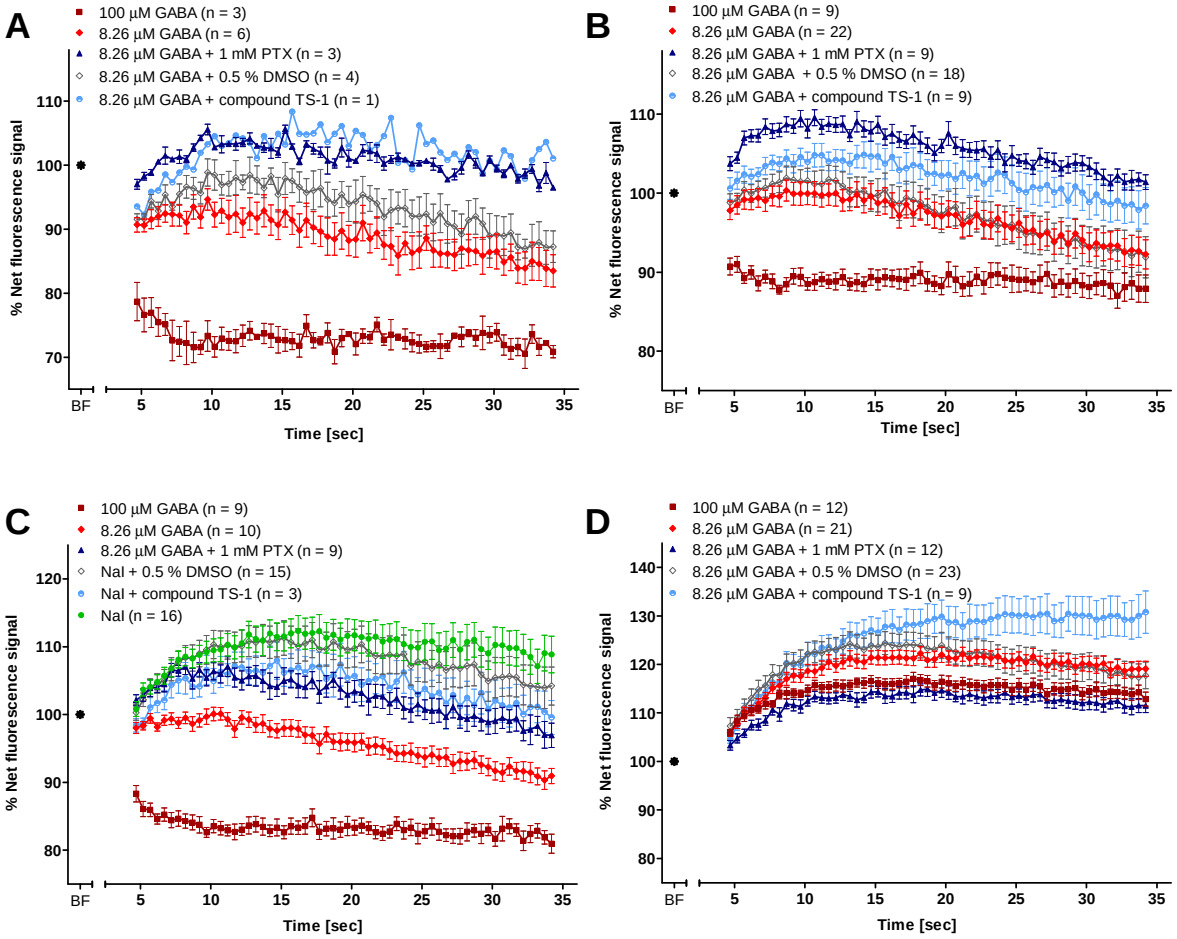

Figure 5.7: Fluorescence signal change after adding test compound TS-1 to HEK293 cells expressing mutant YFP-H148Q/I152L and $\alpha 1\beta 2\varepsilon$ $GABA_A$ receptors.

Fluorescence was measured for 30 seconds after adding (A) 8.26 µM GABA to wells containing compound TS-1 (54.58 nM final concentration; initial screening assay). (B) The assay was repeated at least three times using different plates and batches of cells. Effect of compound TS-1 was significantly different to GABA-control response ($p < 0.01$). (C) Data from no-GABA control plates. NaI test solution only was added to wells containing compound TS-1 (54.58 nM final concentration). (D) Effect of 8.26 µM GABA and 54.58 µM compound TS-1 in cells expressing YFP-H148Q/I152L only. 100 µM GABA, 8.26 µM GABA, 8.26 µM GABA and 1 mM picrotoxin, 8.26 µM GABA and 0.5 % DMSO and in (C) NaI test solution alone served as respective controls. Data correspond to means ± SEM; n states the number of wells measured. Net fluorescence of values was normalised by setting the averaged baseline fluorescence to 100 % and fluorescence changes (after adding solutions) were calculated as percentage of the baseline fluorescence.

Test compounds TS-2 as well as TS-3 inhibited GABA-control responses at concentrations of 55.32 nM and 55.66 nM, respectively, during the initial screening assay. This could be confirmed when repeating the assay using the compounds in triplicates (Figures 5.8 A, B and 5.9 A, B). No effect could be seen in the absence of GABA or on cells expressing YFP-H148Q/I152L only, which was expected (Figures 5.8 C, D and 5.9 C, D).

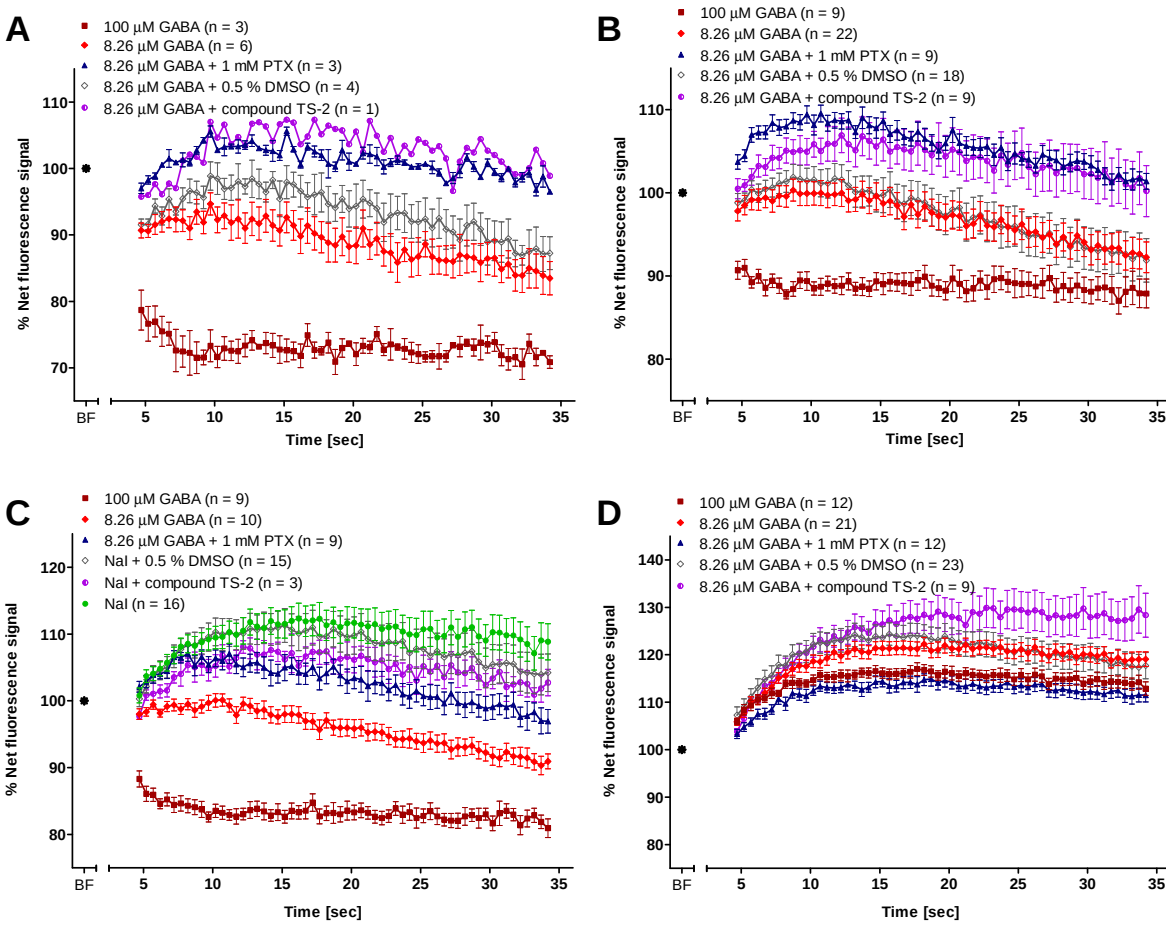

Figure 5.8: Fluorescence signal change after adding test compound TS-2 to HEK293 cells expressing mutant YFP-H148Q/I152L and $\alpha 1\beta 2\varepsilon$ $GABA_A$ receptors.

Fluorescence was measured for 30 seconds after adding (A) 8.26 µM GABA to wells containing compound TS-2 (55.32 nM final concentration) in initial screening assay. (B) The assay was repeated on at least three different plates. Effect of compound TS-2 was significantly different to GABA-control response ($p < 0.01$). (C) Data from no-GABA control plates. NaI test solution only was added to wells containing compound TS-2 (55.32 nM final concentration). (D) Effect of 8.26 µM GABA and 55.32 µM compound TS-2 on cells expressing YFP-H148Q/I152L only. 100 µM GABA, 8.26 µM GABA, 8.26 µM GABA and 1 mM picrotoxin, 8.26 µM GABA and 0.5 % DMSO and in (C) NaI test solution alone served as controls. Data correspond to means ± SEM; n states the number of wells measured. Net fluorescence of values was normalised by setting the averaged baseline fluorescence to 100 % and fluorescence changes (after adding solutions) were calculated as percentage of the baseline fluorescence.

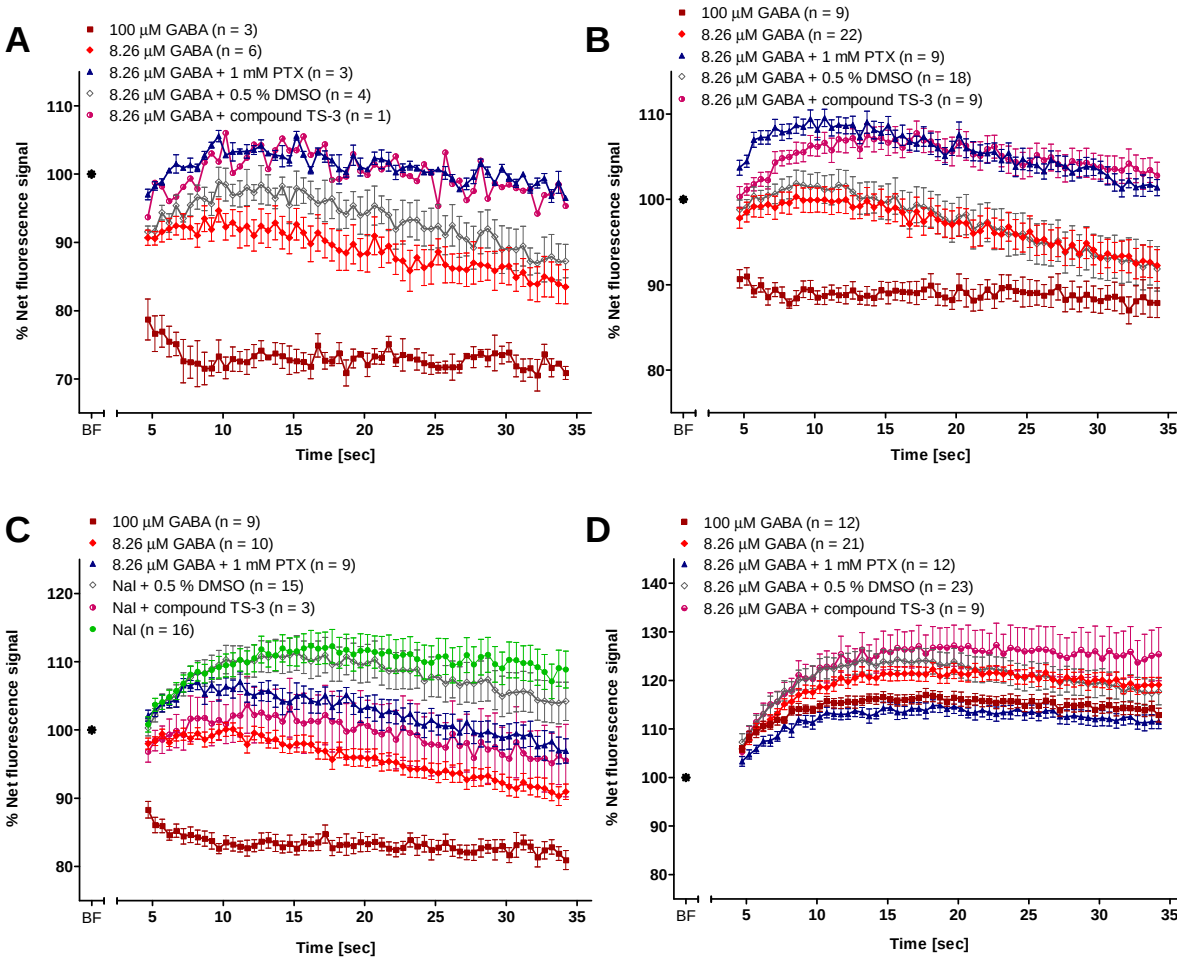

Figure 5.9: Fluorescence signal change after adding test compound TS-3 to HEK293 cells expressing YFP-H148Q/I152L and $\alpha 1\beta 2\varepsilon$ $GABA_A$ receptors.

Fluorescence was measured for 30 seconds after adding (A) 8.26 µM GABA to wells containing compound TS-3 (55.66 nM final concentration) in initial screening assay. (B) The assay was repeated on three different plates. Effect of compound TS-3 was significantly different to GABA-control response ($p < 0.01$). (C) Data from no-GABA control plates. NaI test solution only was added to wells containing compound TS-3 (55.66 nM final concentration). (D) Effect of 8.26 µM GABA and 55.66 µM compound TS-3 on cells expressing YFP-H148Q/I152L only. 100 µM GABA, 8.26 µM GABA, 8.26 µM GABA and 1 mM picrotoxin, 8.26 µM GABA and 0.5 % DMSO and in (C) NaI test solution alone served as respective controls. Data correspond to means ± SEM; n states the number of wells measured. Net fluorescence of values was normalised by setting the averaged baseline fluorescence to 100 % and fluorescence changes (after adding solutions) were calculated as percentage of the baseline fluorescence.

Test compound TS-4 inhibited the GABA-control response during the preliminary screening assay (Figure 5.10 A). The assay was repeated using the compound in triplicates. The previously observed effect was less prominent, but still significant (Figure 5.10 B). Controls with test compounds only, in the absence of GABA, or using cells expressing YFP-H148Q/I152L only, showed no YFP quench (see above; Figure 5.10 C, D).

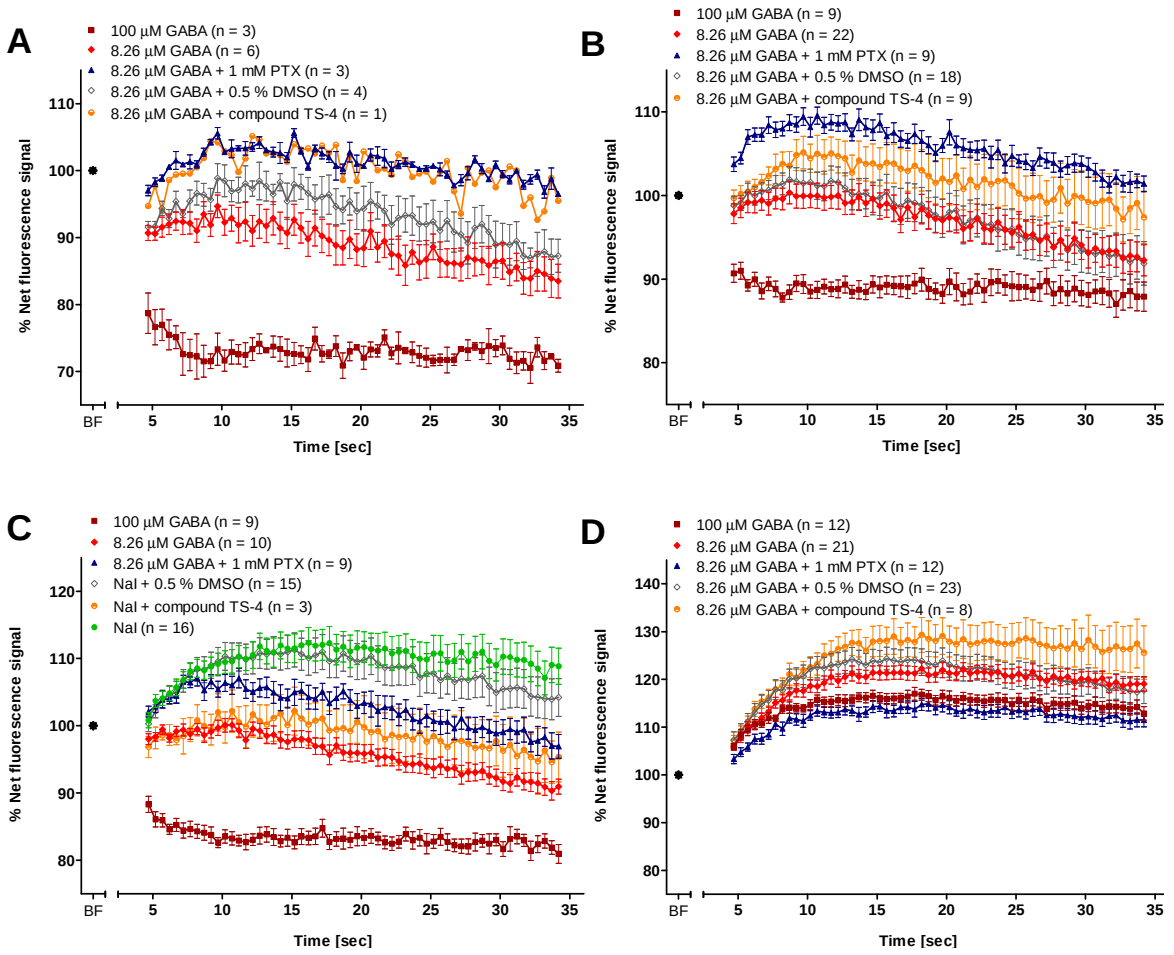

Figure 5.10: Fluorescence signal change after adding test compound TS-4 to HEK293 cells expressing YFP-H148Q/I152L and $\alpha 1\beta 2\varepsilon$ $GABA_A$ receptors.

Fluorescence was measured for 30 seconds after adding (A) 8.26 µM GABA to wells containing compound TS-4 (54 nM final concentrations) in initial screening assay. (B) The assay was repeated in triplicates on three different plates. Effect of compound TS-4 was significantly different to GABA-control response ($p < 0.05$). (C) Data from no-GABA control plates. NaI test solution only was added to wells containing compound TS-4 (54 nM final concentration). (D) Effect of 8.26 µM GABA and 54.01 µM compound TS-4 on cells expressing YFP-H148Q/I152L only. 100 µM GABA, 8.26 µM GABA, 8.26 µM GABA and 1 mM picrotoxin, 8.26 µM GABA and 0.5 % DMSO and in (C) NaI test solution alone served as controls. Data correspond to means ± SEM; n states the number of wells measured. Net fluorescence of values was normalised by setting the averaged baseline fluorescence to 100 % and fluorescence changes (after adding solutions) were calculated as percentage of the baseline fluorescence.

A similar result was obtained for compound TS-5. It inhibited the GABA-control response during the preliminary screening assay (Figure 5.11 A), however, after repeating the assay three times, the inhibition of the GABA-control response was less distinctive, but still significant (Figure 5.11 B). Controls with test compounds only, in the absence of GABA, or using cells expressing YFP-H148Q/I152L only, showed no YFP quench, which was expected (see above; Figure 5.11 C, D).

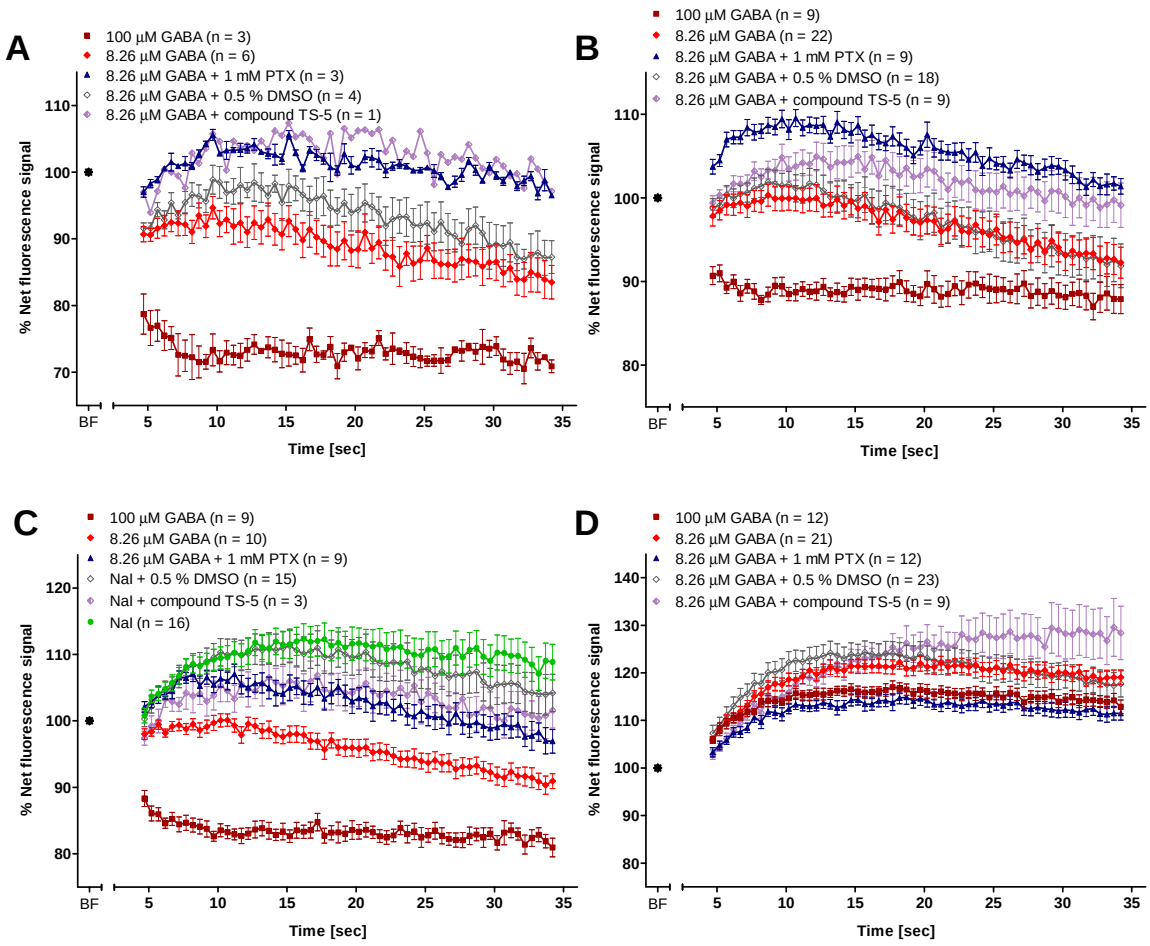

Figure 5.11: Fluorescence signal change after adding test compound TS-5 to HEK293 cells expressing YFP-H148Q/I152L and $\alpha 1\beta 2\varepsilon$ $GABA_A$ receptors.

Fluorescence was measured for 30 seconds after adding (A) 8.26 µM GABA to wells containing compound TS-5 (55.51 nM final concentration; initial screening assay). (B) The assay was repeated three times on different plates. Effect of compound TS-5 was significantly different to GABA-control response ($p < 0.01$). (C) Data from no-GABA control plates. NaI test solution only was added to wells containing compound TS-5 (55.51 nM final concentration). (D) Effect of 8.26 µM GABA and 55.51 µM compound TS-5 on cells expressing YFP-H148Q/I152L only. 100 µM GABA, 8.26 µM GABA, 8.26 µM GABA and 1 mM picrotoxin, 8.26 µM GABA and 0.5 % DMSO and in (C) NaI test solution alone served as controls. Data correspond to means ± SEM; n states the number of wells measured. Net fluorescence of values was normalised by setting the averaged baseline fluorescence to 100 % and fluorescence changes (after adding solutions) were calculated as percentage of the baseline fluorescence.

The results obtained for compounds TS-6 and TS-7 also indicated the inhibition of the GABA-control response in the first test (Figures 5.12 A and 5.13 A). These results could be confirmed after repeating the assay, showing that the compounds triggered an effect significantly different to the GABA-control responses (Figures 5.12 B and 5.13 B; C and D show respective controls used).

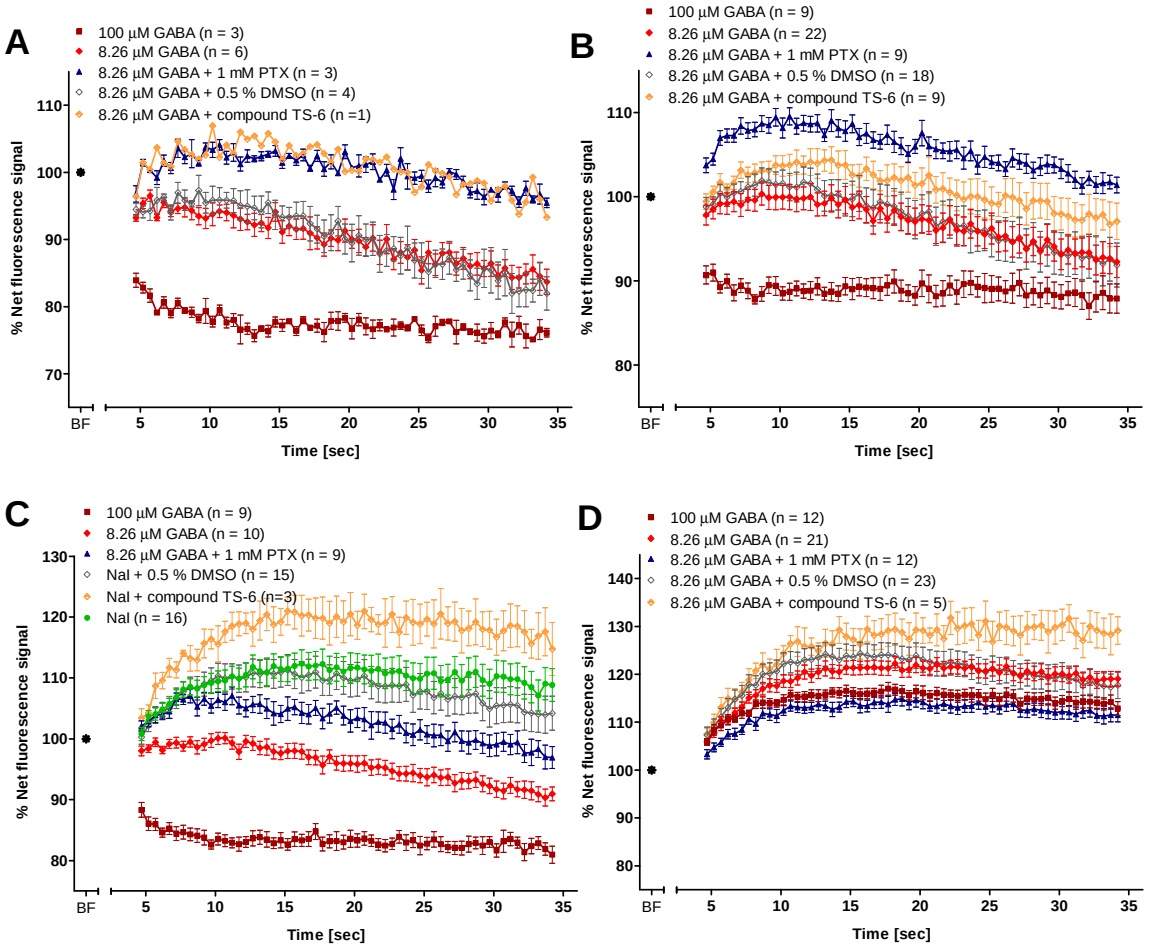

Figure 5.12: Fluorescence signal change after adding test compound TS-6 to HEK293 cells expressing YFP-H148Q/I152L and $\alpha 1\beta 2\varepsilon$ $GABA_A$ receptors.

Fluorescence was measured for 30 seconds after adding (A) 8.26 µM GABA in NaI test solution to wells containing test compound TS-6 (55.02 nM final concentration; initial screening assay). (B) The assay was repeated three times on different plates. Effect of compound TS-6 was significantly different to GABA-control response ($p < 0.01$). (C) Data from no-GABA control plates. NaI test solution only was added to the wells containing compound TS-6 (55.02 nM final concentration). (D) Effect of 8.26 µM GABA and 55.02 µM compound TS-6 on cells expressing YFP-H148Q/I152L only. 100 µM GABA, 8.26 µM GABA, 8.26 µM GABA and 1 mM picrotoxin, 8.26 µM GABA and 0.5 % DMSO and in (C) NaI test solution alone served as controls. Data correspond to means ± SEM; n states the number of wells measured. Net fluorescence of values was normalised by setting the averaged baseline fluorescence to 100 % and fluorescence changes (after adding solutions) were calculated as percentage of the baseline fluorescence.

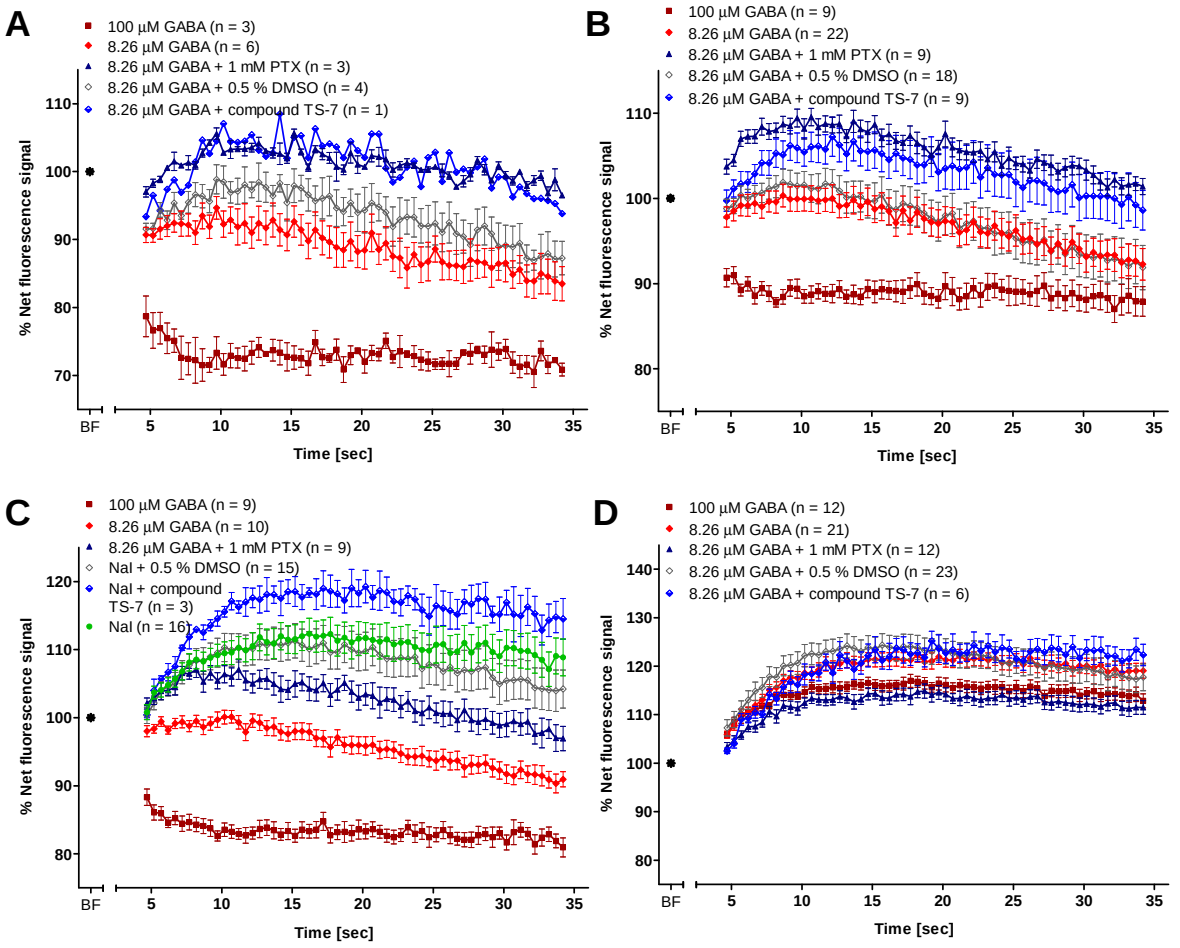

Figure 5.13: Fluorescence signal change after adding test compound TS-7 to HEK293 cells expressing YFP-H148Q/I152L and $\alpha 1\beta 2\varepsilon$ $GABA_A$ receptors.

Fluorescence was measured for 30 seconds after adding (A) 8.26 µM GABA to wells containing compound TS-7 (54.42 nM final concentration; initial screening assay). (B) The assay was repeated three times on different plates using distinct batches of transfected cells. The effect of compound TS-7 was significantly different to GABA-control response ($p < 0.05$). (C) Data from no-GABA control plates. NaI test solution only was added to wells containing compound TS-7 (54.42 nM final concentration). (D) Effect of 8.26 µM GABA and 54.42 µM compound TS-7 on cells expressing YFP-H148Q/I152L only. 100 µM GABA, 8.26 µM GABA, 8.26 µM GABA and 1 mM picrotoxin, 8.26 µM GABA and 0.5 % DMSO and in (C) NaI test solution alone served as controls. Data correspond to means ± SEM; n states the number of wells measured. Net fluorescence of values was normalised by setting the averaged baseline fluorescence to 100 % and fluorescence changes (after adding solutions) were calculated as percentage of the baseline fluorescence.

In contrast to the above compounds, test compounds TS-8 and TS-9 inhibited GABA-control responses during the preliminary screening assay as well as when repeating the assay using the compounds in triplicates on each plate (Figure 5.14 A, B and 5.15 A, B). No effects were observed in the absence of GABA or in cells expressing YFP-H148Q/I152L only (Figures 5.14 C, D and 5.15 C, D).

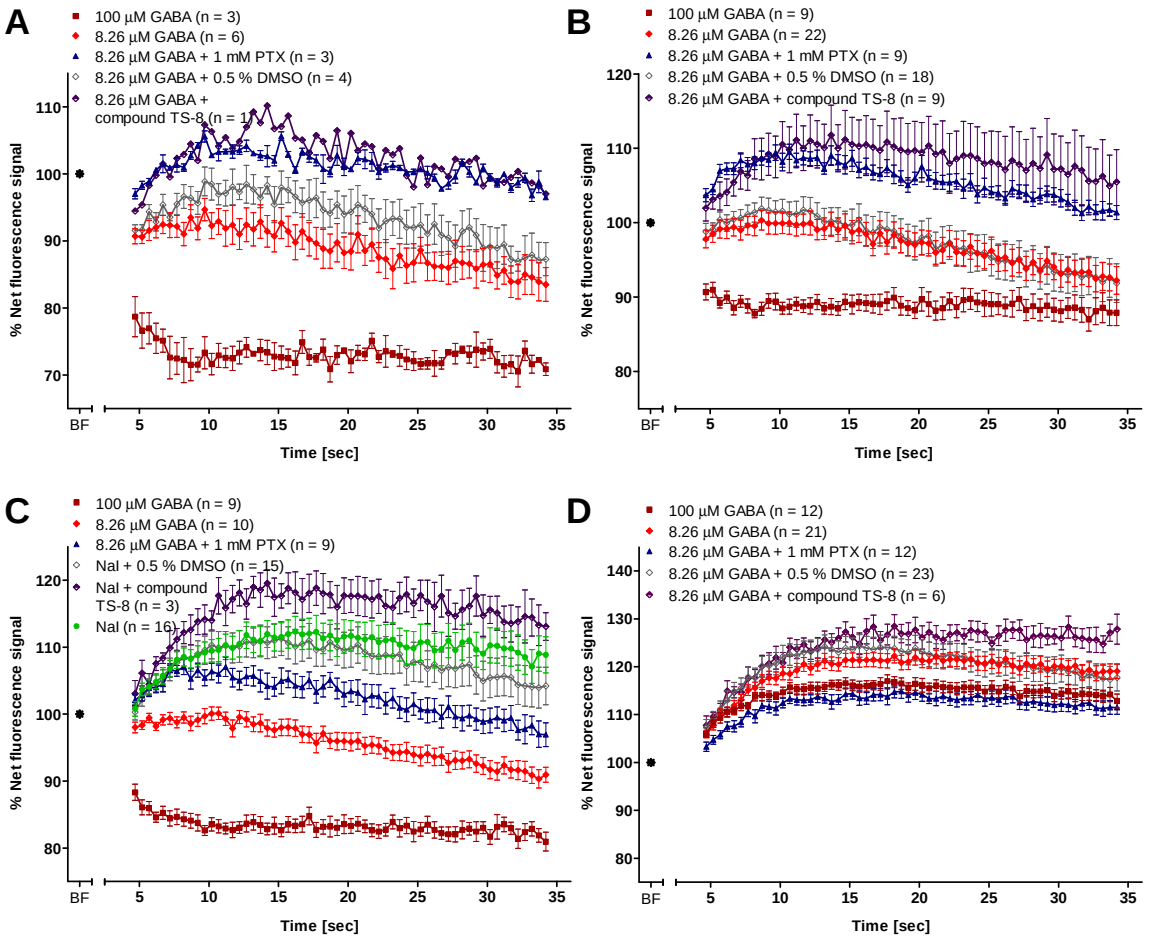

Figure 5.14: Fluorescence signal change after adding test compound TS-8 to HEK293 cells expressing mutant YFP-H148Q/I152L and $\alpha 1\beta 2\varepsilon$ $GABA_A$ receptors.

Fluorescence was measured for 30 seconds after adding (A) 8.26 µM GABA to wells containing compound TS-8 (54.39 nM final concentration; initial screening assay). (B) The assay was repeated three times on different plates. Effect of compound TS-8 was significantly different to GABA-control response ($p < 0.01$). (C) Data from no-GABA control plates. NaI test solution only was added to wells containing compound TS-8 (54.39 nM final concentration). (D) Effect of 8.26 µM GABA and 54.39 µM compound TS-8 on cells expressing YFP-H148Q/I152L only. 100 µM GABA, 8.26 µM GABA, 8.26 µM GABA and 1 mM picrotoxin, 8.26 µM GABA and 0.5 % DMSO and in (C) NaI test solution alone served as controls. Data correspond to means ± SEM; n states the number of wells measured. Net fluorescence of values was normalised by setting the averaged baseline fluorescence to 100 % and fluorescence changes (after adding solutions) were calculated as percentage of the baseline fluorescence.

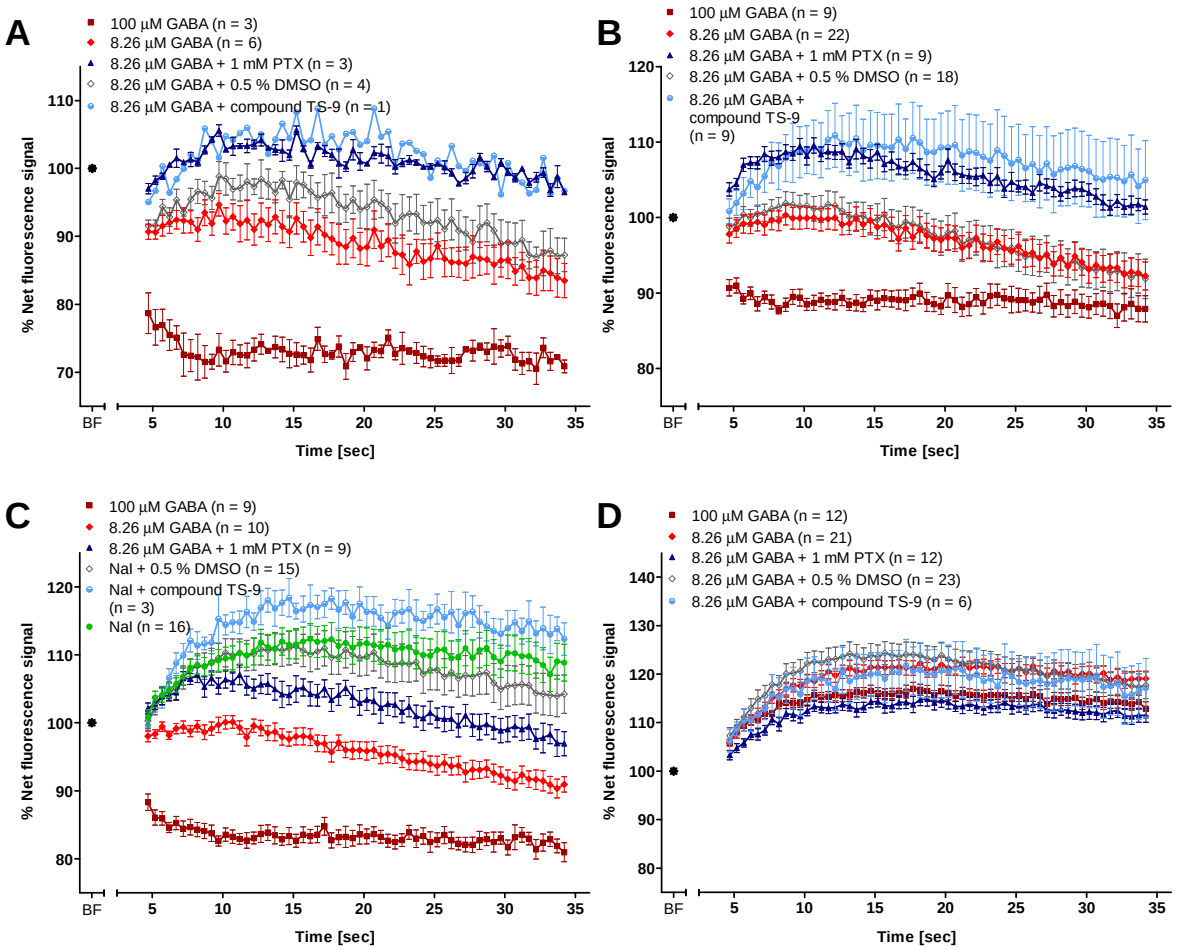

Figure 5.15: Fluorescence signal change after adding test compound TS-9 to HEK293 cells expressing YFP-H148Q/I152L and $\alpha 1\beta 2\varepsilon$ $GABA_A$ receptors.

Fluorescence was measured for 30 seconds after adding (A) 8.26 µM GABA to wells containing compound TS-9 (55.77 nM final concentration; initial screening assay). (B) Screening assay was repeated three times on different plates. Effect of compound TS-9 was significantly different to GABA-control response ($p < 0.05$). (C) Data from no-GABA control plates. NaI test solution only was added to wells containing compound TS-9 (55.77 nM final concentration). (D) Effect of 8.26 µM GABA and 55.77 µM compound TS-9 on cells expressing YFP-H148Q/I152L only. 100 µM GABA, 8.26 µM GABA, 8.26 µM GABA and 1 mM picrotoxin, 8.26 µM GABA with 0.5 % DMSO and in (C) NaI test solution alone served as respective controls. Data correspond to means ± SEM; n states the number of wells measured. Net fluorescence of values was normalised by setting the averaged baseline fluorescence to 100 % and fluorescence changes (after adding solutions) were calculated as percentage of the baseline fluorescence.

Compounds TS-10 and TS-11 also inhibited GABA-control responses during the preliminary screen (Figures 5.16 A and 5.17 A), but the effects were less distinctive after repeating the assays three times (Figures 5.16 B and 5.17 B). Compound TS-10 exhibited a fluorescence quench of about 20 % in cells expressing YFP-H148Q/I152L only that was not seen in cells expressing $GABA_A$ receptors, indicating iodide entrance into the cells (Figure 5.16 D).

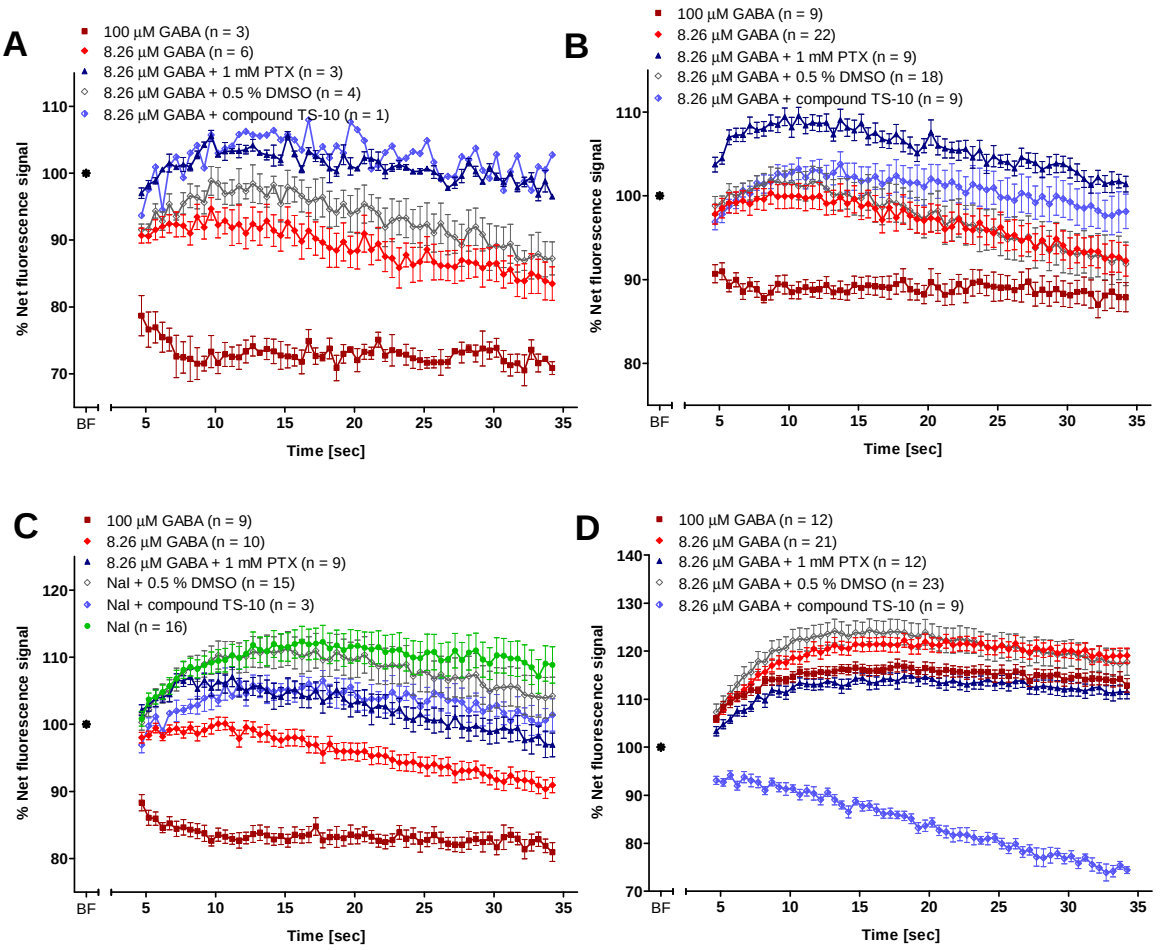

Figure 5.16: Fluorescence signal change after adding test compound TS-10 to HEK293 cells expressing YFP-H148Q/I152L and $\alpha 1\beta 2\varepsilon$ $GABA_A$ receptors.

Fluorescence was measured for 30 seconds after adding (A) 8.26 µM GABA to wells containing compound TS-10 (52.63 nM final concentration; initial screening assay). (B) The assay was repeated three times on different plates. The effect of the compound was significantly different to the GABA-control response ($p < 0.05$). (C) Data from no-GABA control plates. NaI test solution only was added to the wells containing compound TS-10 (52.63 nM final concentration). (D) Effect of 8.26 µM GABA and 52.63 µM compound TS-10 in cells expressing YFP-H148Q/I152L only. 100 µM GABA, 8.26 µM GABA, 8.26 µM GABA and 1 mM picrotoxin, 8.26 µM GABA and 0.5 % DMSO and in (C) NaI test solution alone served as respective controls. Data correspond to means ± SEM; n states the number of wells measured. Net fluorescence of values was normalised by setting the averaged baseline fluorescence to 100 % and fluorescence changes (after adding solutions) were calculated as percentage of the baseline fluorescence.

In contrast, test compound TS-11 showed an increased fluorescence signal in cells expressing YFP-H148Q/I152L only (Figure 5.17 D).

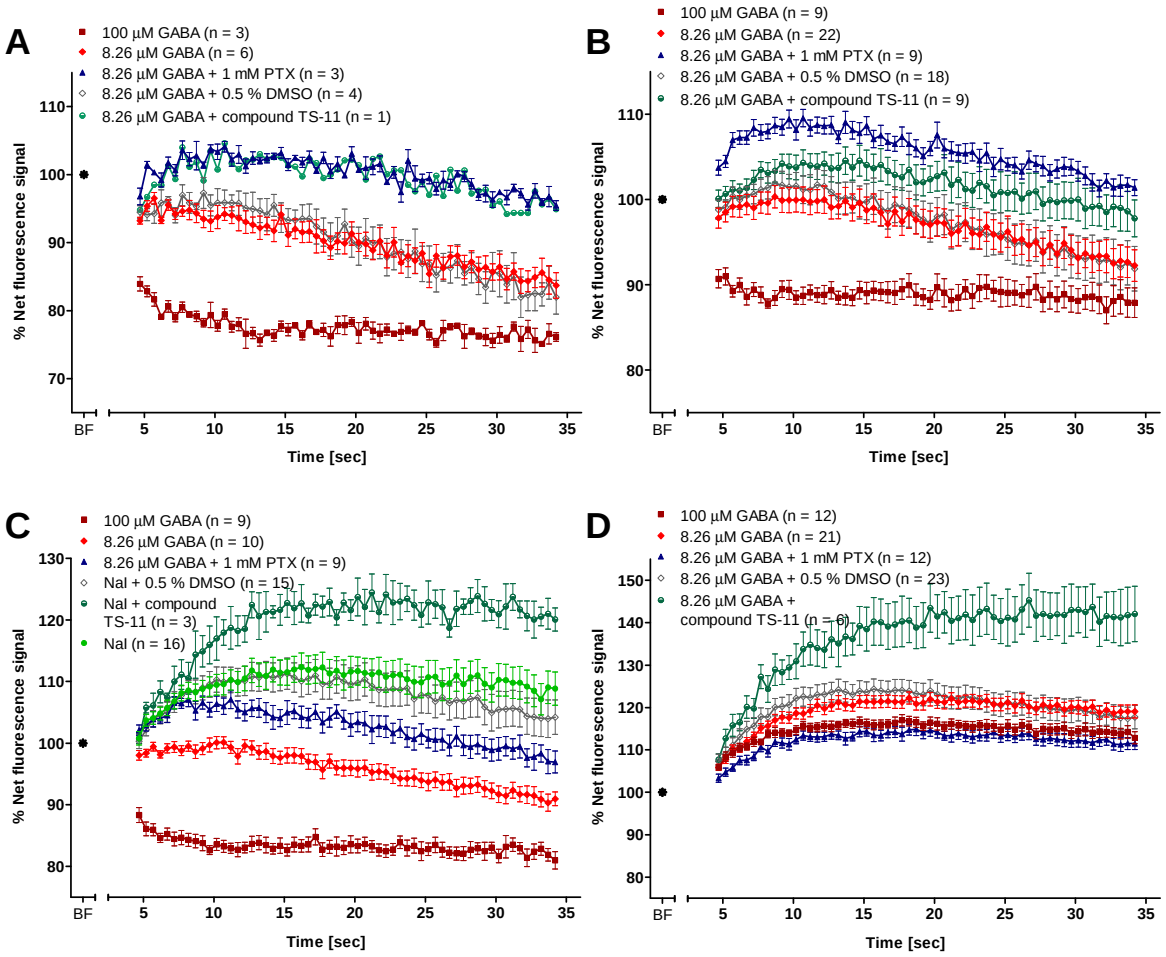

Figure 5.17: Fluorescence signal change after adding test compound TS-11 to HEK293 cells expressing YFP-H148Q/I152L and $\alpha 1\beta 2\varepsilon$ $GABA_A$ receptors.

Fluorescence was measured for 30 seconds after adding (A) 8.26 µM GABA to wells containing compound TS-11 (56.08 nM final concentrations) in initial screening assay. (B) The assay was repeated on three different plates. The effect of the compound was significantly different to the GABA-control response ($p < 0.05$). (C) Data from no-GABA control plates. NaI test solution only was added to wells containing compound TS-11 (56.08 nM final concentration). (D) Effect of 8.26 µM GABA and 56.08 µM compound TS-11 on cells expressing YFP-H148Q/I152L only. 100 µM GABA, 8.26 µM GABA, 8.26 µM GABA and 1 mM picrotoxin, 8.26 µM GABA with 0.5 % DMSO and in (C) NaI test solution alone served as controls. Data correspond to means ± SEM; n states the number of wells measured. Net fluorescence of values was normalised by setting the averaged baseline fluorescence to 100 % and fluorescence changes (after adding solutions) were calculated as percentage of the baseline fluorescence.

Test compound TS-12 inhibited receptor activity in cells expressing $\alpha 1\beta 2\varepsilon$ receptors. Repeating the assay confirmed this result (Figure 5.18 A and B). NaI test solution control and controls with cells lacking the receptors showed no effect upon the presence of the test compound (Figure 5.18 C, D).

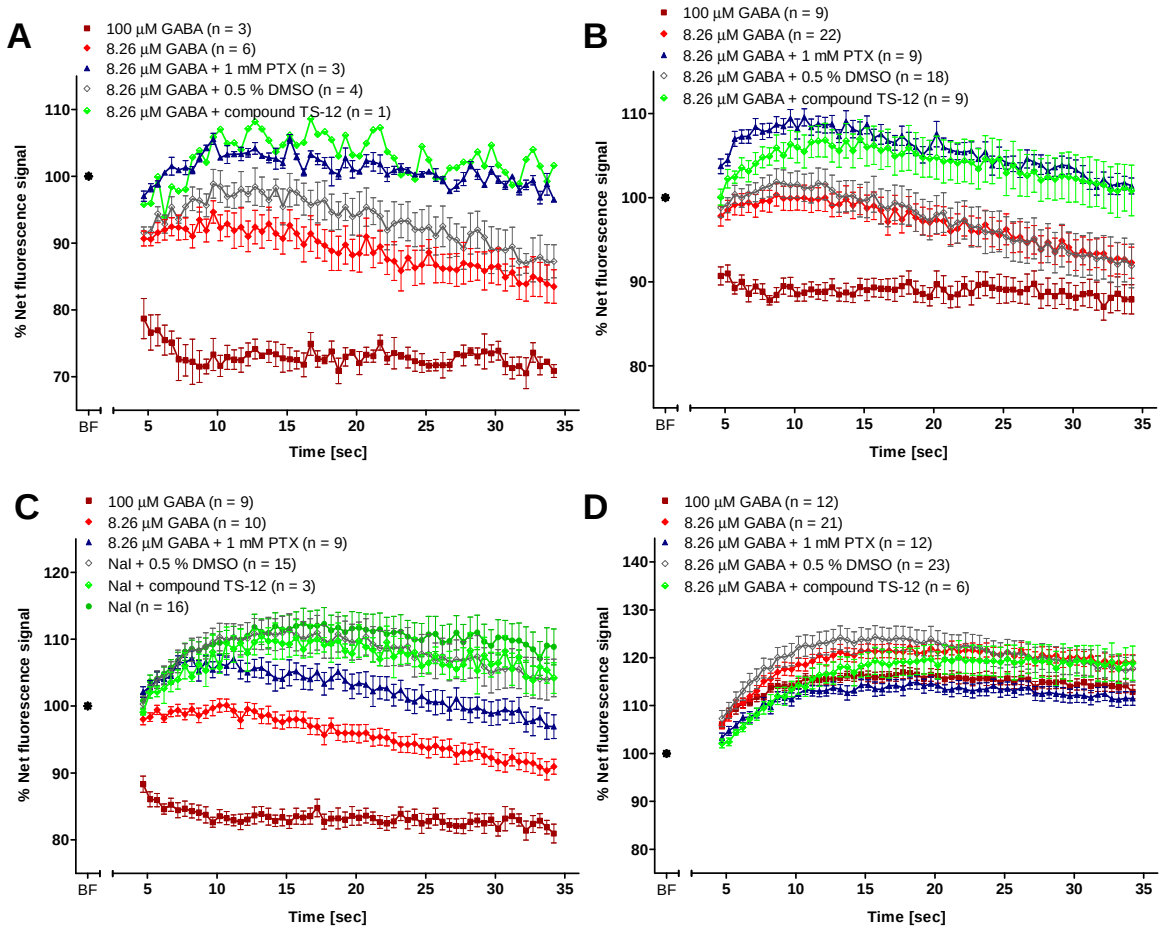

Figure 5.18: Fluorescence signal change after adding test compound TS-12 to HEK293 cells expressing mutant YFP-H148Q/I152L and $\alpha 1\beta 2\varepsilon$ $GABA_A$ receptors.

Fluorescence was measured for 30 seconds after adding (A) 8.26 µM GABA to wells containing compound TS-12 (54.2 nM final concentration; initial screening assay). (B) The assay was repeated three times on different plates. The effect of the compound was significantly different to the GABA-control response ($p < 0.01$). (C) Data from no-GABA control plates. NaI test solution only was added to the wells containing compound TS-12 (54.2 nM final concentration). (D) Effect of 8.26 µM GABA and 54.2 µM compound TS-12 in cells expressing YFP-H148Q/I152L only. 100 µM GABA, 8.26 µM GABA, 8.26 µM GABA and 1 mM picrotoxin, 8.26 µM GABA and 0.5 % DMSO and in (C) NaI test solution alone served as respective controls. Data correspond to means ± SEM; n states the number of wells measured. Net fluorescence of values was normalised by setting the averaged baseline fluorescence to 100 % and fluorescence changes (after adding solutions) were calculated as percentage of the baseline fluorescence.

Results for test compounds TS-13 and TS-14 are depicted in Figures 5.19 and 5.20. The assay results indicated that the compounds inhibited GABA-control responses in cells expressing $\alpha 1\beta 2\varepsilon$ $GABA_A$ receptors. Controls performed in cells expressing mutant YFP-H148Q/I152L only showed increased fluorescence signals compared to the other controls applied (Figures 5.19 and 5.20 D).

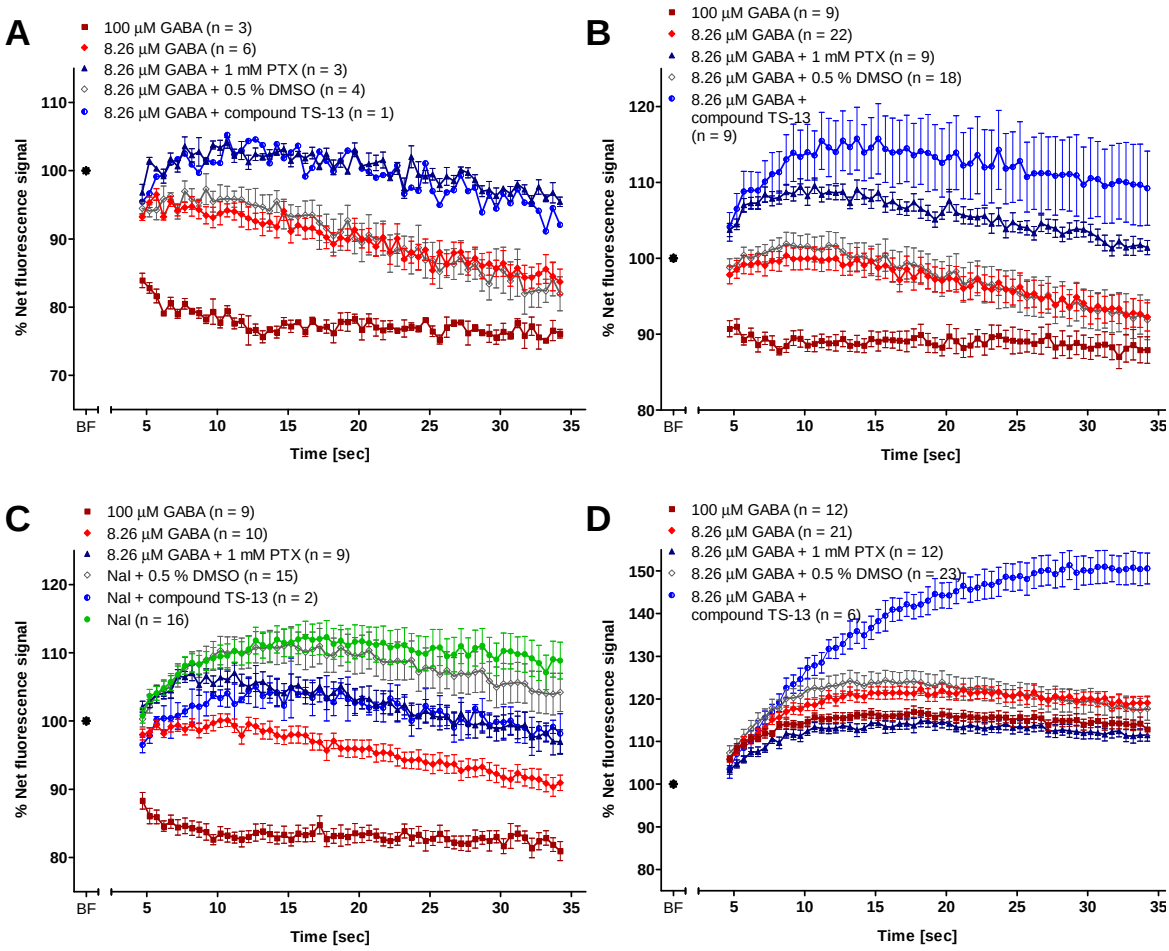

Figure 5.19: Fluorescence signal change after adding test compound TS-13 to HEK293 cells expressing YFP-H148Q/I152L and $\alpha 1\beta 2\varepsilon$ $GABA_A$ receptors.

Fluorescence was measured for 30 seconds after adding (A) 8.26 µM GABA to wells containing compound TS-13 (55.34 nM final concentrations) in initial screening assay. (B) The assay was repeated on three different plates. The effect of compound TS-13 was significantly different to the GABA-control response ($p < 0.01$). (C) Data from no-GABA control plates. NaI test solution only was added to wells containing compound TS-13 (55.34 nM final concentrations). (D) Effect of 8.26 µM GABA and 55.34 µM compound TS-13 in cells expressing mutant YFP-H148Q/I152L only. 100 µM GABA, 8.26 µM GABA, 8.26 µM GABA and 1 mM picrotoxin, 8.26 µM GABA with 0.5 % DMSO and in (C) NaI test solution alone served as controls. Data correspond to means ± SEM; n states the number of wells measured. Net fluorescence of values was normalised by setting the averaged baseline fluorescence to 100 % and fluorescence changes (after adding solutions) were calculated as percentage of the baseline fluorescence.

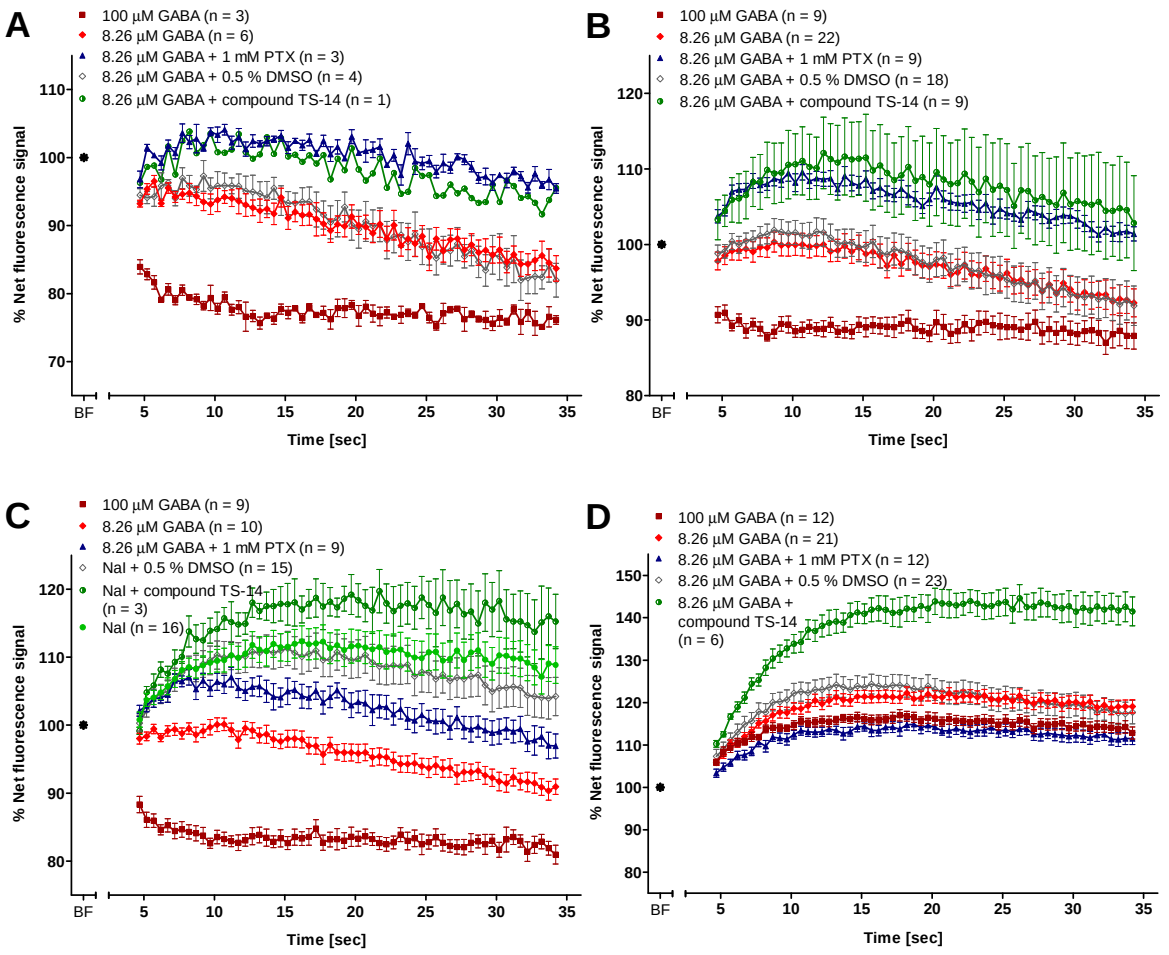

Figure 5.20: Fluorescence signal change after adding test compound TS-14 to HEK293 cells expressing YFP-H148Q/I152L and $\alpha 1\beta 2\varepsilon$ $GABA_A$ receptors.

Fluorescence was measured for 30 seconds after adding (A) 8.26 µM GABA to wells containing compound TS-14 (55.03 nM final concentration) in initial screening assay. (B) The assay was repeated on at least three different plates. The effect of compound TS-14 was significantly different to GABA-control response ($p < 0.05$). (C) Data from no-GABA control plates. NaI test solution only was added to wells containing compound TS-14 (55.03 nM final concentration). (D) Effect of 8.26 µM GABA and 55.03 µM compound TS-14 in cells expressing YFP-H148Q/I152L only. 100 µM GABA, 8.26 µM GABA, 8.26 µM GABA and 1 mM picrotoxin, 8.26 µM GABA and 0.5 % DMSO and in (C) NaI test solution alone served as controls. Data correspond to means ± SEM; n states the number of wells measured. Net fluorescence of values was normalised by setting the averaged baseline fluorescence to 100 % and fluorescence changes (after adding solutions) were calculated as percentage of the baseline fluorescence.

Test compound TS-15 inhibited the effect of GABA at EC_{30} concentrations in HEK293 cells expressing $\alpha 1\beta 2\varepsilon$ receptors (Figure 5.21 A, B). However, when the test compound was applied to cells expressing YFP-H148Q/I152L only, the fluorescence signal decreased slightly to 96.56 $\pm$ 1.18 % compared to the baseline fluorescence, whereas fluorescence signals of all other controls were higher (Figure 5.21 D).

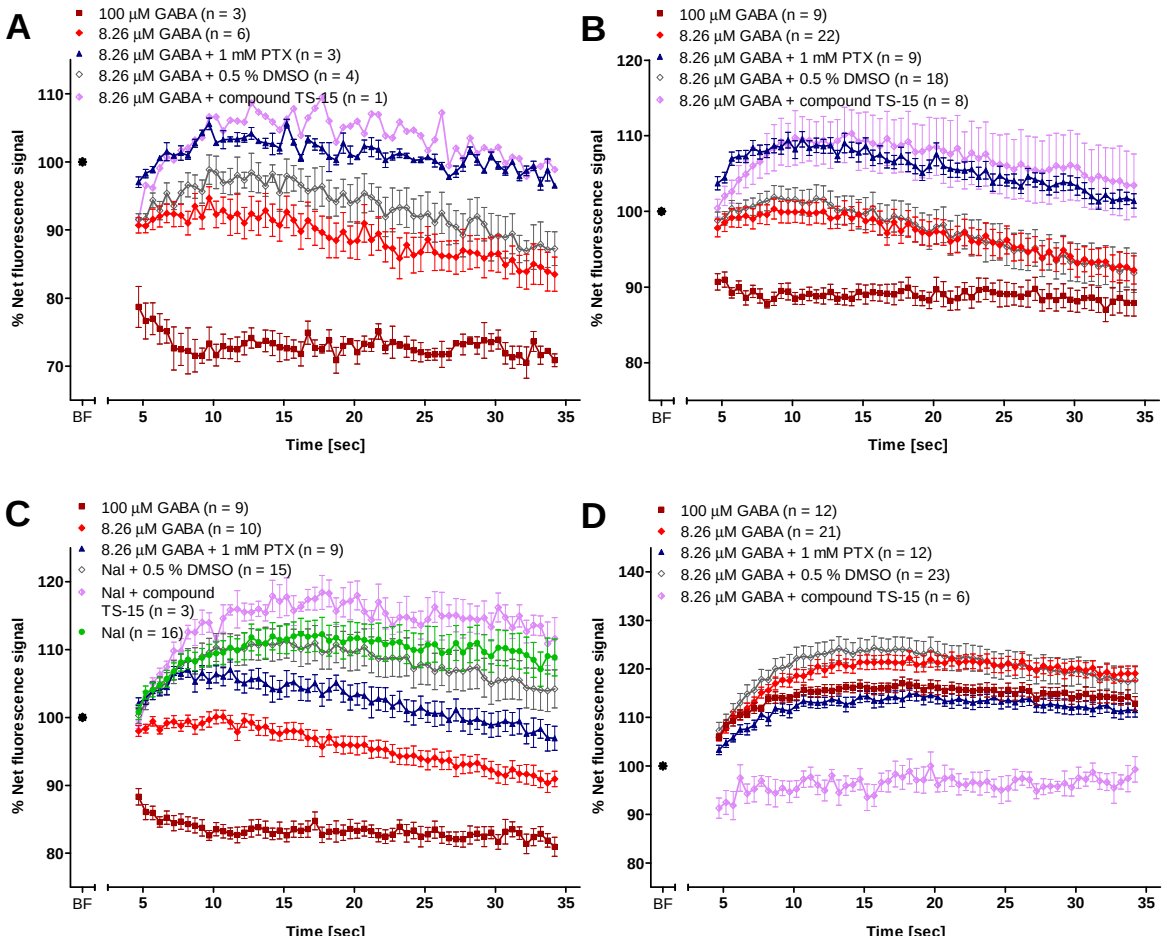

Figure 5.21: Fluorescence signal change after adding test compound TS-15 to HEK293 cells expressing mutant YFP-H148Q/I152L and $\alpha 1\beta 2\varepsilon$ $GABA_A$ receptors.

Fluorescence was measured for 30 seconds after adding (A) 8.26 µM GABA to wells containing compound TS-15 (54.97 nM final concentration; initial screening assay). (B) Assay was repeated three times on different plates. The effect of compound TS-15 was significantly different to the GABA-control response ($p < 0.05$). (C) Data from no-GABA control plates. NaI test solution only was added to wells containing compound TS-15 (54.97 nM final concentration). (D) Effect of 8.26 µM GABA and 54.97 µM compound TS-15 on cells expressing YFP-H148Q/I152L only. 100 µM GABA, 8.26 µM GABA, 8.26 µM GABA and 1 mM picrotoxin, 8.26 µM GABA with 0.5 % DMSO and in (C) NaI test solution alone served as respective controls. Data correspond to means $\pm$ SEM; n states the number of wells measured. Net fluorescence of values was normalised by setting the averaged baseline fluorescence to 100 % and fluorescence changes (after adding solutions) were calculated as percentage of the baseline fluorescence.

The majority of chemical compounds tested that showed an effect on cells expressing $\alpha 1 \beta 2 \varepsilon$ $GABA_A$ receptors inhibited the fluorescence quench, and there were only a few test compounds enhancing receptor activity. Therefore, fluorescence quench increasing compounds that were identified at the second lowest concentration range tested (between 503 and 593 nM) were also examined by repeating the assays with respective controls. Test compound TS-16 triggered a fluorescence quench that was larger than the quench obtained when cells were exposed to 100 µM GABA. This could be confirmed by repeating the assay several times in triplicates (Figure 5.22 A, B). Applying the compound with NaI test solution only also indicated a small effect (Figure 5.22 C). In both cases, the onset of the responses was relatively slow compared to the GABA-control responses. Cells lacking the $GABA_A$ receptors showed no change in fluorescence signal when exposed to the compound, indicating that the response was $GABA_A$ receptor-dependent.

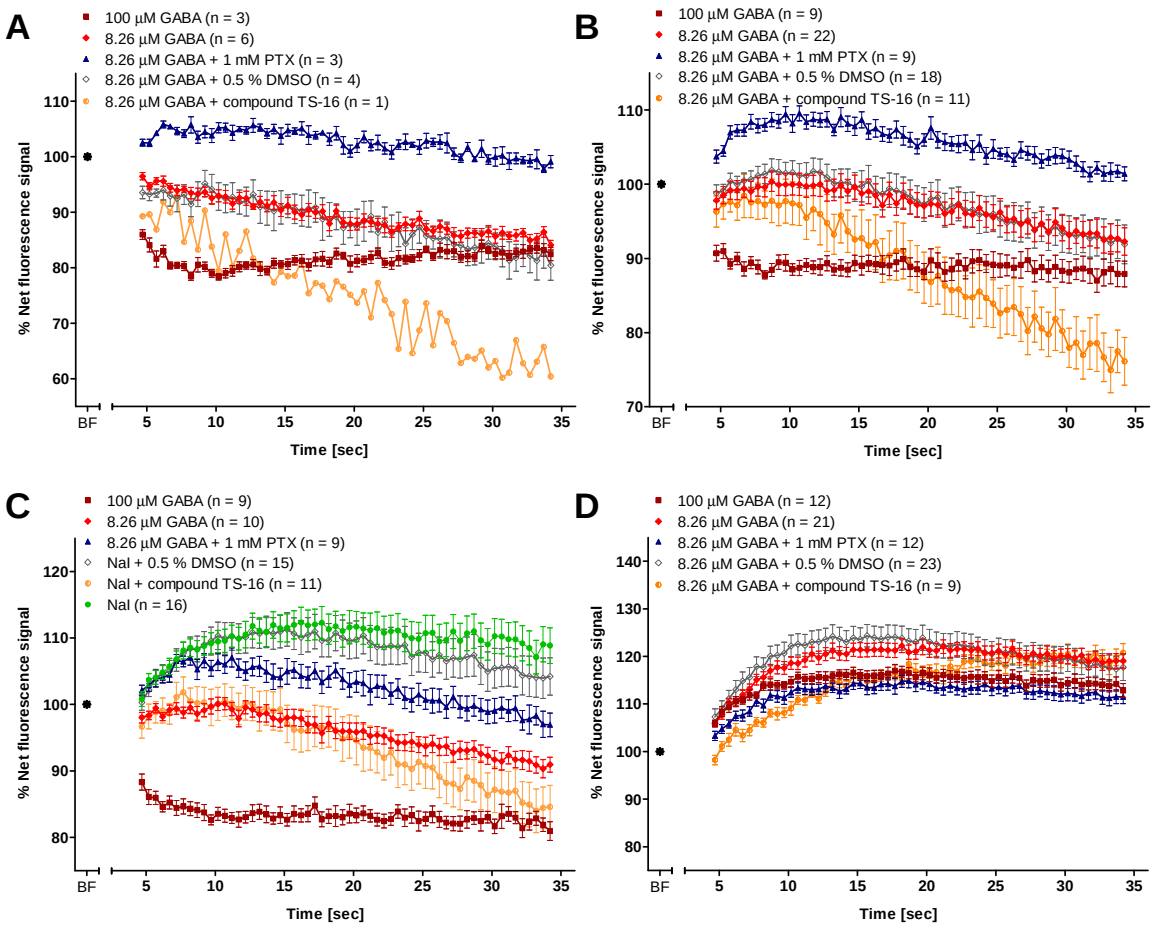

Figure 5.22: Fluorescence signal change after adding test compound TS-16 to HEK293 cells expressing YFP-H148Q/I152L and $\alpha 1\beta 2\varepsilon$ $GABA_A$ receptors.

Fluorescence was measured for 30 seconds after adding (A) 8.26 µM GABA to wells containing compound TS-16 (539.4 nM final concentration) in initial screening assay. (B) The assay was repeated several times using different plates. The effect of compound TS-16 was significantly different to GABA-control response ($p < 0.05$). (C) Data from no-GABA control plates. NaI test solution only was added to the wells containing compound TS-16 (539.4 nM final concentration). (D) Effect of 8.26 µM GABA and 53.94 µM compound TS-16 on cells expressing YFP-H148Q/I152L only. 100 µM GABA, 8.26 µM GABA, 8.26 µM GABA and 1 mM picrotoxin, 8.26 µM GABA and 0.5 % DMSO and in (C) NaI test solution alone served as respective controls. Data correspond to means ± SEM; n states the number of wells measured. Net fluorescence of values was normalised by setting the averaged baseline fluorescence to 100 % and fluorescence changes (after adding solutions) were calculated as percentage of the baseline fluorescence.

In contrast, the increased fluorescence quench triggered by compound TS-17 that was observed during the initial screening assay could not be confirmed when repeating the assay; no significant change could be seen compared to the EC_{30} GABA-control response (Figure 5.23). Similar results were obtained for compounds TS-18 and TS-19. The compounds inhibited the fluorescence change evoked by GABA during the initial screens, but in further replicates no significant effect could be observed (Figures 5.24 and 5.25).

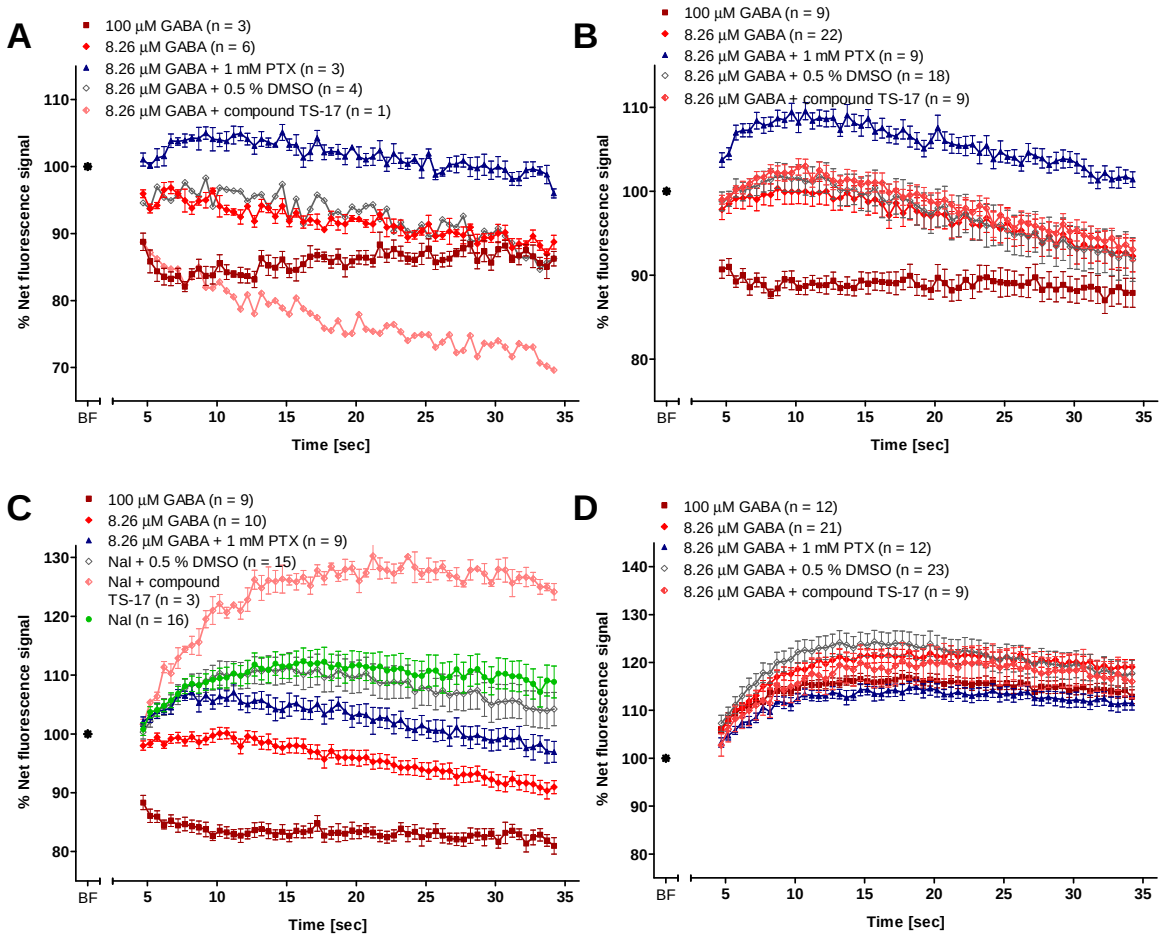

Figure 5.23: Fluorescence signal change after adding test compound TS-17 to HEK293 cells expressing mutant YFP-H148Q/I152L and $\alpha 1\beta 2\varepsilon$ $GABA_A$ receptors.

Fluorescence was measured for 30 seconds after adding (A) 8.26 µM GABA to wells containing compound TS-17 (570 nM final concentration; initial screening assay). (B) The assay was repeated three times on different plates. (C) Data from no-GABA control plates. NaI test solution only was added to the wells containing compound TS-17 (570 nM final concentration). (D) Effect of 8.26 µM GABA and 57 µM compound TS-17 on cells expressing YFP-H148Q/I152L only. 100 µM GABA, 8.26 µM GABA, 8.26 µM GABA and 1 mM picrotoxin, 8.26 µM GABA and 0.5 % DMSO and in (C) NaI test solution alone served as controls. Data correspond to means ± SEM; n states the number of wells measured. Net fluorescence of values was normalised by setting the averaged baseline fluorescence to 100 % and fluorescence changes (after adding solutions) were calculated as percentage of the baseline fluorescence.

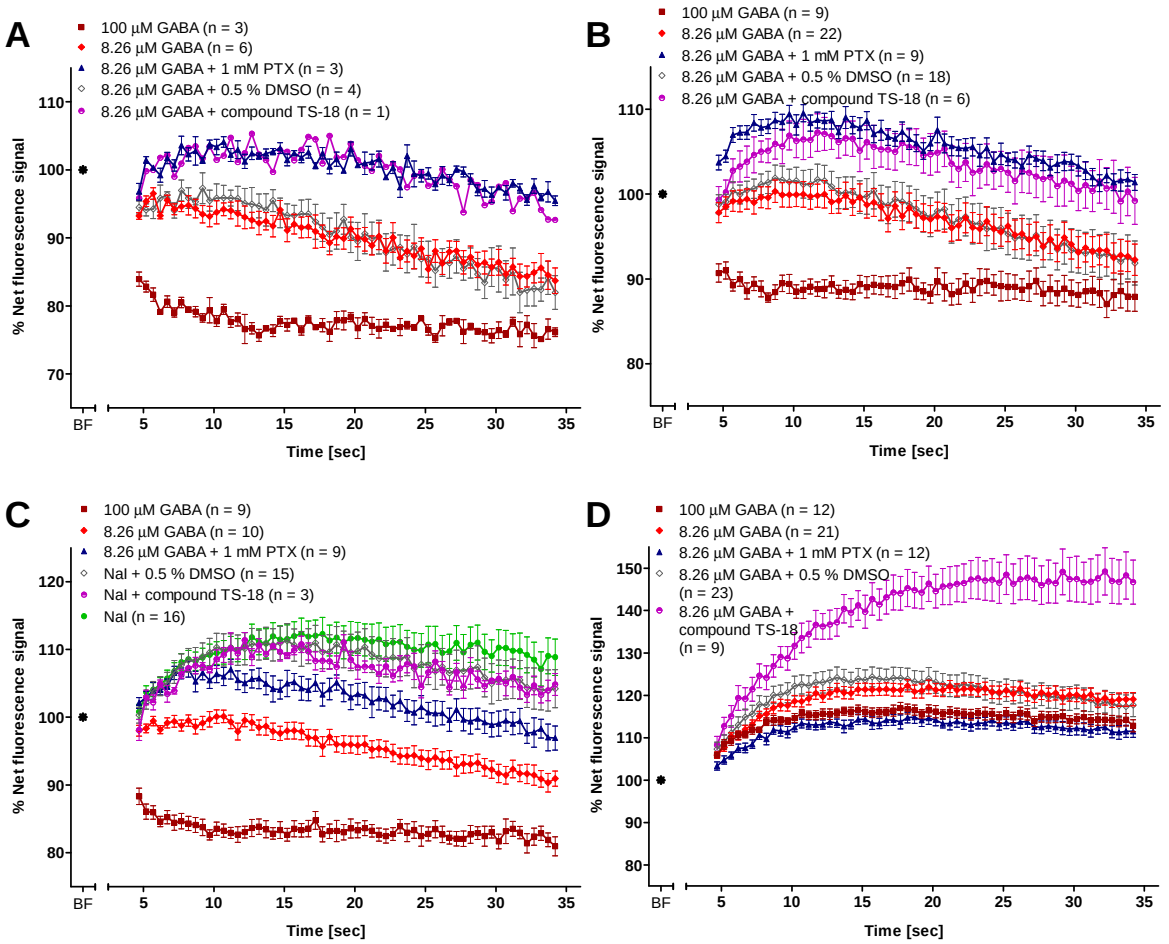

Figure 5.24: Fluorescence signal change after adding test compound TS-18 to HEK293 cells expressing YFP-H148Q/I152L and $\alpha 1\beta 2\varepsilon$ $GABA_A$ receptors.

Fluorescence was measured for 30 seconds after adding (A) 8.26 µM GABA to wells containing compound TS-18 (54.02 nM final concentration) in initial screening assay. (B) The screening assay was repeated on different plates. (C) Data from no-GABA control plates. NaI test solution only was added to wells containing compound TS-18 (54.02 nM final concentration). (D) Effect of 8.26 µM GABA and 54.02 µM compound TS-18 on cells expressing YFP-H148Q/I152L only. 100 µM GABA, 8.26 µM GABA, 8.26 µM GABA and 1 mM picrotoxin, 8.26 µM GABA with 0.5 % DMSO and in (C) NaI test solution alone served as controls. Data correspond to means ± SEM; n states the number of wells measured. Net fluorescence of values was normalised by setting the averaged baseline fluorescence to 100 % and fluorescence changes (after adding solutions) were calculated as percentage of the baseline fluorescence.

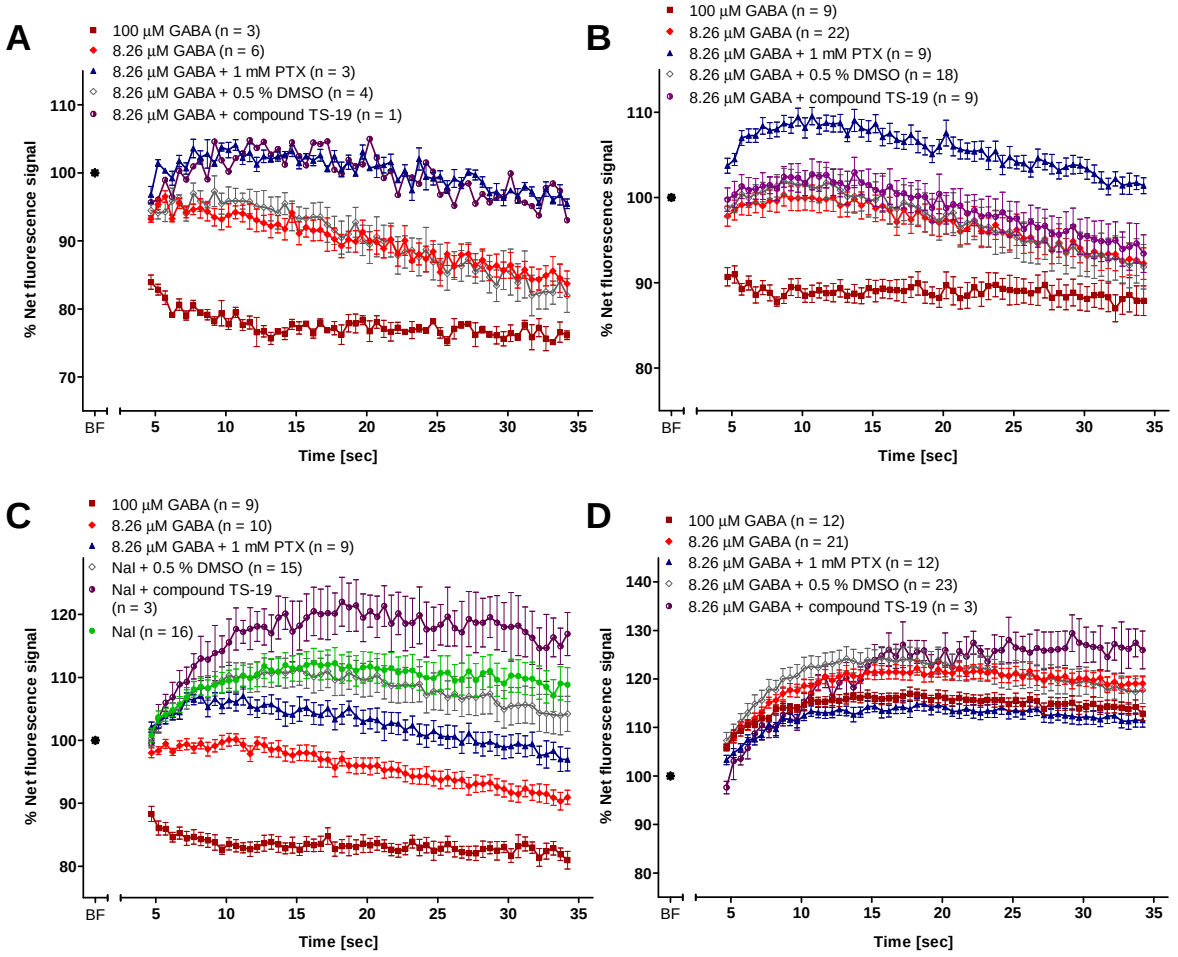

Figure 5.25: Fluorescence signal change after adding test compound TS-19 to HEK293 cells expressing YFP-H148Q/I152L and $\alpha 1\beta 2\varepsilon$ $GABA_A$ receptors.

Fluorescence was measured for 30 seconds after adding (A) 8.26 µM GABA to wells containing compound TS-19 (55.33 nM final concentrations) in initial screening assay. (B) The assay was repeated on three different plates. (C) Data from no-GABA control plates. NaI test solution only was added to wells containing compound TS-19 (55.33 nM final concentration). (D) Effect of 8.26 µM GABA and 55.33 µM compound TS-19 on cells expressing YFP-H148Q/I152L only. 100 µM GABA, 8.26 µM GABA, 8.26 µM GABA and 1 mM picrotoxin, 8.26 µM GABA with 0.5 % DMSO and in (C) NaI test solution alone served as respective controls. Data correspond to means ± SEM; n states the number of wells measured. Net fluorescence of values was normalised by setting the averaged baseline fluorescence to 100 % and fluorescence changes (after adding solutions) were calculated as percentage of the baseline fluorescence.

5.2.3 Investigation of 'hit' compounds on $\alpha 3\beta 2\gamma 2$ receptors

Test compounds were also applied to HEK293 cells expressing mutant YFP-H148Q/I152L and $\alpha 3\beta 2\gamma 2$ $GABA_A$ receptors. In contrast to cells expressing $\alpha 1\beta 2\varepsilon$ $GABA_A$ receptors, the majority of compounds applied to cells expressing $\alpha 3\beta 2\gamma 2$ receptors enhanced the YFP fluorescence quench during the preliminary screening tests. Furthermore, the number of active compounds was less and only seven were left after preliminary screenings at a concentration range of 503 to 593 nM. These were tested further by repeating the assays in several wells per plate and also using further controls, as described above for Section 5.2.2.

Test compounds TS-10, TS-20 and TS-21 elicited enhanced quenching of the mutant YFP compared to the GABA-control response (EC_{30}) in cells expressing $\alpha 3\beta 2\gamma 2$ receptors during the preliminary screens. This was confirmed when repeating the assays using triplicates per plate (Figures 5.26 A, B, 5.27 A, B and 5.28 A, B). The compounds also caused a fluorescence quench when applied in the absence of GABA. However, when test compounds were added to control cells expressing YFP-H148Q/I152L only, a fluorescence quench could also be observed, indicating the interference of some endogenously expressed proteins (Figures 5.26 C, D, 5.27 C, D and 5.28 C, D).

Test compound TS-22 inhibited the GABA-elicited fluorescence quench during the preliminary screens (Figure 5.29 A). Repeating the test confirmed this result, although the effect was less prominent compared to before (Figure 5.29 B). The fluorescence signal was similar to that of the controls when applying compound TS-22 without GABA to the cells. However, performing the assay on cells expressing mutant YFP-H148Q/I152L only, the fluorescence signal was higher than that obtained from the respective controls (100 µM GABA, 8.26 µM GABA, 8.26 µM GABA and 1 mM picrotoxin and 8.26 µM GABA with 0.5 % DMSO; Figure 5.29 C, D).

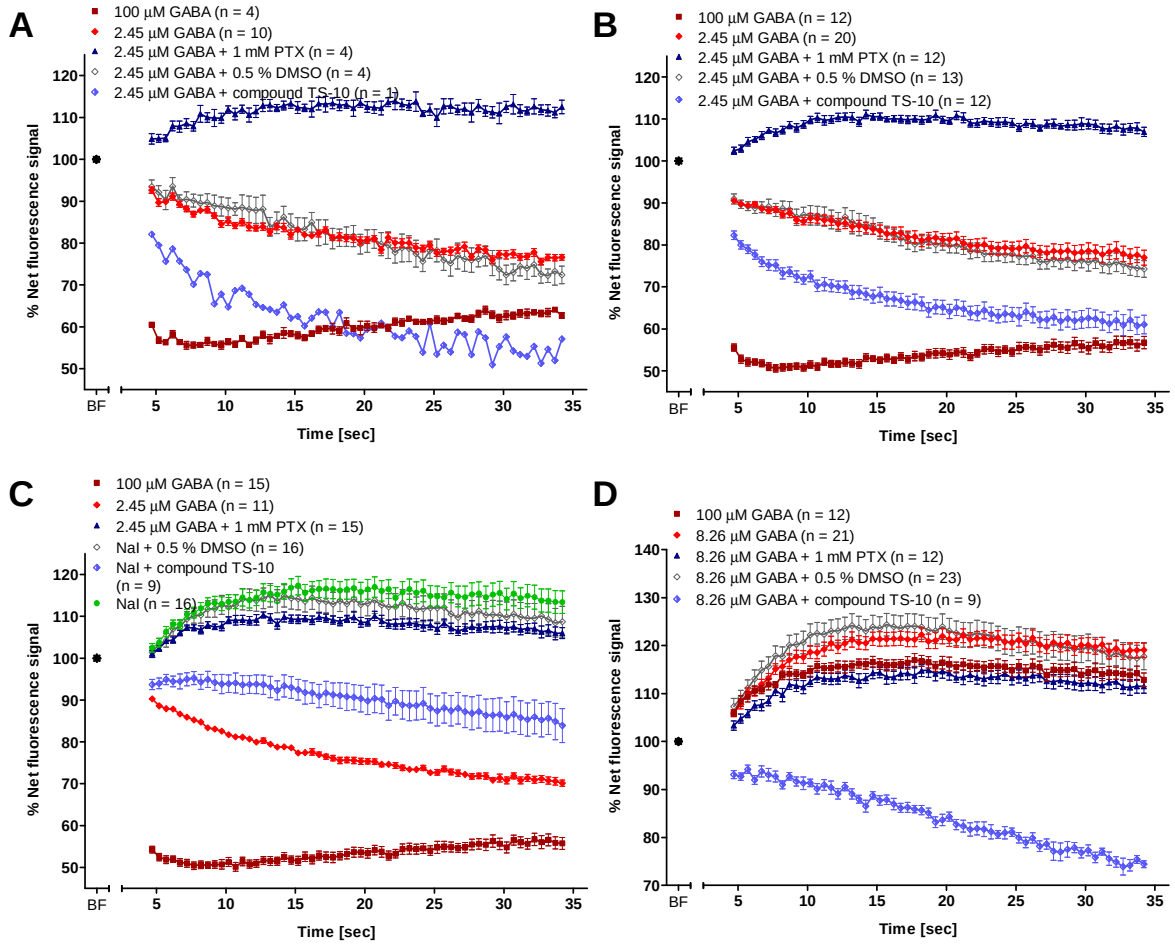

Figure 5.26: Fluorescence signal change after adding test compound TS-10 to HEK293 cells expressing mutant YFP-H148Q/I152L and $\alpha 3\beta 2\gamma 2$ $GABA_A$ receptors.

Fluorescence was measured for 30 seconds after adding (A) 2.45 µM GABA to wells containing 526.3 nM compound TS-10 (final concentrations) in initial screening assay. (B) The assay was repeated in triplicates on different plates. The effect of compound TS-10 was significantly different to GABA-control response ($p < 0.001$). (C) Data from no-GABA control plates. NaI test solution only was added to the wells containing compound TS-10 (526.3 nM final concentration). (D) Effect of 8.26 µM GABA and 52.63 µM compound TS-10 on cells expressing YFP-H148Q/I152L only. 100 µM GABA, 8.26 µM GABA, 8.26 µM GABA and 1 mM picrotoxin, 8.26 µM GABA and 0.5 % DMSO and in (C) NaI test solution alone served as controls. Data correspond to means ± SEM; n states the number of wells measured. Net fluorescence of values was normalised by setting the averaged baseline fluorescence to 100 % and fluorescence changes (after adding solutions) were calculated as percentage of the baseline fluorescence.

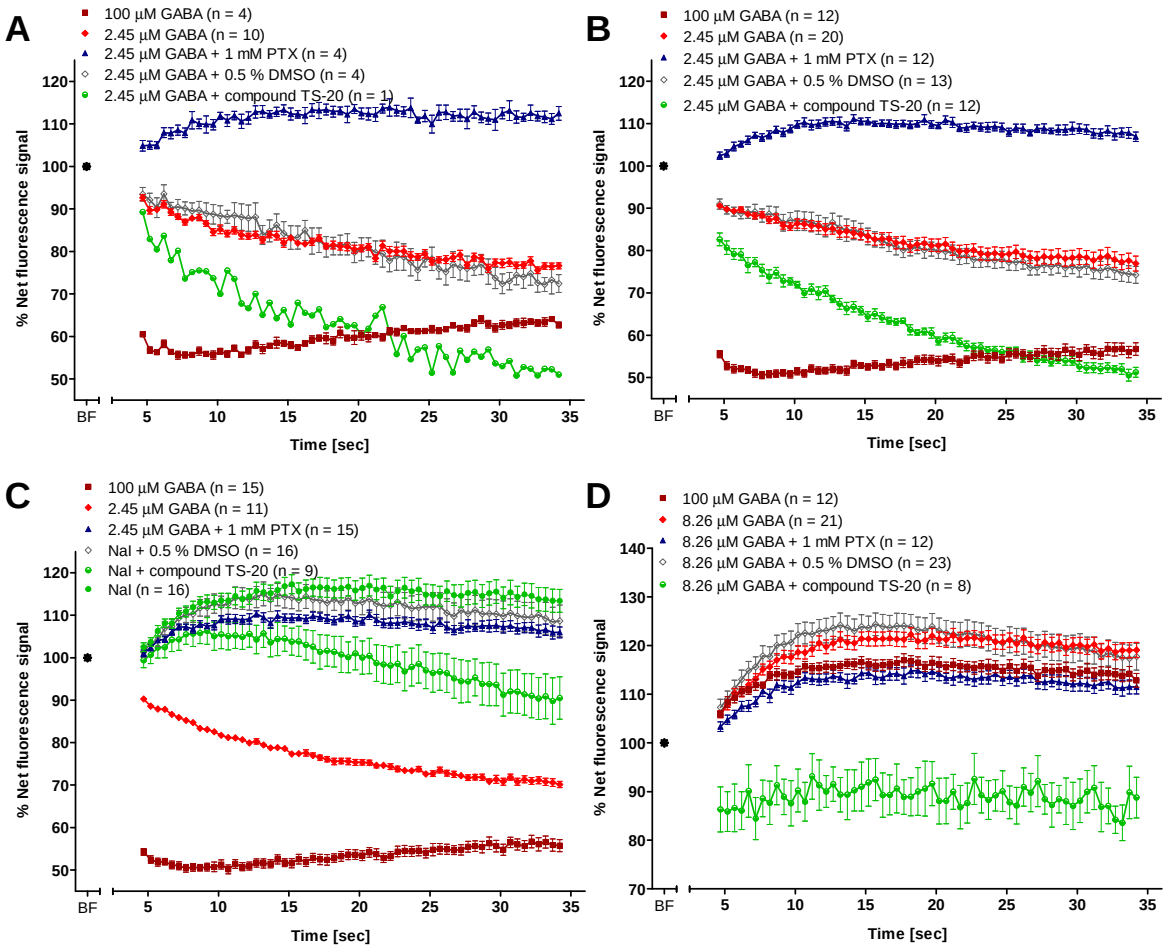

Figure 5.27: Fluorescence signal change after adding test compound TS-20 to HEK293 cells expressing YFP-H148Q/I152L and $\alpha 3\beta 2\gamma 2$ $GABA_A$ receptors.

Fluorescence was measured for 30 seconds after adding (A) 2.45 µM GABA to wells containing 543.1 nM compound TS-20 (final concentrations) in initial screening assay. (B) The assay was repeated on several different plates. The effect of compound TS-20 was significantly different to GABA-control response ($p < 0.001$). (C) Data from no-GABA control plates. NaI test solution only was added to wells containing compound TS-20 (543.1 nM final concentration). (D) Effect of 8.26 µM GABA and 54.31 µM compound TS-20 on cells expressing YFP-H148Q/I152L only. 100 µM GABA, 8.26 µM GABA, 8.26 µM GABA and 1 mM picrotoxin, 8.26 µM GABA with 0.5 % DMSO and in (C) NaI test solution alone served as controls. Data correspond to means ± SEM; n states the number of wells measured. Net fluorescence of values was normalised by setting the averaged baseline fluorescence to 100 % and fluorescence changes (after adding solutions) were calculated as percentage of the baseline fluorescence.

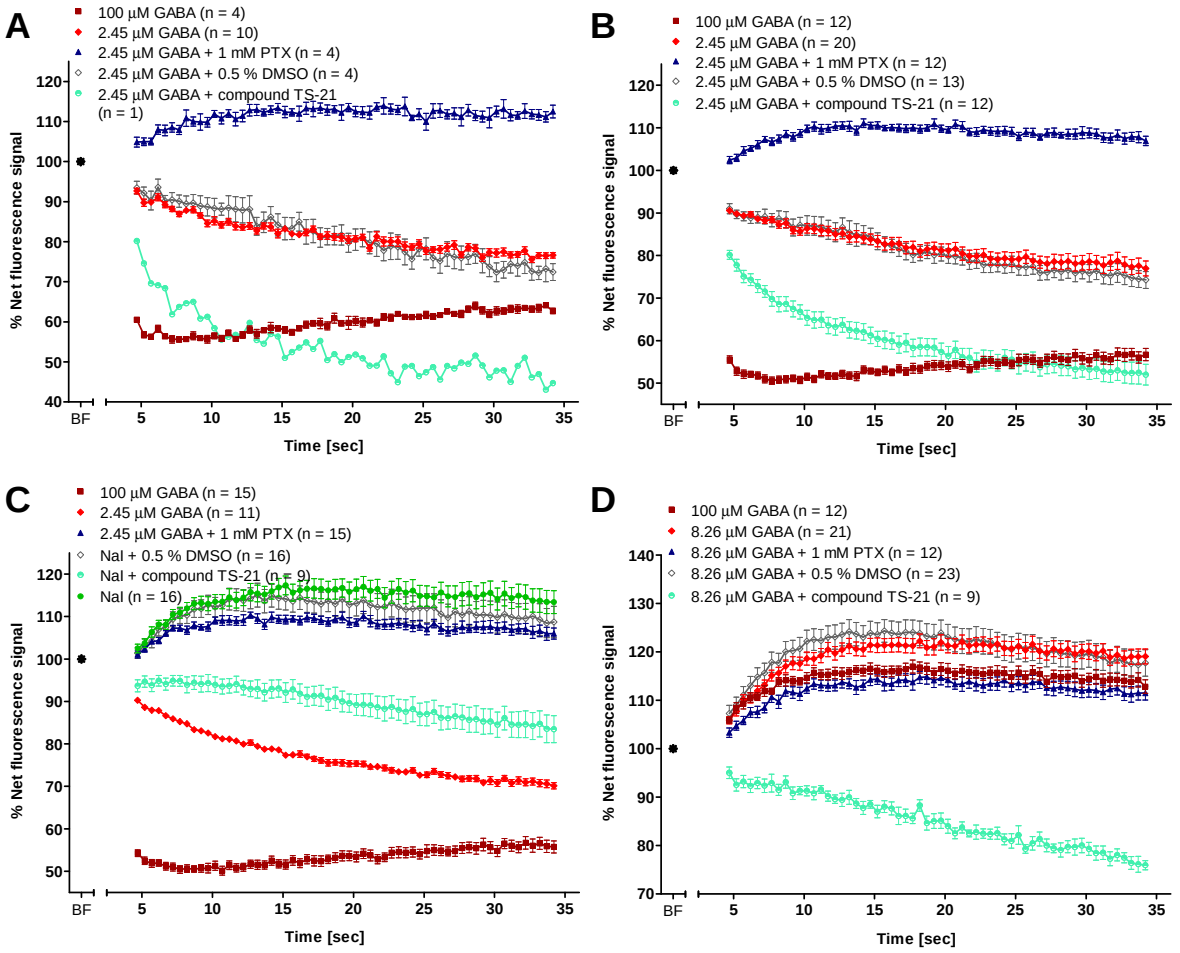

Figure 5.28: Fluorescence signal change after adding test compound TS-21 to HEK293 cells expressing YFP-H148Q/I152L and $\alpha 3\beta 2\gamma 2$ $GABA_A$ receptors.

Fluorescence was measured for 30 seconds after adding (A) 2.45 µM GABA to wells containing 548.9 nM compound TS-21 (final concentrations) in initial screening assay. (B) Screening assay was repeated on different plates. The effect of compound TS-21 was significantly different to GABA-control response ($p < 0.001$). (C) Data from no-GABA control plates. NaI test solution only was added to wells containing compound TS-21 (548.9 nM final concentration). (D) Effect of 8.26 µM GABA and 54.89 µM compound TS-21 was investigated on cells expressing YFP-H148Q/I152L only. 100 µM GABA, 8.26 µM GABA, 8.26 µM GABA and 1 mM picrotoxin, 8.26 µM GABA and 0.5 % DMSO and in (C) NaI test solution alone served as controls. Data correspond to means ± SEM; n states the number of wells measured. Net fluorescence of values was normalised by setting the averaged baseline fluorescence to 100 % and fluorescence changes (after adding solutions) were calculated as percentage of the baseline fluorescence.

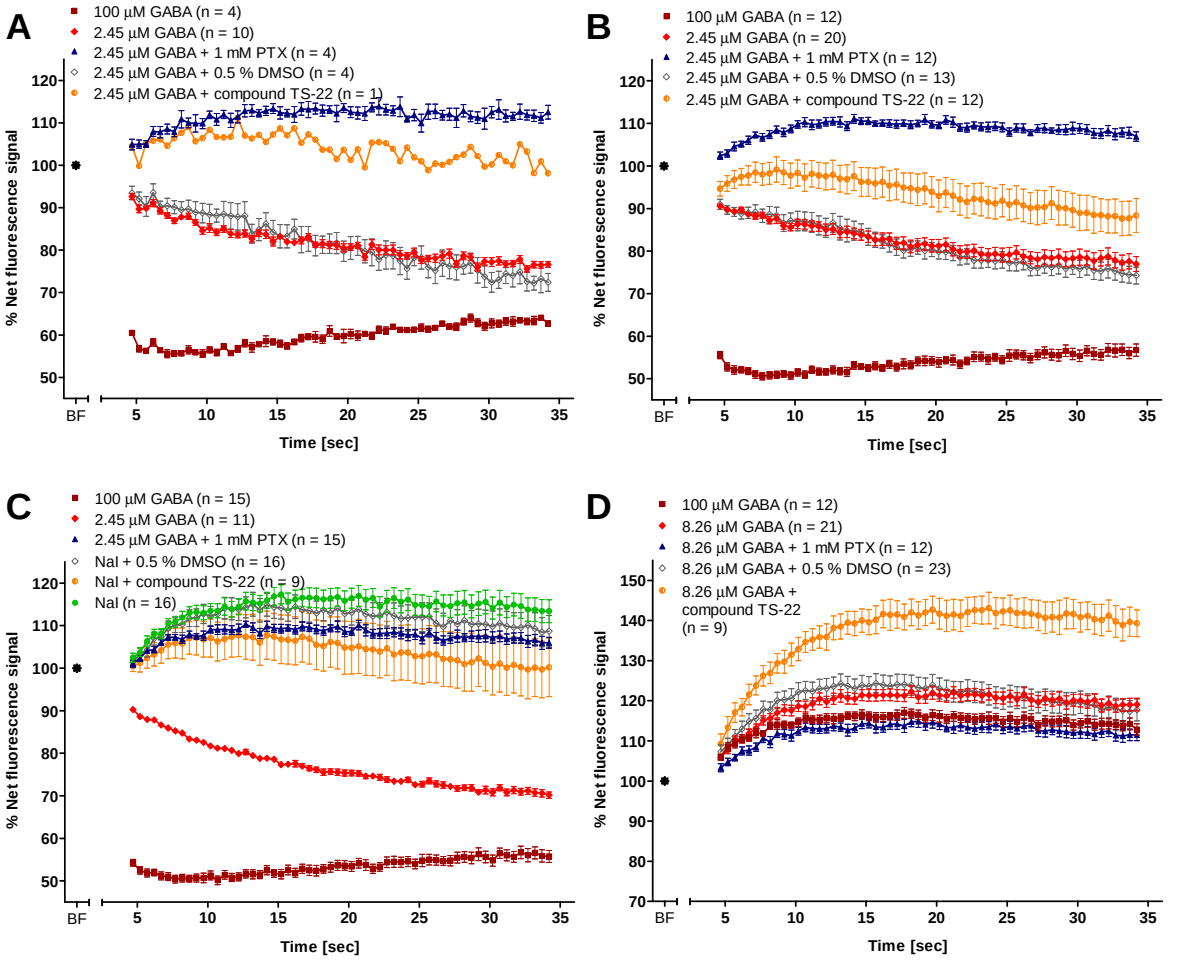

Figure 5.29: Fluorescence signal change after adding test compound TS-22 to HEK293 cells expressing YFP-H148Q/I152L and $\alpha 3\beta 2\gamma 2$ $GABA_A$ receptors.

Fluorescence was measured for 30 seconds after adding (A) 2.45 µM GABA to wells containing 545.8 nM compound TS-22 (final concentrations) in initial screening assay. (B) The assay was repeated on different plates. The effect of compound TS-22 was significantly different to GABA-control response ($p < 0.01$). (C) Data from no-GABA control plates. NaI test solution only was added to wells containing compound TS-22 (545.8 nM final concentration). (D) Effect of 8.26 µM GABA and 54.58 µM compound TS-22 on cells expressing YFP-H148Q/I152L only. 100 µM GABA, 8.26 µM GABA, 8.26 µM GABA and 1 mM picrotoxin, 8.26 µM GABA with 0.5 % DMSO and in (C) NaI test solution alone served as controls. Data correspond to means ± SEM; n states the number of wells measured. Net fluorescence of values was normalised by setting the averaged baseline fluorescence to 100 % and fluorescence changes (after adding solutions) were calculated as percentage of the baseline fluorescence.

Compounds TS-23 and TS-16 had increased the fluorescence quench compared to the GABA-control response in cells expressing $\alpha3\beta2\gamma2$ $GABA_A$ receptors. Results from the former could be confirmed while repeating the assay several times on different plates. The fluorescence quench obtained was 49.19 $\pm$ 3.27 % and therefore slightly higher than the quench obtained for 100 µM GABA (44.15 $\pm$ 1.22 %; Figure 5.30 A, B). The compound also triggered a small fluorescence quench when applied without GABA. No effect was seen in cells lacking $\alpha3\beta2\gamma2$ $GABA_A$ receptors, indicating that the observed YFP quench is $GABA_A$ receptor specific (Figure 5.30 C, D). Similar results were obtained for the latter compound, TS-16. However, the fluorescence quench was weaker (38.15 $\pm$ 3.65 %); no effect was seen when the compound was applied without GABA or to cells lacking the receptor (Figure 5.31).

The positive screening result obtained in the initial screening tests using test compound TS-24 turned out to be false positive. The fluorescence quench could not be confirmed when repeating the assays (Figure 5.32).

The number of test compounds enhancing or inhibiting $GABA_A$ receptor activity determined by the preliminary screening tests (Section 5.2.1) could be further reduced by subtracting false-positive results and those compounds that triggered an effect on cells lacking the receptors when retesting the compounds using triplicates per plate (see above). The remaining compounds exhibiting $GABA_A$ receptor-specific activity could now be further investigated. There were seven compounds left exhibiting a distinctive effect on $\alpha1\beta2\varepsilon$ receptors and three compounds that showed an effect on $\alpha3\beta2\gamma2$ $GABA_A$ receptors.

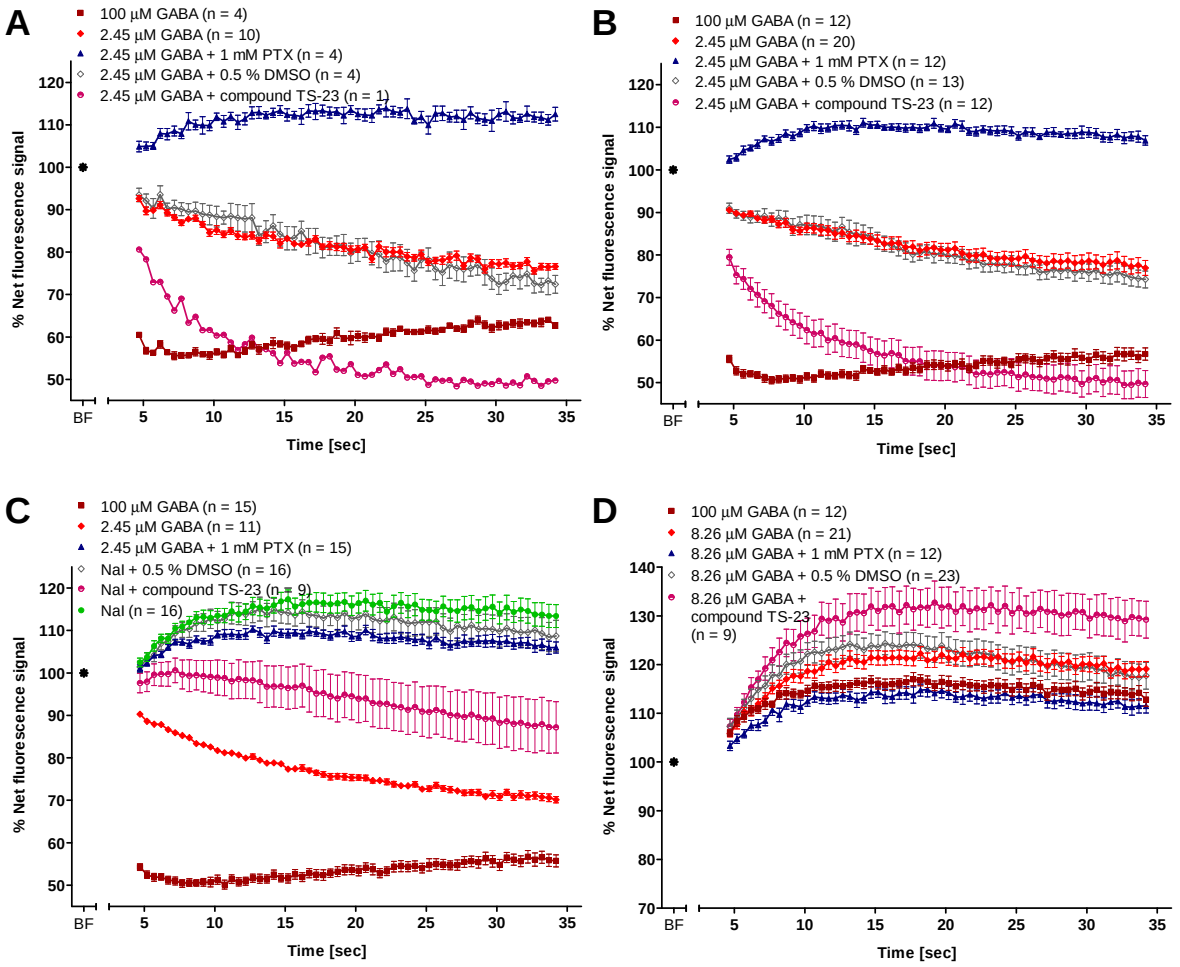

Figure 5.30: Fluorescence signal change after adding test compound TS-23 to HEK293 cells expressing YFP-H148Q/I152L and $\alpha 3\beta 2\gamma 2$ $GABA_A$ receptors.

Fluorescence was measured for 30 seconds after adding (A) 2.45 µM GABA to wells containing 546.6 nM compound TS-23 (final concentrations) in initial screening assay. (B) The assay was repeated on different plates. The effect of compound TS-23 was significantly different to GABA-control response ($p < 0.001$). (C) Data from no-GABA control plates. NaI test solution only was added to wells containing compound TS-23 (546.6 nM final concentration). (D) Effect of 8.26 µM GABA and 54.66 µM compound TS-23 on cells expressing YFP-H148Q/I152L only. 100 µM GABA, 8.26 µM GABA, 8.26 µM GABA and 1 mM picrotoxin, 8.26 µM GABA with 0.5 % DMSO and in (C) NaI test solution alone served as respective controls. Data correspond to means ± SEM; n states the number of wells measured. Net fluorescence of values was normalised by setting the averaged baseline fluorescence to 100 % and fluorescence changes (after adding solutions) were calculated as percentage of the baseline fluorescence.

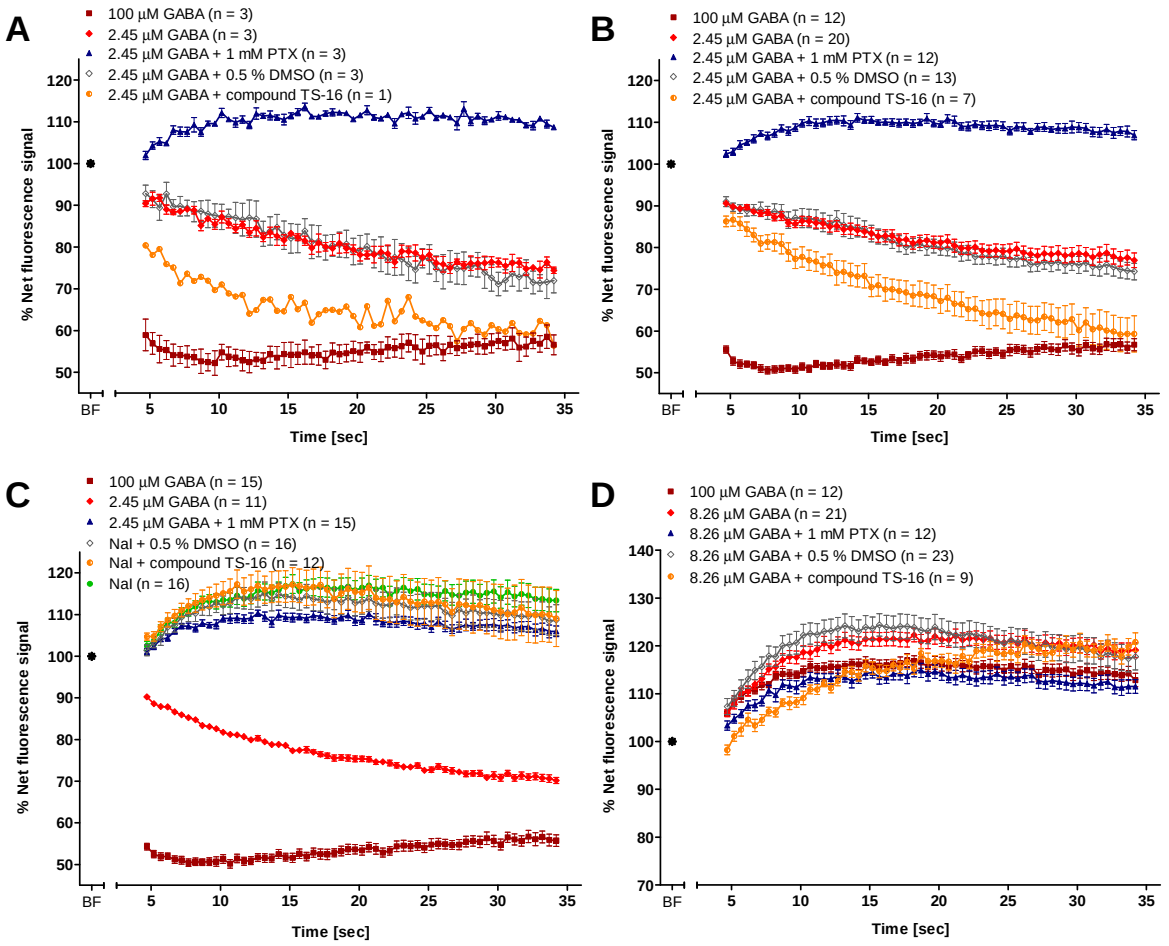

Figure 5.31: Fluorescence signal change after adding test compound TS-16 to HEK293 cells expressing YFP-H148Q/I152L and $\alpha 3\beta 2\gamma 2$ $GABA_A$ receptors.

Fluorescence was measured for 30 seconds after adding (A) 2.45 µM GABA to wells containing 539.4 nM compound TS-16 (final concentrations) in initial screening assay. (B) The assay was repeated on different plates. The effect of compound TS-16 was significantly different to GABA-control response ($p < 0.05$). (C) Data from no-GABA control plates. NaI test solution only was added to wells containing compound TS-16 (539.4 nM final concentration). (D) Effect of 8.26 µM GABA and 53.94 µM compound TS-16 on cells expressing YFP-H148Q/I152L only. 100 µM GABA, 8.26 µM GABA, 8.26 µM GABA and 1 mM picrotoxin, 8.26 µM GABA and 0.5 % DMSO and in (C) NaI test solution alone served as controls. Data correspond to means ± SEM; n states the number of wells measured. Net fluorescence of values was normalised by setting the averaged baseline fluorescence to 100 % and fluorescence changes (after adding solutions) were calculated as percentage of the baseline fluorescence.

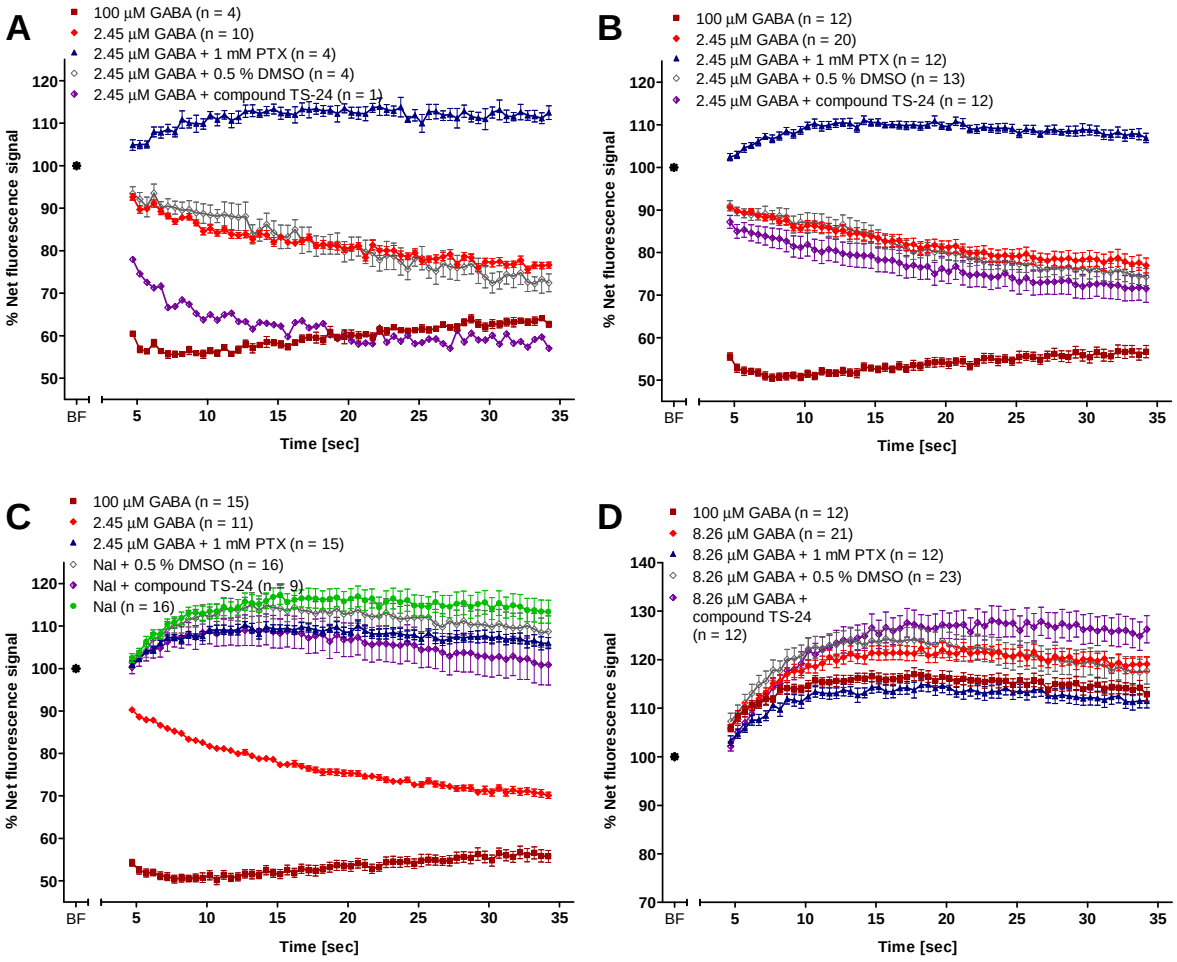

Figure 5.32: Fluorescence signal change after adding test compound TS-24 to HEK293 cells expressing YFP-H148Q/I152L and $\alpha 3\beta 2\gamma 2$ $GABA_A$ receptors.

Fluorescence was measured for 30 seconds after adding (A) 2.45 µM GABA to wells containing 553.6 nM compound TS-24 (final concentrations) in initial screening assay. (B) The assay was repeated on different plates. (C) Data from no-GABA control plates. NaI test solution only was added to wells containing compound TS-24 (553.6 nM final concentration). (D) Effect of 8.26 µM GABA and 55.36 µM compound TS-24 on cells expressing YFP-H148Q/I152L only. 100 µM GABA, 8.26 µM GABA, 8.26 µM GABA and 1 mM picrotoxin, 8.26 µM GABA with 0.5 % DMSO and in (C) NaI test solution alone served as controls. Data correspond to means ± SEM; n states the number of wells measured. Net fluorescence of values was normalised by setting the averaged baseline fluorescence to 100 % and fluorescence changes (after adding solutions) were calculated as percentage of the baseline fluorescence.

5.2.4 Investigation of 'hit' compounds in *Xenopus laevis* oocytes

Next, a selection of the remaining test compounds was examined in more detail using the two-electrode voltage-clamp technique by expressing $\alpha1\beta2\varepsilon$ or $\alpha3\beta2\gamma2$ $GABA_A$ receptors in *Xenopus laevis* oocytes. Test compound TS-3 was selected due to its significant inhibitory effect on cells expressing the $\alpha1\beta2\varepsilon$ receptor and the fact that control experiments confirmed the results (Figure 5.9). Applying increasing concentrations of compound TS-3 with GABA (EC_{30}) to *Xenopus* oocytes expressing $\alpha1\beta2\varepsilon$ receptors did not show significant differences to currents obtained from GABA-control responses (n = 4; Figure 5.33 A, B) and the inhibiting effect of the compound could not be confirmed.

The mutant YFP-based screening assays indicated that test compound TS-16 enhanced both $\alpha1\beta2\varepsilon$ and $\alpha3\beta2\gamma2$ $GABA_A$ receptors expressed in HEK293 cells (Figures 5.22 and 5.31). It was the only test compound identified in the screening assay that enhanced the activity of $\alpha1\beta2\varepsilon$ receptors and, therefore, further investigated. The compound's enhancing effect could be confirmed in oocytes expressing $\alpha3\beta2\gamma2$ receptors (Figure 5.34 A, C). The GABA-control response increased by 65.8 % when applying 10 or 100 µM compound TS-16 together with GABA (EC_{20}) to the oocytes. The compounds EC_{50} was 3.67 µM (n = 7). However, in oocytes expressing $\alpha1\beta2\varepsilon$ receptors, no clear concentration-dependent characteristics could be detected when applying the compound (n = 4; Figure 5.34 A, B). High concentrations of the test compound actually triggered an "outward" current in two of four oocytes. Overall the current traces obtained throughout for $\alpha1\beta2\varepsilon$ receptors expressed in *Xenopus* oocytes were very small compared to traces from other $GABA_A$ receptor subtypes.

Since the results so far obtained for $\alpha1\beta2\varepsilon$ $GABA_A$ receptors were inexplicit, the final compound tested in oocytes was compound TS-23. Compound TS-23 enhanced GABA-evoked YFP quench in the screening assay setup using HEK293 cells expressing $\alpha3\beta2\gamma2$ receptors (Figure 5.30). The results obtained from oocytes confirmed the potentiation of GABA-mediated responses by the compound. At concentrations of 10 µM or higher, the response was about 60 % enhanced compared to the GABA-control response. The EC_{50} of the compound was 1.42 µM (n = 5; Figure 5.35 A, B).

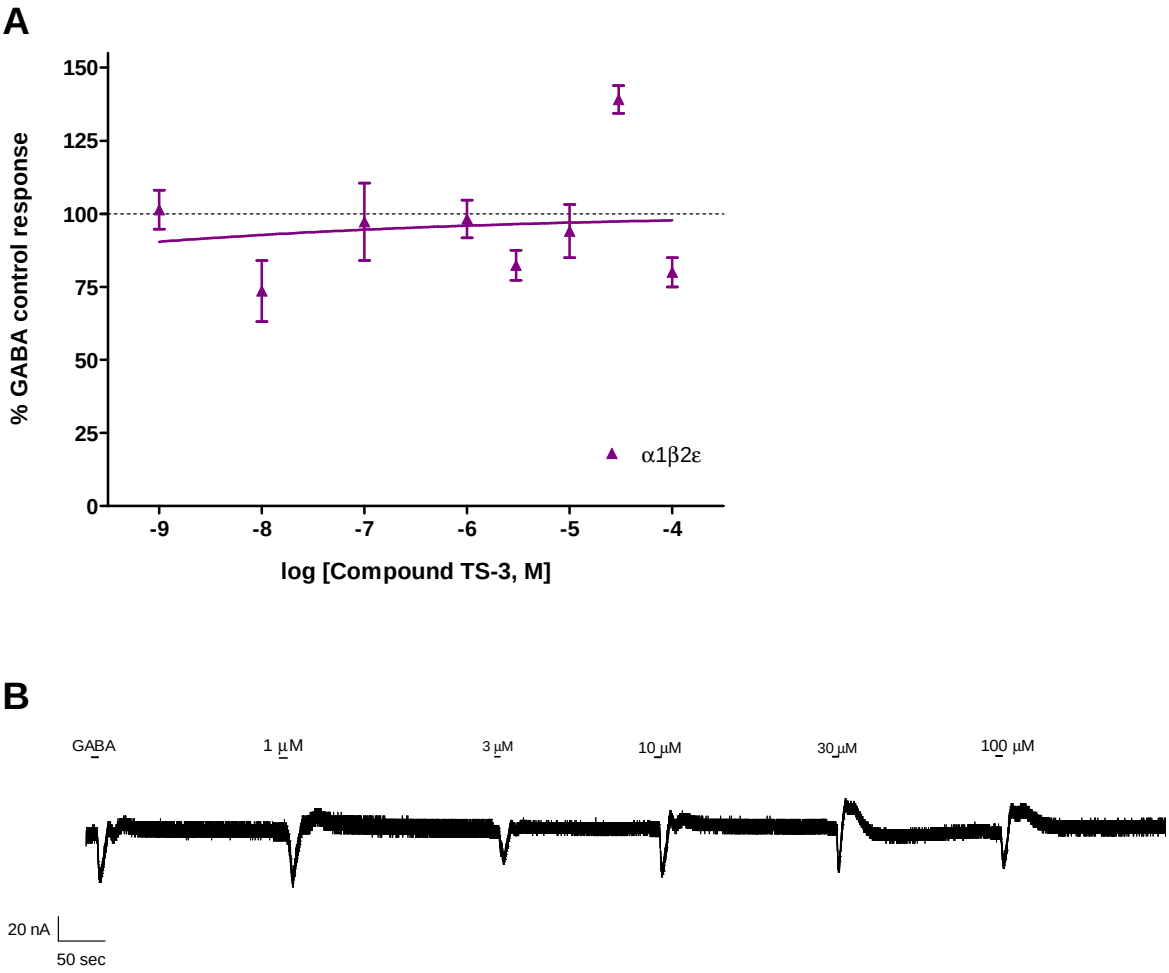

Figure 5.33: Results obtained from oocytes expressing $\alpha 1\beta 2\varepsilon$ receptors after exposure to test compound TS-3 and GABA at EC_{30} concentrations.

(A) Compound TS-3 concentration response analysis using a non-linear regression fit with variable slopes as described in Section 2.3.5 (n = 4). Data points correspond to means ± SEM; n states the number of oocytes examined. (B) Representative current traces evoked by GABA at EC_{30} concentrations alone or in combination with increasing concentrations of compound TS-3. Horizontal bars represent drug application.

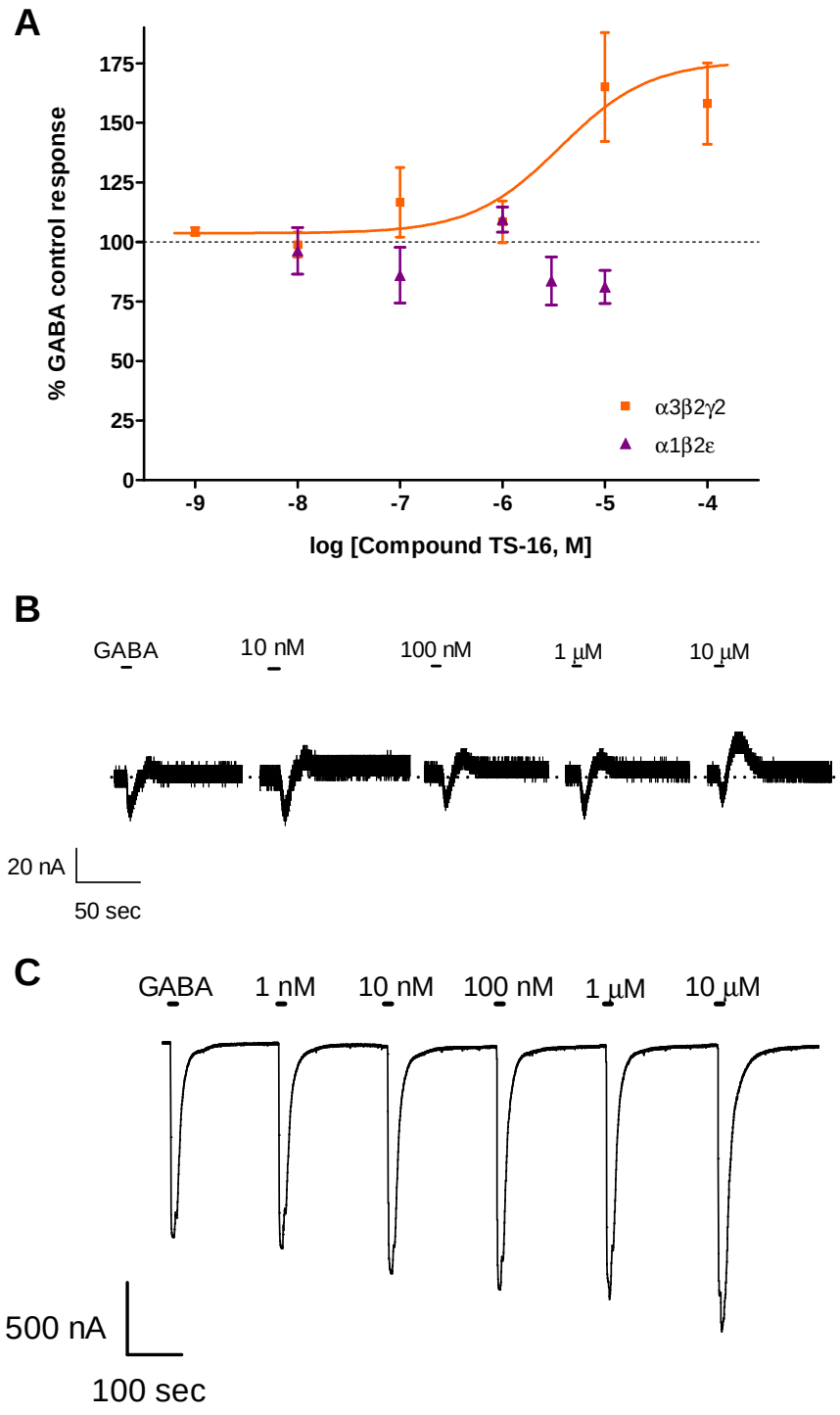

Figure 5.34: Results obtained from oocytes expressing $\alpha 1\beta 2\varepsilon$ or $\alpha 3\beta 2\gamma 2$ receptors after exposure to test compound TS-16 and submaximal GABA concentrations.

(A) Compound TS-16 concentration-response analysis using a non-linear regression fit with variable slopes as described in Section 2.3.5 (n = 4 for $\alpha 1\beta 2\varepsilon$ and n = 7 for $\alpha 3\beta 2\gamma 2$). Data points correspond to means ± SEM; n states the number of oocytes examined. (B) Representative current traces evoked by GABA at EC_{30} concentrations alone or in combination with increasing concentrations of compound TS-16 in oocytes expressing $\alpha 1\beta 2\varepsilon$ receptors. (C) Sample current traces triggered by GABA at EC_{20} concentrations alone or in combination with increasing concentrations of compound TS-16 in oocytes expressing $\alpha 3\beta 2\gamma 2$ receptors. Horizontal bars represent drug application.

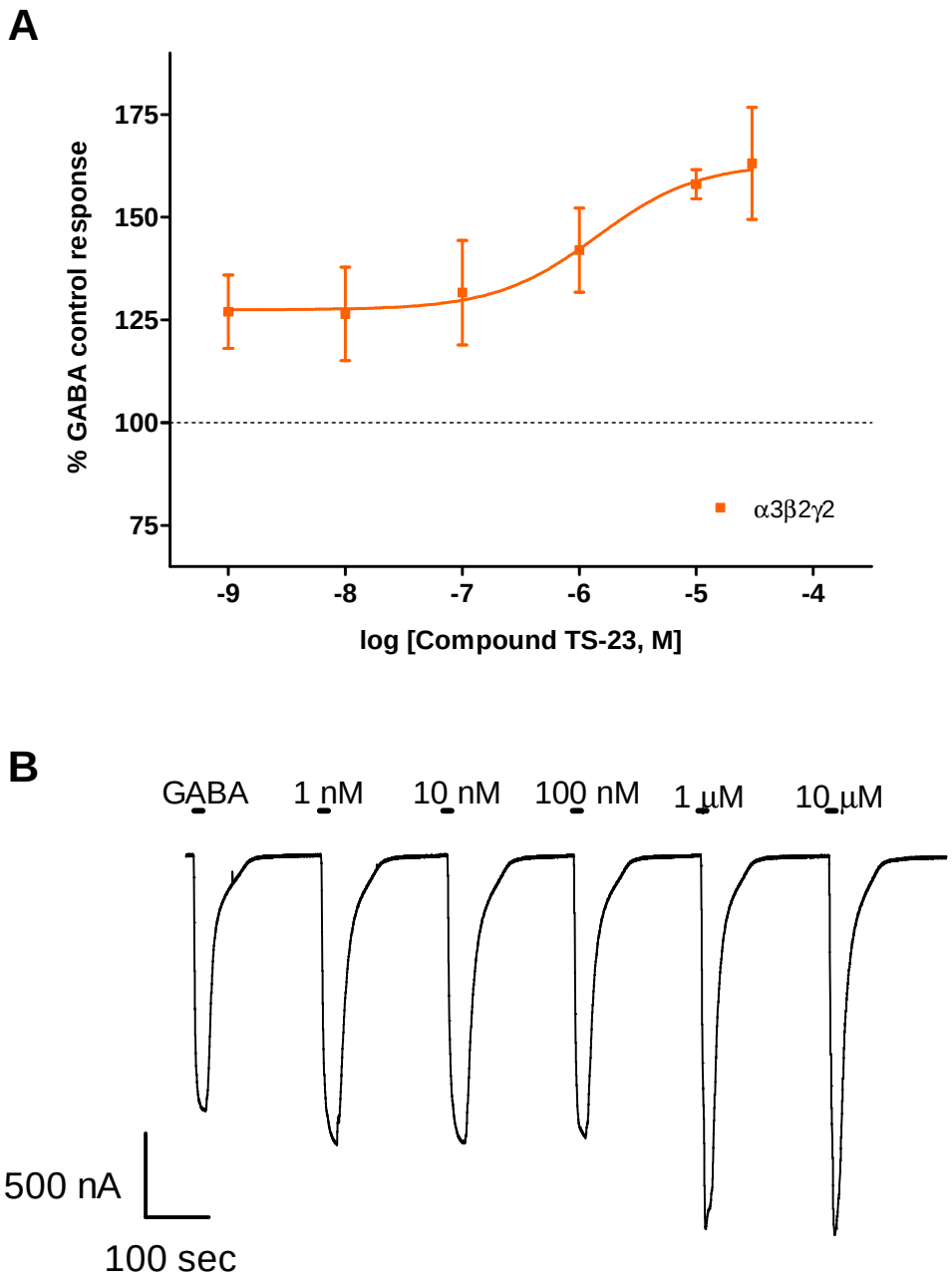

Figure 5.35: Results obtained from oocytes expressing $\alpha 3\beta 2\gamma 2$ receptors after exposure to test compound TS-23 and GABA at EC_{30} concentrations.

(A) Compound TS-23 concentration-response analysis using a non-linear regression fit with variable slopes as described in Section 2.3.5 (n = 5). Data points correspond to means ± SEM; n states the number of oocytes examined. (B) Sample current traces triggered by GABA at EC_{30} concentrations alone or in combination with increasing concentrations of compound TS-23 in oocytes expressing $\alpha 3\beta 2\gamma 2$ receptors. Horizontal bars represent drug application.

5.3 Discussion

After setting up and optimising a cell-based screening assay using the mutant YFP-H148Q/I152L, 800 chemical compounds of the Maybridge HitFinder™ Collection were screened against $\alpha1\beta2\varepsilon$ as well as $\alpha3\beta2\gamma2$ $GABA_A$ receptors expressed in HEK293 cells using a fluorescence plate reader. As mentioned in the previous chapter, the assay setup using cells expressing $\alpha1\beta2\varepsilon$ receptors exhibited a very small signal range and Z'-factor and its suitability to screen for compounds was uncertain. However, it was proposed that YFP quench-inhibiting or -enhancing compounds could be identified visually and, thus, the assay format was applied due to the lack of alternative methods. By screening compounds against both receptor subtypes it was possible to compare compound effects and to identify compounds that were specific to one of the receptor subtypes.

In order to elicit the desired biological action, it is necessary to apply a chemical compound at a specific concentration (Inglese et al., 2006). Moreover, the right compound concentration for the preliminary screening is often chosen according to the capacity of the secondary screening test or further investigations (Willumsen et al., 2003). In this project, compounds were screened initially at relatively high concentrations with the aim to evaluate the hit rate. The majority of the test compounds did show little or no effects. This was expected since in unbiased libraries most compounds do not exhibit activity (Zhang et al., 1999). Nevertheless, the hit rate was relatively high and numerous compounds seemed to exhibit effects by enhancing or inhibiting YFP quenches on the two receptor subtypes. The question arose whether the chosen test compound concentration was too high, and the fluorescence change seen in many samples may have been due to "off-target" or toxic effects, which are sometimes observed at high compound concentrations (Inglese et al., 2006). In a study performing HTS on 5-HT_6Rs, which are G protein-coupled receptors, chemical compounds at a concentration of 10 µM were applied (Kim et al., 2008). However, since the nature of the performed assays and investigated proteins was very different, compound concentrations cannot be compared easily. Here, in order to identify the most potent compounds, their concentrations were gradually decreased and retested until a manageable number of compounds was left for further

investigations.

When examining the preliminary screening results it is striking that the majority of compounds influencing the fluorescence signal in cells expressing $\alpha1\beta2\varepsilon$ receptors are inhibiting the GABA-evoked YFP quench. In contrast, most compounds increased the fluorescence quench in cells expressing $\alpha3\beta2\gamma2$ receptors. Furthermore, the compound concentrations used in the later screens were relatively low, especially after the last dilution. However, since all compounds tested at this concentration inhibited the YFP quench in $\alpha1\beta2\varepsilon$ receptors, it is possible that some inhibited the open, spontaneously active receptor channels before GABA in NaI solution was injected into the wells. The test compounds were added to 50 µl NaCl bathing solution before NaI test solution was injected (50.3 to 59.3 nM was the final concentration of compounds per well).

The preliminary screening tests were performed in singlets and the occurrence of false positive results among the selected compounds was expected, since they are very common in single-dose, single-experiment assay setups (Hann & Oprea, 2004). There are many different reasons for false positive results to occur: it could be due to pipetting errors, cross-contamination or other handling errors, also data handling and analysis. These could have easily happened despite the great care that was taken due to the large amount of compounds and subsequent data obtained that were all handled manually. Further reasons are possible quenching artefacts or auto-fluorescence of compounds, variability of the transfected cells, measurements on the edge of the plate, reagent differences or other effects triggered by a compound independently from the $GABA_A$ receptor subtypes investigated (Gonzalez & Maher, 2002; Gill et al., 2003; Terstappen, 2005; Inglese et al., 2007a; Sui & Wu, 2007; Janzen & Popa-Burke, 2009).

Test compounds exhibiting positive effects during the preliminary screening tests were further examined to eliminate possible false positive results. Thus, the assays were repeated using triplicates as well as additional controls, such as cells lacking the $GABA_A$ receptors and, to check for agonist-independent activity, applying the compounds without submaximal GABA concentrations. Note that the latter control does not function with compounds that

inhibited GABA-control responses. By this means, several test compounds that previously inhibited or enhanced GABA-elicited fluorescence quenches could be ruled out for further testing. Of those, a number of compounds showed a YFP quench on cells lacking the receptors. Hence, it was suggested that the effect seen after applying the compound was caused via endogenously expressed proteins. The same might be the case where the fluorescence signal was higher compared to the other controls used in cells lacking receptors. Although it is not clear, why the fluorescence signal would increase compared to the baseline fluorescence; it could also be some assay artefact, since the fluorescence signal in no-GABA controls did not show a comparable increase. Further compounds could be eliminated due to the fact that the effect seen at first was less prominent or non existent when repeating the assay; the latter may have happened due to pipetting or data handling errors.

After performing the mutant YFP-based assay, from 800 compounds screened, seven were identified to be active on $\alpha1\beta2\varepsilon$ receptors and three on $\alpha3\beta2\gamma2$ $GABA_A$ receptors. To do a different type of assay is a frequently applied method to confirm the activity of a test compound (Zheng et al., 2004). Here, the two-electrode voltage-clamp technique was used to confirm and examine the compound's activities in more detail. Due to time limitations, not all of the identified compounds could be examined in oocytes. The first compound investigated was compound TS-3. This compound showed no effects on cells expressing $\alpha3\beta2\gamma2$ $GABA_A$ receptors, but inhibited the GABA-evoked fluorescence quench in cells expressing $\alpha1\beta2\varepsilon$ receptors in the YFP-based assay. However, this effect could not be confirmed when using the two-electrode voltage-clamp technique and *Xenopus* oocytes. The problem was that currents from oocytes expressing $\alpha1\beta2\varepsilon$ receptors were very small, and therefore it was difficult to distinguish differences between currents elicited by submaximal concentrations of GABA and those evoked by the compound together with GABA. Additionally, some of the valves of the perfusion system were stuck and opened manually. It is therefore likely that the data obtained do not reflect the effect of the test compound but rather unsteadiness of the perfusion of the compound. The next compound examined in oocytes was compound TS-16, which increased the YFP quench on both receptor subtypes tested in HEK293 cells using the YFP-based screening assay. Again, the results obtained for the ε-containing receptor sub-

type were ambiguous. Interestingly, instead of increasing GABA-evoked currents, at higher concentrations an "outward" current could be seen in two of four oocytes tested that was not seen with lower concentrations or GABA alone. This may indicate that, at higher concentrations, the compound blocked the spontaneously open channels. Tests in oocytes expressing $\alpha3\beta2\gamma2$ receptors confirmed the results of the YFP-based assay; the compound enhanced GABA-evoked currents in a concentration-dependent manner. Due to the difficulties with the oocytes expressing the ε-containing receptors, the last investigated compound was compound TS-23, which enhanced the YFP quench in HEK293 cells expressing the $\alpha3\beta2\gamma2$ receptor. The activity of the compound on this receptor subtype could also be confirmed in oocytes.

In summary, performing two-electrode voltage-clamp experiments in oocytes expressing $\alpha3\beta2\gamma2$ $GABA_A$ receptors could confirm the results obtained from the YFP-based screening assay in HEK293 cells. To what extend results are comparable is not certain, since the compounds were only tested at a single concentration using the cell-based screening assay, except when testing GABA-concentration responses (see Section 4.3.3, Chapter 4). Nevertheless, from the results obtained here, it can be concluded that the screening assay is a suitable assay format to screen chemical compound libraries against $\alpha3\beta2\gamma2$ receptors. The EC_{50} values obtained for the two hit compounds were in the low micromolar range. Possible future work may lead to generation and screening of compound analogues which may enhance the potencies of the compounds (see below).

Results obtained for $\alpha1\beta2\varepsilon$ receptors were ambiguous when using the two-electrode voltage-clamp technique and no subtype-selective compound could be identified yet. This may partly be a reflection on the cell-based screening assay that exhibited a small signal range and, thus, low robustness. Nevertheless, it was unexpected that the obtained results could not be confirmed performing the two-electrode voltage-clamp technique in *Xenopus* oocytes. It may be worth trying the patch-clamp method in the future and test the compounds on receptors expressed in HEK293 cells, rather than oocytes, since the compounds were identified using these cells. Furthermore, oocytes are less sensitive during pharmacological investigations compared to mammalian cells (Xu et al., 2001). In the future, the ability to identify hit com-

pounds could also be improved, if the assays signal range and, thus, quality (Z'-factor) could be further enhanced. One possibility to improve the assay's quality could be by manipulating the ε subunit in a way that the continuous activity could be eliminated without influencing agonist or modulator binding properties, because amino acid changes would only be generated in the pore lining of the channel. One would need to keep in mind that there are modulators that bind to residues in the channels pore. However, those are not a priority in the present study mainly seeking test compounds binding elsewhere on the receptor channel (see Section 1.4, Chapter 1).

Originally, it was planned to verify a number of hit compounds and to generate a second-generation library, consisting of structural analogues of the compounds exhibiting the strongest effects during the preliminary screening. Afterwards, pharmacological characteristics of the improved hit compounds could be examined using electrophysiological techniques. In drug screening tests, the screening of hit analogues generated via parallel synthesis is common practice, because a compound's properties towards the target protein can be enhanced (van Niel et al., 2005; Kim et al., 2008; Wafford et al., 2009). Structure-activity relationships generated by screening compound analogues would reveal which structural elements are crucial for biological efficacy and would deliver first-generation tools for examining the *in vivo* function of ε-subunit-containing receptors. In this study, hit compounds were tested immediately after the preliminary screening in oocytes using the two-electrode voltage-clamp technique due to time limitations of this project. In the future, due to the fact that it was possible to screen for compounds modulating $GABA_A$ receptor activity using this assay format, further chemical compounds may be screened and analogues of hit compounds may be subsequently generated to further evaluate and examine their properties.

Chapter 6

General Discussion

$GABA_A$ receptors are targeted by a plethora of different clinically important drugs. However most of them target the receptors non-selectively, hence adverse side effects often occur (Buffett-Jerrott & Stewart, 2002; Möhler et al., 2002; Bateson, 2004; Agid et al., 2007). Nevertheless, the structural diversity of the receptors offers great prospects for finding subunit selective modulatory compounds that would target specific receptor subtypes.

Different receptor subunits confer distinct pharmacological and electrophysiological properties to $GABA_A$ receptor subtypes (Sieghart & Sperk, 2002). The ε subunit has only been investigated in few studies and not much is known about its physiological role *in vivo*. Previous studies that investigated pharmacological properties of ε-containing receptors showed that the subunit confers different properties to the receptor, compared to $\alpha\beta$ or $\alpha\beta\gamma$ receptors, however, no subunit-selective pharmacological profile could be established (Olsen & Sieghart, 2009).

6.1 Pharmacological characterisation of the $\alpha 3\beta 2\varepsilon$ $GABA_A$ receptor

The pharmacological properties of $\alpha 3\beta 2\varepsilon$ $GABA_A$ receptors were investigated using the two-electrode voltage-clamp technique. This subunit combination had not been examined before. Because the $\beta 2$ subunit is the most widely distributed β subunit in the mammalian brain, it

is likely that the subunits form functional channels in some areas of the brain. The data obtained were similar to results obtained in previous recombinant pharmacological studies investigating the ε subunit in combination with different α and β subunits (Davies et al., 1997; Whiting et al., 1997; Thompson et al., 1998; Neelands et al., 1999; Maksay et al., 2003; Ranna et al., 2006). It was shown that the inclusion of the ε subunit into a $GABA_A$ receptor complex changes its pharmacological properties, for example $\alpha3\beta2\varepsilon$ receptors exhibited high agonist sensitivity compared to $\alpha3\beta2$ and $\alpha3\beta2\gamma2$ receptors, but the potency to the anaesthetic etomidate was less compared to $\alpha3\beta2$ receptors. Nevertheless, no ε-selective compounds are known yet. However, it is possible that there is a specific binding site located between the α and ε subunits, probably similar to the benzodiazepine binding site (due to sequence similarities between different subunits) and it was suggested that the ε subunit represents an important future drug target (Whiting, 1999). It was further shown that the ε subunit confers unusual properties to $\alpha3\beta2\varepsilon$ receptors, for example constitutive receptor activity, which was also reported from other recombinant receptor subtypes containing the ε subunit (Whiting et al., 1997; Neelands et al., 1999; Wagner et al., 2005). It is not known, whether ε-containing receptors exhibit spontaneous activity *in vivo* and what implications this would have on the receptors function or localisation.

Many $GABA_A$ receptor subunits exhibit splice versions, however they are usually restricted to a single splice site, whereas the ε subunit exhibits multiple splice sites (Whiting et al., 1997; Wilke et al., 1997; Erlitzki et al., 2000; Sinkkonen et al., 2000; Kasparov et al., 2001). Many of these are expressed in the peripheral tissue, but there are also distinct splice versions present in the brain and the question arises: why are there so many ε subunit splice variants? Wilke et al. (1997) suggested that truncated transcripts may be expressed to down-regulate ε subunit expression or they could have another, as yet unknown, function. The work conducted here showed that the ε_T subunit version expressed in brain (described by Kasparov et al., 2001) is not incorporated into functional receptors when co-expressed with $\alpha3$ and $\beta2$ subunits in *Xenopus* oocytes. Similar results have also been obtained for other ε subunit splice variants and the only functional variant known so far is the ε transcript of 3.5 kb found in brain (Whiting et al., 1997; Davies et al., 2002).

Due to the fact that not much is known about the ε subunit and no specific pharmacology has been identified yet, it was decided to search for ε-selective compounds. Previous studies have screened compound libraries against specific α subunits or δ-subunit-containing receptors (van Niel et al., 2005; Wafford et al., 2009), but no study has been conducted to search for ε-subunit-selective modulatory compounds. Such a compound could be an important pharmacological tool to further study the role of the promiscuous ε subunit and it may also be a key step towards the development of future drugs targeted to ε-containing receptors, for example to treat AD. Therefore, the next goal of the study was to set up a cell-based screening assay to screen the ε-subunit-containing receptor subtype for selective modulatory compounds.

6.2 Search for and setup of a cell-based screening assay

Electrophysiological recording techniques, such as the two-electrode voltage-clamp technique, are labour intensive with low throughput, and hence unsuitable for the screening of compound libraries. Thus, a cell-based screening assay was sought. Several methods exist to screen $GABA_A$ receptors (see Smith & Simpson, 2003; Gilbert et al., 2009b; Verkman & Galietta, 2009). However, only few were relatively easy to set up and did not require specialised measuring devices, but could be performed using fluorescence or absorbance plate readers. Of the three assay formats tested, the last attempted assay approach, applying a mutant YFP, finally gave the desired results. The mutant YFP-H148Q/I152L acts as an iodide-ion indicator protein and was expressed together with $\alpha3\beta2\gamma2$ $GABA_A$ receptors in HEK293 cells. The cells were plated into a 96-well microtitre plate and exposed to high concentrations of the agonist GABA. This activated the expressed receptors facilitating iodide influx into the cells that quenched the YFP, which could be measured using a fluorescence plate reader. Fluorescence quench was prevented when the $GABA_A$ receptor blocker picrotoxin was applied. Kruger et al. (2005) tested the assay format in GlyRs as well as $\alpha1\beta1$ $GABA_A$ receptors and obtained a similar fluorescence quench for the $GABA_A$ receptor subtype as was obtained in this study using $\alpha3\beta2\gamma2$ receptors. After it was shown that the assay format was functional, cells expressing the $\alpha3\beta2\varepsilon$ receptor were tested, but no fluorescence quench

could be detected. Thereupon, several other receptor subtypes were tested, indicating that the maximum fluorescence quench could vary widely, depending on the subunit composition of the expressed receptor. It was proposed that these differences are due to different kinetic and gating properties of the receptor subtypes (that are conferred by different subunits). Furthermore, differences in transfection efficiency also influenced the YFP quench (Gilbert et al., 2009b). However, it was unclear why no fluorescence quench was detected in cells expressing the $\alpha3\beta2\varepsilon$-containing receptor. It was proposed that the constitutive activity of the receptor subtype could have also influenced the result. In a final attempt it was examined whether the inclusion of the $\alpha1$ subunit, instead of the $\alpha3$ subunit, into the receptor complex would change the assays outcome, and, surprisingly, a small fluorescence quench could be detected. Although the YFP quench was less considerable than the one obtained from $\alpha3\beta2\gamma2$ receptors, the $\alpha1\beta2\varepsilon$ receptor subtype was subsequently used in the screening assay.

The results of the mutant YFP screening assay setup once again demonstrated that the ε subunit confers different properties to $GABA_A$ receptors compared to other receptor subunits. During the two-electrode voltage-clamp studies it was noticeable that GABA-evoked currents were smaller in oocytes expressing $\alpha3\beta2\varepsilon$ receptors compared to oocytes expressing $\alpha3\beta2$ or $\alpha3\beta2\gamma2$ receptors. The small signal range obtained in the mutant YFP screening assay setup raised the question whether there is a relation between the two findings. The spontaneous activity observed in recombinant ε-containing receptors influences the current size and probably the signal window of the plate reader assay. However, this is likely not the only reason. It could be that ε-subunit-containing receptors were less efficiently expressed on the cell surface compared to other $GABA_A$ receptors. Gilbert et al. (2009b) showed that cells expressing fewer receptors and YFP (due to different transfection methods) also exhibited a smaller % fluorescence quench.

6.3 Screening of $\alpha 1\beta 2\varepsilon$ and $\alpha 3\beta 2\gamma 2$ $GABA_A$ receptors

After the assay format was optimised and its functionality demonstrated, a chemical compound library was screened against both $\alpha 1\beta 2\varepsilon$ and $\alpha 3\beta 2\gamma 2$ $GABA_A$ receptors expressed in HEK293 cells. The assay setup to screen the former subtype was not optimal for compound screening due to a small signal dynamic range. However, it was possible to distinguish the effect of compounds that inhibited or enhanced the fluorescence quench from the effect evoked by GABA at EC_{30} concentrations. Screening data were compared with those obtained from screening $\alpha 3\beta 2\gamma 2$ receptors in order to identify compounds that were selective to the ε-containing receptor. A similar practice was also used by Wafford et al. (2009) who sought δ-subunit-selective compounds.

The results obtained from the preliminary screening tests demonstrated that most compounds that were active on $\alpha 1\beta 2\varepsilon$ receptors inhibited the receptors activity, whereas it was the opposite for cells expressing $\alpha 3\beta 2\gamma 2$ receptors (most active compounds enhanced the fluorescence quench). Why most of the compounds inhibited the fluorescence quench is not known. It could again have something to do with the spontaneous activity of ε-containing receptors. Next, compounds that showed an effect were further tested using additional controls. By this means, false positive compounds could be eliminated. Several compounds showed effects on cells that did not express the $GABA_A$ receptor subtypes, but only YFP-H148Q/I152L, indicating that changes of the fluorescence signal were due to endogenously expressed proteins rather than the $GABA_A$ receptors investigated. Endogenously expressed proteins in HEK293 cells also likely played a role when setting up the iodide-flux assay that was tested before the mutant YFP-based assay, but failed to give the desired outcome. The data obtained highlighted the importance of controls.

From the 800 compounds that were screened against the two receptor subtypes, only a few were identified as hit compounds. In order to verify their activity, the compounds were tested using the two-electrode voltage-clamp method and *Xenopus laevis* oocytes expressing the respective receptor subtypes. Due to time restrictions only few compounds could be tested. Using oocytes expressing $\alpha 3\beta 2\gamma 2$ receptors confirmed the enhancing effect of compounds

(32) and (38) that were also seen using the plate reader assay. To what degree the results of the two methods were comparable beyond that remains unclear, since the YFP-based assay was only applied using one concentration of the test compounds. Results obtained from oocytes expressing $\alpha 1\beta 2\varepsilon$ receptors could not confirm the activity of the two hit compounds tested. It may be that the assays signal range was too low and the assay indeed was unsuitable to screen compounds against this receptor subtype. However, currents obtained using the two-electrode voltage-clamp technique and oocytes expressing $\alpha 1\beta 2\varepsilon$ receptors were very small. It is, therefore, likely that a different test using HEK293 cells and the more sensitive patch-clamp method could produce results that would confirm the effect of the previously identified hit compounds.

This study as well as the work by Gilbert et al. (2009b) and Kruger et al. (2005) showed that it is possible to set up a cell-based screening assay and screen chemical compound libraries using cells transiently expressing mutant YFP-H148Q/I152L and certain $GABA_A$ receptor subtypes. However, the studies also show that there is further room for improvement of the method in the future. Gilbert et al. (2009b), for example, showed that different transient transfection methods and transfection efficacies influence the YFP % fluorescence quench as well as the GABA EC_{50} values (note that the study was performed using flow cytometry rather than a fluorescence plate reader). The study by Kruger et al. (2005) and the work performed here also indicated inconsistencies in conjunction with the GABA EC_{50} value obtained using the fluorescence plate reader.

6.4 Future Work

This work demonstrated that the mutant YFP-based assay is suitable to screen chemical compound libraries. As indicated above, there are still difficulties associated with the method and no ε-selective compounds could be identified yet. However, the work presents the basis to further search for ε-subunit-selective modulatory compounds. The improvement of the assay's quality and robustness could enhance the chances to identify hit compounds greatly. One factor that might have affected the small YFP quench was the fact that ε-containing

receptors exhibit constitutive activity *in vitro* and the question arose whether a mutation preventing the receptor from opening spontaneously could improve the assay's outcome. The improved assay could be used to screen further chemical compounds against ε-containing $GABA_A$ receptors and hit compounds could be investigated in more detail.

Nevertheless, several promising compounds that showed an effect on ε-containing $GABA_A$ receptors have been identified in this study, which could be continued by verifying the activity of those compounds using further tests, for example the patch-clamp method using HEK293 cells. The next logical step would be to generate structural analogues of hit compounds using parallel synthesis (van Niel et al., 2005; Wafford et al., 2009). This second-generation library could then be screened again to identify compounds with enhanced binding affinity and selectivity. Improved compounds could then be examined in more detail using electrophysiological methods. If the activity of those compounds could be confirmed, they would present important research tools to further study the ε-subunit-containing $GABA_A$ receptor and help to finally elucidate the subunit's function *in vivo*.

6.5 Conclusions

The work conducted showed that $\alpha3\beta2\varepsilon$ $GABA_A$ receptors exhibit similar pharmacological characteristics as other ε-subunit-containing receptor subtypes (Davies et al., 1997; Whiting et al., 1997; Thompson et al., 1998; Neelands et al., 1999; Maksay et al., 2003; Ranna et al., 2006). Inclusion of the ε subunit into the $\alpha3\beta2$ receptor complex conferred distinct pharmacological properties as well as unusual characteristics, such as spontaneous activity, to the receptor subtype.

A cell-based screening assay was established using the mutant YFP-H148Q/I152L expressed in HEK293 cells also expressing $\alpha1\beta2\varepsilon$ or $\alpha3\beta2\gamma2$ receptors. It was demonstrated that the assay format facilitated the screening for compounds that modulate the activity of these receptor subtypes and several interesting hit compounds could be identified, of which several have been further investigated using the two-electrode voltage-clamp technique.

Further work is needed to unequivocally identify ε-subunit-selective compounds. Such compounds are important research tools that would contribute greatly towards the understanding of the physiological functions of ε-containing $GABA_A$ receptor subtypes in the future. In addition, they are prospective candidates for drug development.

Bibliography

Abeliovich, H. (2005). An empirical extremum principle for the Hill coefficient in ligand-protein interactions showing negative cooperativity. Biophysical Journal, 89, 76–79.

Agid, Y., Buzsaki, G., Diamond, D. M., Frackowiak, R., Giedd, J., Girault, J.-A., Grace, A., Lambert, J. J., Manji, H., Mayberg, H., Popoli, M., Prochiantz, A., Richter-Levin, G., Somogyi, P., Spedding, M., Svenningsson, P., & Weinberger, D. (2007). How can drug discovery for psychiatric disorders be improved? Nature Reviews Drug Discovery, 6, 189–201.

An, W. F. & Tolliday, N. J. (2009). Introduction: Cell-based assays for high-throughput screening. In Cell-Based Assays for High-Throughput Screening, vol. 486. (Humana Press), pp. 1–12.

Atack, J. R., Maubach, K. A., Wafford, K. A., O'Connor, D., Rodrigues, A. D., Evans, D. C., Tattersall, F. D., Chambers, M. S., MacLeod, A. M., Eng, W.-S., Ryan, C., Hostetler, E., Sanabria, S. M., Gibson, R. E., Krause, S., Burns, H. D., Hargreaves, R. J., Agrawal, N. G. B., McKernan, R. M., Murphy, M. G., Gingrich, K., Dawson, G. R., Musson, D. G., & Petty, K. J. (2009). *In Vitro* and *in Vivo* properties of 3-tert-butyl-7-(5-methylisoxazol-3-yl)-2-(1-methyl-1h-1,2,4-triazol-5-ylmethoxy)-pyrazolo[1,5-d]-[1,2,4]triazine (MRK-016), a GABA-A receptor alpha5 subtype-selective inverse agonist. Journal of Pharmacology and Experimental Therapeutics, 331, 470–484.

Atack, J. R., Wafford, K. A., Tye, S. J., Cook, S. M., Sohal, B., Pike, A., Sur, C., Melillo, D., Bristow, L., Bromidge, F., Ragan, I., Kerby, J., Street, L., Carling, R., Castro, J. L., Whiting, P., Dawson, G. R., & McKernan, R. M. (2006). TPA023 [7-(1,1-dimethylethyl)-6-(2-ethyl-2h-1,2,4-triazol-3-ylmethoxy)-3-(2-fluorophenyl)-1,2,4-triazolo[4,3-b]pyridazine], an agonist selective for alpha2- and alpha3-containing GABA-A receptors, is a nonsedating anxiolytic in rodents and primates. Journal of Pharmacology and Experimental Therapeutics, 316, 410–422.

Bateson, A. N. (2004). The benzodiazepine site of the GABA-A receptor: an old target with new potential? Sleep Medicine, 5, S9–S15.

Bateson, A. N., Lasham, A., & Darlison, M. G. (1991). gamma-Aminobutyric acidA receptor heterogeneity is increased by alternative splicing of a novel beta-subunit gene transcript. Journal of Neurochemistry, 56, 1437–1440.

Baumann, S. W., Baur, R., & Sigel, E. (2002). Forced subunit assembly in alpha1 beta2 gamma2 GABA-A receptors. Insight into the absolute arrangement. The Journal of Biological Chemistry, 277, 46020–46025.

Baumgartner, W., Islas, L., & Sigworth, F. J. (1999). Two-microelectrode voltage clamp of *Xenopus* oocytes: Voltage errors and compensation for local current flow. Biophysical Journal, 77, 1980–1991.

Belelli, D., Callachan, H., Hill-Venning, C., Peters, J., & Lambert, J. (1996). Interaction of positive allosteric modulators with human and *Drosophila* recombinant GABA receptors expressed in *Xenopus laevis* oocytes. British Journal of Pharmacology, 118, 563–576.

Belelli, D., Casula, A., Ling, A., & Lambert, J. J. (2002). The influence of subunit composition on the interaction of neurosteroids with GABA-A receptors. Neuropharmacology, 43, 651–661.

Belelli, D. & Lambert, J. J. (2005). Neurosteroids: endogenous regulators of the GABA-A receptor. Nature Reviews Neuroscience, 6, 565–575.

Belelli, D., Lambert, J. J., Peters, J. A., Wafford, K., & Whiting, P. J. (1997). The interaction of the general anesthetic etomidate with the gamma-aminobutyric acid type A receptor is influenced by a single amino acid. Proceedings of the National Academy of Sciences, 94, 11031–11036.

Belujon, P., Baufreton, J., Grandoso, L., Boue-Grabot, E., Batten, T., Ugedo, L., Garret, M., & Taupignon, A. (2009). Inhibitory transmission in locus coeruleus neurons expressing GABA-A receptor epsilon subunit has a number of unique properties. Journal of Neurophysiology, 102, 2312–2325.

Benke, D., Fakitsas, P., Roggenmoser, C., Michel, C., Rudolph, U., & Möhler, H. (2004). Analysis of the presence and abundance of GABA-A receptors containing two different types of alpha subunits in murine brain using point-mutated alpha subunits. Journal of Biological Chemistry, 279, 43654–43660.

Berglund, K., Schleich, W., Wang, H., Feng, G., Hall, W., Kuner, T., & Augustine, G. (2008). Imaging synaptic inhibition throughout the brain via genetically targeted Clomeleon. Brain Cell Biology, 36, 101–118.

Boileau, A. J., Baur, R., Sharkey, L. M., Sigel, E., & Czajkowski, C. (2002). The relative amount of cRNA coding for [gamma]2 subunits affects stimulation by benzodiazepines in GABA-A receptors expressed in *Xenopus* oocytes. Neuropharmacology, 43, 695–700.

Boileau, A. J., Li, T., Benkwitz, C., Czajkowski, C., & Pearce, R. A. (2003). Effects of [gamma]2s subunit incorporation on GABA-A receptor macroscopic kinetics. Neuropharmacology, 44, 1003–1012.

Bollan, K. A., Baur, R., Hales, T. G., Sigel, E., & Connolly, C. N. (2008). The promiscuous role of the epsilon subunit in GABA-A receptor biogenesis. Molecular and Cellular Neuroscience, 37, 610–621.

Bonnert, T. P., McKernan, R. M., Farrar, S., le Bourdelles, B., Heavens, R. P., Smith, D. W., Hewson, L., Rigby, M. R., Sirinathsinghji, D. J. S., Brown, N., Wafford, K. A., & Whiting, P. J. (1999). Theta, a novel gamma-aminobutyric acid type A receptor subunit. Proceedings of the National Academy of Sciences of the United States of America, 96, 9891–9896.

Bormann, J. (2000). The 'ABC' of GABA receptors. Trends in Pharmacological Sciences, 21, 16–19.

Bregestovski, P., Waseem, T., & Mukhtarov, M. (2009). Genetically encoded optical sensors for monitoring of intracellular chloride and chloride-selective channel activity. Frontiers in Molecular Neuroscience, 2, 15.

Buddhala, C., Hsu, C.-C., & Wu, J.-Y. (2009). A novel mechanism for GABA synthesis and packaging into synaptic vesicles. Neurochemistry International, 55, 9–12.

Buffett-Jerrott, S. & Stewart, S. (2002). Cognitive and sedative effects of benzodiazepine use. Current Pharmaceutical Design, 8, 45–58.

Celentano, J. & Wong, R. (1994). Multiphasic desensitization of the GABA-A receptor in outside-out patches. Biophysical Journal, 66, 1039–1050.

Cervetto, C. & Taccola, G. (2008). GABA-A and strychnine-sensitive glycine receptors modulate N-methyl-d-aspartate-evoked acetylcholine release from rat spinal motoneurons: A possible role in neuroprotection. Neuroscience, 154, 1517–1524.

Chambers, M. S., Atack, J. R., Carling, R. W., Collinson, N., Cook, S. M., Dawson, G. R., Ferris, P., Hobbs, S. C., O'Connor, D., Marshall, G., Rycroft, W., & MacLeod, A. M. (2004). An orally bioavailable, functionally selective inverse agonist at the benzodiazepine site of GABA-A alpha5 receptors with cognition enhancing properties. Journal of Medicinal Chemistry, 47, 5829–5832.

Chen, C.-L., Yang, Y.-R., & Chiu, T.-H. (1999). Activation of rat locus coeruleus neuron GABA-A receptors by propofol and its potentiation by pentobarbital or alphaxalone. European Journal of Pharmacology, 386, 201–210.

Citron, M. (2010). Alzheimer's disease: strategies for disease modification. Nature Reviews Drug Discovery, 9, 387–398.

Colquhoun, D. (1998). Binding, gating, affinity and efficacy: the interpretation of structure-activity relationships for agonists and of the effects of mutating receptors. British Journal of Pharmacology, 125, 924–947.

Connolly, C. N., Krishek, B. J., McDonald, B. J., Smart, T. G., & Moss, S. J. (1996). Assembly and cell surface expression of heteromeric and homomeric gamma-aminobutyric acid type A receptors. Journal of Biological Chemistry, 271, 89–96.

Crestani, F., Martin, J. R., Möhler, H., & Rudolph, U. (2000). Mechanism of action of the hypnotic zolpidem *in vivo*. British Journal of Pharmacology, 131, 1251–1254.

Darlison, M. G., Pahal, I., & Thode, C. (2005). Consequences of the evolution of the GABA-A receptor gene family. Cellular and Molecular Neurobiology, 25, 607–624.

Dascal, N. (1987). The use of *Xenopus* oocytes for the study of ion channels. CRC Critical Reviews in Biochemistry, 22, 317–387.

Davies, P. A., Hanna, M. C., Hales, T. G., & Kirkness, E. F. (1997). Insensitivity to anaesthetic agents conferred by a class of GABA-A receptor subunit. Nature, 385, 820–823.

Davies, P. A., Kirkness, E. F., & Hales, T. G. (2001). Evidence for the formation of functionally distinct $\alpha\beta\gamma\epsilon$ GABA-A receptors. Journal of Physiology, 537, 101–113.

Davies, P. A., McCartney, M. R., Wang, W., Hales, T. G., & Kirkness, E. F. (2002). Alternative transcripts of the GABA-A receptor epsilon subunit in human and rat. Neuropharmacology, 43, 467–475.

D'Hulst, C., Atack, J. R., & Kooy, R. F. (2009). The complexity of the GABA-A receptor shapes unique pharmacological profiles. Drug Discovery Today, 14, 866–875.

D'Hulst, C. & Kooy, R. F. (2007). The GABA-A receptor: a novel target for treatment of fragile X? Trends in Neurosciences, 30, 425–431.

Dominguez-Perrot, C., Feltz, P., & Poulter, M. O. (1996). Recombinant GABA-A receptor desensitization: the role of the gamma2 subunit and its physiological significance. The Journal of Physiology, 497, 145–159.

Draguhn, A., Verdorn, T. A., Ewert, M., Seeburg, P. H., & Sakmann, B. (1990). Functional and molecular distinction between recombinant rat GABA-A receptor subtypes by Zn^{2+}. Neuron, 5, 781–788.

Ducic, I., Caruncho, H. J., Zhu, W. J., Vicini, S., & Costa, E. (1995). gamma-Aminobutyric acid gating of Cl^- channels in recombinant GABA-A receptors. Journal of Pharmacology and Experimental Therapeutics, 272, 438–445.

Duebel, J., Haverkamp, S., Schleich, W., Feng, G., Augustine, G. J., Kuner, T., & Euler, T. (2006). Two-photon imaging reveals somatodendritic chloride gradient in retinal ON-type bipolar cells expressing the biosensor Clomeleon. Neuron, 49, 81–94.

Dumont, J. (1972). Oogenesis in *Xenopus laevis* (Daudin). I. stages of oocyte development in laboratory maintained animals. Journal of Morphology, 136, 153–179.

Ebert, B., Wafford, K. A., Whiting, P. J., Krogsgaard-Larsen, P., & Kemp, J. A. (1994). Molecular pharmacology of gamma-aminobutyric acid type A receptor agonists and partial agonists in oocytes injected with different alpha, beta, and gamma receptor subunit combinations. Molecular Pharmacology, 46, 957–963.

Erlitzki, R., Gong, Y., Zhang, M., & Minuk, G. (2000). Identification of gamma-aminobutyric acid receptor subunit types in human and rat liver. American Journal of Physiology - Gastrointestinal and Liver Physiology, 279, G733–739.

Ferri, C. P., Prince, M., Brayne, C., Brodaty, H., Fratiglioni, L., Ganguli, M., Hall, K., Hasegawa, K., Hendrie, H., Huang, Y., Jorm, A., Mathers, C., Menezes, P. R., Rimmer, E., & Scazufca, M. (2005). Global prevalence of dementia: a Delphi consensus study. The Lancet, 366, 2112–2117.

Filatov, G. N. & White, M. M. (1995). The role of conserved leucines in the M2 domain of the acetylcholine receptor in channel gating. Molecular Pharmacology, 48, 379–384.

Findlay, G. S., Ueno, S., Harrison, N. L., & Harris, R. A. (2001). Allosteric modulation in spontaneously active mutant [gamma]-aminobutyric acidA receptors in frogs. Neuroscience Letters, 293, 155–158.

Fisher, J. & Macdonald, R. (1997). Functional properties of recombinant GABA-A receptors composed of single or multiple beta subunit subtypes. Neuropharmacology, 36, 1601–1610.

Fritschy, J.-M. & Brünig, I. (2003). Formation and plasticity of GABAergic synapses: physiological mechanisms and pathophysiological implications. Pharmacology & Therapeutics, 98, 299–323.

Galietta, L. J. V., Haggie, P. M., & Verkman, A. S. (2001a). Green fluorescent protein-based halide indicators with improved chloride and iodide affinities. Federation of European Biochemical Societies Letters, 499, 220–224.

Galietta, L. V. J., Jayaraman, S., & Verkman, A. S. (2001b). Cell-based assay for high-throughput quantitative screening of CFTR chloride transport agonists. American Journal of Physiology - Cell Physiology, 281, C1734–1742.

Gao, B., Fritschy, J., Benke, D., & Möhler, H. (1993). Neuron-specific expression of GABA-A-receptor subtypes: Differential association of the [alpha]1- and [alpha]3-subunits with serotonergic and GABAergic neurons. Neuroscience, 54, 881–892.

Gao, B., Hornung, J. P., & Fritschy, J. M. (1995). Identification of distinct GABA-A-receptor subtypes in cholinergic and parvalbumin-positive neurons of the rat and marmoset medial septum-diagonal band complex. Neuroscience, 65, 101–117.

Garret, M., Bascles, L., Boue-Grabot, E., Sartor, P., Charron, G., Bloch, B., & Margolskee, R. (1997). An mRNA encoding a putative GABA-gated chloride channel is expressed in the human cardiac conduction system. Journal of Neurochemistry, 68, 1382–1389.

Gilbert, D., Esmaeili, A., & Lynch, J. W. (2009a). Optimizing the expression of recombinant $\alpha\beta\gamma$ GABA-A receptors in HEK293 cells for high-throughput screening. Journal of Biomolecular Screening, 14, 86–91.

Gilbert, D. F., Islam, R., Lynagh, T. P., Webb, T. I., & Lynch, J. (2009b). High throughput techniques for discovering new glycine receptor modulators and their binding sites. Frontiers in Molecular Neuroscience, 2, 1–10.

Gill, S., Gill, R., Lee, S., Hesketh, J., Fedida, D., Rezazadeh, S., Stankovich, L., & Liang, D. (2003). Flux assays in high throughput screening of ion channels in drug discovery. ASSAY and Drug Development Technologies, 1, 709–717.

Gillet, V. J. (2008). New directions in library design and analysis. Current Opinion in Chemical Biology, 12, 372–378.

Gingrich, K. J., Roberts, W. A., & Kass, R. S. (1995). Dependence of the GABA-A receptor gating kinetics on the alpha-subunit isoform: implications for structure-function relations and synaptic transmission. The Journal of Physiology, 489, 529–543.

Gonzalez, J. & Maher, M. (2002). Cellular fluorescent indicators and voltage/ion probe reader (VIPR) tools for ion channel and receptor drug discovery. Receptors and Channels, 8, 283–295.

Haas, K. & Macdonald, R. (1999). GABA-A receptor subunit gamma2 and delta subtypes confer unique kinetic properties on recombinant GABA-A receptor currents in mouse fibroblasts. The Journal of Physiology, 514, 27–45.

Hadingham, K. L., Wingrove, P., Bourdelles Le, B., Palmer, K. J., Ragan, C. I., & Whiting, P. J. (1993). Cloning of cDNA sequences encoding human alpha2 and alpha3 gamma-aminobutyric acidA receptor subunits and characterization of the benzodiazepine pharmacology of recombinant alpha1-, alpha2-, alpha3- , and alpha5-containing human gamma-aminobutyric acidA receptors. Molecular Pharmacology, 43, 970–975.

Hamill, O., Marty, A., Neher, E., Sakmann, B., & Sigworth, F. (1981). Improved patch-clamp techniques for high-resolution current recording from cells and cell-free membrane patches. Pfluegers Archiv: European Journal of Physiology, 391, 85–100.

Hann, M. M. & Oprea, T. I. (2004). Pursuing the leadlikeness concept in pharmaceutical research. Current Opinion in Chemical Biology, 8, 255–263.

Harris, B. D., Wong, G., Moody, E. J., & Skolnick, P. (1995). Different subunit requirements for volatile and nonvolatile anesthetics at gamma-aminobutyric acid type A receptors. Molecular Pharmacology, 47, 363–367.

Harris, R., Mihic, S., Brozowski, S., Hadingham, K., & Whiting, P. (1997). Ethanol, flunitrazepam, and pentobarbital modulation of GABA-A receptors expressed in mammalian cells and *Xenopus* oocytes. Alcoholism: Clinical and Experimental Research, 21, 444–451.

Harvey, R. J., Kim, H.-C., & Darlison, M. G. (1993). Molecular cloning reveals the existence of a fourth [gamma] subunit of the vertebrate brain GABA-A receptor. Federation of European Biochemical Societies Letters, 331, 211–216.

Haverkamp, S., Wassle, H., Duebel, J., Kuner, T., Augustine, G. J., Feng, G., & Euler, T. (2005). The primordial, blue-cone color system of the mouse retina. The Journal of Neuroscience, 25, 5438–5445.

Hedblom, E. & Kirkness, E. F. (1997). A novel class of GABA-A receptor subunit in tissues of the reproductive system. Journal of Biological Chemistry, 272, 15346–15350.

Hevers, W. & Lüddens, H. (1998). The diversity of GABA-A receptors. Pharmacological and electrophysiological properties of GABA-A channel subtypes. Molecular Neurobiology, 18, 35–86.

Hill-Venning, C., Belelli, D., Peters, J., & Lambert, J. (1997). Subunit-dependent interaction of the general anaesthetic etomidate with the gamma-aminobutyric acid type A receptor. British Journal of Pharmacology, 120, 749–756.

Hogg, R. C., Bandelier, F., Benoit, A., Dosch, R., & Bertrand, D. (2008). An automated system for intracellular and intranuclear injection. Journal of Neuroscience Methods, 169, 65–75.

Hosie, A. M., Clarke, L., da Silva, H., & Smart, T. G. (2009). Conserved site for neurosteroid modulation of GABA-A receptors. Neuropharmacology, 56, 149–154.

Hosie, A. M., Wilkins, M. E., & Smart, T. G. (2007). Neurosteroid binding sites on GABA-A receptors. Pharmacology & Therapeutics, 116, 7–19.

Inglese, J., Auld, D. S., Jadhav, A., Johnson, R. L., Simeonov, A., Yasgar, A., Zheng, W., & Austin, C. P. (2006). Quantitative high-throughput screening: A titration-based approach that efficiently identifies biological activities in large chemical libraries. Proceedings of the National Academy of Sciences, 103, 11473–11478.

Inglese, J., Johnson, R. L., Simeonov, A., Xia, M., Zheng, W., Austin, C. P., & Auld, D. S. (2007a). High-throughput screening assays for the identification of chemical probes. Nature Chemical Biology, 3, 466–479.

Inglese, J., Shamu, C. E., & Guy, R. K. (2007b). Reporting data from high-throughput screening of small-molecule libraries. Nature Chemical Biology, 3, 438–441.

Irnaten, M., Walwyn, W., Wang, J., Venkatesan, P., Evans, C., Chang, K., Andresen, M., Hales, T., & Mendelowitz, D. (2002). Pentobarbital enhances GABAergic neurotransmission to cardiac parasympathetic neurons, which is prevented by expression of GABA-A epsilon subunit. Anesthesiology, 97, 717–724.

Janzen, W. P. & Popa-Burke, I. G. (2009). Advances in improving the quality and flexibility of compound management. Journal of Biomolecular Screening, 14, 444–451.

Jayaraman, S., Haggie, P., Wachter, R. M., Remington, S. J., & Verkman, A. S. (2000). Mechanism and cellular applications of a green fluorescent protein-based halide sensor. The Journal of Biological Chemistry, 275, 6047–6050.

Jechlinger, M., Pelz, R., Tretter, V., Klausberger, T., & Sieghart, W. (1998). Subunit composition and quantitative importance of hetero-oligomeric receptors: GABA-A receptors containing alpha6 subunits. The Journal of Neuroscience, 18, 2449–2457.

Johnstone, T. B. C., Hogenkamp, D. J., Coyne, L., Su, J., Halliwell, R. F., Tran, M. B., Yoshimura, R. F., Li, W.-Y., Wang, J., & Gee, K. W. (2004). Modifying quinolone antibiotics yields new anxiolytics. Nature Medicine, 10, 31–32.

Jones, B. L. & Henderson, L. P. (2007). Trafficking and potential assembly patterns of epsilon-containing GABA-A receptors. Journal of Neurochemistry, 103, 1258–1271.

Jones, B. L., Whiting, P. J., & Henderson, L. P. (2006). Mechanisms of anabolic androgenic steroid inhibition of mammalian epsilon-subunit-containing GABA-A receptors. The Journal of Physiology, 573, 571–593.

Jurd, R., Arras, M., Lambert, S., Drexler, B., Siegwart, R., Crestani, F., Zaugg, M., Vogt, K. E., Ledermann, B., Antkowiak, B., & Rudolph, U. (2003). General anesthetic actions *in vivo* strongly attenuated by a point mutation in the GABA-A receptor beta3 subunit. The Journal of the Federation of American Societies for Experimental Biology, 17, 250–252.

Kar, S., Slowikowski, S., Westaway, D., & Mount, H. (2004). Interactions between beta-amyloid and central cholinergic neurons: implications for Alzheimer's disease. Journal of Psychiatry and Neuroscience, 29, 427–441.

Kash, T. L., Trudell, J. R., & Harrison, N. L. (2004). Structural elements involved in activation of the gamma-aminobutyric acid type A (GABA-A) receptor. Biochemical Society Transactions, 32, 540–546.

Kasparov, S., Davies, K., Patel, U., Boscan, P., Garret, M., & Paton, J. (2001). GABA-A receptor epsilon-subunit may confer benzodiazepine insensitivity to the caudal aspect of the nucleus tractus solitarii of the rat. The Journal of Physiology, 536, 785–96.

Kaufman, D. L., Houser, C. R., & Tobin, A. J. (1991). Two forms of the gamma-aminobutyric acid synthetic enzyme glutamate decarboxylase have distinct intraneuronal distributions and cofactor interactions. Journal of Neurochemistry, 56, 720–723.

Kim, H.-J., Yun, H.-M., Kim, T., Nam, G., Roh, E. J., Kostenis, E., Choo, H.-Y. P., Pae, A. N., & Rhim, H. (2008). Functional human 5-HT6 receptor assay for high throughput screening of chemical ligands and binding proteins. Combinatorial Chemistry & High Throughput Screening, 11, 316–324.

Knoflach, F., Rhyner, T., Villa, M., Kellenberger, S., Drescher, U., Malherbe, P., Sigel, E., & Möhler, H. (1991). The [gamma]3-subunit of the GABA-A-receptor confers sensitivity to benzodiazepine receptor ligands. Federation of European Biochemical Societies Letters, 293, 191–194.

Korpi, E. R., Gründer, G., & Lüddens, H. (2002). Drug interactions at GABA-A receptors. Progress in Neurobiology, 67, 113–159.

Korpi, E. R., Kuner, T., Kristo, P., Kohler, M., Herb, A., Lüddens, H., & Seeburg, P. H. (1994). Small N-terminal deletion by splicing in cerebellar alpha6 subunit abolishes GABA-A receptor function. Journal of Neurochemistry, 63, 1167–1170.

Krishek, B. J., Moss, S. J., & Smart, T. G. (1998). Interaction of H^+ and Zn^{2+} on recombinant and native rat neuronal GABA-A receptors. The Journal of Physiology, 507, 639–652.

Kruger, W., Gilbert, D., Hawthorne, R., Hryciw, D. H., Frings, S., Poronnik, P., & Lynch, J. W. (2005). A yellow fluorescent protein-based assay for high-throughput screening of glycine and GABA-A receptor chloride channels. Neuroscience Letters, 380, 340–345.

Kuner, T. & Augustine, G. J. (2000). A genetically encoded ratiometric indicator for chloride: Capturing chloride transients in cultured hippocampal neurons. Neuron, 27, 447–459.

Labarca, C., Nowak, M. W., Zhang, H., Tang, L., Deshpande, P., & Lester, H. A. (1995). Channel gating governed symmetrically by conserved leucine residues in the M2 domain of nicotinic receptors. Nature, 376, 514–516.

Lamigeon, C., Bellier, J. P., Sacchettoni, S., Rujano, M., & Jacquemont, B. (2001). Enhanced neuronal protection from oxidative stress by co-culture with glutamic acid decarboxylase-expressing astrocytes. Journal of Neurochemistry, 77, 598–606.

Lavoie, A., Tingey, J., Harrison, N., Pritchett, D., & Twyman, R. (1997). Activation and deactivation rates of recombinant GABA-A receptor channels are dependent on alpha-subunit isoform. Biophysical Journal, 73, 2518–2526.

Lipinski, C. A., Lombardo, F., Dominy, B. W., & Feeney, P. J. (2001). Experimental and computational approaches to estimate solubility and permeability in drug discovery and development settings. Advanced Drug Delivery Reviews, 46, 3–26.

Löw, K., Crestani, F., Keist, R., Benke, D., Brunig, I., Benson, J. A., Fritschy, J.-M., Rulicke, T., Bluethmann, H., Möhler, H., & Rudolph, U. (2000). Molecular and neuronal substrate for the selective attenuation of anxiety. Science, 290, 131–134.

Lüscher, B. & Keller, C. A. (2004). Regulation of GABA-A receptor trafficking, channel activity, and functional plasticity of inhibitory synapses. Pharmacology & Therapeutics, 102, 195–221.

Lynch, J. (2005). High-throughput screening of neuronal Cl^- channels: Why and how? Current Neuropharmacology, 3, 207–216.

Lynch, J. W. (2009). Native glycine receptor subtypes and their physiological roles. Neuropharmacology, 56, 303–309.

Macdonald, R. L., Kang, J.-Q., & Gallagher, M. J. (2010). Mutations in GABA-A receptor subunits associated with genetic epilepsies. The Journal of Physiology, 588, 1861–1869.

Maksay, G., Thompson, S. A., & Wafford, K. A. (2003). The pharmacology of spontaneously open alpha1 beta3 epsilon GABA-A receptor-ionophores. Neuropharmacology, 44, 994–1002.

Maniatis, T., Fritsch, E., & Sambrook, J. (1982). Molecular Cloning: a laboratory manual. (New York: Cold Spring Harbor Laboratory Press.).

Marandi, N., Konnerth, A., & Garaschuk, O. (2002). Two-photon chloride imaging in neurons of brain slices. Pflügers Archiv European Journal of Physiology, 445, 357–365.

Markova, O., Mukhtarov, M., Real, E., Jacob, Y., & Bregestovski, P. (2008). Genetically encoded chloride indicator with improved sensitivity. Journal of Neuroscience Methods, 170, 67–76.

Martin, D. L. & Rimvall, K. (1993). Regulation of gamma-aminobutyric acid synthesis in the brain. Journal of Neurochemistry, 60, 395–407.

McGehee, D. S. & Role, L. W. (1996). Presynaptic ionotropic receptors. Current Opinion in Neurobiology, 6, 342–349.

McKernan, R. M. & Whiting, P. J. (1996). Which GABA-A-receptor subtypes really occur in the brain? Trends in Neurosciences, 19, 139–143.

Miko, A., Werby, E., Sun, H., Healey, J., & Zhang, L. (2004). A TM2 residue in the beta1 subunit determines spontaneous opening of homomeric and heteromeric gamma-aminobutyric acid-gated ion channels. Journal of Biological Chemistry, 279, 22833–22840.

Minier, F. & Sigel, E. (2004). Techniques: Use of concatenated subunits for the study of ligand-gated ion channels. Trends in Pharmacological Sciences, 25, 499–503.

Mitchell, E. A., Herd, M. B., Gunn, B. G., Lambert, J. J., & Belelli, D. (2008). Neurosteroid modulation of GABA-A receptors: Molecular determinants and significance in health and disease. Neurochemistry International, 52, 588–595.

Möhler, H. (2006). GABA-A receptor diversity and pharmacology. Cell and Tissue Research, 326, 505–516.

Möhler, H. (2007). Molecular regulation of cognitive functions and developmental plasticity: impact of GABA-A receptors. Journal of Neurochemistry, 102, 1–12.

Möhler, H., Fritschy, J. M., & Rudolph, U. (2002). A new benzodiazepine pharmacology. The Journal of Pharmacology and Experimental Therapeutics, 300, 2–8.

Molokanova, E. & Savchenko, A. (2008). Bright future of optical assays for ion channel drug discovery. Drug Discovery Today, 13, 14–22.

Moragues, N., Ciofi, P., Lafon, P., Odessa, M. F., Tramu, G., & Garret, M. (2000). cDNA cloning and expression of a gamma-aminobutyric acid A receptor epsilon-subunit in rat brain. European Journal of Neuroscience, 12, 4318–4330.

Moragues, N., Ciofi, P., Tramu, G., & Garret, M. (2002). Localisation of GABA-A receptor [epsilon]-subunit in cholinergic and aminergic neurones and evidence for co-distribution with the [theta]-subunit in rat brain. Neuroscience, 111, 657–669.

Mortensen, M., Wafford, K. A., Wingrove, P., & Ebert, B. (2003). Pharmacology of GABA-A receptors exhibiting different levels of spontaneous activity. European Journal of Pharmacology, 476, 17–24.

Moult, P. R. (2009). Neuronal glutamate and GABA-A receptor function in health and disease. Biochemical Society Transactions, 37, 1317–1322.

Navarro, J. F., Burón, E., & Martín-López, M. (2002). Anxiogenic-like activity of L-655,708, a selective ligand for the benzodiazepine site of GABA-A receptors which contain the alpha-5 subunit, in the elevated plus-maze test. Progress in Neuro-Psychopharmacology and Biological Psychiatry, 26, 1389–1392.

Neelands, T. R., Fisher, J. L., Bianchi, M., & Macdonald, R. L. (1999). Spontaneous and gamma-aminobutyric acid (GABA)-activated GABA-A receptor channels formed by epsilon subunit-containing isoforms. Molecular Pharmacology, 55, 168–178.

Olsen, R. W., Chang, C.-S. S., Li, G., Hanchar, H. J., & Wallner, M. (2004). Fishing for allosteric sites on GABA-A receptors. Biochemical Pharmacology, 68, 1675–1684.

Olsen, R. W. & Sieghart, W. (2008). International union of pharmacology. LXX. subtypes of gamma-aminobutyric acidA receptors: Classification on the basis of subunit composition, pharmacology, and function. update. Pharmacological Reviews, 60, 243–260.

Olsen, R. W. & Sieghart, W. (2009). GABA-A receptors: Subtypes provide diversity of function and pharmacology. Neuropharmacology, 56, 141–148.

Pape, J. R., Bertrand, S. S., Lafon, P., Odessa, M. F., Chaigniau, M., Stiles, J. K., & Garret, M. (2009). Expression of GABA-A receptor [alpha]3-, [theta]-, and [epsilon]-subunit mRNAs during rat CNS development and immunolocalization of the [epsilon] subunit in developing postnatal spinal cord. Neuroscience, 160, 85–96.

Pirker, S., Schwarzer, C., Wieselthaler, A., Sieghart, W., & Sperk, G. (2000). GABA-A receptors: immunocytochemical distribution of 13 subunits in the adult rat brain. Neuroscience, 101, 815–850.

Pistis, M., Belelli, D., Peters, J. A., & Lambert, J. J. (1997). The interaction of general anaesthetics with recombinant GABA-A and glycine receptors expressed in *Xenopus laevis* oocytes: a comparative study. British Journal of Pharmacology, 122, 1707–1719.

Piston, D. W. & Kremers, G.-J. (2007). Fluorescent protein FRET: the good, the bad and the ugly. Trends in Biochemical Sciences, 32, 407–414.

Pless, S. & Lynch, J. (2008). Illuminating the structure and function of Cys-loop receptors. Clinical and Experimental Pharmacology and Physiology, 35, 1137–1142.

Pritchett, D. B., Lüddens, H., & Seeburg, P. H. (1989a). Type I and type II GABA-A-benzodiazepine receptors produced in transfected cells. Science, 245, 1389–1392.

Pritchett, D. B. & Seeburg, P. H. (1990). Gamma-aminobutyric acidA receptor alpha 5-subunit creates novel type II benzodiazepine receptor pharmacology. Journal of Neurochemistry, 54, 1802–1804.

Pritchett, D. B., Sontheimer, H., Shivers, B. D., Ymer, S., Kettenmann, H., Schofield, P. R., & Seeburg, P. H. (1989b). Importance of a novel GABA-A receptor subunit for benzodiazepine pharmacology. Nature, 338, 582–585.

Ranna, M., Sinkkonen, S., Moykkynen, T., Uusi-Oukari, M., & Korpi, E. (2006). Impact of epsilon and theta subunits on pharmacological properties of alpha3beta1 GABA-A receptors expressed in *Xenopus* oocytes. BioMed Central Pharmacology, 6, 1.

Reynolds, D. S., Rosahl, T. W., Cirone, J., O'Meara, G. F., Haythornthwaite, A., Newman, R. J., Myers, J., Sur, C., Howell, O., Rutter, A. R., Atack, J., Macaulay, A. J., Hadingham, K. L., Hutson, P. H., Belelli, D., Lambert, J. J., Dawson, G. R., McKernan, R., Whiting, P. J., & Wafford, K. A. (2003). Sedation and anesthesia mediated by distinct GABA-A receptor isoforms. The Journal of Neuroscience, 23, 8608–8617.

Rohrbough, J. & Spitzer, N. (1996). Regulation of intracellular Cl^- levels by Na^+-dependent Cl^- cotransport distinguishes depolarizing from hyperpolarizing GABA-A receptor-mediated responses in spinal neurons. The Journal of Neuroscience, 16, 82–91.

Rudolph, U., Crestani, F., Benke, D., Brunig, I., Benson, J. A., Fritschy, J.-M., Martin, J. R., Bluethmann, H., & Möhler, H. (1999). Benzodiazepine actions mediated by specific [gamma]-aminobutyric acidA receptor subtypes. Nature, 401, 796–800.

Rudolph, U., Crestani, F., & Möhler, H. (2001). GABA-A receptor subtypes: dissecting their pharmacological functions. Trends in Pharmacological Sciences, 22, 188–194.

Rudolph, U. & Möhler, H. (2004). Analysis of GABA-A receptor function and dissection of the pharmacology of benzodiazepines and general anesthetics through mouse genetics. Annual Review of Pharmacology and Toxicology, 44, 475–498.

Rudolph, U. & Möhler, H. (2006). GABA-based therapeutic approaches: GABA-A receptor subtype functions. Current Opinion in Pharmacology, 6, 18–23.

Sandell, E. B. & Kolthoff, I. M. (1937). Micro determination of iodine by a catalytic method. Microchimica Acta, 1, 9–25.

Sanna, E., Mascia, M. P., Klein, R. L., Whiting, P. J., Biggio, G., & Harris, R. A. (1995). Actions of the general anesthetic propofol on recombinant human GABA-A receptors: influence of receptor subunits. The Journal of Pharmacology and Experimental Therapeutics, 274, 353–360.

Sanna, E., Murgia, A., Casula, A., & Biggio, G. (1997). Differential subunit dependence of the actions of the general anesthetics alphaxalone and etomidate at gamma-aminobutyric acid type A receptors expressed in *Xenopus laevis* oocytes. Molecular Pharmacology, 51, 484–490.

Saxena, N. C. & Macdonald, R. L. (1994). Assembly of GABA-A receptor subunits: role of the delta subunit. The Journal of Neuroscience, 14, 7077–7086.

Scheller, M. & Forman, S. A. (2002). Coupled and uncoupled gating and desensitization effects by pore domain mutations in GABA-A receptors. The Journal of Neuroscience, 22, 8411–8421.

Schofield, P. R., Darlison, M. G., Fujita, N., Burt, D. R., Stephenson, F. A., Rodriguez, H., Rhee, L. M., Ramachandran, J., Reale, V., Glencorse, T. A., Seeburg, P., & Barnard, E. A. (1987). Sequence and functional expression of the GABA-A receptor shows a ligand-gated receptor super-family. Nature, 328, 221–227.

Seltzer, B. (2010). Galantamine-ER for the treatment of mild-to-moderate Alzheimer's disease. Clinical Interventions in Aging, 5, 1–6.

Sergeeva, O. A., Andreeva, N., Garret, M., Scherer, A., & Haas, H. L. (2005). Pharmacological properties of GABA-A receptors in rat hypothalamic neurons expressing the epsilon-subunit. The Journal of Neuroscience, 25, 88–95.

Sieghart, W. (2000). Unraveling the function of GABA-A receptor subtypes. Trends in Pharmacological Sciences, 21, 411–413.

Sieghart, W. & Sperk, G. (2002). Subunit composition, distribution and function of GABA-A receptor subtypes. Current Topics in Medicinal Chemistry, 2, 795–816.

Sigel, E. (1990). Use of *Xenopus* oocytes for the functional expression of plasma membrane proteins. The Journal of Membrane Biology, 117, 201–221.

Sigel, E. & Baur, R. (2000). Electrophysiological evidence for the coexistence of alpha1 and alpha6 subunits in a single functional GABA-A receptor. Journal of Neurochemistry, 74, 2590–2596.

Sigel, E. & Buhr, A. (1997). The benzodiazepine binding site of GABA-A receptors. Trends in Pharmacological Sciences, 18, 425–429.

Sigel, E. & Minier, F. (2005). The *Xenopus* oocyte: System for the study of functional expression and modulation of proteins. Molecular Nutrition and Food Research, 49, 228–234.

Simon, J., Wakimoto, H., Fujita, N., Lalande, M., & Barnard, E. A. (2004). Analysis of the set of GABA-A receptor genes in the human genome. Journal of Biological Chemistry, 279, 41422–41435.

Sinkkonen, S. T., Hanna, M. C., Kirkness, E. F., & Korpi, E. R. (2000). GABA-A receptor epsilon and theta subunits display unusual structural variation between species and are enriched in the rat locus ceruleus. The Journal of Neuroscience, 20, 3588–3595.

Smith, A. & Simpson, P. (2003). Methodological approaches for the study of GABA-A receptor pharmacology and functional responses. Analytical and Bioanalytical Chemistry, 377, 843–851.

Smith, A. J., Alder, L., Silk, J., Adkins, C., Fletcher, A. E., Scales, T., Kerby, J., Marshall, G., Wafford, K. A., McKernan, R. M., & Atack, J. R. (2001). Effect of alpha subunit on allosteric modulation of ion channel function in stably expressed human recombinant gamma-aminobutyric acidA receptors determined using ^{36}Cl ion flux. Molecular Pharmacology, 59, 1108–1118.

Smith, G. B. & Olsen, R. W. (1995). Functional domains of GABA-A receptors. Trends in Pharmacological Sciences, 16, 162–168.

Snodgrass, S. (1978). Use of ^{3}H-muscimol for GABA receptor studies. Nature, 273, 392–394.

Stephenson, F. A., Duggan, M. J., & Pollard, S. (1990). The gamma 2 subunit is an integral component of the gamma-aminobutyric acidA receptor but the alpha 1 polypeptide is the principal site of the agonist benzodiazepine photoaffinity labeling reaction. The Journal of Biological Chemistry, 265, 21160–21165.

Sternfeld, F., Carling, R. W., Jelley, R. A., Ladduwahetty, T., Merchant, K. J., Moore, K. W., Reeve, A. J., Street, L. J., O'Connor, D., Sohal, B., Atack, J. R., Cook, S., Seabrook, G., Wafford, K., Tattersall, F. D., Collinson, N., Dawson, G. R., Castro, J. L., & MacLeod, A. M. (2004). Selective, orally active gamma-aminobutyric acidA alpha5 receptor inverse agonists as cognition enhancers. Journal of Medicinal Chemistry, 47, 2176–2179.

Sui, Y. & Wu, Z. (2007). Alternative statistical parameter for high-throughput screening assay quality assessment. Journal of Biomolecular Screening, 12, 229–234.

Tang, W. & Wildey, M. J. (2004). Development of a colorimetric method for functional chloride channel assay. Journal of Biomolecular Screening, 9, 607–613.

Tang, W. & Wildey, M. J. (2006). Methods for measuring chloride channel conductivity. World Intellectual Property Organization: International Publication Number WO 2006/009986 A1, p. 26 January.

Terstappen, G. C. (2005). Ion channel screening technologies today. Drug Discovery Today: Technologies, 2, 133–140.

Thomas, P. & Smart, T. G. (2005). HEK293 cell line: A vehicle for the expression of recombinant proteins. Journal of Pharmacological and Toxicological Methods, 51, 187–200.

Thompson, S., Bonnert, T., Whiting, P., & Wafford, K. (1998). Functional characteristics of recombinant human GABA-A receptors containing the epsilon-subunit. Toxicology Letters, 100-101, 233–238.

Thompson, S., Whiting, P., & Wafford, K. (1996). Barbiturate interactions at the human GABA-A receptor: dependence on receptor subunit combination. British Journal of Pharmacology, 117, 521–527.

Thompson, S. A., Bonnert, T. P., Cagetti, E., Whiting, P. J., & Wafford, K. A. (2002). Overexpression of the GABA-A receptor epsilon subunit results in insensitivity to anaesthetics. Neuropharmacology, 43, 662–668.

Tsien, R. Y. (1998). The green fluorescence protein. Annual Review of Biochemistry, 67, 509–544.

Ueno, S., Zorumski, C., Bracamontes, J., & Steinbach, J. H. (1996). Endogenous subunits can cause ambiguities in the pharmacology of exogenous gamma-aminobutyric acidA receptors expressed in human embryonic kidney 293 cells. Molecular Pharmacology, 50, 931–938.

Uusi-Oukari, M., Heikkilä, J., Sinkkonen, S., Mäkelä, R., Hauer, B., Homanics, G., Sieghart, W., Wisden, W., & Korpi, E. (2000). Long-range interactions in neuronal gene expression: Evidence from gene targeting in the GABA-A receptor [beta]2-[alpha]6-[alpha]1-[gamma]2 subunit gene cluster. Molecular and Cellular Neuroscience, 16, 34–41.

van Niel, M. B., Wilson, K., Adkins, C. H., Atack, J. R., Castro, J. L., Clarke, D. E., Fletcher, S., Gerhard, U., Mackey, M. M., Malpas, S., Maubach, K., Newman, R., O'Connor, D., Pillai, G. V., Simpson, P. B., Thomas, S. R., & MacLeod, A. M. (2005). A new pyridazine series of GABA-A alpha5 ligands. Journal of Medicinal Chemistry, 48, 6004–6011.

Verdoorn, T. A. (1994). Formation of heteromeric gamma-aminobutyric acid type A receptors containing two different alpha subunits. Molecular Pharmacology, 45, 475–480.

Verkman, A. S. & Galietta, L. J. V. (2009). Chloride channels as drug targets. Nature Reviews Drug Discovery, 8, 153–171.

Waagepetersen, H. S., Sonnewald, U., & Schousboe, A. (1999). The GABA paradox: multiple roles as metabolite, neurotransmitter, and neurodifferentiative agent. Journal of Neurochemistry, 73, 1335–1342.

Wachter, R. M., Elsliger, M.-A., Kallio, K., Hanson, G. T., & Remington, S. J. (1998). Structural basis of spectral shifts in the yellow-emission variants of green fluorescent protein. Structure, 6, 1267–1277.

Wachter, R. M. & Remington, S. J. (1999). Sensitivity of the yellow variant of green fluorescent protein to halides and nitrate. Current Biology, 9, R628–R629.

Wafford, K. A., Bain, C. J., Whiting, P. J., & Kemp, J. A. (1993). Functional comparison of the role of gamma subunits in recombinant human gamma-aminobutyric acidA/benzodiazepine receptors. Molecular Pharmacology, 44, 437–442.

Wafford, K. A., van Niel, M. B., Ma, Q. P., Horridge, E., Herd, M. B., Peden, D. R., Belelli, D., & Lambert, J. J. (2009). Novel compounds selectively enhance [delta] subunit containing GABA-A receptors and increase tonic currents in thalamus. Neuropharmacology, 56, 182–189.

Wagner, C., Friedrich, B., Setiawan, I., Lang, F., & S., B. (2000). The use of *Xenopus laevis* oocytes for the functional characterization of heterologously expressed membrane proteins. Cellular Physiology and Biochemistry, 10, 1–12.

Wagner, D. A., Goldschen-Ohm, M. P., Hales, T. G., & Jones, M. V. (2005). Kinetics and spontaneous open probability conferred by the epsilon subunit of the GABA-A receptor. The Journal of Neuroscience, 25, 10462–10468.

Watkins, P. B., Zimmerman, H. J., Knapp, M. J., Gracon, S. I., & Lewis, K. W. (1994). Hepatotoxic effects of tacrine administration in patients with Alzheimer's disease. JAMA: The Journal of the American Medical Association, 271, 992–998.

Whiting, P., Bonnert, T., McKernan, R., Farrar, S., Bourdelles, B. l., Heavens, R., Smith, D., Hewson, L., Rigby, M., Sirinathsinghji, J., Thompson, S., & Wafford, K. (1999). Molecular and functional diversity of the expanding GABA-A receptor gene family. Annals of the New York Academy of Sciences, 868, 645–653.

Whiting, P., McKernan, R. M., & Iversen, L. L. (1990). Another mechanism for creating diversity in gamma-aminobutyrate type A receptors: RNA splicing directs expression of two forms of gamma 2 phosphorylation site. Proceedings of the National Academy of Sciences of the United States of America, 87, 9966–9970.

Whiting, P. J. (1999). The GABA-A receptor gene family: new targets for therapeutic intervention. Neurochemistry International, 34, 387–390.

Whiting, P. J. (2006). GABA-A receptors: a viable target for novel anxiolytics? Current Opinion in Pharmacology, 6, 24–29.

Whiting, P. J., McAllister, G., Vassilatis, D., Bonnert, T. P., Heavens, R. P., Smith, D. W., Hewson, L., O'Donnell, R., Rigby, M. R., Sirinathsinghji, D. J. S., Marshall, G., Thompson, S. A., & Wafford, K. A. (1997). Neuronally restricted RNA splicing regulates the expression of a novel GABA-A receptor subunit conferring atypical functional properties. The Journal of Neuroscience, 17, 5027–5037.

Wilke, K., Gaul, R., Klauck, S. M., & Poustka, A. (1997). A gene in human chromosome band Xq28 (GABRE) defines a putative new subunit class of the GABA-A neurotransmitter receptor. Genomics, 45, 1–10.

Willumsen, N. J., Bech, M., Olesen, S.-P., Jensen, B. S., Korsgaard, M. P. G., & Christophersen, P. (2003). High throughput electrophysiology: New perspectives for ion channel drug discovery. Receptors and Channels, 9, 3–12.

Wisden, W., Herb, A., Wieland, H., Keinanen, K., Luddens, H., & Seeburg, P. H. (1991). Cloning, pharmacological characteristics and expression pattern of the rat GABA-A receptor [alpha]4 subunit. Federation of European Biochemical Societies Letters, 289, 227–230.

Witchel, H. J., Milnes, J. T., Mitcheson, J. S., & Hancox, J. C. (2002). Troubleshooting problems with in vitro screening of drugs for QT interval prolongation using HERG K^+ channels expressed in mammalian cell lines and *Xenopus* oocytes. Journal of Pharmacological and Toxicological Methods, 48, 65–80.

Wohlfarth, K. M., Bianchi, M. T., & Macdonald, R. L. (2002). Enhanced neurosteroid potentiation of ternary GABA-A receptors containing the delta subunit. The Journal of Neuroscience, 22, 1541–1549.

Wong, G., Sei, Y., & Skolnick, P. (1992). Stable expression of type I gamma-aminobutyric acidA/benzodiazepine receptors in a transfected cell line. Molecular Pharmacology, 42, 996–1003.

Wood, C., Williams, C., & Waldron, G. J. (2004). Patch clamping by numbers. Drug Discovery Today, 9, 434–441.

Xu, J., Wang, X., Ensign, B., Li, M., Wu, L., Guia, A., & Xu, J. (2001). Ion-channel assay technologies: quo vadis? Drug Discovery Today, 6, 1278–1287.

Yuede, C. M., Donga, H., & Csernansky, J. G. (2007). Anti-dementia drugs and hippocampal-dependent memory in rodents. Behavioural Pharmacology, 18, 347–363.

Zhang, J., Sato, M., & Tohyama, M. (1991). Region-specific expression of the mRNAs encoding beta subunits (beta 1, beta 2, and beta 3) of GABA-A receptor in the rat brain. The Journal of Comparative Neurology, 303, 637–57.

Zhang, J.-H., Chung, T. D. Y., & Oldenburg, K. R. (1999). A simple statistical parameter for use in evaluation and validation of high throughput screening assays. Journal of Biomolecular Screening, 4, 67–73.

Zheng, W., Spencer, R. H., & Kiss, L. (2004). High throughput assay technologies for ion channel drug discovery. ASSAY and Drug Development Technologies, 2, 543–552.

Appendices

Appendix A

Vector maps

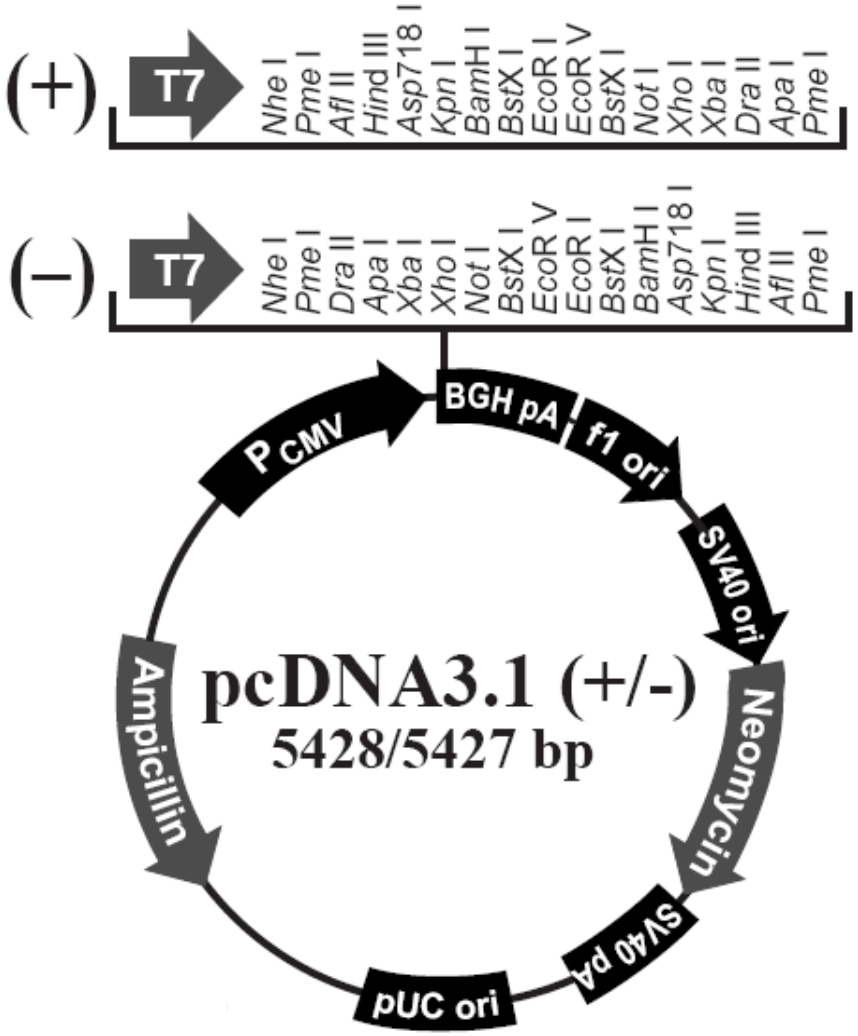

Figure A.1: Vector map pcDNA3.1 (Invitrogen)

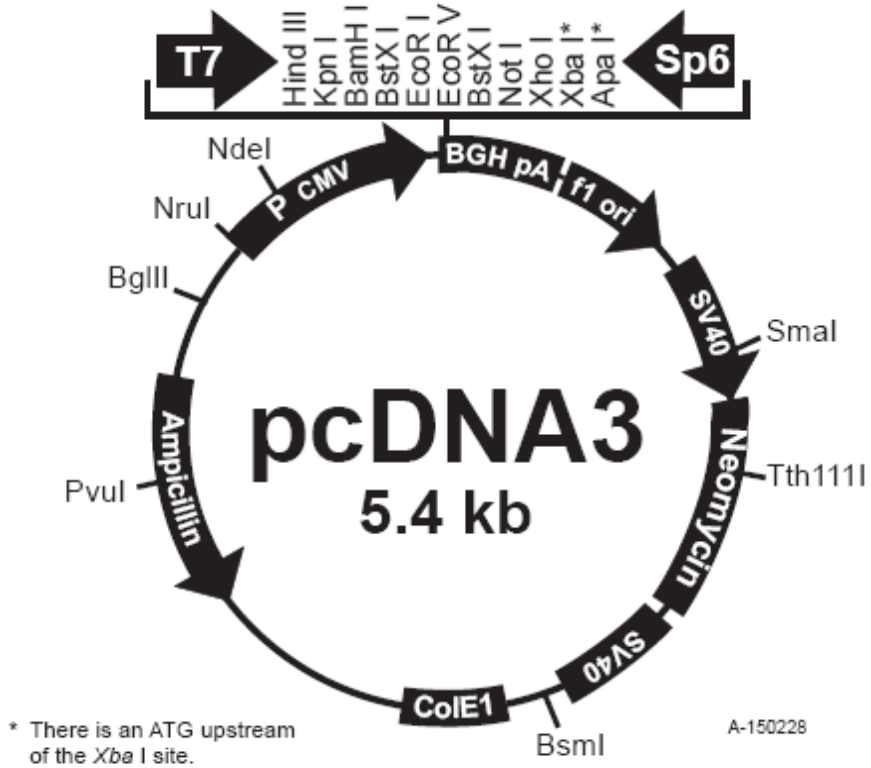

Figure A.2: Vector map pcDNA3 (Invitrogen)

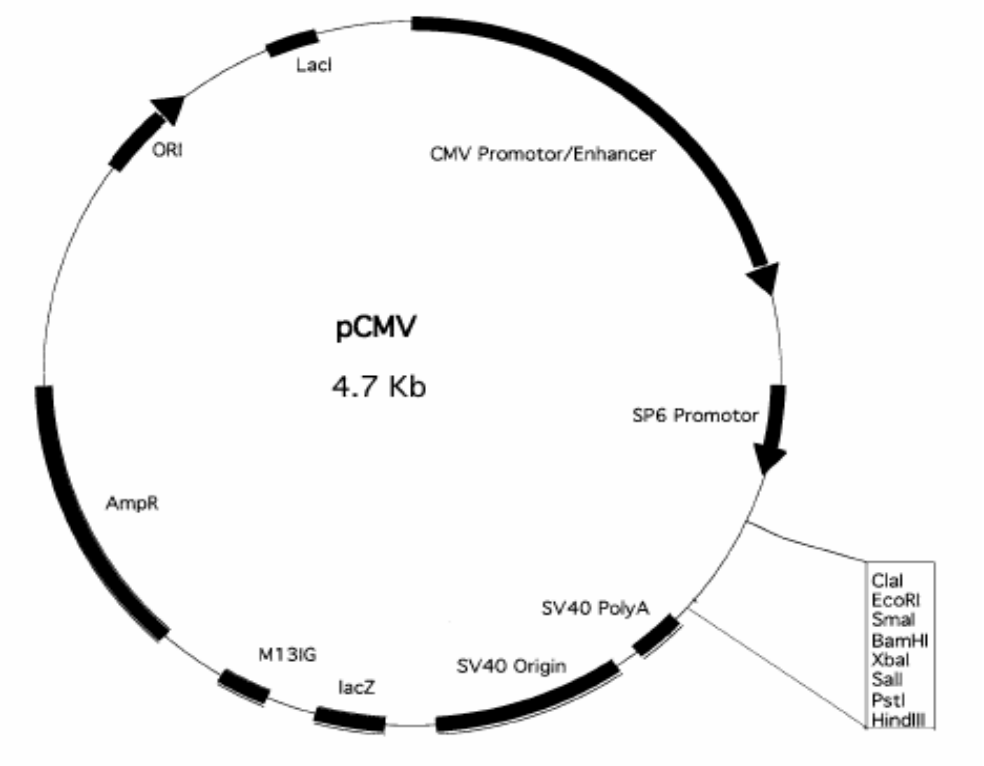

Figure A.3: Vector map pCMV (from Professor Erwin Sigel)

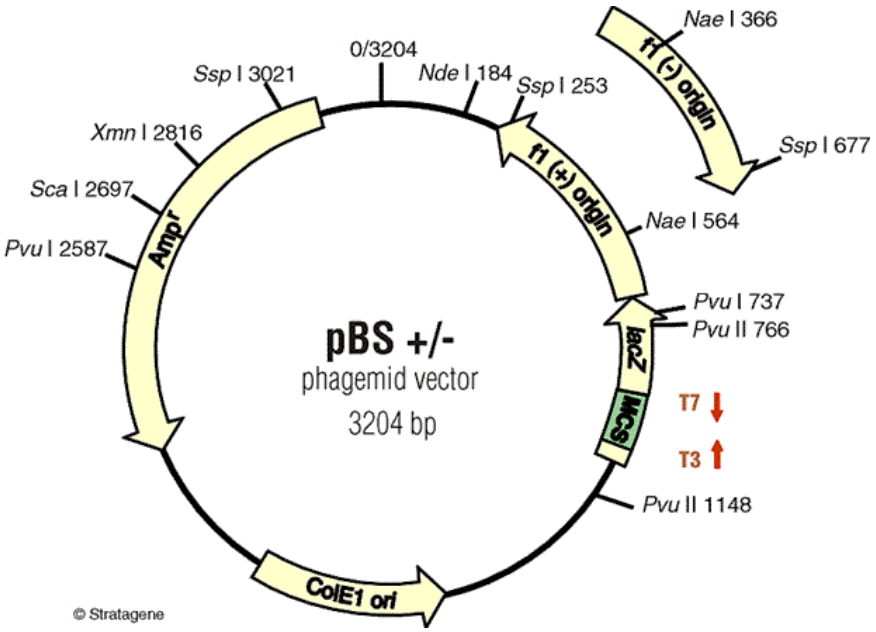

Figure A.4: Vector map pBS (Stratagene)

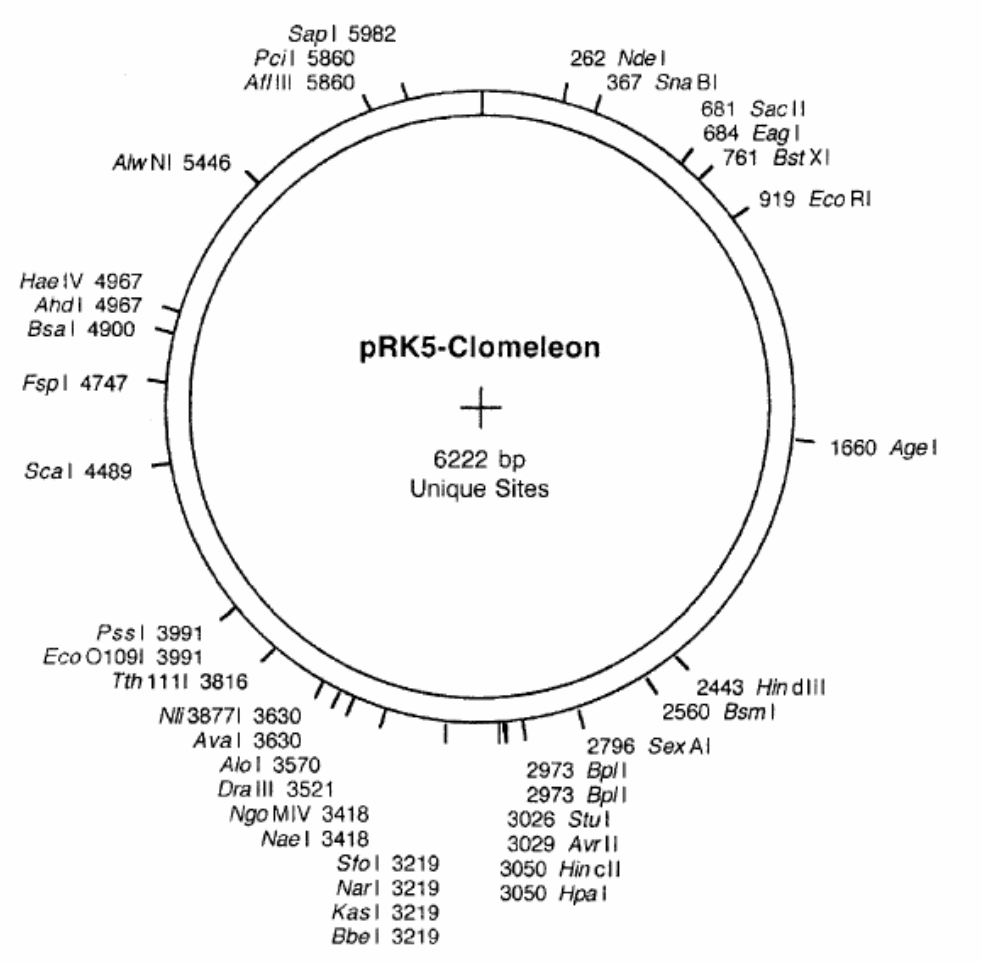

Figure A.5: Vector map pRK5-Clomeleon (from Dr Thomas Kuner)

Appendix B

Additional Graphs

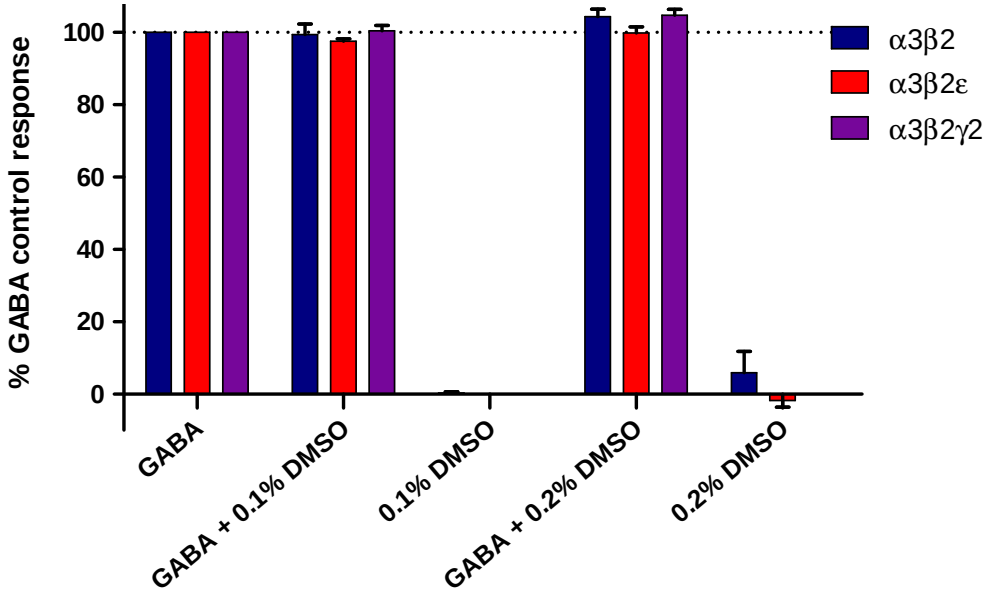

Figure B.1: Effect of DMSO on oocytes expressing $\alpha 3\beta 2$, $\alpha 3\beta 2\varepsilon$ and $\alpha 3\beta 2\gamma 2$ $GABA_A$ receptor subtypes.

Columns represent mean responses of different concentrations of DMSO alone or with GABA (EC_{20} concentrations) on the receptor subtypes. $\alpha 3\beta 2$: n = 4 for GABA-control response, n = 3 for GABA + 0.1 % DMSO, n = 3 for 0.1 % DMSO, n = 3 for GABA + 0.2 % DMSO, n = 3 for 0.2 % DMSO. $\alpha 3\beta 2\varepsilon$: n = 4 for GABA-control response, n = 3 for GABA + 0.1 % DMSO, n = 2 for 0.1 % DMSO, n = 3 for GABA + 0.2 % DMSO, n = 3 for 0.2 % DMSO. $\alpha 3\beta 2\gamma 2$: n = 9 for GABA-control response, n = 5 for GABA + 0.1 % DMSO, n = 3 for 0.1 % DMSO, n = 4 for GABA + 0.2 % DMSO, n = 5 for 0.2 % DMSO. Data are means $\pm$ SEM; n represents the number of oocytes examined. Currents were normalised to the maximal response induced by GABA at EC_{20} concentrations.

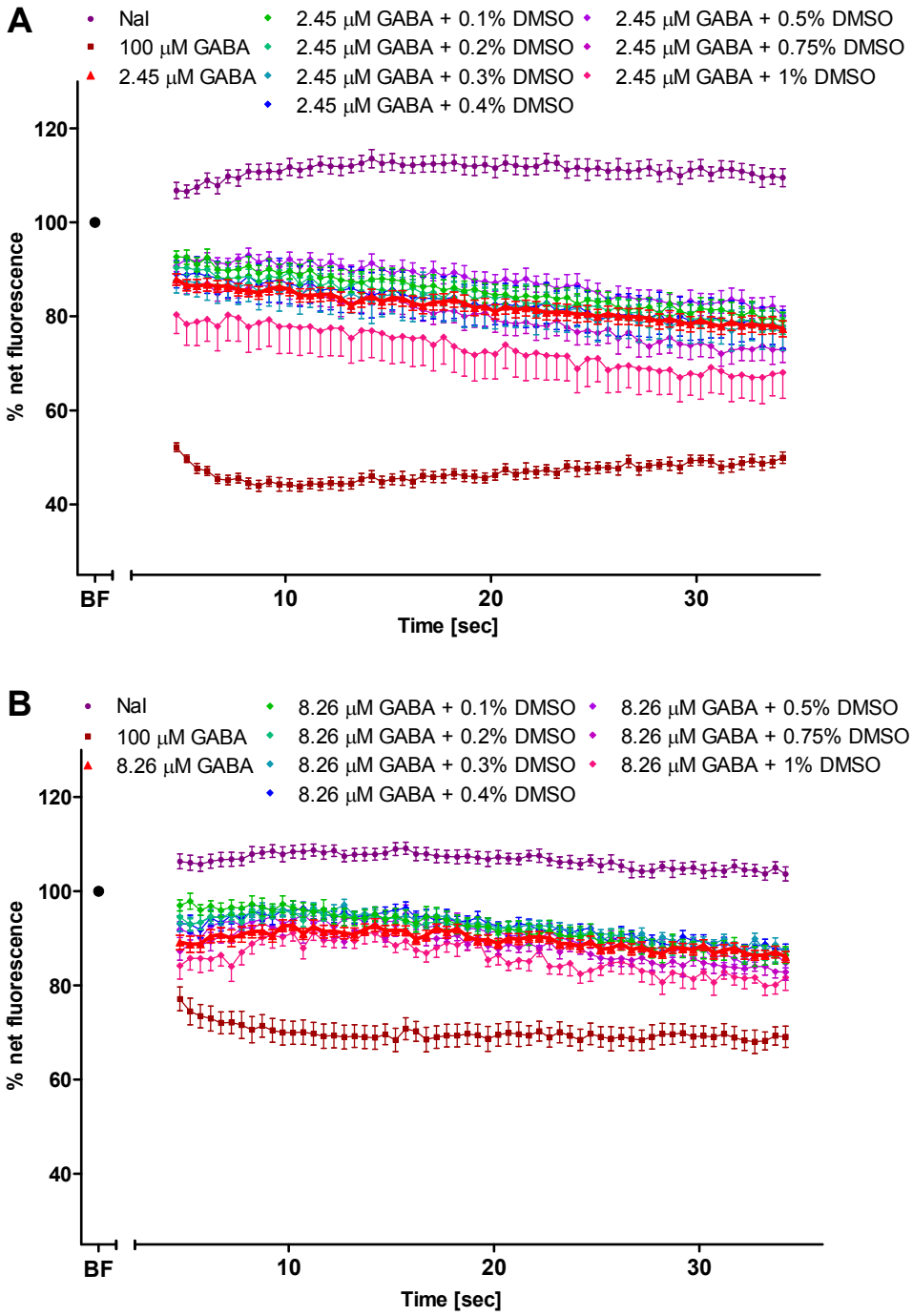

Figure B.2: Fluorescence signal of mutant YFP-H148Q/I152L in response to different concentrations of DMSO in HEK293 cells also expressing $\alpha 3\beta 2\gamma 2$- (A) or $\alpha 1\beta 2\varepsilon$ $GABA_A$ receptors .

Fluorescence was measured for 30 seconds after addition of NaI test solution only or together with 100 µM GABA, EC_{30} GABA or EC_{30} GABA and 0.1 to 1 % DMSO. Net fluorescence was normalised by setting the averaged baseline fluorescence to 100 % and fluorescence changes (after adding solutions) were calculated as percentage of the baseline fluorescence.

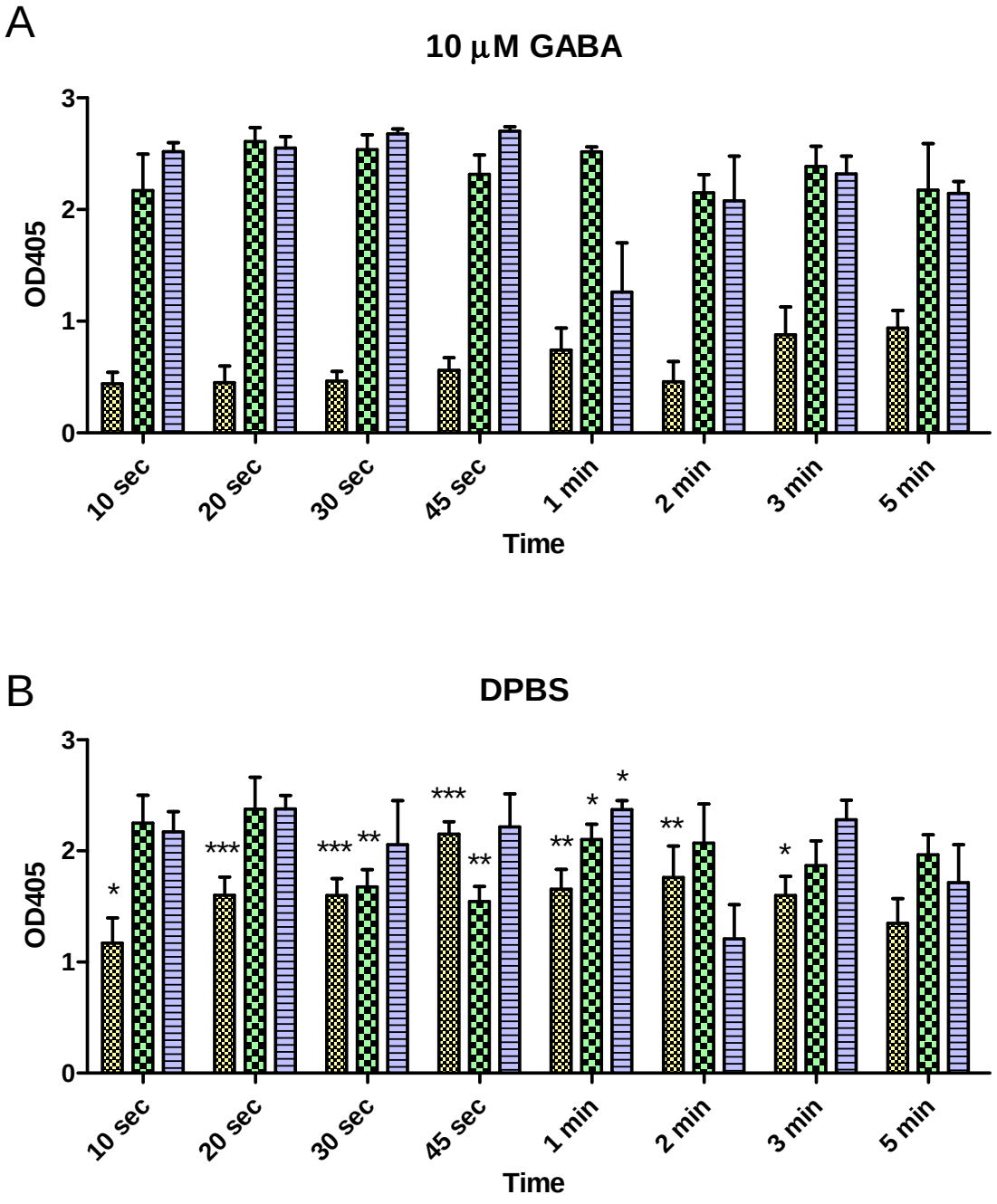

Figure B.3: OD405 values from iodide-flux assay in HEK293 cells expressing $\alpha 3\beta 2\gamma 2$ $GABA_A$ receptors. Before performing the SK assay, 10 µM GABA or DPBS were incubated for ten seconds to five minutes, respectively.

*Readings represent data from SK assay from undiluted cell lysate from assays, which were repeated three times (first assay = yellow columns, second = green columns, third = blue columns). Values are means ± SD from six data points each. * indicates p < 0.05, ** = p < 0.01, *** = p < 0.001 comparing GABA-treated cells (A) with their respective DPBS controls (B).*

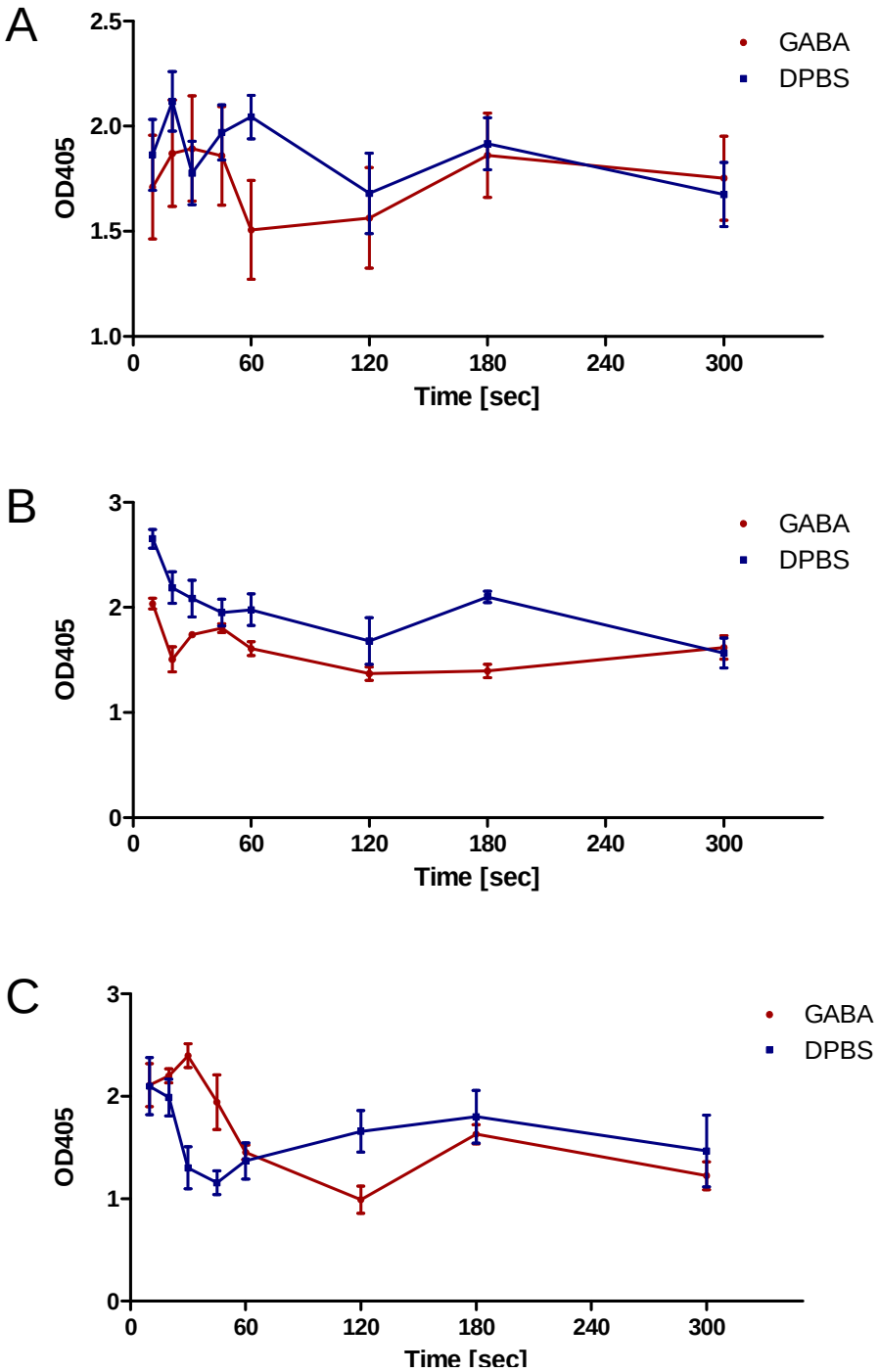

Figure B.4: OD405 values from iodide-flux assay in HEK293 cells expressing $\alpha 3\beta 2\gamma 2$ $GABA_A$ receptors. Before performing the SK assay, 10 µM GABA or DPBS were incubated for ten seconds to five minutes, respectively.

Readings represent data from SK assay from (A) undiluted cell lysate from assays (n = 18). (B) Values obtained from diluted cell supernatant, 2:3 (n = 6) or (C) 1:5 (n = 6). Values are means ± SEM.

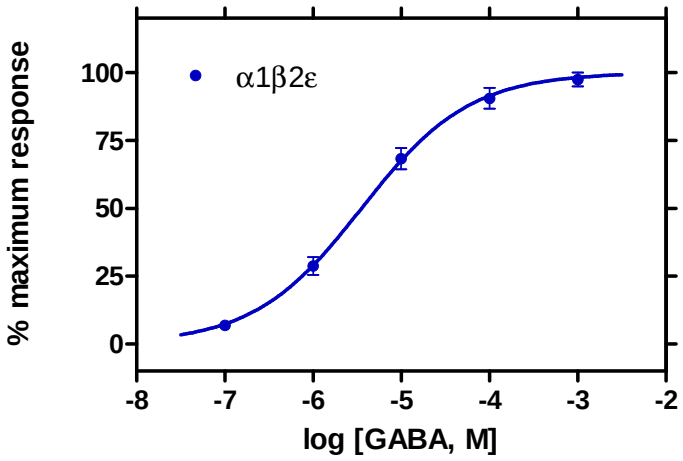

Figure B.5: GABA concentration-response curve for $\alpha 1\beta 2\varepsilon$ $GABA_A$ receptors (n = 4) expressed in *Xenopus laevis* oocytes. The data correspond to means ± SEM; n states the number of oocytes tested. The EC_{50} value was 3.553 ± 0.52 µM and the Hill coefficient 0.71. Curves were fitted using a non-linear regression fit with variable slopes as described in Section 2.3.5.

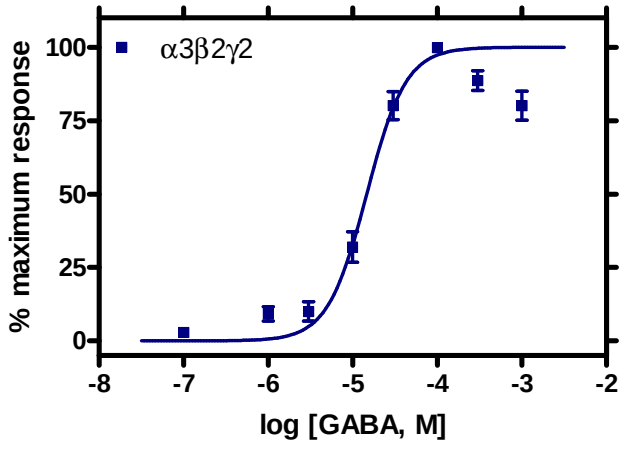

Figure B.6: GABA concentration-response curve for $\alpha 3\beta 2\gamma 2$ $GABA_A$ receptors (n = 10) expressed in HEK293 cells. The data correspond to means ± SEM; n states the number of cells clamped. The EC_{50} value was 14.65 µM and the Hill coefficient 1.88. Curves were fitted using a non-linear regression fit with variable slopes as described in Section 2.3.5.